MECHANISTIC STUDIES IN PORPHOBILINOGEN BIOSYNTHESIS

Sharon Deena George

A Thesis Submitted for the Degree of PhD
at the
University of St Andrews

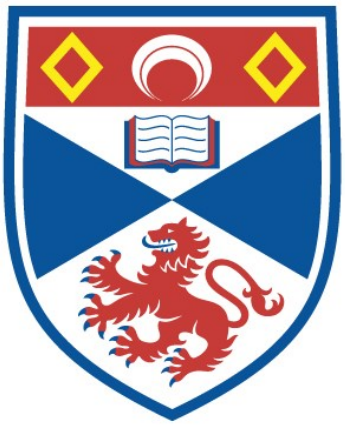

1993

MECHANISTIC STUDIES IN PORPHOBILINOGEN BIOSYNTHESIS

a thesis presented by

SHARON DEENA GEORGE, M.Sc.

to the

UNIVERSITY OF ST. ANDREWS

in application for

THE DEGREE OF DOCTOR OF PHILOSOPHY

St. Andrews

September 1992

ProQuest LLC.
789 East Eisenhower Parkway
P.O. Box 1346
Ann Arbor, MI 48106 – 1346

DECLARATION

I, Sharon Deena George, hereby certify that this thesis has been composed by myself, that it is a record of my own work, and that it has not been accepted in partial or complete fulfilment of any other degree or professional qualification.

Signed Date 14.10.92

I was admitted to the Faculty of Science of the University of St. Andrews under Ordinance General No.12 on October 1st 1989 and as a candidate for the degree of Ph.D. on September 1st 1990.

Signed Date 14.10.92

I hereby certify that the candidate has fulfilled the conditions of the Resolution and Regulations appropriate to the Degree of Ph.D.

Signature of Supervisor

Date

COPYRIGHT

In submitting this thesis to the University of St. Andrews, I understand that I am giving permission for it to be made available for use in accordance with the regulations of the University Library for the time being in force, subject to any copyright vested in the work not being affected thereby. I also understand that the title and abstract will be published, and that a copy of the work may be made and supplied to any *bonafide* library or research worker.

Dedicated with love and gratitude

to my

husband and parents

ACKNOWLEDGEMENTS

I would like to extend my profound thanks to Dr. A. R. Butler my supervisor, for giving me the opportunity to carry out this work and for his excellent and inspiring supervision during its progress.

I am extremely grateful to Professor D. Cole-Hamilton and Professor C. Vincent for the use of facilities in the department and to Dr. S. Arumugam and Dr. F. G. Riddel for their excellent advice and assistance in the optimal utilisation of the 500 MHz NMR spectrometer.

I would like to express my heartfelt thanks to Dr. D. M. G. Lloyd for specialist advice and to Dr. S. M. Glidewell for her untiring help and support in the laboratory.

My indebtedness to the technical staff in the department is manifest: Mr. J. R. Bews (computing), Mrs. M. B. Parker (stores), Mr. J. Ward and Mr. D. Wilkie (electrical workshop), Mr. J. Rennie, Mr. R. E. Cathcart and Mr. D. Clarke (mechanical workshop), Mr. C. F. M. Smith (glassblower), Mr. C. Millar (mass spectrometry), Mrs. S. Smith (elemental analysis) and Mrs. M. H. Smith (NMR).

I would also like to acknowledge with deep gratitude, financial assistance from The Royal Society who have supported my research in the purchase of labelled materials and The Rollo Trust for the provision of a research studentship.

To my occassionally abandoned husband Sheru, I give my sincere thanks for his patience and constant encouragement which have been invaluable in the preparation of this work.

Most of all I am deeply grateful to my parents, for their unstinting support and encouragement throughout my academic career and who have always given me the opportunity to realise my full potential.

ABBREVIATIONS AND SYMBOLS

A	absorbance
ALA	5-aminolevulinic acid
ALA.HCl	5-aminolevulinic acid hydrochloride
ALA dehydratase	5-aminolevulinic acid dehydratase
ALA synthase	5-aminolevulinic acid synthase
ATP	adenosine triphosphate
BES	N,N-bis(2-hydroxyethyl)-2-amino-ethanesulphonic acid
BTDA	boron trifluoride-diacetic acid complex
copro'gen III	coproporphyrinogen III
copro'gen oxidase	coproporphyrinogen III oxidase
DMAB	*p*-N,N-dimethylaminobenzaldehyde
DOVA	dioxovalerate
DMF	N,N-dimethylformamide
DSS	2,2-dimethyl-2-silapentane-5-sulphonate
DTT	dithioerythreitol
EDTA	ethylenediaminetetraacetic acid
HAT	2-hydroxy-3-aminotetrahydropyran-1-one
HEPES	N-(2-hydroxyethyl)piperazine-N'-(2-ethanesulphonic acid)
IUPAC	International Union of Pure and Applied Chemistry
IUB	International Union of Biochemistry
k	rate constant
KPi	potassium phosphate

MMTS	methylmethanethiosulphonate
MOPS	3-(N-morpholino)propanesulphonic acid
NADPH	reduced nicotinamide adenine dinucleotide phosphate
N,N-dimethyl-ALA.HCl	N,N-dimethyl-5-aminolevulinic acid hydrochloride
PBG	porphobilinogen
PBG deaminase	porphobilinogen deaminase
PBGS	porphobilinogen synthase
PIPES	piperazine-N,N'-bis(2-ethane-sulphonic acid)
PLP	pyridoxal 5'-phosphate
proto'gen IX	protoporphyrinogen IX
proto'gen oxidase	protoporphyrinogen IX oxidase
r	buffer ratio
t	time
TES	N-tris(hydroxymethyl)methyl-2-aminoethanesulphonic acid
TMS	trimethylsilane
tRNA	transfer ribonucleic acid
uro'gen III	uroporphyrinogen III
uro'gen III synthase	uroporphyrinogen III synthase
uro'gen decarboxylase	uroporphyrinogen III decarboxylase
λ	wavelength

ABSTRACT

[4-^{13}C]ALA.HCl (50% enriched) and [^{15}N]ALA.HCl (50% enriched) have been synthesised and utilised in mechanistic studies. The synthesis of the former was achieved *via* a modified literature procedure, employing [2-^{13}C]glycine (99.8% enriched) as the starting material. The NMR spectral data of the labelled materials have been fully characterised.

^{13}C NMR studies of [4-^{13}C]ALA.HCl (50% enriched) have demonstrated the forms of ALA and its autocondensation products under physiological conditions. ^{17}O and ^{1}H NMR studies have confirmed the existence of the alternative forms of ALA and its condensation products at neutral pH. The non-enzymatic cyclic dimerisation of ALA leads to the formation of 2,5-bis(2-carboxyethyl)pyrazine and under some circumstances, pseudo-PBG. The condensation products of ALA under a variety of conditions have been identified from their NMR spectra and mechanisms for their formation are proposed.

The condensation of ALA and its 5-methyl analogue with a variety of carbonyl compounds have been investigated and the products (novel substituted pyrroles in some cases) characterised by their melting points, elementary analyses, mass spectra and NMR spectra. A hydrogen bonded enaminoketone in a chelated ring has been identified as the intermediate in the reaction between ALA and 1,1,1-trifluoropentane-2,4-dione, by ^{1}H and ^{15}N NMR spectroscopy.

^{13}C NMR kinetics of the reaction between ALA and pentane-2,4-dione has revealed that the reaction proceeds *via* an enaminoketone intermediate. The nature of the intermediate species in the above reaction was confirmed by ^{15}N NMR

spectroscopy. On the basis of the kinetic evidence obtained for the reaction between ALA and 1,1,1-trifluoropentane-2,4-dione, a mechanism has been proposed for the Knorr and Fischer-Fink pyrrole syntheses.

Studies with the bovine liver enzyme, ALA dehydratase, has revealed that it is very specific in the reaction that it catalyses; the Knorr-type dimerisation of two molecules of ALA to form PBG. The substrate analogues, levulinic acid and the methyl ester of ALA were found to be a non-competitive inhibitor and a very poor substrate of the enzyme respectively. The substrate analogues, N,N-dimethyl-ALA and 5-methyl-ALA do not bind to the enzyme and therefore do not affect the rate of production of PBG. A mechanism has been postulated for PBG biosynthesis, similar to the one proposed for the Knorr pyrrole synthesis.

Stopped-flow kinetics of the reaction between *p*-nitrophenyl-diazonium tetrafluoroborate and bilirubin ditaurate disodium salt has revealed that diazonium ions are solely responsible for the cleavage of the central methylene bridge of the bilirubin conjugate molecule. On the basis of the above evidence, a mechanism has been proposed for the diazo coupling reaction.

CONTENTS

page

CHAPTER 2 SYNTHESES OF [4-^{13}C]ALA.HCl AND [^{15}N]ALA.HCl

CHAPTER 4 THE KNORR AND FISCHER-FINK CONDENSATIONS OF ALA AND 5-METHYL-ALA

CHAPTER ONE

INTRODUCTION

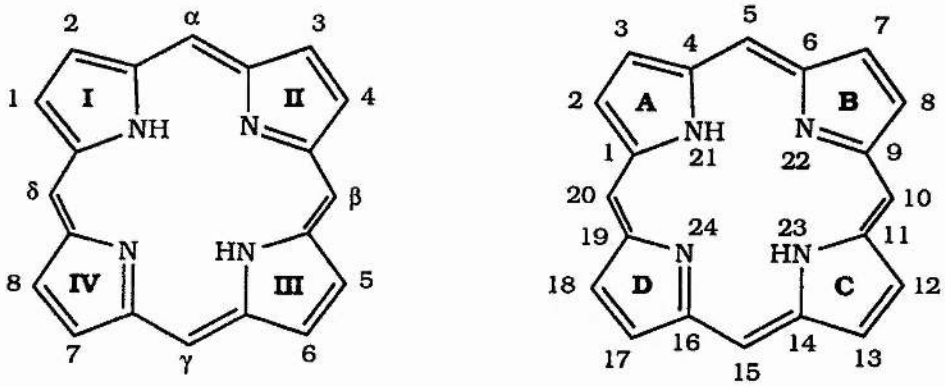

Figure 1.1 Structures of the parent systems, porphin (Fischer) and porphyrin (IUPAC-IUB) showing the numeration of the four pyrrole rings.

1.1 General Introduction.

Porphyrins and porphyrin derivatives play a vital role in the biochemistry of all living systems. They form the backbone of pigments, such as haem and chlorophylls, which have a wide biological distribution. Porphyrins and their derivatives are also present in a wide variety of other biocatalysts such as cytochromes, vitamin B_{12} and the prosthetic groups of enzymes e.g. peroxidases and catalases.

The bare tetrapyrrolic nucleus referred to as 'porphin' in the Fischer nomenclature[1-3] is a unique biological structure. It consists of a macrocycle of four 'pyrrole-type' rings designated I, II, III and IV linked by four methine bridges α, β, γ and δ (Fig. 1.1). This is a rigid planar structure from which porphyrins are derived, by the substitution of some or all of the peripheral carbon atoms (C_1 to C_8) by a variety of side chains. The type of side chain determines the physical characteristics of the porphyrin.

The more recent IUPAC-IUB[4] nomenclature has defined a new numbering system for porphyrins, which brings porphyrin numeration in line with that of the biosynthetically related corinnoid system. The parent system in the revised nomenclature is called porphyrin. The numbering of ring positions including nitrogen and the use of letters to denote individual rings is also shown in Fig. 1.1.

The normal biological intermediate is not this highly conjugated porphyrin, but the hexahydroporphyrin, the porphyrinogen (Fig. 1.2) in which each of the methine bridges and the two pyrrolenine nitrogen atoms are hydrogenated. Porphyrinogens are colourless and unconjugated in contrast to the conjugated and brilliantly coloured porphyrins which fluoresce red

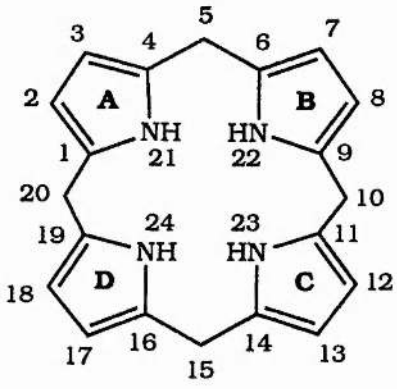

PORPHYRINOGEN

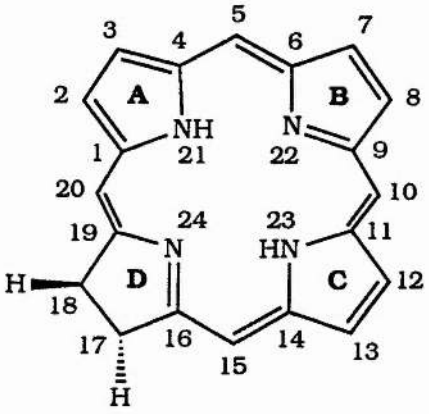

CHLORIN NUCLEUS

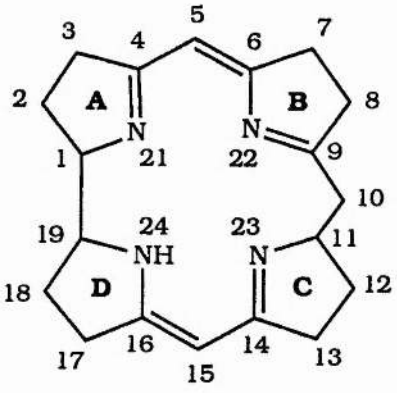

CORRIN NUCLEUS

Figure 1.2 Stuctures of porphyrinogen, the chlorin nucleus and the corrin nucleus.

in light of wavelength around 400 nm. The chemistry of these compounds is well described by Marks,[5] Smith[6] and Dolphin[7] and various other aspects are discussed by Falk[8,9] and Adler.[10]

A derivative of the porphyrin nucleus is the chlorin nucleus (Fig. 1.2), a 17,18-dihydroporphyrin, in which saturation is traditionally shown in ring D. Another highly modified form of the porphyrin nucleus is the corrin nucleus (Fig. 1.2). An important attribute arising from the complex ring structures of porphyrins and porphyrin derivatives, and the available ligand binding sites within them, is their ability to bind metals. Haem, an iron containing porphyrin complex usually bound to various proteins is central to many biological oxidations, especially those associated with drugs. Haemoproteins are also used as oxygen carriers. Chlorophylls, the magnesium complexes of the chlorin nuclei, are central in solar energy utilisation in the biosphere. Thus, all known photosynthetic organisms show porphyrin dependent metabolism. Deficiency of vitamin B_{12} (cyanocobalamin), the key natural product containing the corrin nucleus and a central cobalt atom, results in pernicious anaemia.

As well as the systematic formation of porphyrins in biological systems, abiotic synthesis of porphyrins has been described in which a primitive chemical system has produced porphyrin like compounds through the high entropy of their formation.[11-14] Such synthesis is important in the ontogenesis of terrestrial life since it would have facilitated the emergence of life forms by increasing the efficiency of oxido-reductive processes.[15-16] As a consequence, porphyrins are found in fossil like forms and have even been identified in rocks from the moon.[17-18]

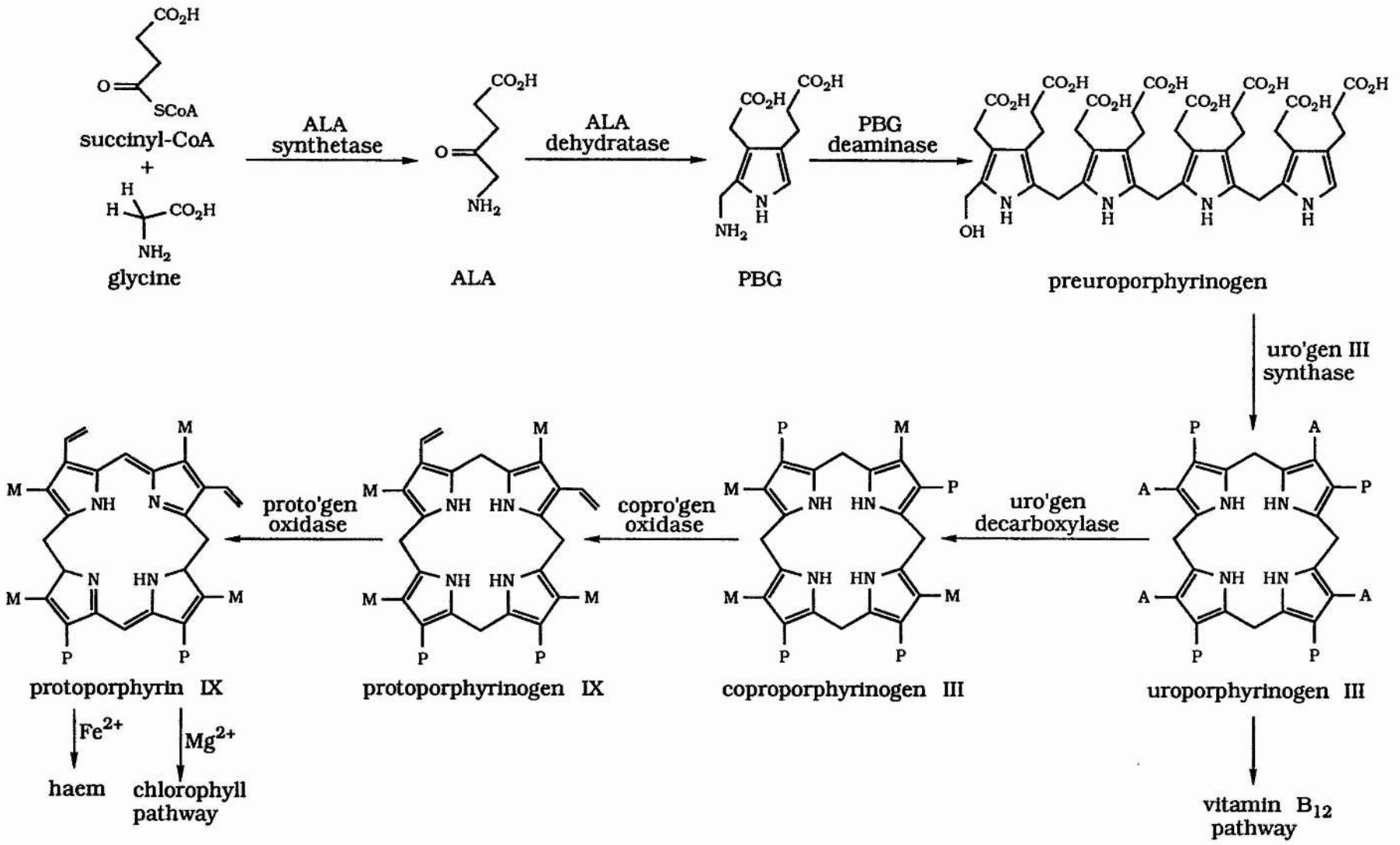

Scheme 1.1 Summary pathway for the biosynthesis of haem, chlorophylls and corrins. M = CH_3, A = CH_2CO_2H, P = $CH_2CH_2CO_2H$.

1.2 Overall pathway for the biosynthesis of haem, chlorophylls and corrins.

The biosynthesis of the tetrapyrrole ring system typifies the economy of biosynthetic effort, requiring only a few enzymic stages to form the complex tetrapyrrole structure from simple precursor molecules. The initial biosynthetic sequence for the synthesis of haem, chlorophylls and corrins, is the same and in each case utilizes porphyrinogens as direct intermediates of the final product.[19]

They all begin with the biosynthesis of the highly reactive aminoketone, 5-aminolevulinic acid (ALA). There are two distinct routes by which ALA is produced. The first operates in animals and some bacteria utilising glycine and succinyl-CoA. Recently, a second route involving the carbon skeleton of glutamate was identified, and has been shown to operate in plants and some anaerobic bacteria. Once formed, ALA dimerises by the action of the enzyme 5-aminolevulinic acid dehydratase (ALA dehydratase) also known as porphobilinogen synthase (PBGS) to form the monopyrrole, porphobilinogen (PBG). The enzyme porphobilinogen deaminase (PBG deaminase) brings about the head-to-tail condensation of four molecules of PBG to generate the highly unstable linear tetrapyrrole, preuroporphyrinogen or 1-hydroxymethylbilane. Cyclisation of preuroporphyrinogen proceeds by the action of the enzyme uroporphyrinogen III synthase (uro'gen III synthase) with rearrangement of ring D to form uroporphyrinogen III (uro'gen III). Uro'gen III is the universal tetrapyrrole precursor from which porphyrins, chlorophylls, corrins and all other tetrapyrroles are derived. Uro'gen III may through methylation form sirroheme, corrins or F_{430}. Alternatively, it may be biosynthesised into haem or

the chlorophylls.

The route to haem involves the decarboxylation of uro'gen III at all four acetate side chains by the action of the enzyme uroporphyrinogen III decarboxylase (uro'gen decarboxylase) to give coproporphyrinogen III (copro'gen III). Two of the propionate groups of copro'gen III are then oxidatively decarboxylated by the enzyme coproporphyrinogen III oxidase (copro'gen oxidase) to form protoporphyrinogen IX (proto'gen IX). The enzyme protoporphyrinogen IX oxidase (proto'gen oxidase) then oxidises proto'gen IX to form protoporphyrin IX. Insertion of Fe^{2+} into the centre of protoporphyrin IX by the enzyme ferrochelatase, gives haem, which is found as such in haemoglobin, myoglobin, cytochromes b and P-450, erythrocruonin, peroxidases and catalases. Introduction of Mg^{2+} into protoporphyrin IX on the other hand, is the first step on the route to the chlorophylls. A schematic representation of these pathways is shown in Scheme 1.1.

1.3 Early investigations on the biosynthesis of the tetrapyrrole ring.

The elucidation of the early stages in the tetrapyrrole biosynthetic pathway was largely complete by the end of the 1950s and all the intermediates with the exception of preuroporphyrinogen had been characterised. The major contributions stemmed from the investigations carried out by Shemin and his co-workers in the United States and the group of Neuberger in the United Kingdom. Central to their methodology was the use of isotopes in order to follow the path by which precursors were incorporated into haem. The use of orally administered [^{15}N]glycine established that this amino acid was the most efficient precursor of the haem nitrogen atoms.[20] Subsequently, experiments carried out with [^{14}C]glycine, using enzyme extracts from avian erythrocytes established that the C-2 carbon atom, but not the carboxyl carbon of glycine was incorporated into eight positions in the haem macrocyclic ring.[21,22] This was deduced by degrading the labelled haem to ethylmethylmaleimide and hematinic acid. The maleimides were then further degraded by methods which permitted the isolation and positional assignment of each of the carbon atoms present in the haem macrocycle. Additional labelling experiments using 1-[^{14}C]acetate and 2-[^{14}C]acetate established that the remaining carbon atoms of haem were derived from an asymmetrical four-carbon compound arising from the tricarboxylic acid cycle,[23] and a succinyl derivative, succinyl-CoA, was suggested as a possible candidate. Subsequently, experimental proof for the involvement of succinyl-CoA was obtained from *in vitro* experiments using avian erythrocyte preparations.[24] The findings of these pioneering

studies (summarised in Fig. 1.3) established the origin of all the carbon and nitrogen atoms in haem and apply to all tetrapyrroles biosynthesised in mammalian, avian and some bacterial systems.

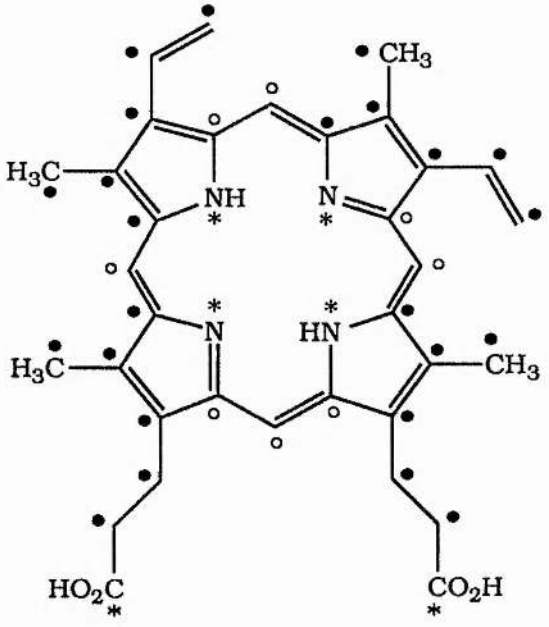

Figure 1.3 Origin of carbon and nitrogen atoms in protoporphyrin IX. * = N of glycine; * = CO_2H carbon of acetate; • = CH_3 carbon of acetate; o = CH_2 carbon of glycine.

The labelling data obtained from the incorporation experiments with radioactive glycine and acetate, and especially the observation that the carboxyl carbon atom of glycine was not incorporated into haem, led to the hypothesis that glycine and succinyl-CoA condensed together to form 2-amino-3-ketoadipic acid which yields ALA on decarboxylation.[25] This was confirmed when [5-^{14}C]ALA was chemically synthesised and shown to be incorporated into haem in high yield and with a labelling pattern identical to that given by [2-^{14}C]glycine.[26]

At the time ALA was first described, the existence of the next intermediate in the porphyrin biosynthetic pathway, PBG, had

already been known for several years, having been isolated from the urine of patients suffering from acute intermittent porphyria.[27] However, its role as an intermediate in the haem biosynthetic pathway was not recognised until its structure had been elucidated by X-ray crystallography[28] and found to be similar to that postulated for the haem precursor pyrrole. It then became apparent that two molecules of ALA could account for all the carbon and nitrogen atoms of PBG. PBG was subsequently shown to act as an excellent precursor for porphyrins[29] and its role as an intermediate was finally confirmed when it was shown to be formed enzymatically from ALA.[30,31]

1.4 Biosynthesis of ALA.

1.4.1 Occurrence and properties of ALA synthases (EC 2·3·1·37).

The first step, the rate controlling step of haem biosynthesis, is the condensation of succinyl-CoA and glycine to form ALA (Scheme 1.2).

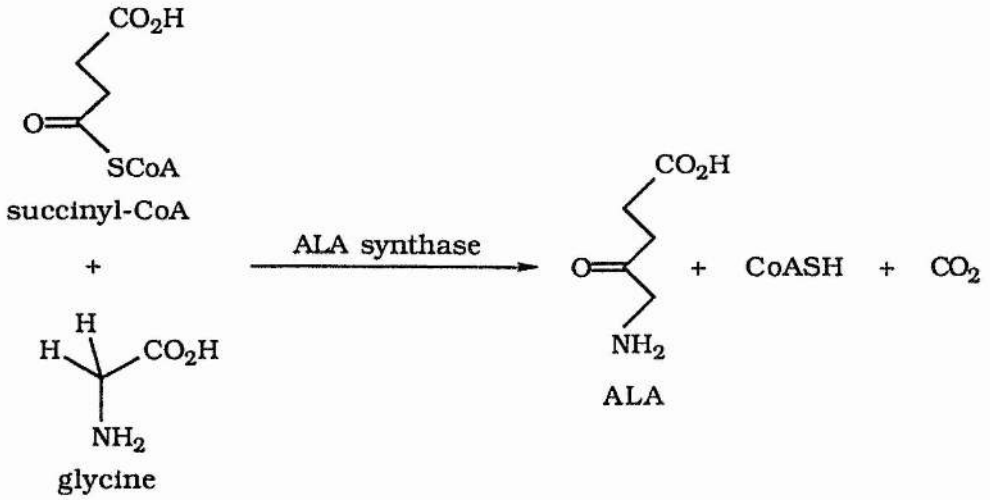

Scheme 1.2 The ALA synthase reaction.

The enzyme ALA synthase, responsible for this reaction was

described simultaneously by Shemin and his co-workers in bacterial extracts[32] and by Neuberger and his group in avian preparations.[24] Since then, the enzyme has been purified from many sources including *Rhodobacter spheroids*,[33] livers of rat[34] and chicken embryos.[35] *Euglena gracilis* [36] and yeast.[37]

In eukaryotes, the enzyme is located in the mitochondrion. Although succinyl-CoA is generated by other enzyme systems such as methylmalonyl-CoA mutase, succinate thiokinase and acetoacetyl-CoA : succinate transferase, the major source of succinyl-CoA for haem biosynthesis is from the tricarboxylic acid cycle.

Experiments with chick embryo liver[38] and yeast[39] have established that the enzyme is first synthesised in the cytosol as a pre-enzyme which is transported across the mitochondrial membrane and processed to give the mature form.

Haem is an important regulator acting as both a feedback inhibitor of the enzyme directly and also as a regulator at the nucleic acid level. Evidence for the presence of both an inhibitor and an activator of the enzyme have been obtained which indicates that it may be regulated through sulphur-containing metabolites such as the trisulphides of cysteine and glutathione.[40] These compounds are able to activate ALA synthase *in vitro* by converting a low activity form to a high activity form.

All the ALA synthases purified to date appear to exist as homodimers with subunit molecular weights varying from 40,000 to 60,000. The enzyme is absolutely specific for glycine, but not for succinyl-CoA. The methyl ester of succinyl-CoA is also a good substrate whereas glutaryl-CoA and acetyl-CoA are poor substrates.

All ALA synthases require the cofactor pyridoxal 5'-phosphate

(PLP) for full catalytic activity.[41] The activity of the *Rhodopseudomonas spheroids* enzyme is maximal at 50 mM PLP[42] but the nature of the interaction of the coenzyme with the enzyme is so complex that it is not possible to determine the binding constant with any precision.

Spectroscopic studies[43] indicate that at pH 5 or pH 8.5, the enzyme-PLP link is largely in the form of a Schiff base absorbing at 420 nm. At pH 7.2, where the enzyme is catalytically active, experimental evidence is more consistent with the presence of a carbinolamine or equivalent structure, absorbing at 333 nm. Treatment of the holoenzyme with sodium borohydride leads to inactivation of the enzyme at pH either side of pH 7,[44] although at neutral pH, the enzyme is not inactivated to any great extent by the reagent. This suggests that at neutral pH, PLP is bound in a less reactive form, possibly as a carbinolamine substituted by an enzyme thiol rather than as a fully formed Schiff base as has been previously suggested.[43]

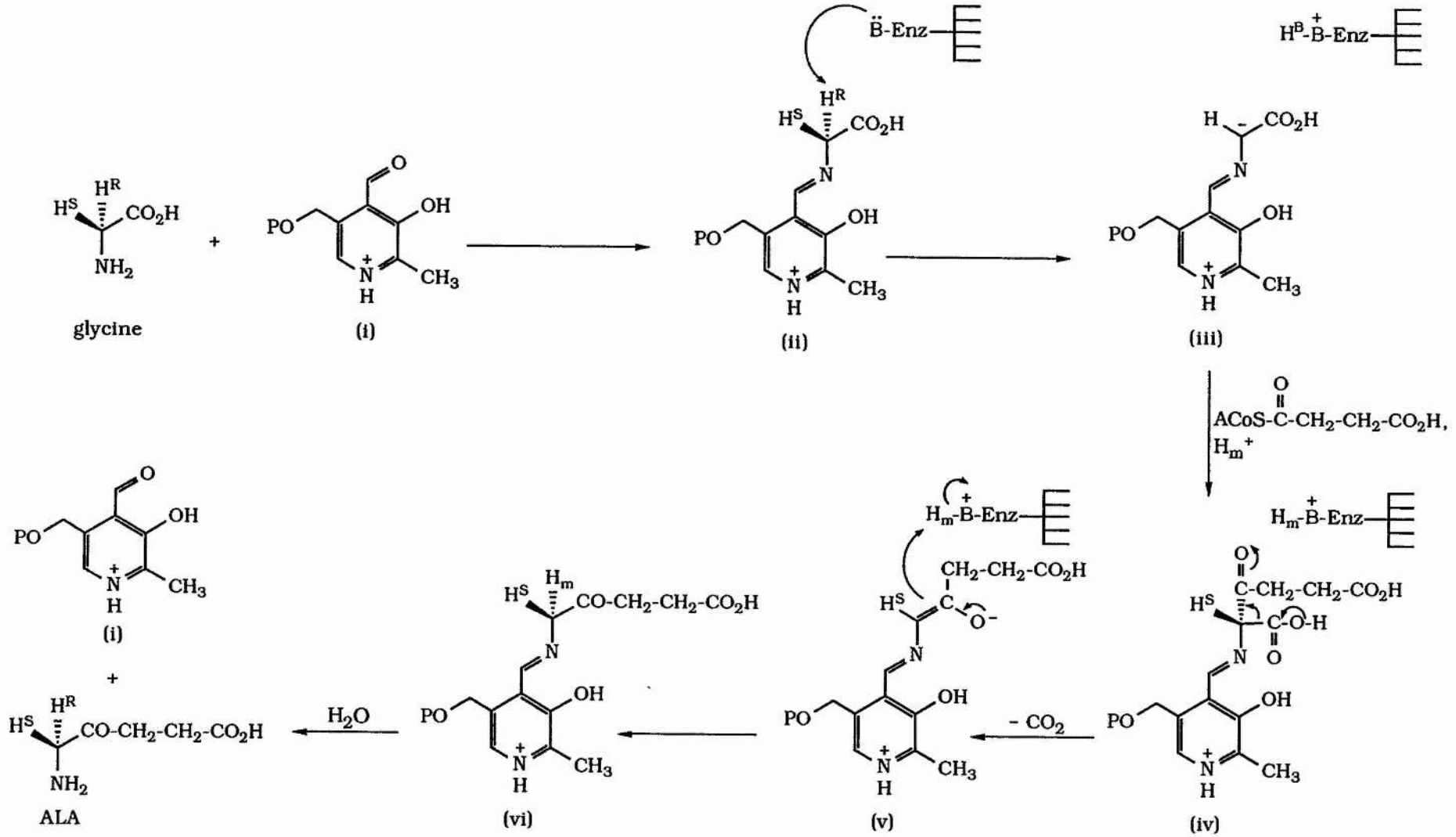

Scheme 1.3 Mechanism and steric course of the ALA synthase reaction.

1.4.2 Mechanism of ALA synthase.

Most of the mechanistic details of the ALA synthase reaction have been deduced from investigations with the enzyme isolated from *Rhodopseudomonas spheroids*. In common with other PLP catalysed enzyme reactions,[45] the first event in the synthesis of ALA involves the binding of glycine to the PLP-enzyme complex [Scheme 1.3(i)] to form an enzyme-PLP-glycine Schiff base complex [Scheme 1.3(ii)]. It has been established that the latter generates a stabilised carbanion at the glycine-α-carbon atom [Scheme 1.3(iii)] by the loss of a proton,[46] this being the *pro*-R hydrogen atom.[47] This conclusion was strengthened by the finding that in the absence of the second substrate, succinyl-CoA, the enzyme catalyses a partial reaction in which the *pro*-R hydrogen atom of glycine is exchanged with the protons of the solvent.[48] Reaction of succinyl-CoA with the enzyme-PLP-glycine carbanion intermediate yields an enzyme-PLP-α-amino-β-ketoadipic acid complex [Scheme 1.3(iv)].

Experimental evidence[47] has shown that further transformation of this intermediate into ALA occurs by decarboxylation to generate the enzyme-bound intermediate enol [Scheme 1.3(v)] which is then protonated stereospecifically to form the enzyme-pyridoxal 5'-phosphate Schiff base of ALA [Scheme 1.3(vi)]. The *pro*-S hydrogen atom of glycine is retained in the biosynthesis[49] and incorporated into the *pro*-S configuration at the C-5 position of ALA. This suggests that of the two crucial conversions [Scheme 1.3(ii to iv) and (iv to vi)] one proceeds by an inversion and the other by a retention of configuration. The conclusion that the *pro*-S hydrogen atom of glycine is incorporated into the *pro*-S hydrogen atom at the C-5 position of ALA was strengthened by the finding that in the absence of either substrate,

the enzyme catalyses the exchange of the *pro*-R hydrogen atoms at the C-5 position of ALA.[50] In the mechanism of the ALA synthase reaction, it is assumed that in the conversion of (iii) to (iv) (Scheme 1.3) the hydrogen H^R abstracted by the basic group on the enzyme exchanges with the protons of the medium (H_m^+).

1.5 Biosynthesis of ALA from glutamate.

Investigators were puzzled for many years by their inability to detect the enzyme ALA synthase in higher plants. The problem was solved by Beale and Castelfranco[51] when they demonstrated that ALA was derived from the carbon skeleton of glutamate in greening cucumber cotyledons. Further experiments with [^{14}C]-labelled glutamate in greening barley showed that it was incorporated into ALA with the carbon skeleton intact and with C-1 of glutamate giving rise to C-5 of ALA.[52]

Much of the earlier work on ALA formation from five-carbon precursors by intact chloroplasts and unpurified cell extracts has been reviewed by Beale.[53] The existence of the C-5 pathway has been confirmed in barley,[54] *Euglena gracilis*,[55] the green algae *Chlamydomonas reinhardtii* [56] and *Chlorella vulgaris*,[57] the red alga *Cyanidium caldarium*,[58] the cyanobacteria *Synechocystis* and *Synechococcus*,[59] the prochlorophyte *Prochlorothrix*[59] and the photosynthetic bacterium *Chlorobium*.[60] Similar or identical reaction mechanisms appear to operate in all cases.

1.5.1 Mechanism of ALA formation from glutamate.

The elucidation of the pathway by which glutamate is transformed into ALA has been the subject of intensive research over the last decade. The enzymes have been characterised most

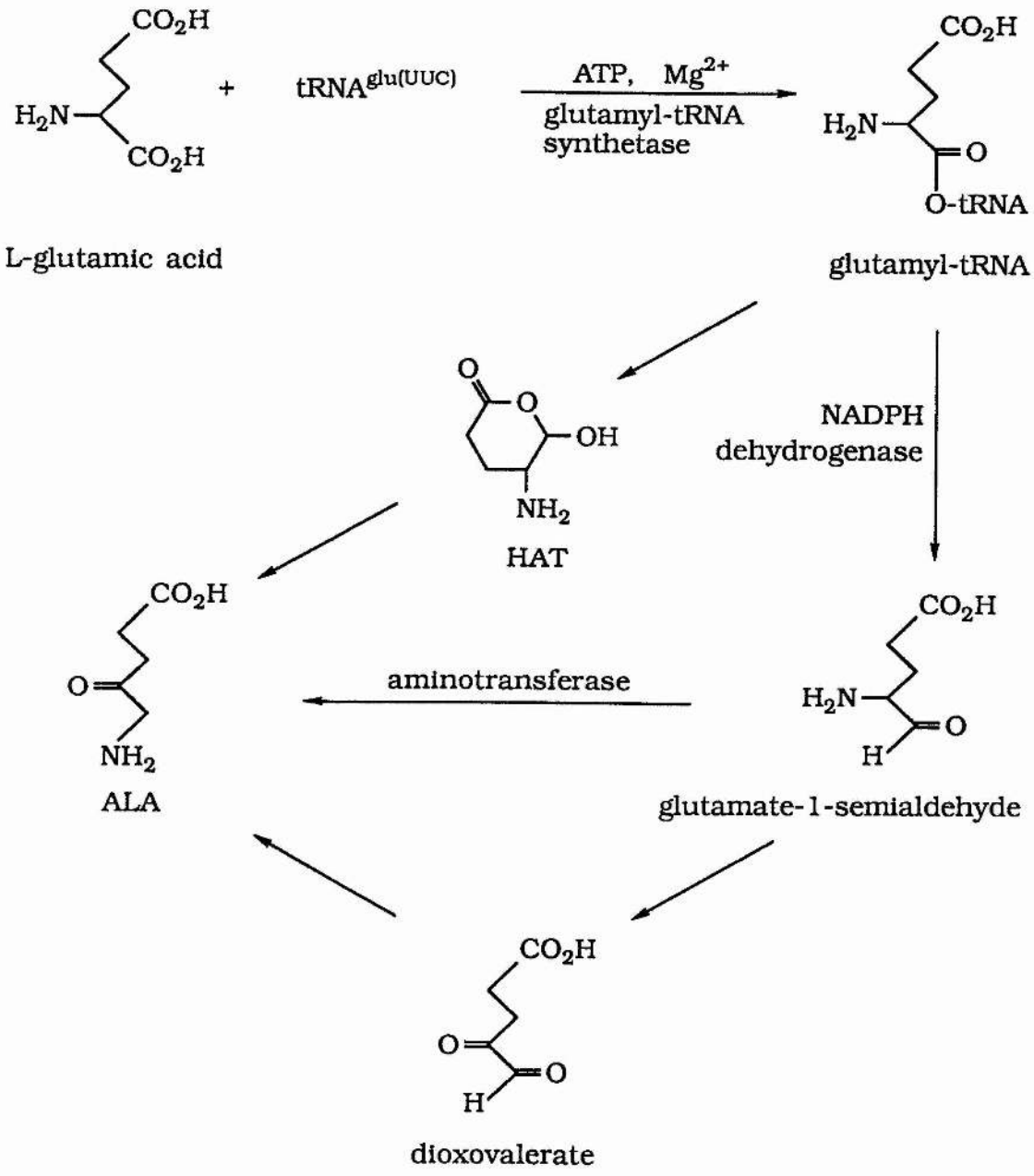

Scheme 1.4 Glutamate pathway for the biosynthesis of ALA.

fully in barley and it is assumed, though not proven, that similar enzymes are operative in algae and bacteria. Altogether, three enzymes have been detected in extracts of greening barley.[61] In addition, the involvement of $tRNA^{glu}$ has also been established.[62-64]

The first enzyme, glutamate-tRNA synthetase catalyses the coupling of glutamate to $tRNA^{glu}$, a reaction which requires ATP and magnesium ions. The glutamyl-tRNA is then reduced by a second enzyme in an NADPH requiring reaction. The product of this reduction has been characterised as glutamate-1-semialdehyde[66] or its hydrated hemiacetal form.[67] However, some of the reported properties of the product are inconsistent with the presence of a 2-aminoaldehyde group and Jordan *et al*[68] have suggested that 2-hydroxy-3-aminotetrahydropyran-1-one (HAT), the cyclised form of glutamate-1-semialdehyde is the true precursor of ALA. The plausible mechanism of the third enzyme, an aminotransferase has been proposed by Hoober *et al*[67] in which the glutamate-1-semialdehyde binds to the enzyme which contains a pyridoxamine phosphate cofactor at the active site. The amino group transaminates with the substrate to yield an enzyme-bound 4,5-diaminovalerate intermediate. This is transformed into ALA by donating the amino group in the C-4 position to the pyridoxal 5'-phosphate to regenerate the pyridoxamine 5'-phosphate-enzyme ready to receive the next substrate. This mechanism explains why an amino donor other than the substrate is required and is also consistent with the NMR experiments of Mau and Wang[69] which showed that there was intermolecular transfer of the amino group during the reaction. The likely involvement of the cyclic intermediate (HAT) as a substrate need not affect the above mechanism since the transaminase would ring open the compound

as the first step in the mechanism.

Experiments carried out with *Scenedesmas* have revealed that in this organism 4,5-dioxovalerate is a better precursor for ALA than glutamate-l-semialdehyde. The presence of the enzyme L-alanine-4,5-dioxovalerate transaminase has been presented as evidence for a two stage transformation of glutamate-l-semialdehyde into ALA. It is possible that variations on the pathway shown in Scheme 1.4 exist in different organisms with 4,5-dioxo-valerate as an intermediate between glutamate-l-semialdehyde and ALA in *Scenedesmas* but not in barley. The formation of ALA from glutamate through dioxovalerate (DOVA) has been shown to be present in bovine liver[70] and labelled DOVA has been incorporated into ALA and haem in rats.[71]

In vivo and *in vitro* results indicate that in higher plants, green algae, red algae and cyanobacteria all cellular tetrapyrroles are formed from glutamate. Some photosynthetic bacteria have the glutamate pathway, while others have the glycine pathway. *Euglena gracilis* is uniquely able to form plastid tetrapyrroles from glutamate while simultaneously forming mitochondrial haems from glycine and succinate.

1.6 Biosynthesis of porphobilinogen.

1.6.1 Occurrence and properties of ALA dehydratases (EC 4·2·1·24)

The enzyme ALA dehydratase was intially shown to be present in ox liver[31] and avian erythrocytes.[30] The enzyme has since been shown to be present in virtually all living organisms and has been highly purified from a variety of sources including human erythrocytes,[72,73] bovine liver,[74,75] yeast,[76] spinach,[77] and *Rhodospseudomonas spheroids.*[78]

The reaction catalysed by the enzyme involves the dimerisation of two molecules of ALA in a Knorr reaction with the elimination of two molecules of water, to form PBG as shown in Scheme 1.5.

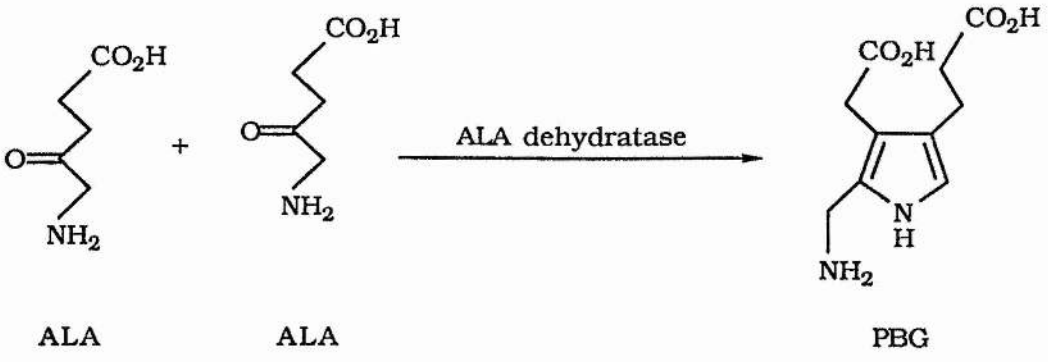

ALA ALA PBG

Scheme 1.5 The ALA dehydratase reaction.

There are comprehensive reviews of the properties of ALA dehydratases in the literature.[79,80,81] The mammalian and avian enzymes are zinc metalloenzymes, all of which have pH optima in the range 6.3 to 7.0 and are inhibited by EDTA. Dehydratases of this class have molecular weights of about 280,000, made up of eight identical subunits of molecular weight 35,000.

The bacterial enzymes have very different properties with pH optima from 8 to 8.5 and a requirement for monovalent cations such as K^+ for maximal activity. Although bacterial enzymes are not inhibited by EDTA and are not activated by zinc ions, this does not necessarily preclude the presence of a very tight zinc binding site. The enzyme from *Rhodopseudomonas spheroids* has a molecular weight of 240,000 and has been shown to exist as an octamer.[82] Dehydratases from plants[77] and yeast[76] also seem to be zinc metalloenzymes as judged by their susceptibility to EDTA, however their pH optima are somewhat higher than those of the mammalian

enzymes.

Electron microscopy of the bovine ALA dehydratase has revealed that the eight subunits are arranged at the corners of a cube with dihedral symmetry.[83] Recent experimental evidence[84] has shown that the octamer is a dimer of tetramers and that each tetramer is a dimer of dimers. The conclusions from these studies are consistent with the enzyme structure being composed of four functional dimers. In this connection, there is a considerable amount of evidence to suggest that the bovine enzyme, at least, exhibits half-site reactivity.[80] The ALA dehydratase from *Rhodopseudomonas spheroids* has also been shown to dissociate into four functional tetramers in the absence of potassium ions.[82]

A common feature of all dehydratases is the remarkable sensitivity of their sulfhydryl groups to oxygen or to thiol reagents. On exposure of the native bovine enzyme to oxygen there is a rapid loss of enzyme activity which is associated with the oxidation of two highly reactive -SH groups of two cysteine residues at the active site to form an S-S bond.[85-88] Full catalytic activity can be restored on treatment of the enzyme with an exogenous thiol.[89] Chemical modification by reagents directed toward alkylation of cysteine inactivate the enzyme e.g. N-ethylmaleimide,[90] *p*-chloromercuri-benzoate,[91] iodoacetic acid,[85,92,93] iodoacetamide,[85] 3- and 5-halo-levulinic acids[88] and 5,5'-dithiobis(2-nitrobenzoic acid).[94] Studies with the human ALA dehydratase labelled with $^{65}Zn^{2+}$[95] have shown that -SH groups are involved with the binding of the metal ion.

The metal requirements for the dehydratase enzymes have been investigated largely with the mammalian enzymes, especially those isolated from human erythrocytes and bovine liver. It has been established that one zinc ion is bound per subunit, eight per

octamer, on the basis of experiments with both nonradioactive zinc[86,87] and with ^{65}Zn.[95] Whether zinc is essential for catalytic activity is still in doubt. Investigations by Tsukamoto *et al* [86,87] suggest that zinc plays only a conformational role and is not essential for activity. Bevan *et al* [74] have suggested that only four zinc ions per octamer are required for full catalytic activity and that only half the subunits may be catalytically active at one time. Jaffe *et al* [96] have confirmed both observations that four Zn^{2+}/mol of octameric apoenzyme are necessary for full catalytic activity and that holoenzyme isolated in the presence of 10 μM $ZnCl_2$ contains eight Zn^{2+}/octamer. The additional four binding sites are believed to be catalytically unimportant. Using $^{65}Zn^{2+}$ Gibbs and Jordan[97] have demonstrated that when only four zinc ions are bound per octamer, the enzyme is half active and that eight zinc ions are necessary for full catalytic activity.

Zinc has also been shown to activate the enzyme *in vivo* in humans[98] and to be essential for the *de novo* synthesis of the enzyme in fungi.[99] Cadmium displaces $^{65}Zn^{2+}$ from the enzyme more rapidly than nonlabelled zinc,[95] in keeping with the higher affinity of the enzyme for cadmium ions.[80] Substitution by ^{113}Cd ions at the zinc binding site yields an active enzyme with a single ^{113}Cd NMR resonance at 79.0 ppm. This signal is not affected by the addition of ALA, suggesting that the substrate is not interacting directly with the metal ion.[100]

Evidence from X-ray absorption spectroscopy[101] has revealed that zinc is ligated to three sulphur atoms. The stoichiometry of three sulphur ligands to Zn(II) concurs with the findings of Jaffe *et al* [96] that methylmethanethiosulphonate (MMTS) modification of ALA dehydratase at a stoichiometry of three per subunit results in

complete loss of the intrinsic Zn(II). The availability of the cDNA sequence from the human ALA dehydratase has provided the opportunity to examine the derived primary structure of the human enzyme and to suggest the possible location of these three sulphydryl groups.[102] A sequence is present close to the consensus zinc binding sites as deduced from sequences described in other zinc metalloenzymes.[103] This sequence contains four cysteine residues, two of which are the oxygen-sensitive groups responsible for the formation of the S-S bond. In addition, there are two histidine residues one of which is thought to interact with the zinc ion based on evidence from inactivation studies.[86] However, whether the putative metal binding site comprises these histidines is not known. The proposed metal-binding site sequence runs from residues 119 to 132 in the human enzyme with the four amino acids proposed as metal ligands indicated (x). This sequence is identical to that determined for the rat[104] and is similar to the primary protein structure derived from the *E. coli* gene sequence,[105] with all but one of the putative cysteine residues and both histidine residues conserved (*).

Human enzyme	C^x	D	V	C^x	L	C	P	Y	T	S	H^x	G	H	C^x	G
Rat enzyme	C	D*	V	C*	L	C*	P	Y*	T*	S*	H*	G*	H*	C*	G*
E. coli enzyme	S	D*	T	C*	F	C*	E	Y*	T*	S*	H*	G*	H*	C*	G*

The *E. coli* enzyme, if it is typical of other bacterial enzymes would also seem to have the metal binding site. The structural differences may, however, make a difference in the tightness of the metal binding which could account for the lack of EDTA inhibition

seen in the bacterial enzymes.

One of the most interesting properties of the mammalian ALA dehydratases is their reaction with and inactivation by lead ions. The activities of human[98] and rat[106] erythrocyte ALA dehydratases are inhibited by lead, both *in vivo* and *in vitro*, although, zinc is able to overcome this inhibition. Such is the sensitivity of the dehydratase to lead *in vivo*, that its activity has been used to monitor plasma lead levels in humans with lead poisoning.[107] One of the effects of lead poisoning,[108] which directly relates to the inhibition of the ALA dehydratase enzyme is the sharp rise of ALA in the blood[109-111] and the severe accompanying abdominal pain, peripheral neuropathy, hypertension and mental dysfunction caused by this compound. ALA has been shown to act as a 4-aminobutyric acid agonist and found to inhibit the activity of the mammalian spinal motor neurons probably *via* 4-aminobutyric acid inhibitory synapses.[112] The most obvious mechanism by which lead inhibits the mammalian dehydratases is thought to be by displacement of zinc. However, recent studies[97] have shown that lead completely inactivates the $^{65}Zn^{2+}$ labelled human enzyme, but that only half the radioactivity is displaced from the enzyme. These findings suggest that either half-site reactivity is involved or that zinc and lead may interact with the human enzyme at more than one site.[113] It is also possible that binding of lead to only half the subunits in the octamer, may cause a confirmational change which accounts for the loss of all the activity.

There are three other diseases in which large amounts of ALA are produced and excreted in the urine with clinical features resembling those of lead poisoning; hereditary tyrosinaemia,[114] plumboporphyria[115] and acute intermittent porphyria.[116]

Hereditary tyrosinaemia is an autosomal recessive inborn error of metabolism due to a deficiency of 4-fumarylacetate hydrolase.[117] As a result, the metabolite, succinylacetone (4,6-dioxoheptanoic acid) accumulates. Succinylacetone is an extremely potent competitive inhibitor of ALA dehydratase[118] and in hereditary tyrosinaemia, both plasma concentration and urinary excretion of ALA are increased. The porphyrias are a heterogeneous group of inherited disorders that have been linked to enzymatic defects in the haem biosynthetic pathway.[119-121] These disorders range from mild photosensitivity to severe mutilating sun sensitivity and from mild abdominal pain to life threatening hepatic failure. There are however no dermatological manifestations in acute intermittent porphyria. Plumboporphyria is the result of an inherent defect in ALA dehydratase and acute intermittent porphyria is caused by a defect in PBG deaminase, the next enzyme in the haem biosynthetic pathway.

1.6.2. Current knowledge of the ALA dehydratase reaction.

The ALA dehydratase reaction proceeds *via* a Schiff base intermediate[122] formed between one molecule of ALA and an active group on the enzyme. The enzymic group involved with the binding of ALA to the enzyme from *Rhodopseudomonas spheroids* [123] and from human erythrocytes[124] has been identified as the ε-amino group of a lysine residue.

The Schiff base forms between the enzyme and C_4 of the first ALA which binds to its active site.[125,126] Labelling studies with [5-^{13}C]ALA and [5-^{14}C]ALA, have demonstrated that this ALA becomes the P-side of PBG in the case of the bovine liver[125] and the human red blood cell enzyme[126] respectively [(*) in Scheme 1.6].

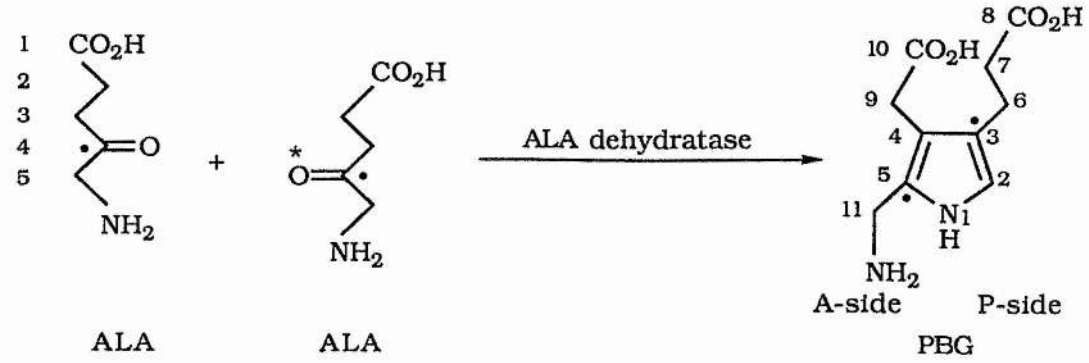

Scheme 1.6 Formation of [3,5-^{13}C]PBG from [4-^{13}C]ALA. * denotes the site of P-side Schiff base formation; • denotes ^{13}C labelled positions.

The C_5 proton of P-side ALA is extracted from the *pro*-R position.[127,128] Octameric enzyme requires four Zn(II) for full catalytic activity.[74,96] Schiff base trapping studies indicate four active sites per octamer or eight sites with strong negative cooperativity,[129] though others have presented data to support eight active sites per octamer.[86,97] Modification of ALA dehydratase with the small reversible sulfhydryl reagent, MMTS, introduced by Smith *et al*,[130] forms a protein that is completely inactive toward PBG production, is free of Zn(II), is highly stable and can be fully reactivated by the addition of 2-mercaptoethanol and Zn(II) or Cd(II).[96] MMTS modified enzyme forms the Schiff base intermediate,[129] but cannot bind A-side ALA and cannot therefore catalyse PBG formation. Thus, the formation of a Schiff base between P-side ALA and the active site lysine residue requires neither Zn(II) nor reduced enzyme sulfhydryl group. Recently, Jaffe and Markham[131,132] have shown that for the complex formed from [4-^{13}C]ALA and/or [5-^{13}C]ALA and MMTS modified ALA dehydratase, the predominant species is a Schiff base adduct, with C_5 of ALA *trans* to the lysine methylene and the protonation of the two nitrogens opposite, as shown in Fig. 1.4.

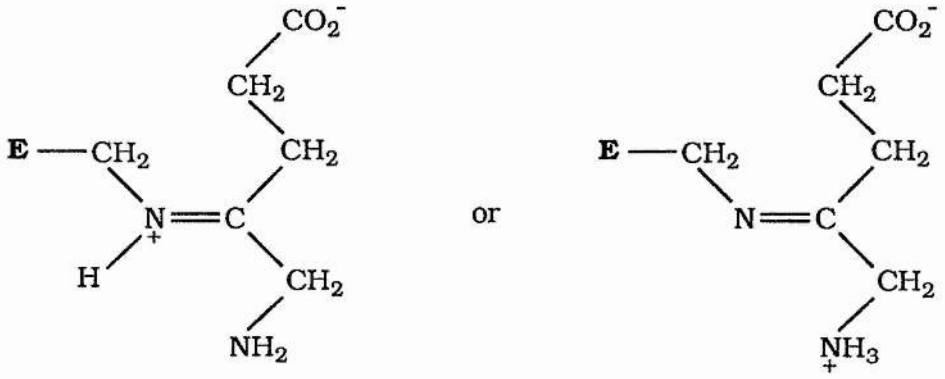

Figure 1.4 Stereochemistry and possible protonation states of the P-side Schiff base intermediate; **E** = enzyme.

The ^{13}C chemical shift[133] of the complex formed between [3,3-^{2}H,3-^{13}C]ALA and MMTS modified ALA dehydratase has confirmed the *E* stereochemistry of the imine double bond. By comparison with model imines[133] formed between [^{15}N]ALA and hydrazine and hydroxylamine, the ^{15}N chemical shift of the Schiff base adduct formed between [^{15}N]ALA and MMTS modified ALA dehydratase, suggests that the amino group is in an environment resembling partial deprotonation. Deprotonation of the amino group would facilitate formation of a Schiff base between the amino group of the enzyme-bound Schiff base and C_4 of the second ALA substrate. This is the first evidence supporting carbon-nitrogen bond formation as the initial site of interaction between the two ALA substrate molecules.

The numerous reports on half-site reactivity need to be further studied. Half the subunits of the bovine dehydratase are modified on reduction with borohydride in the presence of [4-^{14}C]ALA, suggesting that half-site reactivity may be operative.[81,129] Studies[88] with the active-site-directed reagent, 5-chlorolevulinic acid have also revealed an element of half-site reactivity. Aspects of half-site reactivity of ALA dehydratases have

been discussed in detail elsewhere.[80]

Studies of dissociation and rehybridisation of bovine liver ALA dehydratase attached to Sepharose suggested that dimer formation was necessary for PBG formation.[134] It was therefore suggested that one ALA reacts with one type of subunit to form a Schiff base and another ALA is bound non-covalently to a second type of subunit, which maybe of similar composition to the subunit that binds ALA by Schiff base formation.[135] The proof of this hypothesis would lie in establishing the non-identity of the subunits. Wu *et al*[83] rigorously demonstrated that bovine liver ALA dehydratase was an octamer composed of eight subunits which were indistinguishable by sedimentation equilibrium in 6 M guanidine hydrochloride or by polyacrylamide gel electrophoresis in the presence of sodium dodecyl sulphate. Investigations of subunit composition by primary sequence analysis of bovine liver ALA dehydratase by Hohberger[136] revealed that the NH_2-terminal sequences were blocked and that the number of peptides on tryptic digest was equal to that predicted by the amino acid composition. However there exists an intriguing report that only half of the NH_2-terminal residues of the bovine enzyme are acylated, suggesting a subtle difference in subunit structure.[137]

An alternative concept of the active site would not necessarily involve adjacent alignment of two ALA binding sites on separate subunits, but rather, the formation of PBG at a site within individual subunits. Thus differences in opinion exist concerning the nature of the active site (requiring half alignment on adjacent subunits or total site within subunits) and the number of active sites (four versus eight).

The enzyme groups from mammalian sources responsible for

catalysis have not been identified with any certainty with the exception of the active site lysine[124] (K252 in the human and rat enzymes and K247 in the *E. coli* enzyme). Photoinactivation studies by Tsukamato *et al*[86] have also implicated two histidines. They subsequently demonstrated the presence of two conserved histidines at the likely zinc binding site, one of which appears to be involved as a catalytic group.[87] A close study of the gene and cDNA-derived protein sequences reveal several potential catalytic residues in areas of high conservation. The wealth of knowledge emanating from molecular biology studies suggest that many of the above questions will soon be answered.

Information on the following stages in the biosynthesis of haem, chlorophylls and corrins is available in comprehensive accounts.[134-139]

References.

1. H. Fischer and H. Orth, 'Die Chemie des Pyrrols', Vol. I, p. 327, Akad. Verlagsges., Leipzig, 1934.
2. H. Fischer and H. Orth, 'Die Chemie des Pyrrols', Vol. II, Part 1, Akad. Verlagsges., Leipzig, 1937.
3. H. Fischer and A. Stern, 'Die Chemie des Pyrrols', Vol. II, Part 2, Akad. Verlagsges., Leipzig, 1940.
4. IUPAC/IUB, *Eur. J. Biochem.*, 1980, **108**, 1.
5. G. S. Marks, 'Heme and Chlorophyll - Chemical, Biochemical and Medicinal Aspects', Van Nostrand Rheinhold, Princeton, New Jersey, 1969.
6. K. M. Smith (ed.), 'Porphyrins and Metalloporphyrins', p. 3, Elsevier, New York, 1975.
7. D. Dolphin (ed.), 'The Porphyrins', 7 volumes, Academic Press, New York, 1979.
8. J. E. Falk, R. Lemberg and R. K. Morton, (eds.), 'Haematin Enzymes', 2 volumes, Pergamon Press, New York, 1961.
9. J. E. Falk (ed.), 'Porphyrins and Metalloporphyrins', Elsevier, New York, 1964.
10. A. D. Adler (ed.), *Ann. N. Y. Acad. Sci.*, 1973, **206**, 1.
11. S. L. Miller, *Ann. N. Y. Acad. Sci.*, 1957, **69**, 260.
12. G. W. Hodgson and B. L. Baker, *Nature*, 1967, **216**, 29.
13. C. I. Simionescu, R. Mora and B. C. Simionescu, *Bioelectrochem. Bioenerget.*, 1975, **5**, 1.
14. C. I. Simionescu, B. C. Simionescu, R. Mora and L. Keanca, *Orig. Life*, 1978, **9**, 103.
15. J. A. Mercer-Smith and D. C. Mauzerall, *Photochem. Photobiol.*, 1984, **39**, 397.

16. J. A. Mercer-Smith, A. Raudino and D. C. Mauzerall, *Photochem. Photobiol.*, 1985, **42**, 239.

17. R. Bonnett and F. Czechowski, *J. Chem. Soc., Perkin Trans. 1*, 1984, 125.

18. G. W. Hodgson, *Ann. N. Y. Acad. Sci.*, 1972, **194**, 86.

19. G. H. Tait, *in* 'Heme and Hemoproteins', (F. De Matteis and W. N. Aldridge, eds.), p. 1, Springer-Verlag, Berlin, 1978.

20. D. Shemin and D. Rittenberg, *J. Biol. Chem.*, 1945, **159**, 567.

21. D. Shemin, I. M. London and D. Rittenberg, *J. Biol. Chem.*, 1950, **83**, 757.

22. H. M. Muir and A. Neuberger, *Biochem. J.*, 1950, **47**, 97.

23. D. Shemin and J. Wittenberg, *J. Biol. Chem.*, 1951, **192**, 315.

24. K. D. Gibson, W. G. Laver and A. Neuberger, *Biochem. J.*, 1958, **70**, 71.

25. D. Shemin and C. S. Russell, *J. Am. Chem. Soc.*, 1953, **75**, 4873.

26. D. Shemin, C. S. Russell and T. Abramsky, *J. Am. Chem. Soc.*, 1955, **215**, 613.

27. R. G. Westall, *Nature*, 1952, **170**, 614.

28. O. Kennard, *Nature*, 1953, **171**, 876.

29. J. E. Falk, E. I. B. Dresel and C. Rimington, *Nature*, 1953, **172**, 292.

30. R. Schmid and D. Shemin, *J. Am. Chem. Soc.*, 1955, **77**, 506.

31. K. D. Gibson, A. Neuberger and J. J. Scott, *Biochem. J.*, 1955, **61**, 618.

32. G. Kikuchi, A. Kumar, P. Talmage and D. Shemin, *J. Biol. Chem.*, 1958, **233**, 1214.

33. G. R. Warnick and B. F. Burnham, *J. Biol. Chem.*, 1971, **146**, 6880.

34. A. Ohashi and G. Kikuchi, *J. Biochem.*, 1979, **85**, 239.

35. I. A. Borthwick, G. Srivastava, J. D. Brooker, B. K. May and W. H. Elliot, *Eur. J. Biochem.*, 1983, **129**, 615.

36. V. Dzelzkalns, T. Foley and S. I. Beale, *Arch. Biochem. Biophys.*, 1982, **216**, 196.

37. C. Volland and F. Felix, *Eur. J. Biochem.*, 1984, **142**, 551.

38. I. A. Borthwick, G. Srivastava, A. R. Day, B. A. Pirola, M. A. Snoswell, B. K. May, and W. H. Elliot, *Eur. J. Biochem.*, 1985, **150**, 481.

39. D. Urban-Grimal, C. Volland, T. Garnier, P. Dehoux and R. Labbe-Bois, *Eur. J. Biochem.*, 1986, **156**, 511.

40. A. Neuberger, J. D. Sandy and G. H. Tait, *Biochem. J.*, 1973, **136**, 477.

41. P. M. Jordan and D. Shemin, *in* 'The Enzymes', (P. D. Boyer, ed.), 3rd ed., Vol. 7, p. 339, Academic Press, New York, 1972.

42. G. R. Warnick and B. F. Burnham, *J. Biol. Chem.*, 1971, **246**, 6880.

43. M. Fanica-Gaignier and J. Clement-Metral, *Eur. J. Biochem.*, 1973, **40**, 19.

44. P. M. Jordan and A. Laghai, (unpublished observations).

45. E. E. Snell and S. diMari, *in* 'The Enzymes', (P. D. Boyer, ed.), 3rd ed., Vol. 2, p. 335, Academic Press, New York, 1970.

46. M. Akhtar and P. M. Jordan, *J. Chem. Soc., Chem. Commun.*, 1968, 1691.

47. Z. Zaman, P. M. Jordan and M. Akhtar, *Biochem. J.*, 1973, **135**, 257.

48. A. Laghai and P. M. Jordan, *Biochem. Soc. Trans.*, 1976, **4**, 52.

49. M. M. Abboud, P. M. Jordan and M. Akhtar *J. Chem. Soc., Chem. Commun.*, 1974, 1691.

50. A. Laghai and P. M. Jordan, *Biochem. Soc. Trans.*, 1977, **5**, 299.

51. S. I. Beale and P. A. Castelfranco, *Plant Physiol.*, 1974, **53**, 291.

52. S. I. Beale, S. P. Gough and S. Granick, *Proc. Nat. Acad. Sci. U.S.A.*, 1975, **72**, 2717.

53. S. I. Beale, *in* 'Chloroplast Biogenesis', (N. R. Baker and J. Barber, eds.), p. 133, Elsevier, Amsterdam, 1984.

54. S. P. Gough and C. G. Kannangara, *Calsberg Res. Commun.*, 1977, **42**, 459.

55. S. M. Mayer, J. D. Weinstein and S. I. Beale, *J. Biol. Chem.*, 1987, **262**, 12541.

56. W.-Y. Wang, D.-D. Huang, D. Strachan, S. P. Gough and C. G. Kannangara, *Plant Physiol.*, 1984, **74**, 569.

57. J. D. Weinstein and S. I. Beale, *Arch. Biochem. Biophys.*, 1985, **239**, 87.

58. J. D. Weinstein, S. M. Mayer and S. I. Beale, *in* 'Regulation of Chloroplast Differentiation', (G. Akoyunoglou and H. Senger, eds.), p. 43, A. R. Liss, New York, 1986.

59. S. Rieble and S. I. Beale, *J. Biol. Chem.*, 1988, **263**, 8864.

60. S. Rieble, J. G. Ormerod and S. I. Beale, *Plant Physiol.*, 1988, **86S**: 60.

61. W.-Y. Wang, S. P. Gough and C. G. Kannangara, *Calsberg Res. Commun.*, 1981, **46**, 243.

62. C. G. Kannangara, S. P. Gough, R. P. Oliver and S. K. Rasmussen, *Calsberg Res. Commun.*, 1984, **49**, 417.

63. A. Schon, G. Krupp, S. P. Gough, S. Berry-Lowe, C. G. Kannangara and D. Soll, *Nature*, 1986, **322**, 281.

64. D.-D. Huang and W.-Y. Wang, *J. Biol. Chem.*, 1986, **261**, 13451.

65. P. Bruyant and C. G. Kannangara, *Calsberg Res. Commun.*, 1987, **52**, 99.

66. G. Houen, S. P. Gough and C. G. Kannangara, *Calsberg Res. Commun.*, 1983, **48**, 567.

67. J. K. Hoober, A. Kahn, D. Ash, S. Gough and C. G. Kannangara, *Calsberg Res. Commun.*, 1988, **53**, 11.

68. P. M. Jordan, R. P. Sharma and M. J. Warren, (unpublished observations).

69. Y.-H. L. Mau and W.-Y. Wang, *Plant Physiol.*, 1988, **86**, 793.

70. L. Varticovski, J. P. Kushner, and B. F. Burnham, *J. Biol. Chem.*, 1980, **355**, 3742.

71. K. A. Morton, J. P. Kushner, J. G. Straka and B. F. Burnham, *J. Clin. Invest.*, 1983, **71**, 1744.

72. R. M. Anderson and R. J. Desnick, *J. Biol. Chem.*, 1979, **254**, 6924.

73. P. N. B. Gibbs, A. G. Chaudhry and P. M. Jordan, *Biochem. J.*, 1985, **230**, 25.

74. D. R. Bevan, P. Bodlaender and D. Shemin, *J. Biol. Chem.*, 1980, **255**, 2030.

75. P. M. Jordan and J. S. Seehra, *Methods Enzymol.*, 1986, **123**, 427.

76. O. L. Clara de Barriero, *Biochim. Biophys. Acta*, 1967, **139**, 479.

77. W. Leidgens, C. Lutz and H. A. W. Schneider, *Eur. J. Biochem.*, 1983, **135**, 75.

78. D. L. Nandi, K. F. Baker-Cohen and D. Shemin, *J. Biol. Chem.*, 1968, **243**, 1224.

79. D. Shemin, *in* 'The Enzymes', (P. D. Boyer, ed.), 3rd ed., Vol. 7, p. 323, Academic Press, New York, 1972.

80. A. M. Cheh and J. B. Neilands, *Struct. Bonding*, 1976, **29**, 123.

81. D. Shemin, *Phil. Trans. R. Soc. Lond. B.*, 1976, **273**, 109.

82. D. Gurne, J. Chen and D. Shemin, *Proc. Nat. Acad. Sci. U.S.A.*, 1977, **74**, 1383.

83. W. Wu, D. Shemin, K. E. Richards and R. C. Williams, *Proc. Nat. Acad. Sci. U.S.A.*, 1974, **69**, 2585.

84. P. M. Jordan and A. G. Chaudhry, (unpublished observations).

85. G. F. Barnard, R. Itoh, L. H. Hohberger and D. Shemin, *J. Biol. Chem.*, 1977, **252**, 8965.

86. I. Tsukamato, T. Yoshinaga and S. Sano, *Biochim. Biophys. Acta*, 1979, **570**, 167.

87. I. Tsukamato, T. Yoshinaga and S. Sano, *Int. J. Biochem.*, 1980, **12**, 751.

88. J. S. Seehra and P. M. Jordan, *Eur. J. Biochem.*, 1981, **113**, 435.

89. A. M. del C. Batlle, A. M. Ferramola and M. Grinstein, *Biochem. J.*, 1967, **104**, 244.

90. P. M. Jordan and M. G. Gore, (unpublished observations).

91. E. L. Wilson, P. E. Burger and E. B. Dowdle, *Eur. J. Biochem.*, 1972, **29**, 563.

92. A. G. Chaudhry, M. G. Gore and P. M. Jordan, *Biochem. Soc. Trans.*, 1976, **4**, 301.

93. P. M. Jordan, M. G. Gore and A. G. Chaudhry, *Biochem. Soc. Trans.*, 1976, **4**, 762.

94. J. S. Seehra, M. G. Gore, A. G. Chaudhry and P. M. Jordan, *Eur. J. Biochem.*, 1981, **114**, 263.

95. P. N. B. Gibbs and P. M. Jordan, *Biochem. Soc. Trans.*, 1981, **9**, 232.

96. E. K. Jaffe, S. P. Salowe, N. T. Chen and P. A. DeHaven, *J. Biol. Chem.*, 1984, **259**, 5032.

97. P. N. B. Gibbs and P. M. Jordan, (unpublished observations).

98. P. A. Meredith and M. R. Moore, *Biochem. Soc. Trans.*, 1980, **6**, 760.

99. H. Komai and J. B. Neilands, *Arch. Biochem. Biophys.*, 1968, **124**, 456.

100. R. Sommer and D. Beyersmann, *J. Inorg. Biochem.*, 1984, **20**, 131.

101. S. S. Hasnain, E. M. Wardell, C. D. Garner, M. Schlosser and D. Bayersmann, *Biochem. J.*, 1985, **230**, 625.

102. J. G. Wetmer, D. F. Bishop, C. Cantelmo and R. J. Desnick, *Proc. Nat. Acad. Sci. U.S.A.*, 1986, **83**, 7703.

103. M. Kozak, *Nucl. Acids Res.*, 1984, **12**, 857.

104. T. R. Bishop, L. P. Frelin and S. H. Boyer, *Nucl. Acids Res.*, 1986, **14**, 10115.

105. Y. Echelard, J. Dymetryszyn, M. Drolet and A. Sasarman, *Mol. Gen. Genet.*, 1988, **214**, 503.

106. V. N. Vinelli, D. S. Klauder, M. A. Karaffa and H. G. Petering, *Biochem. Biophys. Res. Commun.*, 1975, **65**, 303.

107. J. J. Chisholm, *Sci. Amer.*, 1971, **224**, 15.

108. M. R. Moore and A. Goldberg, *in* 'Dietary and Environmental Lead - Human Health Effects', (K. R. Mahaffey, ed.), p. 261, Elsevier, Amsterdam, 1985.

109. J. Gentz, S. Johansson, B. Lindblad, S. Lindstedt and R. Zetterstrom, *Clin. Chim. Acta*, 1969, **23**, 257.

110. M. R. Moore, P. A. Meredith and A. Goldberg, *in* 'Lead Toxicity', (R. D. Singhal and J. A. Thomas, eds.), p. 79, Urban and Schwartzenberg, Baltimore, 1980.

111. E. K. Silbergeld, R. E. Hruska, D. Bradley, J. M. Lamon and B. C. Frykholm, *Environ. Res.*, 1982, **29**, 459.

112. J. Bagust, P. M. Jordan, M. E. M. Kelley and G. A. Kerkut, *Neurosci. Lett.*, 1985, **21**, S84.

113. P. N. B. Gibbs, M. G. G. Gore and P. M. Jordan, *Biochem. J.*, 1985, **225**, 573.

114. M. G. Cutler, M. R. Moore and F. G. Ewart, *Psychopharmachology*, 1979, **61**, 131.

115. S. Thunell, L. Holmberg and J. Lundgren, *J. Clin. Chem., Clin. Biochem.*, 1987, **25**, 5.

116. A. Kappas, S. Sassa and K. E. Anderson, *in* 'The Metabolic Basis of Inherited Disease' (J. B. Stanbury, J. B. Wyngaarden, D. S. Fredrickson, J. J. Goldstein and M. S. Brown, eds.), 5th ed., McGraw-Hill, New York, 1963.

117. B. O. Lindblad, S. Lindstedt and G. Steen, *Proc. Nat. Acad. Sci. U.S.A.*, 1977, **74**, 4641.

118. S. Sassa and A. Kappas, *J. Clin. Invest.*, 1983, **71**, 625.

119. S. Sassa and A. Kappas, *in* 'Advances in Human Genetics', (H. Harns, ed.), Vol. 11, Plenum Press, New York, 1981.

120. G. H. Elder, *Sem. Liver Dis.*, (R. Schmid, ed.), 1982, **2**, 87.

121. C. Rimington, *Scand. J. Clin. Lab. Invest.*, 1985, **45**, 291.

122. D. L. Nandi and D. Shemin, *J. Biol. Chem.*, 1968, **243**, 1236.

123. D. L. Nandi, *Z. Naturforsch. C. Biosci.*, 1978, **33**, 799.

124. P. N. B. Gibbs and P. M. Jordan, *Biochem. J.*, 1986, **236**, 447.

125. P. M. Jordan and J. S. Seehra, *FEBS Lett.*, 1980, **114**, 283.

126. P. M. Jordan and P. N. B. Gibbs, *Biochem. J.*, 1985, **227**, 1015.

127. M. M. Abboud and M. Akhtar, *J. Chem. Soc., Chem. Commun.*, 1976, 1007.

128. A. G. Chaudhry and P. M. Jordan, *Biochem. Soc. Trans.*, 1976, **4**, 760.

129. E. K. Jaffe and D. Hanes, *J. Biol. Chem.*, 1986, **261**, 9348.

130. D. J. Smith, E. T. Maggio and G. L. Kenyon, *Biochemistry*, 1975, **14**, 766.

131. E. K. Jaffe and G. D. Markham, *Biochemistry*, 1987, **26**, 4258.

132. E. K. Jaffe and G. D. Markham, *Biochemistry*, 1988, **27**, 4475.

133. E. K. Jaffe, G. D. Markham and J. S. Rajagopalan, *Biochemistry*, 1990, **29**, 8345.

134. A. M. del C. Battle, A. M. Stella, A. M. Ferramola. Y. Sopena, E. Wider de Xifrae and H. A. Sancovich, *Int. J. Biochem.*, 1978, **9**, 401.

135. A. M. del C. Battle and A. M. Stella, *Int. J. Biochem.*, 1978, **9**, 861.

136. L. H. Hohberger, Ph.D. dissertation, Northwestern University, 1979.

137. B. Lingner and T. Kleinschmidt, *Z. Naturforsch. C. Biosci.*, 1983, **38**, 1059.

138. A. R. Battersby and E. McDonald, *in* 'Porphyrins and Metalloporphyrins', (K. M. Smith, ed.), p. 61, Elsevier, New York, 1975.

139. D. Dolphin (ed.), 'The Porphyrins', Vol. 6, Academic Press, New York, 1979.

140. S. Granick and S. I. Beale, *Adv. Enzymol.*, 1978, **46**, 33.

141. M. Akhtar and P. M. Jordan, *in* 'Comprehensive Organic Chemistry', (E. Haslam, ed.), Vol. 5, p. 1121, Pergamon Press, New York, 1979.

142. F. J. Leeper, *Nat. Prod. Rep.*, 1985, **2**, 19.

143. H. A. Dailey (ed.), 'Biosynthesis of Heme and Chlorophylls', McGraw-Hill, New York, 1990.

CHAPTER TWO

SYNTHESES OF [4-^{13}C]ALA.HCl AND [^{15}N]ALA.HCl

2.1 Introduction.

The dimerisation of ALA to form PBG by the action of the enzyme ALA dehydratase, is the second committed step in the haem metabolic pathway[1] and is also one which has been least investigated. As illustrated in Scheme 2.1, one molecule of ALA forms the P (propionyl) side of PBG with its amino nitrogen being incorporated into the pyrrole ring, and the second molecule of ALA forms the A (acetyl) side of PBG retaining its free amino group. The overall reaction must involve a number of bond making and bond breaking steps, some of which may be catalysed and some not. The characterisation of each of these stages is essential if one is to understand the enzyme mechanism at the molecular level.

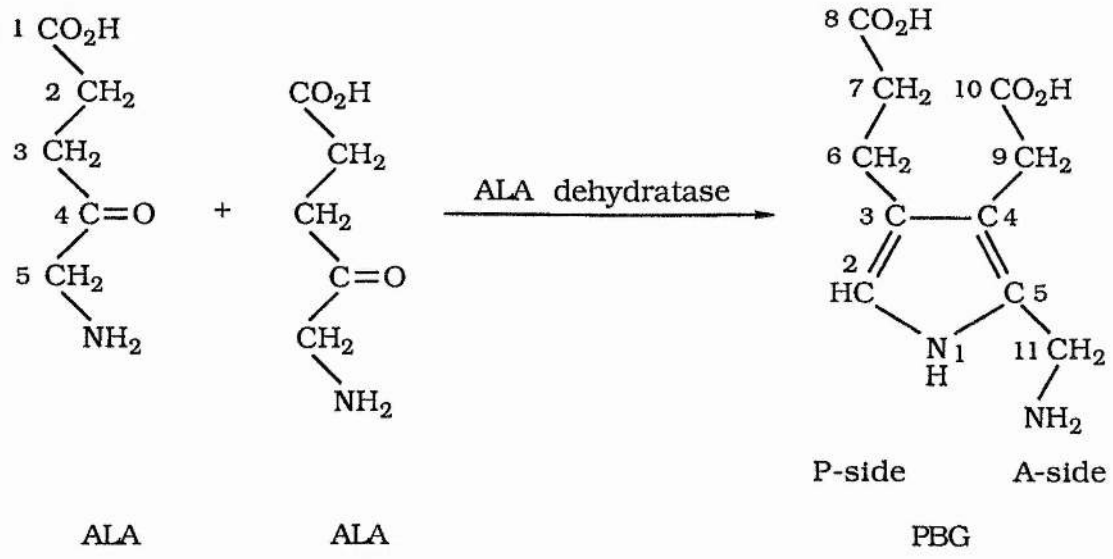

Scheme 2.1 ALA dehydratase catalysed dimerisation of ALA to form PBG.

Implicit to the understanding of the catalytic events which occur at the active site of ALA dehydratase, is a knowledge of the order in which the two molecules of ALA bind to the enzyme prior to condensation. Steady state kinetics[2] can often provide this information and can also provide evidence for the participation of

covalent intermediates. In the case of ALA dehydratase, steady state kinetics cannot be employed, since the two substrate molecules are identical and therefore in kinetic terms cannot be evaluated independently.

An alternative strategy however, is the use of high field NMR involving a single-turnover enzyme approach, in which the two substrate molecules which participate in the reaction are distinguished from one another by isotopic labelling. Jordan and Seehra[3] have used this approach, to establish that the molecule of ALA bound to the enzyme in the form of a Schiff base is the one which becomes the P-side of PBG.

Because of its non-intrusive nature, high resolution NMR has long been recognised as a potential probe of the active site chemistry of enzyme catalysed reactions. MacKenzie *et al* [4] predict a promising future for the use of ^{13}C NMR to study enzyme-substrate complexes below 50,000 daltons, using cryosolvents to prolong the lifetime of enzyme-bound intermediates. ^{13}C and ^{15}N NMR, as probes of enzyme catalysed reactions, suffer from the natural 1.1% and 0.37% abundances of ^{13}C and ^{15}N respectively. The low natural abundances of ^{13}C and ^{15}N therefore dictates the synthesis of ALA enriched at specific sites with carbon-13 and nitrogen-15, for its use in mechanistic studies.

Jaffe *et al* have recently reported ^{13}C NMR studies of [4-^{13}C] ALA (90% enriched)[5] and [5,5-^{2}H, 5-^{13}C]ALA (99% enriched)[6] bound to the 280,000 dalton protein, ALA dehydratase, as well as ^{13}C and ^{15}N NMR studies[7] of [3,3-^{2}H, 3-^{13}C]ALA (99% enriched) and [^{15}N]ALA (95% enriched) bound to ALA dehydratase. These studies have elucidated the structures of enzyme-bound product and a Schiff base intermediate.

ALA.HCl has been synthesised in several ways [8-33] and some of the routes have been used for the preparation of material labelled with nitrogen-15,[11-14] tritium at positions 2 and 3,[27] carbon-13 at positions 2[33] and 5,[32,33] and carbon-14 at positions 1,[26] 2,[26] 4,[16,25,28,30] and 5. [13,16,17,30] These different synthetic procedures are particularly useful when specific labelling at the various positions of ALA is needed.

For various aspects of our study, which will be explained in appropriate sections of the text, [^{15}N]ALA.HCl (50% enriched) and [4-^{13}C]ALA.HCl (50% enriched) were synthesised. From a survey of the above reported procedures, the method of Neuberger and Scott[12] was selected for the synthesis of [^{15}N]ALA.HCl (50%enriched) and a combination of the methods of Pichat and Herbert[16] and Tschudy and Collins[20] were adopted for the synthesis of [4-^{13}C]ALA.HCl (50% enriched).

Carbon-13 isotopic enrichment at the 4-position of ALA was chosen, because from a ^{13}C NMR perspective, the 4-position has several advantages. The carbonyl group at the 4-position of ALA becomes the aromatic carbons at C_3 and C_5 of PBG (Scheme 2.1). During this transformation, the carbonyl carbon must undergo large changes in bonding, subsequently leading to large changes in its ^{13}C chemical shift during the course of the reaction. Therefore, enzyme-bound substrate, possible reaction intermediates and product are anticipated to be readily distinguished from each other in the ^{13}C NMR spectrum. Furthermore, the enriched carbons of both substrate and product are quaternary carbons, thereby eliminating dipolar interactions with directly attached protons as a relaxation mechanism, leading to the prediction of relatively narrow lines (< 50 Hz).[34,35] This is true even for a totally

immobilised carbon bound to this large protein of 280,000 daltons.[36]

2.2 Experimental.

2.2.1 Materials.

Glycine (BDH), phthalic anhydride, sodium metal (Fisons), potassium hydroxide pellets, toluene (Fisons, analaR), diazald, potassium phthalimide, succinic anhydride, carbitol, *p*-cymene, diethylmalonate, dipentene, 48% hydrobromic acid, thionyl chloride (Aldrich), N,N-dimethylformamide (Lancaster Synthesis), absolute ethanol (Hayman, analaR), methylene chloride (Ellis and Everard), diethyl ether, glacial acetic acid, petroleum ether (60-80 °C) (Rhône Poulenc Ltd.) ethyl acetate and 37% hydrochloric acid (Rhône Poulenc Ltd., analaR) were used as received unless otherwise specified.

Molecular sieves Type 3A, 1-2 mm beads, were purchased from Lancaster Synthesis and molecular sieves Type 4A, 1/16 inch pellets, were purchased from Rhône Poulenc Ltd.

[^{15}N]glycine (99% enriched) and [2-^{13}C]glycine (99% enriched) were purchased from MSD Isotopes Inc., and used as received.

The deuteriated solvents for NMR were purchased from GOSS and used as received.

2.2.2 Instrumentation and General Techniques.

A. Melting points.

Routine melting points were determined with open glass capillaries using an Electrothermal melting point apparatus and were uncorrected.

B. Elemental Analysis.

Elemental analyses were performed with a Carlo-Erba Instrumentazione model 1106 CHN analyser.

C. Mass Spectrometry.

Mass spectra were recorded on a Finnigan MAT INCOS 50 mass spectrometer. Fragment ions are indicated as m/z units with relative intensities (%) in parentheses.

D. NMR Spectroscopy.

^{1}H NMR spectra were obtained at 300.134 MHz on a Bruker AM 300 spectrometer using 32 K data points. Unless otherwise specified, ^{1}H spectra were acquired at room temperature, using a pulse width of 2.5 μs (8.5 μs for a 90° flip angle), a recycle time of 5.2 s and a spectral width of 4500 Hz.

^{13}C NMR spectra were obtained at 75.469 MHz on a Bruker AM 300 spectrometer using 32 K data points. Unless otherwise specified, ^{13}C spectra were acquired at room temperature, using a pulse width of 2.0 μs (3.9 μs for a 90° flip angle), a recycle time of 2.3 s and a spectral width of 20,000 Hz. All ^{13}C NMR spectra were ^{1}H decoupled.

Unless otherwise specified, chemical shifts (δ) for ^{1}H and ^{13}C NMR spectra are reported in ppm downfield of TMS (δ = 0) [or DSS (δ = 0) in the case of aqueous solutions] as internal standard and coupling constants *J*, are given in Hz.

^{15}N NMR spectra were obtained at 30.412 MHz on a Bruker AM 300 spectrometer using 32 K data points. Unless otherwise specified, ^{15}N spectra were acquired at room temperature, using a pulse width of 6.5 μs (26 μs for a 90° flip angle), a recycle time of 1.7 s and a spectral width of 18518.52 Hz. All ^{15}N NMR spectra were ^{1}H decoupled and were referenced with respect to external

nitromethane (with 20% CD_3OD to provide the lock signal) set at δ 380.23.

E. Drying and purification of solvents.

Commercially available solvents were used without further purification unless otherwise indicated.

Dry DMF was prepared[37] by keeping the commercially available solvent in contact with molecular sieves Type 4A ($1/16$ inch pellets) for 48 hours in a dark bottle. The solvent was then distilled under nitrogen at reduced pressure. Heating was gentle and the temperature kept below 50 °C. The distillate (after discarding the first 20 ml), b.p. 48-50 °C/15 mmHg, was stored over molecular sieves Type 4A in a dark bottle.

Diethyl ether was purified[38] by shaking 500 ml of it in a large separatory funnel with 5 ml of a solution containing ferrous sulphate (6 g) and concentrated H_2SO_4 (6 ml) in water (110 ml). The aqueous solution was then removed, the ether washed with water and dried for 24 hours over $CaCl_2$ (50 g). It was then filtered and further dried by allowing it to stand over sodium wire in a dark bottle for 24 hours. The ether was then heated under reflux with sodium wire and distilled, b.p. 35 °C/760 mmHg.

Super-dry ethanol was prepared from the commercial absolute ethanol according to the method of Lund and Bjernum.[38] Magnesium turnings (5 g), iodine (0.5 g) and commercial absolute ethanol (50-75 ml) were placed in a 2 litre round-bottomed flask fitted with a double surface condenser and a calcium chloride guard tube. The reaction mixture was warmed until a vigorous evolution of hydrogen set in and the iodine disappeared. Heating was continued until all the magnesium was converted into magnesium ethoxide.

Commercial absolute ethanol (1 litre) was then added and the mixture refluxed for 30 minutes. The condenser was then reassembled for downward distillation and the ethanol gently distilled, b.p. 78 °C/760 mmHg, into a receiver flask containing molecular sieves Type 3A, after discarding the first 20 ml of the distillate. The super-dry ethanol was stored as such with the receiver flask well stoppered.

Thionyl chloride was purified[39] from impurities of sulphur chlorides and sulphuryl chlorides by the distillation of technical thionyl chloride (250 ml) with dipentene (23 ml). A thermometer was immersed to the bottom of the mixture and the distillation stopped when the temperature of the residual liquid reached 84-86 °C. The colourless material thus obtained was then redistilled b.p. 76.5 °C/760 mmHg and the distillate stored in a dark bottle.

Synthetic methanol was stored over molecular sieves Type 3A and used as such.

2.2.3 Synthesis of ALA.HCl from phthalic anhydride and glycine.

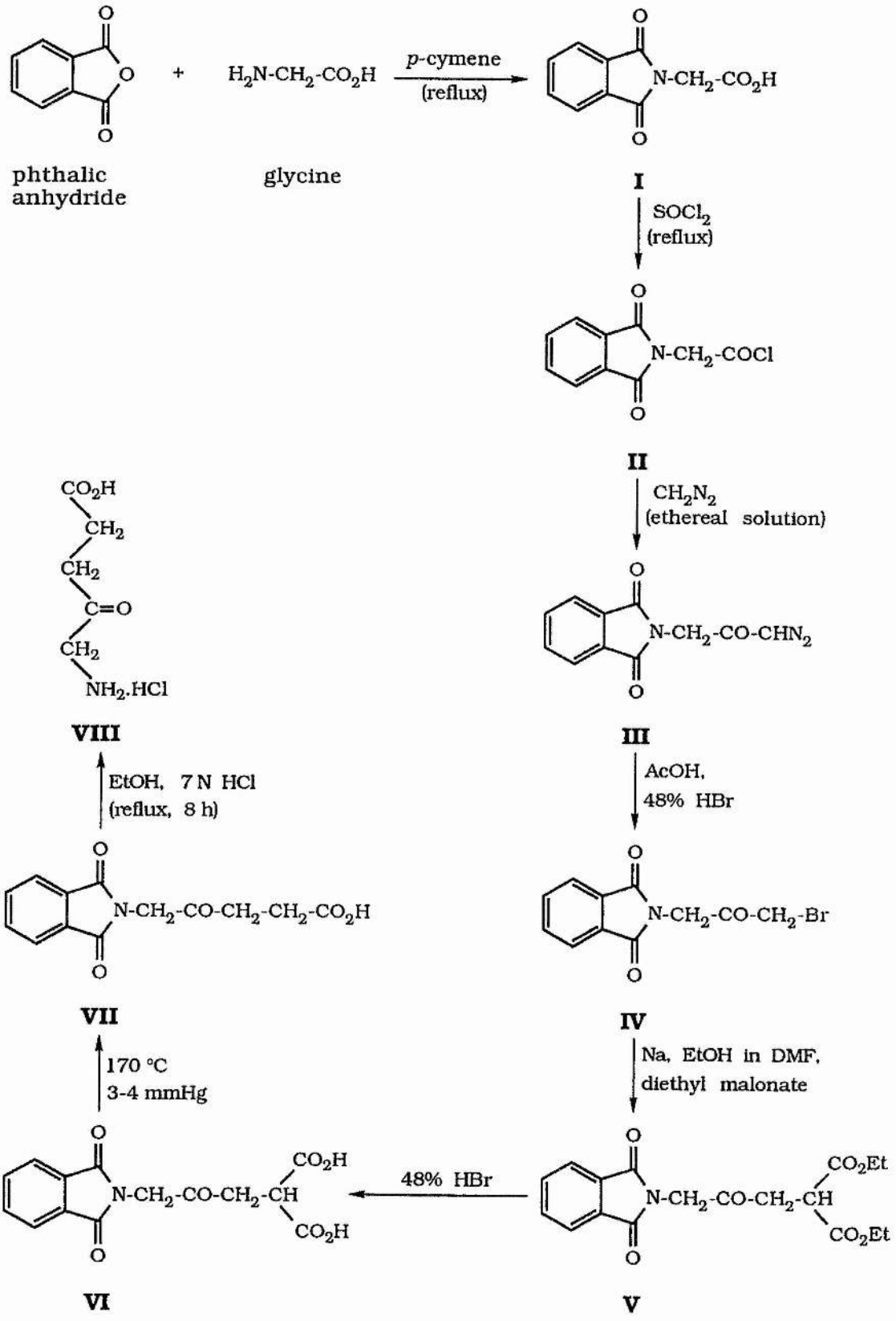

Scheme 2.2

2.2.3.1 Synthesis of N-phthaloylglycine (I).

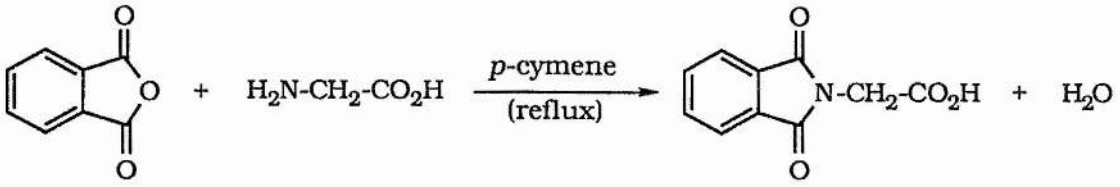

phthalic anhydride | glycine | N-phthaloylglycine

N-phthaloylglycine was prepared according to the method of O'Neill *et al*.[40] Phthalic anhydride (11.84 g, 0.08 mol) and glycine (6 g, 0.08 mol) were suspended in *p*-cymene (100 ml) and the mixture refluxed in an apparatus equipped with a Dean-Stark trap. When approximately 60% of the theoretical amount of water had collected, the *p*-cymene was removed by distillation under reduced pressure and the residue crystallised from aqueous ethanol. The product was obtained as white needles (14.0 g, 85.4%), after recrystallisation from aqueous ethanol, m.p. 192-193 °C. (lit.,[41] 191-192 °C) (Found: C, 58.1; H, 3.1; N, 6.7. $C_{10}H_7NO_4$ requires C, 58.5; H, 3.4; N, 6.8%); m/z 205 (M^+, 2%), 161 (64) 160 (M^+- CO_2H, 100), 147 (1), 133 (9), 119 (13), 104 (17), 77 (20), 76 (19), 66 (4), 50 (10), and 28 (30); δ_H [$(CD_3)_2C=O$] 4.44 (2 H, s, N*CH*$_2$) and 7.91 (4 H, m, Ar*H*); δ_C [$(CD_3)_2C=O$] 39.2, 124.1, 133.0, 135.4, 168.0 and 169.0.

2.2.3.2 Synthesis of N-phthaloylglycylchloride (II).

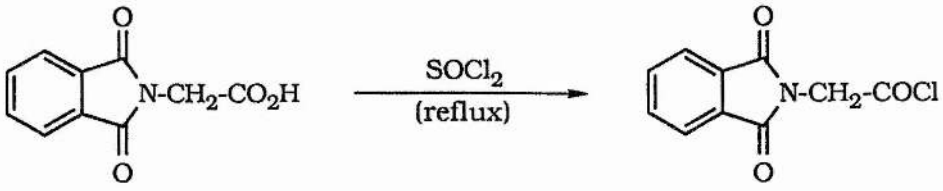

N-phthaloylglycine | N-phthaloylglycylchloride

N-phthaloylglycylchloride was prepared according to the method of Balenović *et al*.[42] N-phthaloylglycine (14.0 g, 0.068 mol) was refluxed with thionyl chloride (24.0 g, 0.2 mol) during one hour. After distillation of the unchanged thionyl chloride with added dry toluene at reduced pressure, the product was recrystallised from petroleum ether (b.p. 60-80 °C) (12.05 g, 79.3%) as pale yellow needles, m.p. 84 °C (lit.,[42] 84-85 °C) (Found: C, 54.0; H, 2.6; N, 6.2. $C_{10}H_6ClNO_3$ requires C, 53.7; H, 2.7; N, 6.3%); m/z 225 (M^++ 2, 3%), 223 (M^+, 9), 161 (73), 160 (100), 147 (2), 133 (31), 104 (72), 77 (67), 76 (77), 66 (60), 50 (58), 38 (25), and 28 (37); δ_H ($CDCl_3$) 4.83 (2 H, s, N*CH*$_2$), 7.80 (2 H, m, Ar*H*) and 7.92 (2 H, m, Ar*H*); δ_C ($CDCl_3$) 47.6, 124.0, 131.6, 134.7, 166.6 and 169.1.

2.2.3.3 Synthesis of 1-diazo-3-phthalimidopropan-2-one (III).

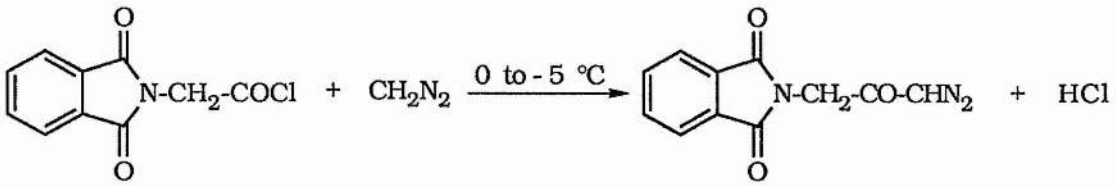

N-phthaloylglycyl-chloride

1-diazo-3-phthalimido-propan-2-one

1-diazo-3-phthalimidopropan-2-one was prepared according to the method of Balenović *et al*.[42] A solution of the recrystallised N-phthaloylglycylchloride (12.05 g, 0.054 mol) in anhydrous ether (400 ml) was gradually added to an ethereal solution (300 ml) of diazomethane (0.16 mol) (preparation described below) kept in an ice-salt mixture at 0 to -5 °C. Crystals of the diazoketone separated at once. After standing overnight, the crystals were filtered and recrystallised from ethyl acetate (10.57 g, 85.5%) as fine white

needles, m.p. 168 °C (dec.) [lit.,[42] 168 °C (dec.)] (Found: C, 57.6; H, 2.6; N, 18.1. $C_{11}H_7N_3O_3$ requires C, 57.65; H, 3.1; N, 18.3%); m/z 201 (M^+- N_2, 33%), 161 (29), 160 (100), 147 (3), 133 (9), 104 (23), 77 (27), 76 (30), 50 (18) and 28 (38); δ_H ($CDCl_3$) 4.44 (2 H, s, NCH_2), 5.40 (1 H, s, CHN_2), 7.75 (2 H, m, Ar*H*) and 7.89 (2 H, m, Ar*H*); δ_C ($CDCl_3$) 44.2, 53.8, 123.7, 132.0, 134.3, 167.6 and 186.5.

2.2.3.3.1 Synthesis of diazomethane.

An ethereal solution of diazomethane, free from ethanol is required in the above Arndt-Eistert reaction with N-phthaloyl-glycylchloride and was prepared by the method of DeBoer and Backer.[43]

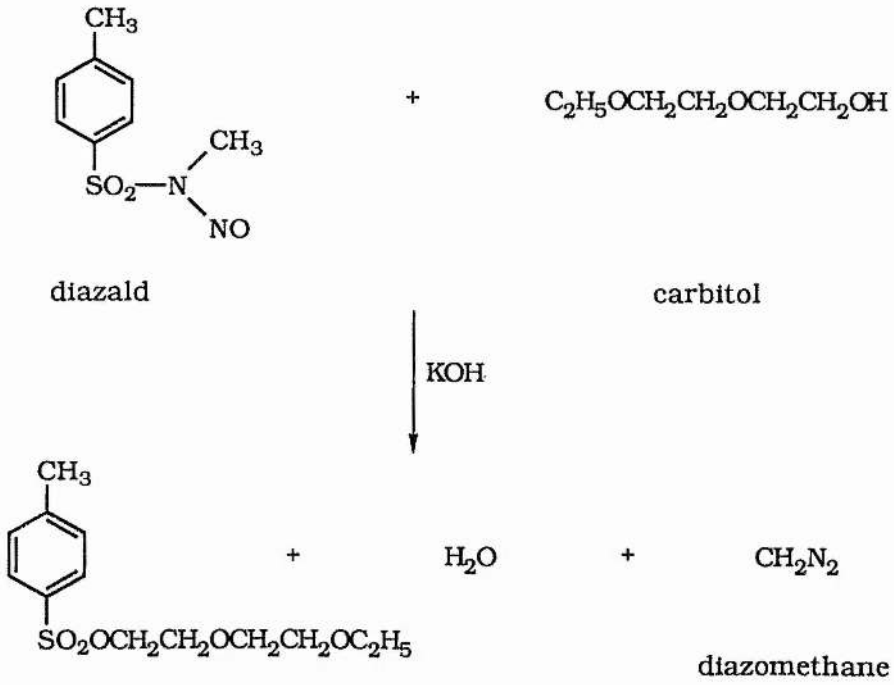

A conical flask with a side arm was fitted with a short length of plastic tubing, the other end of which passes below the surface of ether in a round bottomed flask which is placed in an ice-salt

mixture. In the conical flask were placed potassium hydroxide pellets (15.0 g, 0.27 mol) dissolved in water (25 ml), carbitol (88 ml), ether (25 ml) and the Teflon coated bar of a magnetic stirrer. The conical flask was heated in a water bath at 70-75 °C, the stirrer started and a solution of diazald (54.0 g, 0.25 mol) in ether (315 ml) added at a regular rate by means of a syringe, inserted into the stopper of the conical flask. As soon as all the diazald solution was added, additional ether was swirled in the beaker which contained the diazald solution and added to the conical flask, until the distillate was colourless. The ethereal solution of diazomethane was then dried over potassium hydroxide pellets for 3 hours, and contains approximately 64% diazomethane.[44]

2.2.3.4 Synthesis of 1-bromo-3-phthalimidopropan-2-one (IV).

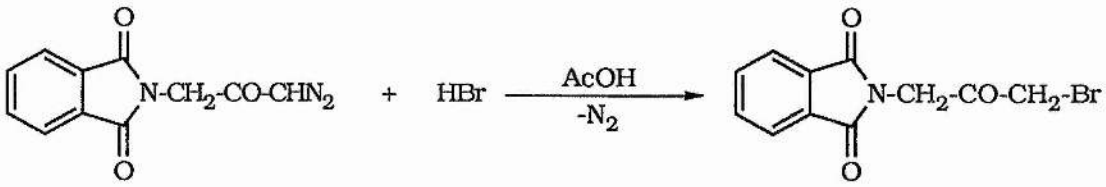

1-diazo-3-phthalimido-propan-2-one

1-bromo-3-phthalimido-propan-2-one

1-bromo-3-phthalimidopropan-2-one was prepared according to the method of Balenović and Bregant.[45] A suspension of 1-diazo-3-phthalimidopropan-2-one (10.57 g, 0.046 mol) in glacial acetic acid (57 ml) was treated with 48% HBr (11.5 ml). On stirring the reaction mixture, nitrogen evolution took place. After standing for 1 hour at room temperature, the reaction was complete. The mixture was then diluted with water (450 ml) and the crystals filtered off in a Buchner funnel and dried *in vacuo* over phosphorus pentoxide.

They were recrystallised from toluene (12.28 g, 94.7%) as fine white crystals, m.p. 147 °C (lit.,[46] 147-148 °C) (Found: C, 46.7; H, 2.6; N, 4.95. $C_{11}H_8BrNO_3$ requires C, 46.85; H, 2.9; N, 5.0%); m/z 283 (M^++ 2, 2%), 281 (M^+, 3), 202 (6), 161 (57), 160 (100), 147 (1), 133 (14), 104 (35), 77 (35), 76 (41), 50 (21) and 28 (15); δ_H [$(CD_3)_2C$=O] 4.47 (2 H, s, NCH_2), 4.84 (2 H, s, CH_2Br) and 7.91 (4 H, s, Ar*H*); δ_C [$(CD_3)_2C$=O] 33.1, 45.1, 124.1, 133.0, 135.4, 168.0 and 195.8.

2.2.3.5 Synthesis of ethyl 2-ethoxycarbonyl-5-phthalimido-levulinate (V).

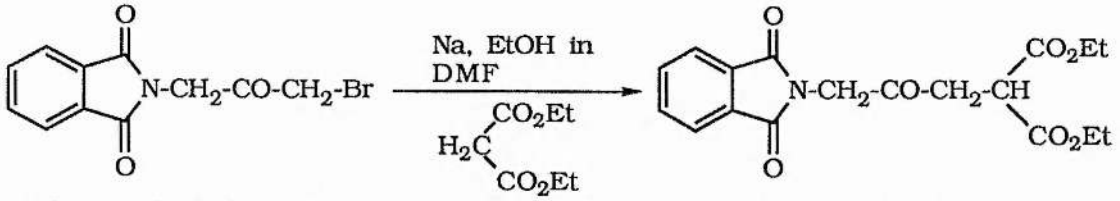

1-bromo-3-phthalimido-propan-2-one

ethyl 2-ethoxycarbonyl-5-phthalimidolevulinate

Ethyl 2-ethoxycarbonyl-5-phthalimidolevulinate was prepared according to the method Tschudy and Collins.[20] To a solution of sodium (1.06 g) in dry ethanol (24.5 ml), was added dry DMF (61.5 ml) and diethylmalonate (7.4 ml). After allowing this to stand for 15 minutes, a solution of 1-bromo-3-phthalimidopropan-2-one (12.28 g, 0.044 mol) in DMF (160 ml) was added. The temperature gradually rose to above room temperature. The mixture was allowed to stand overnight and then evaporated to dryness *in vacuo* . The residue was extracted with methylene chloride and the sodium bromide filtered off. The methylene chloride extract was evaporated *in vacuo* and the residual oil crystallised from a very large volume of petroleum ether (b.p. 60-80 °C). The product was

obtained as fine white crystals (6.24 g, 39.3%), m.p. 84 °C (lit.,[20] 84 °C) (Found: C, 59.8; H, 4.7; N, 3.9. $C_{18}H_{19}N_7$ requires C, 59.8; H, 5.3; N, 3.9%); m/z 361 (M^+, 0.3%), 316 (15), 270 (5), 242 (7), 202 (10), 201 (88), 173 (73), 161 (17), 160 (72), 147 (82), 133 (6), 127 (54), 104 (65), 77 (20), 76 (61), 50 (25) and 28 (100); δ_H ($CDCl_3$) 1.27 (6 H, t, *J* 7.17, 2 x CH_2CH_3), 3.15 (2 H, d, *J* 7.08, CH_2CH), 3.91 (1 H, t, *J* 7.24, CH_2CH) 4.21 (4 H, m, *J* 7.01, 2 x CH_2CH_3), 4.57 (2 H, s, NCH_2), 7.73 (2 H, m, Ar*H*) and 7.87 (2 H, m, Ar*H*); δ_C ($CDCl_3$) 14.0, 38.5, 46.4, 46.9, 61.9, 123.6, 132.1, 134.2, 167.4, 168.3 and 199.3.

2.2.3.6 Synthesis of 2-carboxy-5-phthalimidolevulinic acid (VI).

ethyl 2-ethoxycarbonyl-5-phthalimidolevulinate

2-carboxy-5-phthalimido-levulinic acid

2-carboxy-5-phthalimidolevulinic acid was prepared according to the method of Tschudy and Collins.[20] Ethyl 2-ethoxycarbonyl-5-phthalimidolevulinate (6.24 g, 0.017 mol) was suspended in 48% HBr (62 ml) and allowed to stand at room temperature overnight. It was then heated on a steam bath until all the compound dissolved. The solution was allowed to cool and then evaporated to dryness *in vacuo*. The residue was recrystallised from water, (3.42 g, 66%) as fine white crystals, m.p. 171 °C (lit.,[20] 171-172 °C) (Found: C, 54.7; H, 3.75; N, 4.4. $C_{14}H_{11}NO_7$ requires C, 55.1; H, 3.6; N, 4.6%); m/z 305 (M^+, 5%), 215 (7), 202 (5), 189 (23), 161 (100), 160 (98), 133 (25), 117 (43), 104 (38), 103 (19),

76 (47), 50 (18), 45 (60). δ_H [$(CD_3)_2C$=O] 3.29 (2 H, d, *J* 8.04, CH_2CH), 3.90 (1 H, t, *J* 8.04, CH_2CH), 4.70 (2 H, s, NCH_2) and 7.90 (4 H, s, Ar*H*); δ_C [$(CD_3)_2C$=O] 39.3, 47.0, 47.1, 124.0, 133.0, 135.3, 168.1, 170.1 and 201.2.

2.2.3.7 Synthesis of 5-phthalimidolevulinic acid (VII).

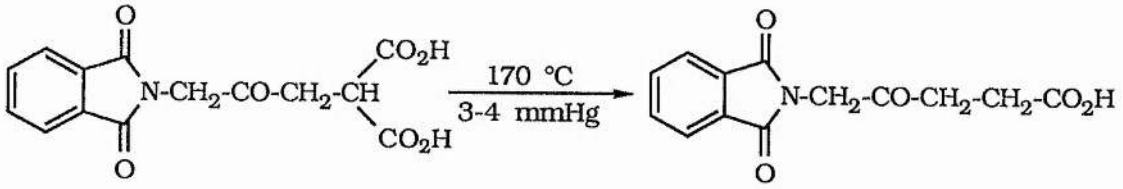

2-carboxy-5-phthalimido-levulinic acid

5-phthalimidolevulinic acid

5-phthalimidolevulinic acid was prepared according to the method of Tschudy and Collins.[20] 2-Carboxy-5-phthalimidolevulinic acid (3.42 g, 0.011 mol) was heated to 170 °C at a pressure of 3 to 4 mmHg until the evolution of gas ceased. The glass-like residue was crystallised from boiling water (1.78 g, 62.0%) as fine white crystals, m.p. 157-158 °C (lit.,[12] 158.5 °C) (Found: C, 59.7; H, 4.2; N, 5.3. $C_8H_{11}NO_5$ requires C, 59.8; H, 4.2; N, 5.4%); m/z 261 (M^+, 2%), 244 (M^+- OH, 3), 216 (M^+- CO_2H, 4), 161 (100), 160 (79), 147 (14), 133 (7), 104 (17), 77 (7), 76 (13), 50 (5) and 28 (32); δ_H [$(CD_3)_2C$=O] 2.62 (2 H, t, *J* 6.56, CH_2CO_2H), 2.93 (2 H, t, *J* 6.56, $CH_2CH_2CO_2H$), 4.63 (2 H, s, NCH_2) and 7.89 (4 H, s, Ar*H*); δ_C [$(CD_3)_2C$=O] 27.9, 35.1, 47.1, 123.8, 133.1, 135.3, 168.2, 173.7 and 202.4.

2.2.3.8 Synthesis of 5-aminolevulinic acid hydrochloride (VIII).

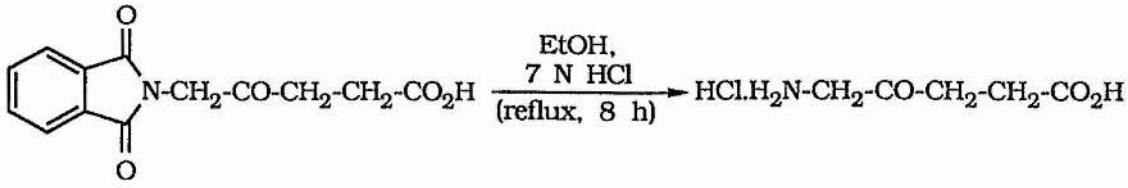

5-phthalimidolevulinic acid

5-aminolevulinic acid hydrochloride

+

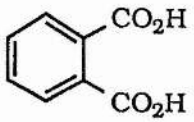

phthalic acid

5-aminolevulinic acid was prepared according to the method of Tschudy and Collins.[20] A mixture of 5-phthalimidolevulinic acid (2.78 g, 0.0068 mol), 95% ethanol (1.8 ml) and 7 N HCl (18 ml) were refluxed for 8 hours and allowed to cool overnight. The phthalic acid was filtered off and the filtrate evaporated to dryness *in vacuo* . The residue was crystallised from a mixture of dry ethanol and dry diethyl ether. 5-aminolevulinic acid hydrochloride (0.986 g, 86.6%) was obtained as yellow crystals, m.p. 148-150 °C (lit.,[20] 148 °C) (Found: C, 35.75; H, 6.5; N, 8.2. $C_5H_{10}NO_3Cl$ requires C, 35.85; H, 6.0; N, 8.4%); m/z 131 (M^+- HCl, 0.5%), 114 (7), 101 (1), 86 (2), 73 (1), 57 (3), 55 (10), 45 (19), 44 (12), 38 (86), 37 (20), 36 (100), 35 (58), 30 (63) and 28 (61); δ_H (D_2O) 2.74 (2 H, t, *J* 6.32, CH_2CO_2H), 2.91 (2 H, t, *J* 6.32, $CH_2CH_2CO_2H$) and 4.14 (2 H, s, CH_2NH_2); δ_C (D_2O) 30.1, 37.0, 49.8, 179.4, and 206.7.

2.2.4 Synthesis of ALA.HCl from methyl 5-chlorolevulinate and potassium phthalimide.

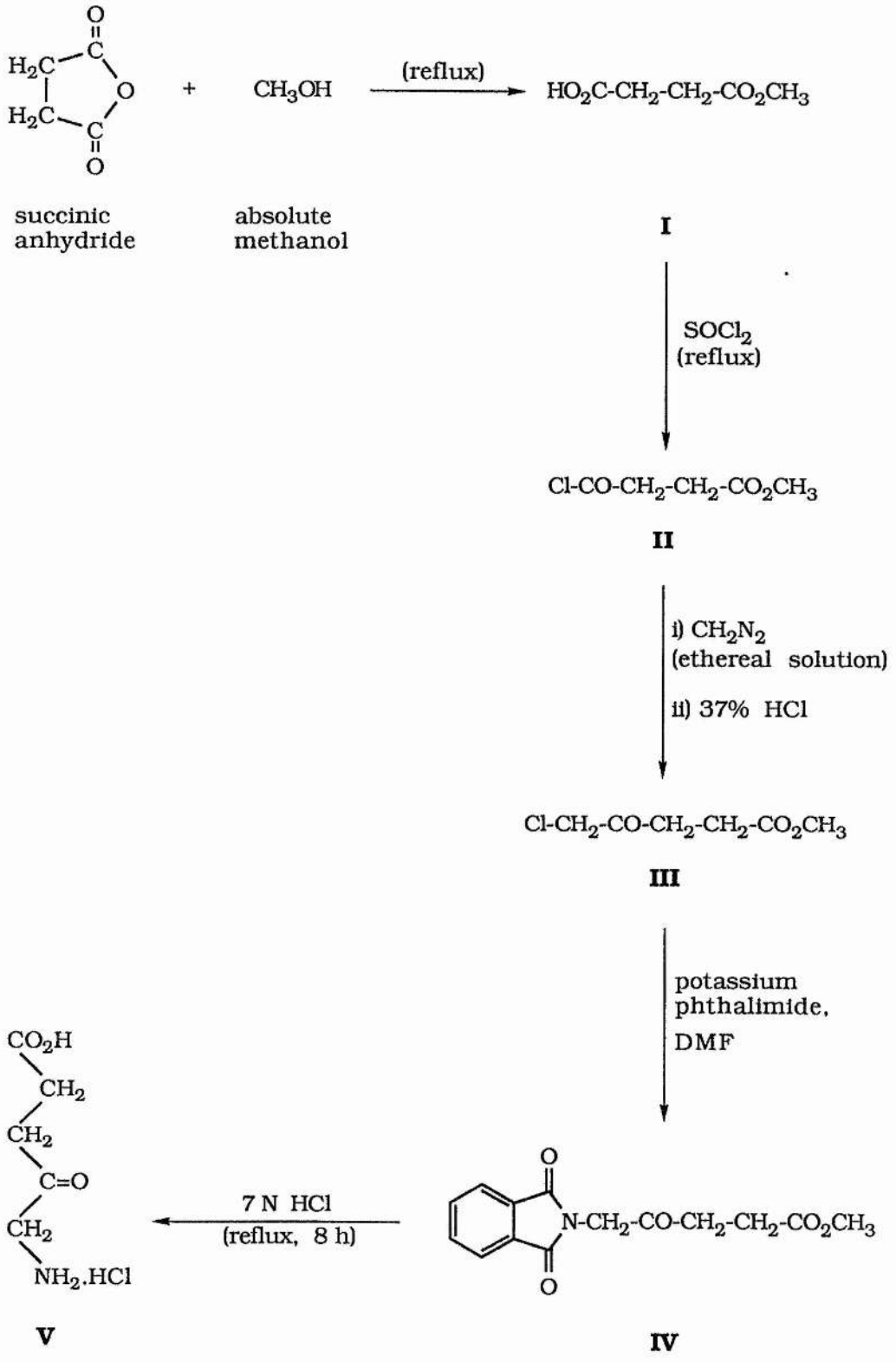

Scheme 2.3

2.2.4.1 Synthesis of methyl hydrogen succinate (I).

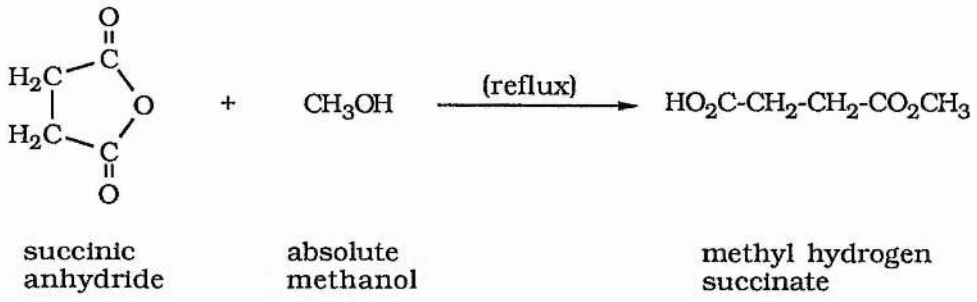

Methyl hydrogen succinate was prepared according to the method of Cason.[47] A mixture of succinic anhydride (50.0 g, 0.5 mol) and dry methanol (24.5 ml) was refluxed in a 500 ml round bottomed flask on a steam-bath. After 35 minutes, the mixture was stirred vigorously until it became homogeneous. This required 15 minutes. The flask was then half immersed in a steam bath for an additional 30 minutes. The excess methanol was removed by distillation under reduced pressure (water pump) from a steam bath. The crude product was recrystallised from toluene-cyclohexane (61.0 g, 92.4%) as white crystals, m.p. 57 °C (lit.,[47] 57-58 °C) (Found: C, 45.65; H, 6.1. $C_5H_8O_4$ requires C, 45.45; H, 6.1%); m/z 133 (M^++ 1, 1%), 132 (M^+, 0.7), 114 (62), 101 (92), 100 (64), 88 (36), 73 (69), 59 (71), 55 (82), 45 (100), 31 (31), 29 (100) and 28 (83); δ_H (D_2O) 2.68 (4 H, s, $CH_2CH_2CO_2H$) and 3.70 (3 H, s, CO_2CH_3); δ_C (D_2O) 31.5, 55.1, 178.4 and 179.7.

2.2.4.2 Synthesis of methyl 3-chloroformylpropanoate (II).

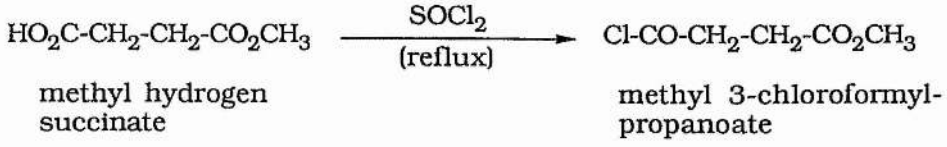

Methyl 3-chloroformylpropanoate was prepared according to the method of Cason.[47] A mixture of methyl hydrogen succinate (48.3 g, 0.37 mol) and thionyl chloride (53 ml, 0.73 mol) was placed in a 500 ml round-bottomed flask bearing a reflux condenser and the solution warmed in a water bath at 30-40 °C for 3 hours. The condenser was replaced by a modified Claisen still head and the excess thionyl chloride removed on a steam bath under reduced pressure (water pump). The crude product was then Kugelrohr distilled to give methyl 3-chloroformylpropanoate (45.21 g, 81.2%) as a colourless liquid, b.p. 53-65 °C/3 mmHg (lit.,[47] 92-94 °C/ 18 mmHg) (Found: C, 40.4; H, 4.7. $C_5H_7ClO_3$ requires C, 39.9; H, 4.7%); m/z 119 (M^+- OMe, 74%), 115 (M^+- Cl, 100), 101 (13), 87 (32), 63 (35), 59 (84), 55 (92), 45 (31), 36 (100) and 28 (90); δ_H ($CDCl_3$) 2.70 (2 H, t, *J* 6.52, $CH_2CO_2CH_3$), 3.24 (2 H, t, *J* 6.52, $CH_2CH_2CO_2CH_3$) and 3.71 (3 H, s, CO_2CH_3); δ_C ($CDCl_3$) 29.2, 41.9, 52.2, 171.5 and 173.2.

2.2.4.3 Synthesis of methyl 5-chlorolevulinate (III).

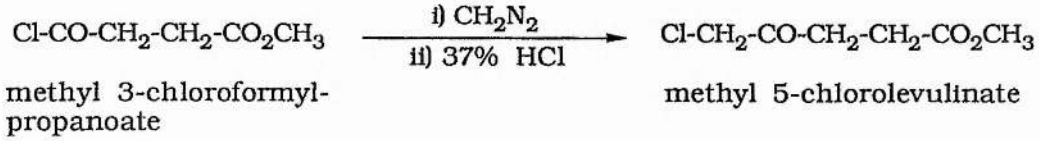

methyl 3-chloroformyl-propanoate

methyl 5-chlorolevulinate

Methyl 5-chlorolevulinate was prepared according to the method of Neuberger and Scott.[12] To a solution of diazomethane (approximately 0.16 mol) in dry ether (300 ml), (prepared in exactly the same way and in the same scale as in Section 2.2.3.3.1) cooled to 0 to -5 °C in an ice-salt mixture was added with mechanical stirring, a solution of methyl 3-chloroformylpropanoate (10.0 g, 0.066 mol) in dry ether (30 ml), during two hours. The

mixture was allowed to warm to room temperature overnight. An equivalent molecular amount of 37% HCl (5.52 ml, 0.066 mol) was gradually added with stirring to the ethereal solution of the diazoketone. This resulted in a rapid evolution of nitrogen after which the solution was practically colourless. The solution was concentrated to about 100 ml *in vacuo* from a bath at room temperature. It was then washed with water (3 x 30 ml), to remove HCl and the combined water washings were extracted with ether (6 x 20 ml), since the ketone ester is quite soluble in water. The combined ether extracts were dried over anhydrous Na_2SO_4 and the solvent removed under reduced pressure. The residual material was Kugelrohr distilled to give methyl 5-chlorolevulinate (4.69 g, 43.2%) as a colourless liquid, b.p. 79-80 °C/1 mmHg (lit.,[12] 92-94 °C/2-3 mmHg) (Found: C, 46.8; H, 6.35. $C_6H_9ClO_3$ requires C, 47.1; H, 6.2%); m/z 133 (M^+- OMe, 4%), 132 (45), 115 (44), 114 (77), 104 (6), 86 (2), 45 (60) and 28 (100); δ_H ($CDCl_3$) 2.66 (2 H, t, *J* 6.56, $CH_2CO_2CH_3$), 2.90 (2 H, t, *J* 6.56, $CH_2CH_2CO_2CH_3$), 3.68 (3 H, s, CO_2CH_3) and 4.19 (2 H, s, CH_2Cl); δ_C ($CDCl_3$) 27.8, 34.3, 48.3, 52.0, 172.9 and 201.3.

2.2.4.4 Synthesis of methyl 5-phthalimidolevulinate (IV).

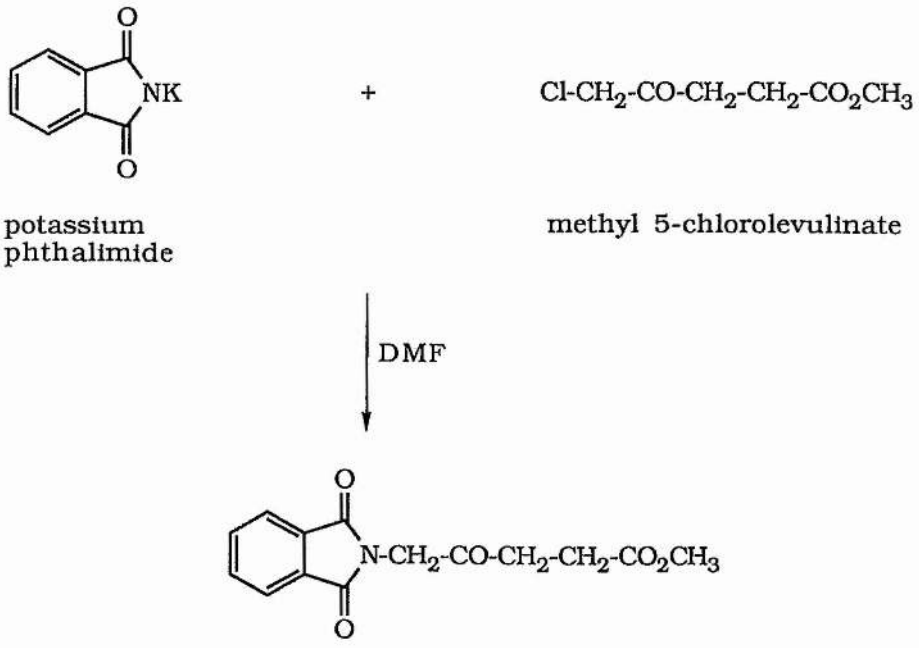

methyl 5-phthalimidolevulinate

Methyl 5-phthalimidolevulinate was prepared according to the method of Neuberger and Scott.[12] Potassium phthalimide (4.0 g, 0.02 mol) was dissolved in anhydrous DMF (20 ml). To this was added methyl 5-chlorolevulinate (3.29 g, 0.02 mol) which was washed in with DMF (2 ml). The mixture was stirred for half an hour and then warmed at 60 °C for an hour. The cooled reaction mixture was filtered to remove KCl and any unreacted potassium phthalimide. Methylene chloride (40 ml) and water (120 ml) were added to the filtrate. The aqueous phase was decanted and washed twice with methylene chloride (12 ml). The methylene chloride extracts were washed with 0.2 N NaOH (15 ml) and then with water until the washings were colourless. The combined methylene chloride extracts were dried over anhydrous Na_2SO_4 and the solvent evaporated under reduced pressure. The residual material

was recrystallised from boiling water (2.87 g, 52.2%) as fine white crystals, m.p. 96 °C (lit.,[12] 96-97 °C) (Found: C, 61.3; H, 4.9; N, 5.1. $C_{14}H_{13}NO_5$ requires C, 61.1; H, 4.8; N, 5.1%); m/z 275 (M^+, 0.3%), 244 (M^+- OMe, 3), 216 (7), 160 (25), 133 (5), 115 (100), 104 (12), 87 (9), 77 (15), 76 (13), 55 (25), 50 (6), 32 (18) and 28 (86); δ_H ($CDCl_3$) 2.67 (2 H, t, *J* 6.71, $CH_2CO_2CH_3$), 2.86 (2 H, t, *J* 6.71, $CH_2CH_2CO_2CH_3$) 3.69 (3 H, s, CO_2CH_3), 4.56 (2 H, s, NCH_2), 7.74 (2 H, m, Ar*H*) and 7.88 (2 H, m, Ar*H*); δ_C ($CDCl_3$) 27.6, 34.5, 46.5 52.0, 123.6, 132.0, 134.2, 167.6, 172.6 and 200.7.

2.2.4.5 Synthesis of 5-aminolevulinic acid hydrochloride (V).

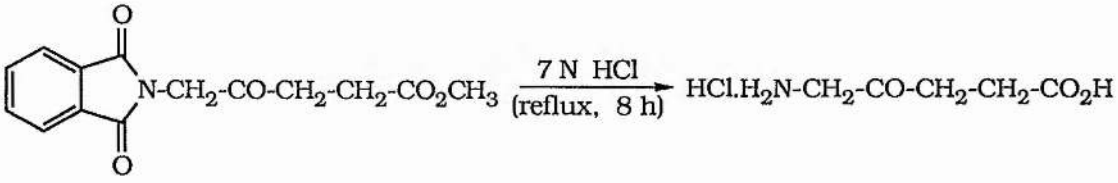

methyl 5-phthalimidolevulinate

5-aminolevulinic acid hydrochloride

+

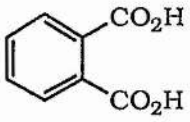

phthalic acid

5-aminolevulinic acid hydrochloride was prepared according to the method of Neuberger and Scott.[12] Methyl 5-phthalimidolevulinate (2.87 g, 0.01 mol) was refluxed for 8 hours in 7 N HCl (30 ml). After the solution was cooled, phthalic acid was removed by filtration and the mother liquor concentrated to dryness *in vacuo*. 5-aminolevulinic acid hydrochloride was obtained (1.01 g, 60.3%) as pale yellow crystals, m.p. 144 °C [lit.,[12] 145 °C (dec.)] (Found: C, 35.8; H, 6.2; N, 8.2. $C_5H_{10}ClNO_3$ requires C, 35.85;

H, 6.0; N, 8.4%); m/z 131 (M^+- HCl, 0.7%), 114 (2), 101 (2), 86 (1), 73 (3), 57 (2), 55 (11), 45 (11), 44 (52), 38 (98), 37 (68), 36 (100), 35 (92), 30 (31) and 28 (60); δ_H (D_2O) 2.71 (2 H, t, *J* 6.33, CH_2CO_2H), 2.90 (2 H, t, *J* 6.33, $CH_2CH_2CO_2H$) and 4.13 (2 H, s, CH_2NH_2); δ_C (D_2O) 30.1, 37.1, 49.8, 179.6 and 206.7.

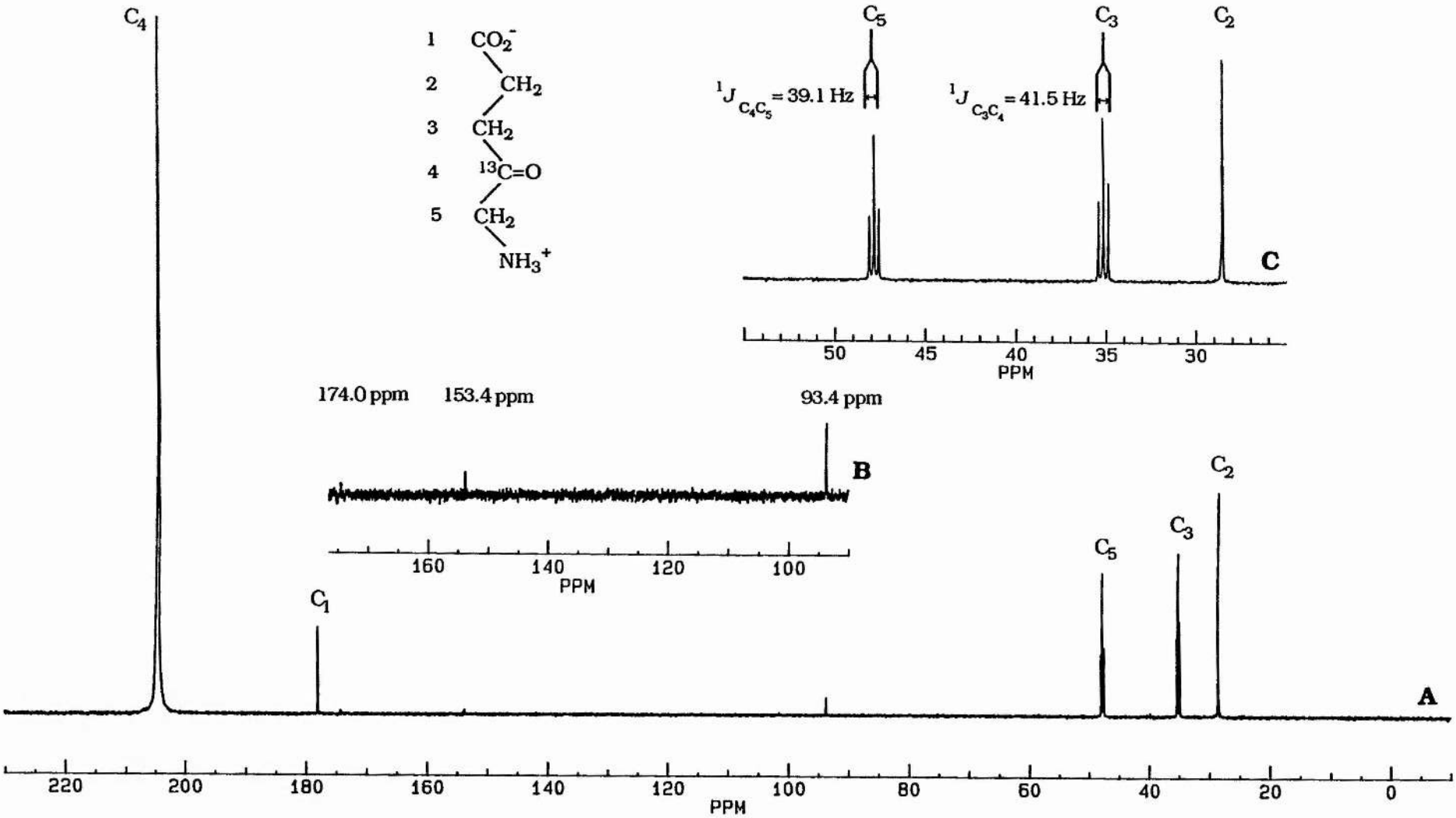

Figure 2.1 (A) ^{1}H decoupled, 75.469 MHz ^{13}C NMR spectrum of 0.25 M [4-^{13}C]ALA.HCl (50% enriched) in 0.1 M KPi buffer, pH 6.8, at 37 °C. **(B)** 4-fold vertical expansion of (A) between 90 and 175 ppm (identical chemical shift scale). **(C)** 3-fold horizontal expansion of (A) between 25 and 55 ppm.

2.3 Results and Discussion.

[4-^{13}C]ALA.HCl (50% enriched) was prepared following the route described in Section 2.2.3, starting with a mixture of phthalic anhydride (20.0 g, 0.135 mol), [2-^{13}C]glycine (99% enriched) (5.0 g, 0.066 mol) and unlabelled glycine (5.0 g, 0.067 mol). The yield of product based on glycine was 1.25 g, 5.63%.

[^{15}N]ALA.HCl (50% enriched) was prepared following the route described in Section 2.2.4 by reacting potassium [^{15}N] phthalimide (99% enriched) (1.0 g, 0.005 mol) and unlabelled potassium phthalimide (1.0 g, 0.005 mol) with methyl-5-chloro-levulinate (1.48 g, 0.009 mol). The yield of product based on potassium phthalimide was 1.0 g, 43.7%.

The ^{13}C NMR spectrum of 0.25 M [4-^{13}C]ALA.HCl (50% enriched), [Fig. 2.1(A)] was obtained in 0.1 M KPi buffer, pH 6.8, at a probe temperature of 37 °C. A D_20 capillary insert was used to provide the lock signal and the chemical shift reference was external dioxane set at δ 67.4. The ^{13}C NMR spectrum [Fig. 2.1 (A)] shows a very strong enhancement of the C_4 carbonyl resonance at 204.2 ppm. The chemical shift assignments for C_1, C_2, C_3 and C_5 are 177.7, 28.2, 34.8 and 47.5 ppm respectively. Three additional signals are observed at δ 93.4, δ 153.4 and δ 174.0, the significance of which will be explained in Chapter 3. Fig. 2.1(B) is a 4-fold vertical expansion of Fig. 2.1(A) between 90 and 175 ppm, identifying the resonances at δ 93.4, δ 153.4 and δ 174.0. Fig. 2.1(C) is a 3-fold horizontal expansion of Fig. 2.1(A) between 25 and 55 ppm showing the natural abundance methylene carbons C_2, C_3 and C_5.

Since the C_4 carbonyl carbon of ALA is 50% enriched in ^{13}C, 50% of the C_3 and C_5 resonances appear as single parent signals,

due to the absence of any coupling with the 50% ^{12}C at C_4. The remaining 50% of the C_3 and C_5 resonances appear as satellite peaks of 25% intensity each, due to coupling with the 50% ^{13}C at C_4. (i.e. the satellite peaks are one half the intensity of the parent peak). One satellite peak lies at higher field and the other at lower field than the parent signal, their spacing being equal to the one bond C-C coupling constant ($^1J_{C_3C_4}$ = 41.5 Hz and $^1J_{C_4C_5}$ = 39.1 Hz). One bond carbon-carbon coupling constants in hydrocarbons vary over a wide range depending on the hybridisation of the two carbon atoms involved. In terms of the 's' character of the two bonding hybrid orbitals, $^1J_{CC}$ has been described by the expression,[48]

$$^1J_{C_XC_Y} = \frac{7.3\ (\%s_X)\ (\%s_Y)}{100} - 17\ \text{Hz}$$

Thus, substituting the values for the percentage 's' character of the bonding orbitals concerned, the upper limit for the one bond carbon-carbon coupling constant between an sp^2 and an sp^3 hybrid orbital [C_4 and C_3 or C_4 and C_5 of [4-^{13}C]ALA.HCl (50% enriched)] is 43.8 Hz.

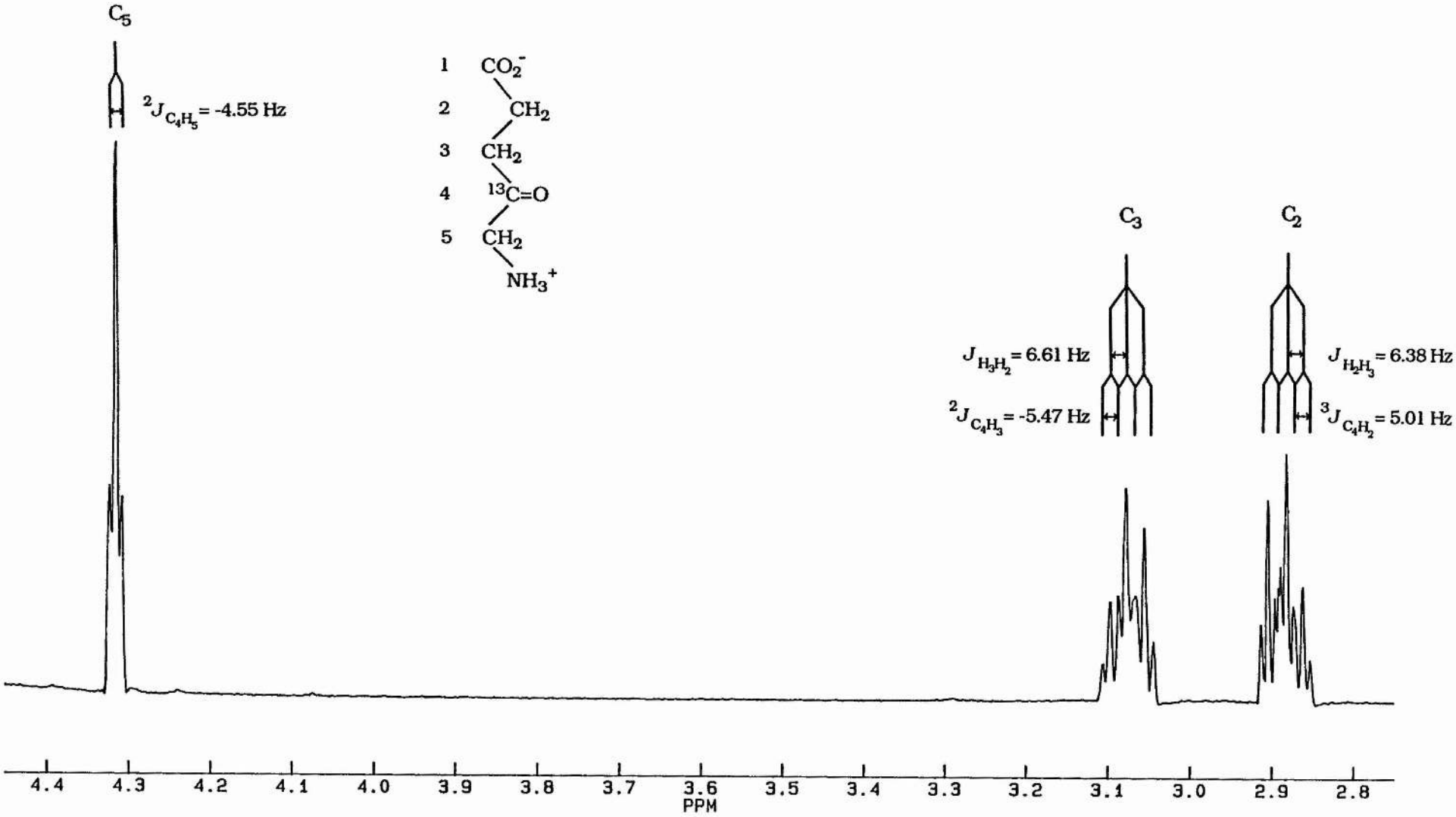

Figure 2.2 300.134 MHz ^{1}H NMR spectrum of 0.5 M [4-^{13}C]ALA.HCl (50% enriched) in 0.1 M KPi buffer, pH 6.8, at 37 °C, identifying the C_2, C_3 and C_5 resonances.

The ^1H NMR spectrum of 0.5 M [4-^{13}C]ALA.HCl (50% enriched) (Fig. 2.2) was obtained in 0.1 M KPi buffer, pH 6.8, at a probe temperature of 37 °C. A D_2O capillary insert was used to provide the lock signal and the chemical shift reference was external dioxane set at δ 3.7. The ^1H spectrum was processed using resolution enhancement.

The chemical shift assignments for the 2-CH_2, 3-CH_2 and 5-CH_2 methylene protons are 2.88, 3.08 and 4.32 ppm respectively. The 2-CH_2 methylene protons are split into a triplet due to coupling with the adjacent 3-CH_2 methylene protons ($J_{H_2H_3}$ = 6.38 Hz) and each peak of this triplet is accompanied by two satellite peaks, one at higher field and the other at lower field than the parent signal, due to a three bond C-H coupling. The spacing between the satellite peaks is equal to this three bond C-H coupling constant ($^3J_{C_4H_2}$ = 5.01 Hz). The 3-CH_2 methylene protons are split into a triplet due to coupling with the adjacent 2-CH_2 methylene protons ($J_{H_3H_2}$ = 6.61 Hz) and each peak of this triplet is accompanied by two satellite peaks, one at higher field and the other at lower field than the parent signal, due to a two bond C-H coupling. The spacing between the satellite peaks is equal to this two bond C-H coupling constant ($^2J_{C_4H_3}$ = -5.47 Hz). The 5-CH_2 methylene protons appear as a single peak and is accompanied by two satellite peaks, one at higher field and the other at lower field than the parent signal, due to a two bond C-H coupling. The spacing between the satellite peaks is equal to this two bond C-H coupling constant ($^2J_{C_4H_5}$ = -4.55 Hz). For the same reasons explained previously, the satellite peaks are about one half the intensities of the parent peaks.

Typical two bond C-H coupling constants range from -6 Hz to

-4 Hz.[49] (Signs are most probably negative.[50]) Detailed discussions and reference data for two bond C-H coupling constants are given in the literature.[51,52] Three bond C-H coupling constants depend in a manner similar to three bond H-H coupling constants on the dihedral angle, ϕ.[49] (This is the famous Karplus relationship[53,54] relating the proton-proton spin-spin coupling constant in the fragment H-C-C-H, to the dihedral angle). The Karplus curve[55] together with some observed values of $^{3}J_{CH}$ [57,58] are given in the literature.

A striking observation with [4-^{13}C]ALA.HCl (50% enriched) is that $^{3}J_{C_4H_2}$ is not smaller than $^{2}J_{C_4H_3}$ in magnitude. The fact that spin-spin coupling constants do not decrease monotonically with the number of bonds separating the interacting nuclei has been reported in the past,[59] although the factors causing such anomalous spin-spin coupling constants are not clear at all.

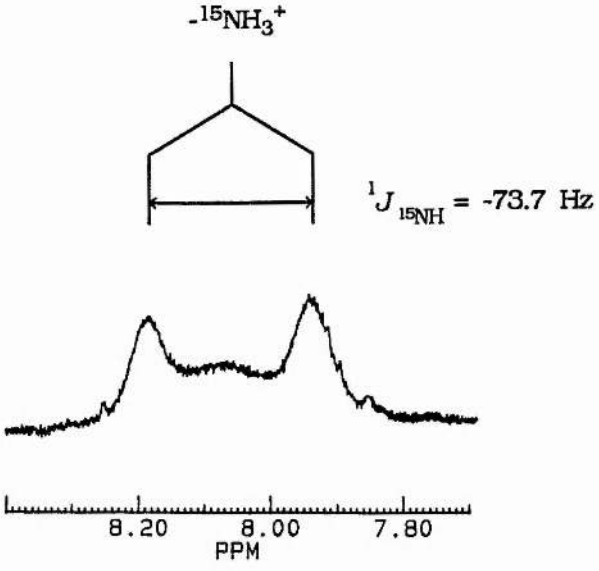

Figure 2.3 300.134 MHz ^{1}H NMR spectrum of 1 M [^{15}N]ALA.HCl (50% enriched) in 0.1 M KPi buffer, pH 6.8, at 37 °C, identifying the $-^{15}NH_3^+$ resonance.

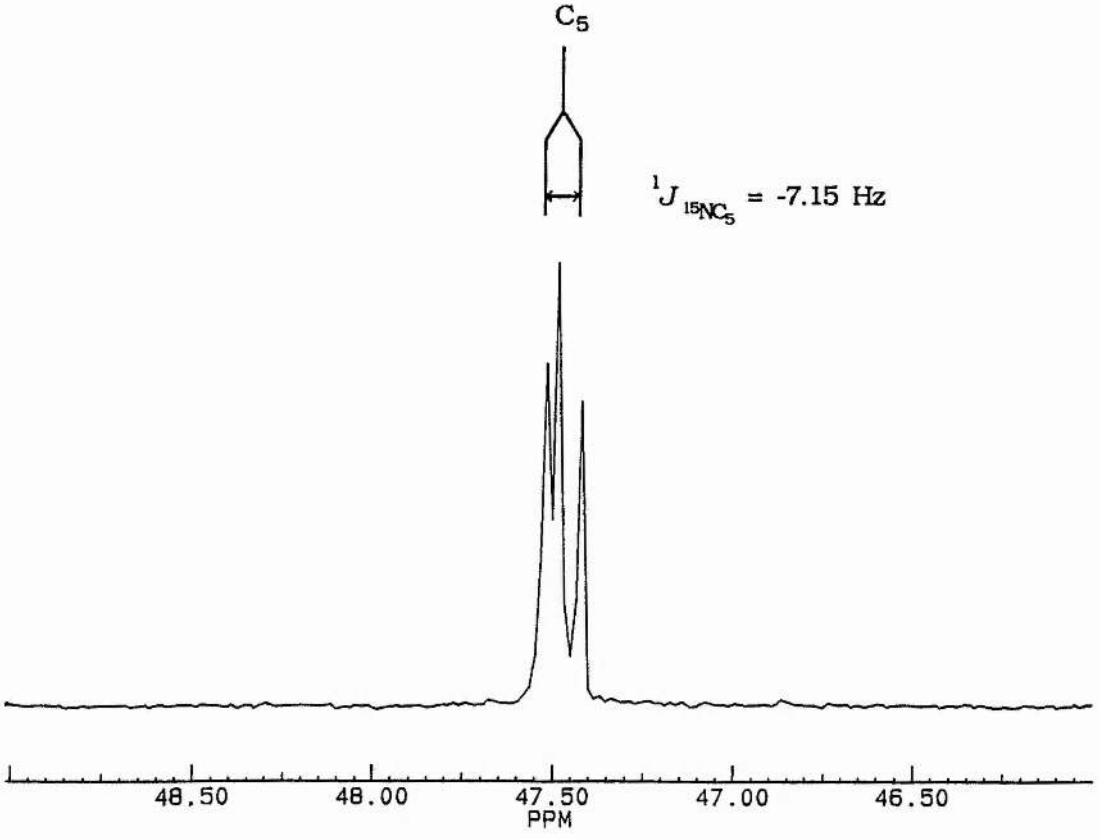

Figure 2.4 ^{1}H decoupled 75.469 MHz ^{13}C NMR spectrum of 1 M [^{15}N]ALA.HCl (50% enriched) in 0.1 M KPi buffer, pH 6.8, at 37 °C, identifying the C_5 resonance.

The ^{1}H NMR spectrum of 1 M [^{15}N]ALA.HCl (50% enriched) (Fig. 2.3), identifying the resonance of the amino group, was obtained in 0.1 M KPi buffer, pH 6.8, at a probe temperature of 37 °C. A D_2O capillary insert was used to provide the lock signal and the chemical shift resonance was external dioxane set at δ 3.7. The resonance of the amino group appears as 2 satellite peaks one on either side of a broad $-^{14}NH_3^+$ resonance centred at 8.07 ppm. The satellite peaks arise, due to the coupling of the protons of the amino group with ^{15}N. The one bond ^{15}N-H coupling constant, $^{1}J_{^{15}NH} = -73.7$ Hz.

Because of its small magnetic moment, μ, one bond couplings to protons which are dominated by the Fermi contact mechanism are negative for ^{15}N.[60] Also, $^{1}J_{^{15}NH}$ falls into regions of ~75, 90 and 135 Hz for pyramidal, trigonal and linear bonding to nitrogen respectively.[60] The one bond ^{15}N-H coupling constant of -73.7 Hz for [^{15}N]ALA.HCl (50% enriched) necessarily corresponds to a $-NH_3^+$ group (i.e. pyrimidal bonding to nitrogen) suggesting that the amino group is protonated under these conditions.

Two bond ^{15}N-H couplings across a saturated carbon, lie between 0 to 2 Hz and in the case of [^{15}N]ALA.HCl (50% enriched), $^{2}J_{^{15}NH_5}$ cannot be resolved.

The ^{13}C NMR spectrum of 1 M [^{15}N]ALA.HCl (50% enriched) (Fig. 2.4) identifying the C_5 resonance at 47.5 ppm accompanied by two satellite peaks one at higher field and the other at lower field than the parent signal, was obtained in 0.1 M KPi buffer, pH 6.8, at a probe temperature of 37 °C. A D_2O capillary insert was used to provide the lock signal, and the chemical shift resonance was external dioxane set at δ 67.4. The ^{13}C NMR spectrum (Fig. 2.4) processed using resolution enhancement, reveals the one bond

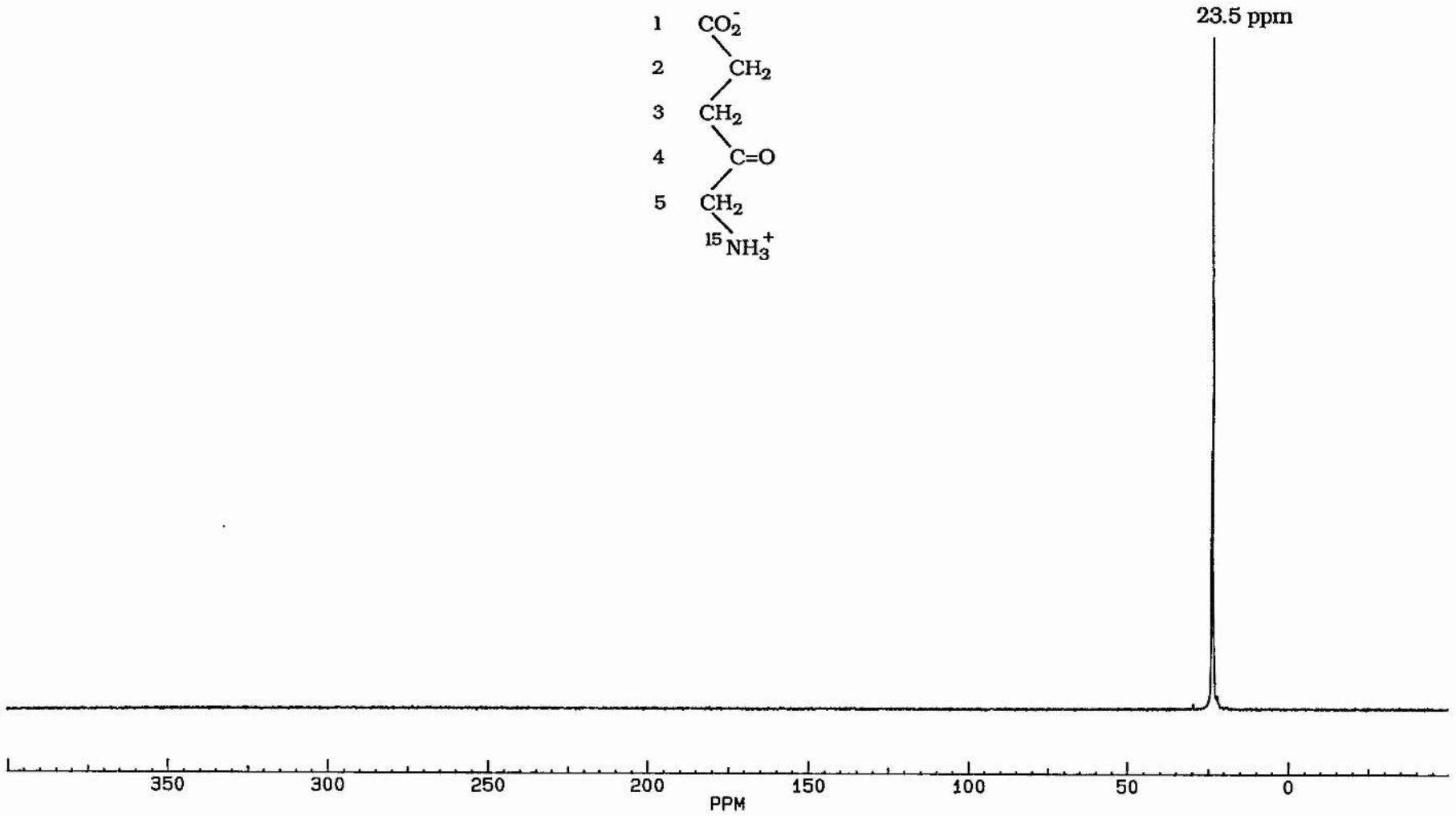

Figure 2.5 ^{1}H decoupled, 30.412 MHz ^{15}N NMR spectrum of 1 M [^{15}N]ALA.HCl (50% enriched) in 0.1 M KPi buffer, pH 6.8, at 37 °C, identifying the -$^{15}NH_3^+$ resonance.

^{15}N-C coupling constant, $^{1}J_{^{15}NC_5}$ = -7.15 Hz. For reasons explained previously, the intensity of the satellite peaks is one half that of the parent signal.

For most molecules, $^{1}J_{^{15}NC}$ is negative, as is expected if the Fermi contact mechanism dominates the coupling interaction.[60] A useful guide to the magnitude of $^{1}J_{^{15}NC}$ is given by the expression,[61]

$$^{1}J_{^{15}NC} = \frac{(\%s_N)\ (\%s_C)}{80}$$

Thus, substituting the appropriate values for the percentage 's' character for the two sp^3 hybrid orbitals concerned, the upper limit for the one bond nitrogen-carbon coupling constant is -7.81 Hz.

The ^{15}N NMR spectrum of 1 M [^{15}N]ALA.HCl (50% enriched) (Fig. 2.5) was obtained in 0.1 M KPi buffer, pH 6.8, at a probe temperature of 37 °C. A D_20 capillary insert was used to provide the lock signal. The ^{15}N NMR spectrum (Fig. 2.5), shows a single peak at δ 23.5 corresponding to the $-^{15}NH_3^+$ resonance of [^{15}N]ALA.HCl (50% enriched).

Aliphatic amine hydrochlorides have a ^{15}N chemical shift range of 15 to 75 ppm.[62]

References.

1. Reviewed by:

a) L. Bogorad, *in* 'The chlorophylls', (L. P. Vernon and G. R. Seeley, eds.), p. 481, Academic Press, New York, 1966.

b) B. F. Burnham, *in* 'Metabolic Pathways', (D. M. Greenberg ed.), Vol. III, 3rd ed., p. 403, Academic Press, New York, 1969.

c) A. R. Battersby and E. McDonald, *in* 'Porphyrins and Metalloporphyrins', (K. M. Smith, ed.), p. 61, Elsevier, New York, 1975.

d) D. Dolphin (ed.), 'The Porphyrins', Vol. 6, Academic Press, New York, 1976.

e) S. Granick and S. I. Beale, *Adv. Enzymol.*, 1978, **46**, 33.

f) M. Akhtar and P. M. Jordan, *in* 'Comprehensive Organic Chemistry', (E. Haslam, ed.), Vol. 5, p. 1121, Pergamon Press, New York, 1979.

g) F. J. Leeper, *Nat. Prod. Reports*, 1985, **2**, 19.

h) H. A. Dailey (ed.), 'Biosynthesis of Heme and Chlorophylls', p. 55, McGraw-Hill, New York, 1990.

2. W. W. Cleland, *Enzymes*, 3rd ed., 1970, **2**, 1.

3. P. M. Jordan and J. S. Seehra, *FEBS Lett.*, 1980, **114**, 283.

4. N. E. MacKenzie, J. P. G. Malthouse and A. I. Scott, *Science*, 1984, **225**, 883.

5. E. K. Jaffe and G. D. Markham, *Biochemistry*, 1987, **26**, 4258.

6. E. K. Jaffe and G. D. Markham, *Biochemistry*, 1988, **27**, 4475.

7. E. K. Jaffe, G. D. Markham and J. S. Rajagopalan, *Biochemistry*, 1990, **29**, 8345.

8. R. W. Wynn and A. H. Corwin, *J. Org. Chem.*, 1950, **15**, 203.

9. D. Shemin and C. S. Russell, *J. Am. Chem. Soc.*, 1953, **75**, 4873.

10. A. Neuberger and J. J. Scott, *Nature*, 1953, **172**, 1093.
11. V. M. Radinov and M. A. Gubareva, *J. Gen. Chem. (U.S.S.R.)*, 1953, **23**, 1951. *(Chem. Abs.*, 1955, **49**, 1007i).
12. A. Neuberger and J. J. Scott, *J. Chem. Soc.*, 1954, 1820.
13. D. Shemin, C. S. Russell and T. Abramsky, *J. Biol. Chem.*, 1955, **215**, 613.
14. L. Pichat, M. Hucleux and M. Herbert, *Bull. Soc. Chim. Fr.*, 1956, 1750.
15. A. Neuberger, J. J. Scott and L. Shuster, *Biochem. J.*, 1956, **64**, 137.
16. L. Pichat and M. Herbert, *Bull. Soc. Chim. Fr.*, 1957, 673.
17. D. Shemin *in* 'Methods in Enzymology' (S. P. Colowick and N. O. Kaplan, eds.), Vol. 4, p 648, Academic Press, New York, 1957.
18. A. A. Marie and R. A. Raphael, *J. Chem. Soc.*, 1958, 2624.
19. A. W. Schrecker and M. M. Trail, *J. Am. Chem. Soc.*, 1958, **80**, 6077.
20. D. P. Tschudy and A. Collins, *J. Org. Chem.*, 1958, **24**, 556.
21. W. G. Laver, A. Neuberger and J. J. Scott, *J. Chem. Soc.*, 1959, 1474.
22. W. G. Laver, A. Neuberger and J. J. Scott, *J. Chem. Soc.*, 1959, 1483.
23. W. R. Hearn and M. F. Wildfeuer, *Anal. Biochem.*, 1961, **2**, 140.
24. F. Sparatore and W. Cumming, *Biochem. Prep.*, 1963, **10**, 6.
25. L. Pichat, J. Loheac and M. Herbert, *Bull. Soc. Chim. Fr.*, 1966, **3**, 3268.
26. L. Pichat, J. Loheac, M. Herbert and G. Chatelain, *Bull. Soc. Chim. Fr.*, 1966, **3**, 3271.

27. L. Pichat, J. Loheac and M. Herbert, *Bull. Soc. Chim. Fr.*, 1966, **3**, 3564.

28. A. E. A. Mitta, A. M. Ferramola, H. A. Sancovich and M. Grinstein, *J. Labelled Cpds.*, 1967, **3**, 20.

29. N. Aronova, N. N. Makhova and S. I. Savialov, *U.S.S.R. Patent*, 1970, 266,773. (*Chem. Abs.*, 1970, **73**, 4584g).

30. L. Pichat, J. P. Beancourt and M. Herbert, *Radioisotopy*, 1971, **12**, 519.

31. N. I. Aronova, N. N. Makhova, S. I. Savialov and B. Yu. Volkenshten, *German Patent*, 1973, 2,208,800. (*Chem. Abs.*, 1973, **79**, 125,863w).

32. A. R. Battersby, E. Hunt, E. McDonald and J. Moron, *J. Chem. Soc., Perkin Trans. 1*, 1973, 2917.

33. A. I. Scott, C. A. Townsend, K. Okada, M. Kajiwara, R. J. Cushley and P. J. Whitman, *J. Am. Chem. Soc.*, 1974, **96**, 8069.

34. R. S. Norton, A. O. Clouse, R. Addleman and A. Allerhand, *J. Am. Chem. Soc.*, 1977, **99**, 79.

35. E. Oldfield, R. S. Norton and A. Allerhand, *J. Biol. Chem.*, 1975, **250**, 6368.

36. A. Allerhand, *Methods Enzymol.*, 1979, **61**, 458.

37. J. Juillard, *Pure Appl. Chem.*, 1977, **49**, 885.

38. 'Vogel's Textbook of Practical Organic Chemistry', 4th ed., Longman Inc., New York, 1978.

39. W. Rigby, *Chem. Ind.*, 1969, 1508.

40. J. J. O'Neill, F. P. Veitch and T. Wagner-Jauregg, *J. Org. Chem.*, 1956, **21**, 363.

41. E. Drechsel, *J. prakt. Chem.*, 1883, **27**, 418.

42. K. Balenović, N. Bregant, D. Cerar and M. Tkalčić, *J. Org. Chem.*, 1951, **16(ii)**, 1308.

43. Th. J. DeBoer and H. J. Backer, *Org. Syn.*, 1956, Vol. 36, 16.

44. F. Arndt, *Org. Syn.*, 1948, Coll. Vol. II, 165.

45. K. Balenovic and L. Bregant, *J. Org. Chem.*, 1952, **17(ii)**, 1328.

46. S. Gabriel, *Ber.*, 1911, **44**, 1905.

47. J. Cason, *Org. Syn.*, Coll. Vol II, 169.

48. F. J. Weigert and J. D. Roberts, *J. Am. Chem. Soc.*, 1972, **94**, 6021.

49. F. W. Wehrli and T.Wirthlin, 'Interpretation of Carbon-13 NMR spectra', Heyden, London, 1976.

50. E. Sackmann and H. Dreeskamp, *Spectrochim. Acta*, 1965, **21**, 2005.

51. J. B. Stothers, 'Carbon-13 Nuclear Magnetic Resonance Spectroscopy', Academic Press, New York, 1972.

52. J. L. Marshall, D. E. Miiller, S. A. Conn, R. Seinwell and A. M. Ihrig, *Acc. Chem. Res.*, 1974, **7**, 333.

53. M. Karplus, *J. Chem. Phys.*, 1959, **30**, 11.

54. M. Karplus, *J. Am. Chem. Soc.*, 1963, **85**, 2870.

55. R. Wasylishen and J. Schaefer, *Can. J. Chem.*, 1972, **50**, 2710.

56. J. A. Schwarcz and A. S. Perlin, *Can. J. Chem.*, 1972, **50**, 3667.

57. R. U. Lemieux, T. L. Nagabushan and B. Paul, *Can. J. Chem.*, 1972, **50**, 773.

58. L. T. J. Delbaere, M. N. G. James and R. U. Lemieux, *J. Am. Chem. Soc.*, 1973, **95**, 7866.

59. G. J. Karabatsos, *J. Am. Chem. Soc.*, 1961, **83**, 1230.

60. G. C. Levy and R. L. Lichter, 'Nitrogen-15 Nuclear Magnetic Resonance Spectroscopy', Wiley-Interscience, 1979.

61. G. Binsch, J. B. Lambert, B. W. Roberts and J. D. Roberts, *J. Am. Chem. Soc.*, 1964, **86**, 5564.

62 G. J. Martin, M. L. Martin and J. P. Goursnard, '^{15}N NMR Spectroscopy', Vol. 18, Springer-Verlag-Berlin, 1981.

CHAPTER THREE

THE NON-ENZYMATIC CYCLIC DIMERISATION OF ALA

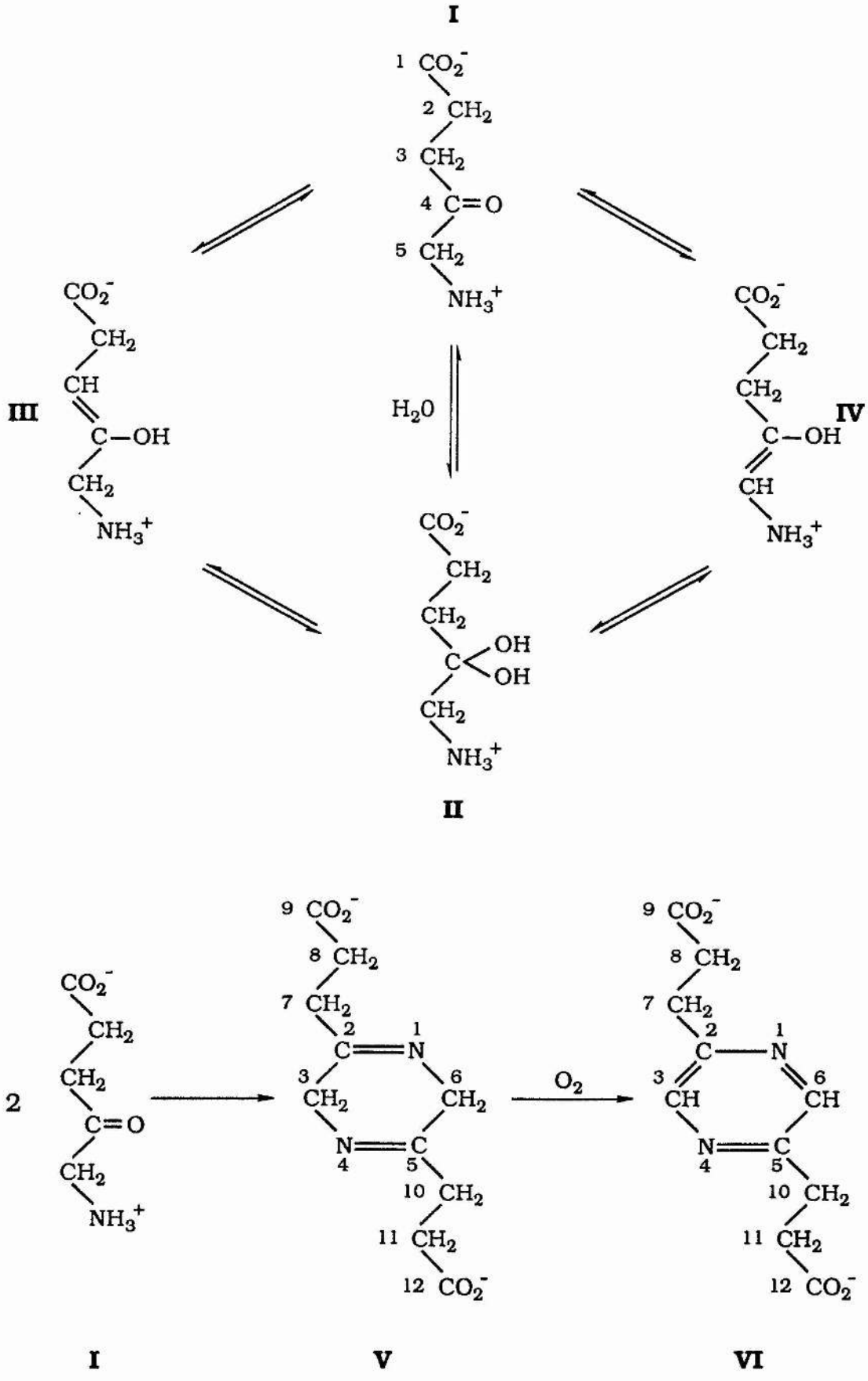

Scheme 3.1

3.1 Introduction.

To date, all the proposed reaction mechanisms of the ALA dehydratase catalysed dimerisation of ALA to form PBG consider only the ketone tautomer of ALA as either substrate. In order to understand fully the enzymatic or physiological behaviour of ALA, it is essential to characterise its non-enzymatic aqueous chemistry. ALA, a 4-keto-5-amino acid, can exist in a number of forms in solution. The question of the forms of ALA present under physiological conditions was first addressed by Michini and Jaffe.[1]

NMR studies with [4-^{13}C]ALA.HCl (50% enriched) suggest that under physiological conditions, ALA rapidly equilibrates between the ketone (I), the hydrate at C_4 (II), the C_3-C_4 enol (III) and the C_4-C_5 enol (IV) as illustrated in Scheme 3.1. The latter two tautomers can each exist as two stereoisomers, *E* or *Z*. These alternative structures of ALA may be significant in the enzymatic synthesis or utilisation of ALA. They may therefore be biologically important as active site structures for the three enzymes which form ALA namely, ALA synthase,[2] glutamate-1-semialdehyde transaminase[3] and L-alanine:4,5-dioxovalerate transaminase[4] as well as ALA dehydratase,[5] which is the sole enzyme for ALA utilisation. NMR studies have also elucidated the structures of the condensation products of ALA (V and VI in Scheme 3.1) formed under physiological conditions. The alternative forms of ALA or its autocondensation products may serve as the active neurotoxin in lead poisoning and in many neuropathic porphyrias[6] (acute intermittent porphyria and plumboporphyria) characterised by elevated ALA levels. A pyrazine, probably a derivative of ALA has been reported in the urine of patients suffering from acute intermittent porphyria.[7]

The ^{13}C NMR spectrum of [4-^{13}C]ALA.HCl (50% enriched) in potassium phosphate (KPi) buffer was used to observe directly the equilibrium distribution of the forms of ALA and demonstrated that the predominant species in solution is the ketone. The mole fraction of the hydrate is about 0.49%. Although direct observation of the enol forms of ALA has not been achieved from the ^{13}C NMR spectrum of [4-^{13}C]ALA.HCl (50% enriched), enol formation has been indirectly demonstrated by monitoring hydrogen exchange at the C_3 and C_5 methylene groups of ALA by ^1H NMR in D_2O. In the past however, extreme conditions of acid or base have been utilised to incorporate deuterium and/or tritium into the C_3 or C_5 positions of ALA through enolisation.[8-10]

3.2 Experimental.

3.2.1 Materials.

ALA.HCl, D_2O (99.8%) and GAL-PAC were purchased from Sigma Chemical Company. The GAL-PAC powder was reconstituted with 3.8 litres of water to prepare a 0.1 M KPi buffer solution, pH 7.6, which was adjusted to pH 6.8 by the addition of 1 M HCl. Where required, KPi buffer was lyophilised in 0.5 ml aliquots, which were then lyophilised from D_2O (99.8%) and stored dry until needed. [4-^{13}C]ALA.HCl (50% enriched) was prepared as described in Section 2.2.3. Celite, 1,4-dioxane, disodium hydrogen phosphate, formaldehyde (37 weight % solution in water), manganese chloride, 10% palladium on charcoal, sodium acetate trihydrate, sodium hydrogen carbonate and sodium hydroxide pellets were purchased from Aldrich Chemical Company. Glacial acetic acid was purchased from Rhône Poulenc Limited and $H_2{}^{17}O$ (12% atom) from Yeda Isotopes Limited, Israel.

Sodium acetate-acetic acid buffer, pH 4.6, was prepared by mixing 49 ml of 0.1 M $NaOAc.3H_2O$ and 51 ml of 0.1 M AcOH.[11] Carbonate buffer, pH 10, was prepared by mixing 50 ml of 0.05 M $NaHCO_3$ and 10.7 ml of 0.1 M NaOH and diluting to 100 ml with distilled water.[11] Phosphate buffer, pH 11.9, was prepared by mixing 50 ml of 0.05 M Na_2HPO_4 and 23 ml of 0.1 M NaOH and diluting to 100 ml with distilled water.[11]

3.2.2 Instrumentation and General Techniques.

^1H and ^{13}C NMR spectra were obtained in exactly the same way as described in Section 2.2.2 D. Unless otherwise specified, ^1H spectra were referenced with respect to external dioxane set at δ 3.7 and ^{13}C spectra were referenced with respect to external dioxane set at δ 67.4.

^{17}O NMR spectra were obtained at 67.798 MHz on a Bruker MSL 500 spectrometer using 16 K data points. ^{17}O spectra were acquired unlocked in a 10 mm high resolution probe using a pulse width of 26 μs (27 μs for a 90° flip angle) a recycle time of 0.41 s and a spectral width of 100,000 Hz. They were referenced with respect to water as an internal standard, set at δ 0 and were ^1H decoupled.

Unless otherwise specified, all spectra were acquired at a probe temperature of 37 °C.

The Griffin digital pH meter used for all pH measurements was checked against a known standard before each measurement and pH values were all recorded at 25 °C.

3.3 Results and Discussion.

3.3.1 ^{13}C NMR of [4-^{13}C]ALA.HCl (50% enriched).

The ^{13}C NMR spectrum of 0.25 M [4-^{13}C]ALA.HCl (50% enriched) in 0.1 M KPi buffer, pH 6.8 (Fig. 2.2), reveals eight signals when processed with a 2 Hz exponential line broadening function. The spectrum was acquired using a D_2O capillary insert to provide the lock signal. The signals are of similar line width and were therefore approximately quantified by peak integrals. The chemical shift assignments of the predominant ketone isomer are listed in Table 3.1 and an explanation for the observed splitting patterns of the C_3 and C_5 resonances has been made in Chapter 2. Three additional resonances are observed at δ 174.0, 153.4 and 93.4 respectively, at 0.10, 0.23 and 0.49% the intensity of the C_4 carbonyl resonance. The signal at δ 93.4 is assigned to the C_4 carbon atom of the hydrate (II) (Scheme 3.1), on the basis of the ^{13}C chemical shifts for hydrates which appear in the region, 85-100 ppm[12] and on the basis of ^{17}O NMR studies described below. The signals at δ 174.0 and 153.4 are assigned to the C_2,C_5 carbon atoms of the dihydropyrazine (V) and pyrazine (VI) products respectively (Scheme 3.1), formed by the dimerisation of two molecules of ALA. ^{13}C NMR studies of the condensation products of ALA described below formed the basis of the latter assignments. The C_4 carbon atom of II and the C_2,C_5 carbon atoms of V and VI are all derived from the isotopically enriched C_4 carbon atom of ALA and are therefore enriched in ^{13}C to the extent of 50%. As a result, they are readily detected in the ^{13}C NMR spectrum of [4-^{13}C] ALA.HCl (50% enriched) even when present in such a small amounts in solution (0.06%-0.5%).

Table 3.1 $^{13}C^{(a)}$ and $^{1}H^{(b)}$ NMR chemical shifts of I, II, III and IV (Scheme 3.1).

Compound	Carbon	Chemical shift[(c)]	Proton	Chemical shift[(d)]
I	C_1	177.7		
	C_2	28.2	2-CH_2	2.70 (t), J =6.38 Hz
	C_3	34.8	3-CH_2	2.90 (t), J =6.38 Hz
	C_4	204.2	5-CH_2	4.14 (s)
	C_5	47.5		
II	C_4	93.4	2-CH_2	2.56 (t), J =7.74 Hz
			3-CH_2	2.06 (t), J =7.74 Hz
			5-CH_2	3.10 (s)
V	C_2,C_5	174.0	3,6-CH_2	4.11 (s)
			7,10-CH_2	2.49 (t), J =6.38 Hz
			8,11-CH_2	2.63 (t), J =6.38 Hz
VI	C_2,C_5	153.4	3,6-CH	8.48 (s)
			7,10-CH_2	2.78 (t), J =6.38 Hz
			8,11-CH_2	3.11 (t), J =6.38 Hz

(a) ^{13}C NMR chemical shifts were obtained with 0.25 M [4-^{13}C] ALA.HCl (50% enriched) in 0.1 M KPi buffer, pH 6.8, at 37 °C, using a D_2O capillary insert.

(b) ^{1}H NMR chemical shifts were obtained with 1 M ALA.HCl in lyophilised 0.1 M KPi buffer, pH 6.8 (99.8% D_2O), at 37 °C.

(c) In ppm, with reference to external dioxane set at δ 67.4.

(d) In ppm, with reference to external dioxane set at δ 3.7.

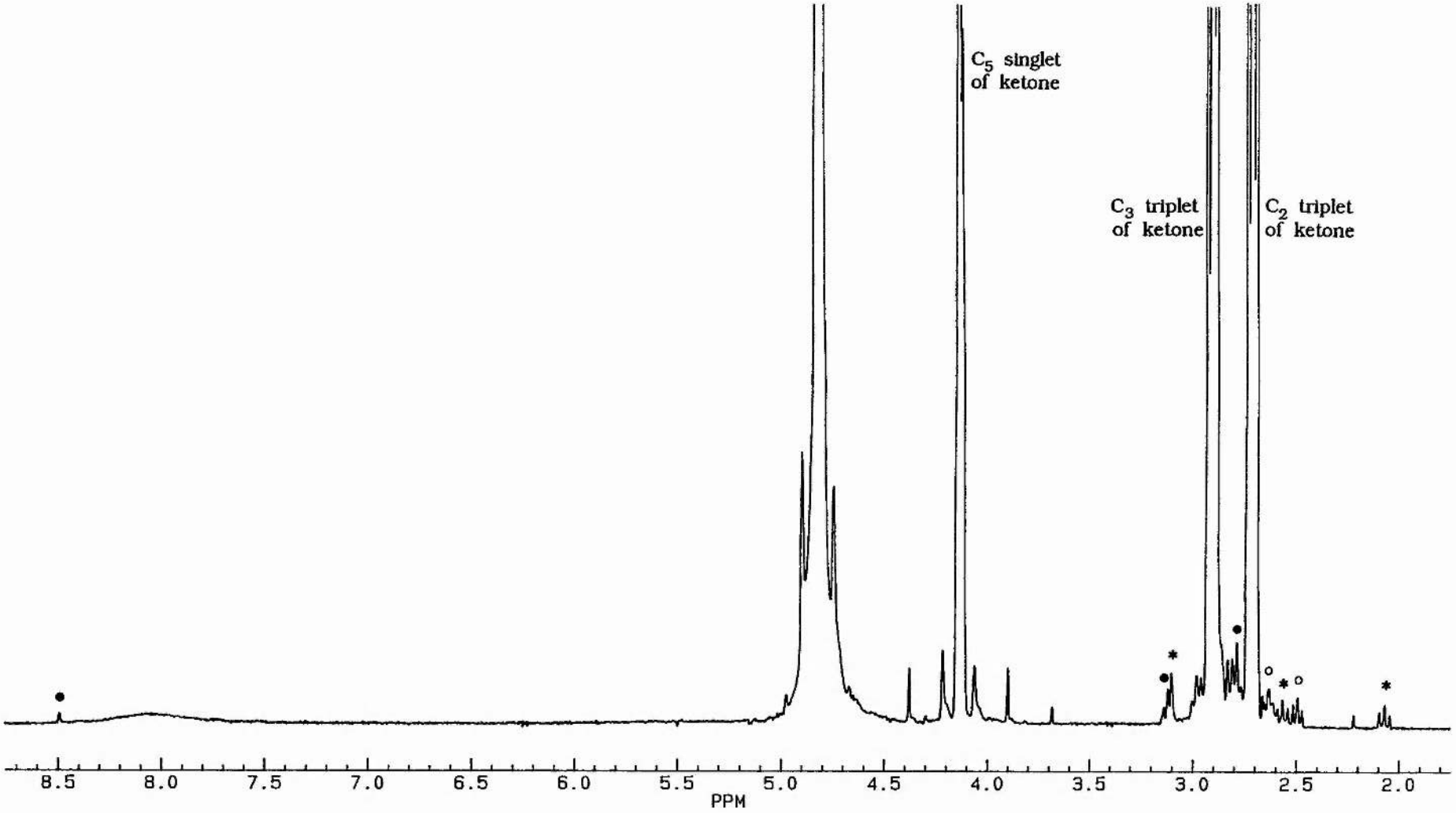

Figure 3.1 300.134 MHz ^{1}H NMR spectrum of 1 M ALA.HCl in 0.1 M lyophilised KPi buffer, pH 6.8 (99.8% D_2O), at 37 °C; * denotes peaks of the hydrate form of ALA; ∘ denotes peaks of the dihydropyrazine; • denotes peaks of the pyrazine.

3.3.2 ^{1}H NMR to probe the structures of the minor forms of ALA.

The ^{1}H NMR spectrum of a 1 M solution of unlabelled ALA.HCl in 0.1 M lyophilised KPi buffer, pH 6.8 (99.8%, D_2O) (Fig 3.1), contains three major peaks (Table 3.1), corresponding to the ketone form (I) (Scheme 3.1) of ALA; a singlet at 4.14 ppm from the C_5 methylene and two triplets at 2.90 and 2.70 ppm from the C_3 and C_2 methylenes respectively. A further three sets of peaks (Table 3.1) each contain a singlet and two triplets shown to be coupled by homonuclear decoupling.

The methylene protons of the hydrate form (II) of ALA (Scheme 3.1) are expected to exhibit a set of ^{1}H NMR signals upfield from the corresponding ketone methylene groups. The α-methylene protons of the hydrate are predicted to be 0.7-0.9 ppm upfield from those of the ketone isomer, and the β–methylene protons are expected to be 0.14-0.20 ppm upfield from the parent signal.[13] One set of resonances of almost equal intensity fall within this prediction; there is a singlet 1.04 ppm upfield from the C_5 methylene signal, a triplet 0.84 ppm upfield from the C_3 methylene signal and a second triplet 0.14 ppm upfield from the C_2 methylene signal of the ketone form of ALA (indicated by * in Fig. 3.1). The two triplets are shown to be coupled by homonuclear decoupling. On the basis of this spectrum, 0.4% is the mole fraction of the hydrate form of ALA in aqueous solution, calculated from the intensities of the C_2 methylene protons of the ketone and hydrate forms of ALA.

The singlet at 4.11 ppm and the two spin-spin coupled triplets at 2.63 and 2.49 ppm are assigned to the C_3,C_6, C_7,C_{10} and C_8,C_{11} methylene protons respectively of the dihydropyrazine (V) (Scheme 3.1) (indicated by ◦ in Fig. 3.1). The singlet at 4.11

ppm which lies masked by the C_5 resonance of the ketone form of ALA at 4.14 ppm, can only be observed by applying a Gaussian multiplication function on the free induction decay. This optimises resolution enhancement of the spectrum. The singlet at 8.48 ppm and the two spin-spin coupled triplets at 3.11 and 2.78 ppm are assigned to the C_3,C_6 methine and C_7,C_{10} and C_8,C_{11} methylene protons respectively of the pyrazine (VI) (Scheme 3.1) (indicated by • in Fig. 3.1). An examination of the intensities of the C_2 protons of the ketone isomer and the C_8,C_{11} methylene protons of V and VI suggests that the upper limit for the mole fractions of V and VI in aqueous solution are 0.64% and 0.69% respectively.

3.3.3 Oxygen Exchange at C_4 of ALA to probe the existence of the C_4 hydrate.

Supporting evidence for the formation and breakdown of the hydrate of ALA was demonstrated by monitoring oxygen exchange at C_4.[1,14] Oxygen exchange was followed by ^{18}O incorporation from $H_2{}^{18}O$ into [4-^{13}C]ALA.HCl (90% enriched) by ^{13}C NMR. The ^{13}C chemical shift change expected when ^{18}O replaces ^{16}O in an aldehyde or ketone is 0.045-0.050 ppm upfield.[15] When [4-^{13}C] ALA.HCl (90% enriched) was dissolved in 0.1 M KPi buffer, pH 6.8, 50% $H_2{}^{18}O$, the incorporation of ^{18}O into C_4 was complete in less than 20 minutes at room temperature ($t_{1/2} < 5$ min), demonstrating the facile formation and breakdown of the C_4 hydrate. The observed isotope shift was -0.046 ppm (3.5 Hz) at 37 °C.

We have further supplemented evidence for the formation and breakdown of the hydrate of ALA, by monitoring ^{17}O exchange at C_4 of ALA by ^{17}O NMR spectroscopy not hitherto reported. The ^{17}O spectra of a large number of liquid organic compounds have been studied by Christ *et al.*[16] Their data provide the basis for the systematisation of the ^{17}O chemical shifts. They showed that the ^{17}O resonances of neat aldehydes and ketones fall in the range 530 to 595 ppm relative to $H_2{}^{17}O$ as an external standard at 0 ppm, while the ^{17}O resonances of the hydroxyl group of alcohols fall near the water line (-37 to +70 ppm). In aqueous solutions of carbonyl compounds, known to be hydrated, an ^{17}O resonance due to the *gem*-diol grouping should appear and is expected to fall in the range of the ^{17}O shift, characteristic of the hydroxylic oxygen. Greenzaid *et al* [13] were able to detect signals in this range due to hydrated species of a number of carbonyl compounds. This group of workers have also found the ^{17}O NMR chemical shifts of the

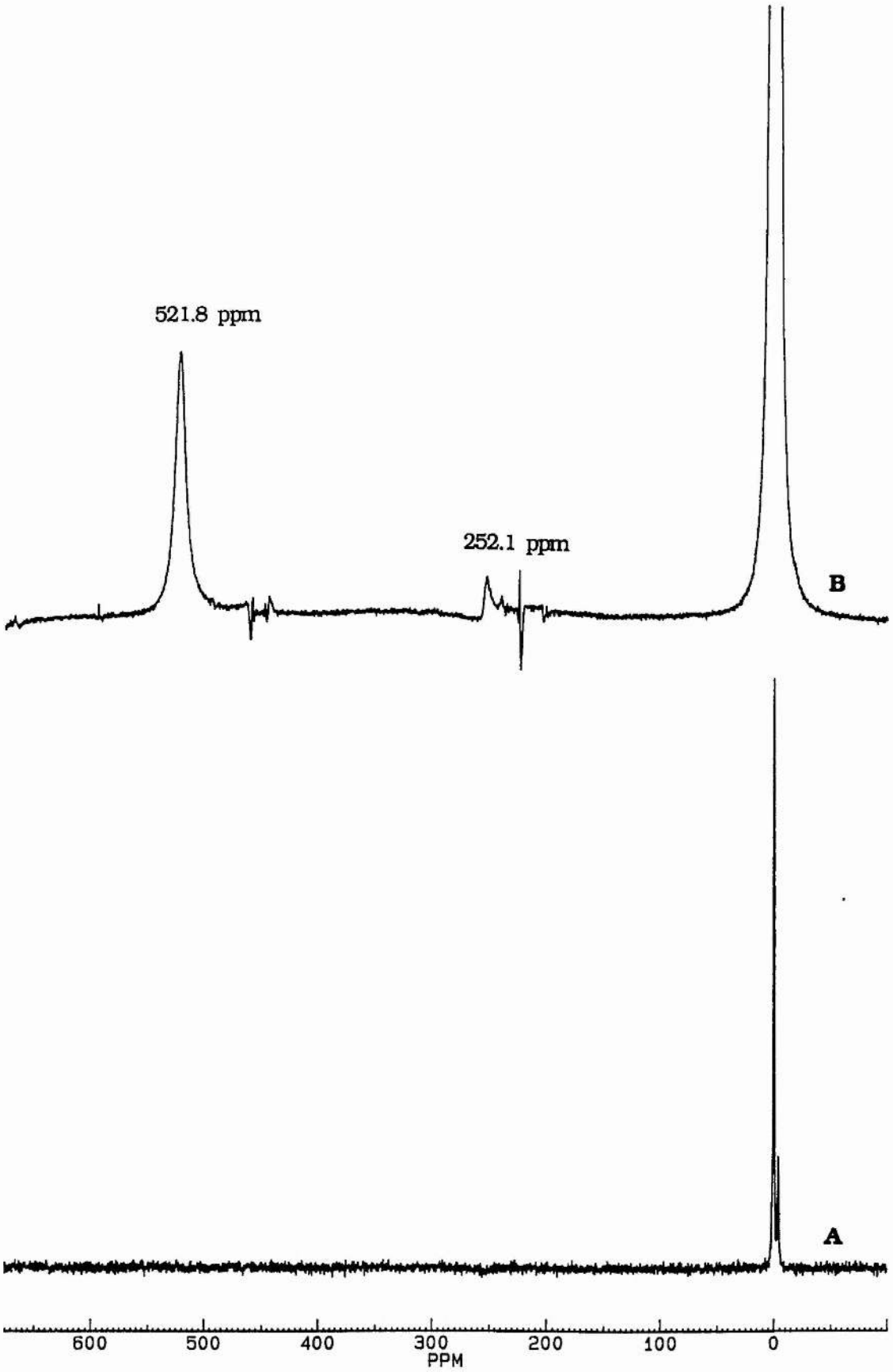

Figure 3.2 ^{1}H decoupled 67.798 MHz ^{17}O NMR spectra of 1 M ALA.HCl at 37 °C, **(A)** in ordinary H_2O and **(B)** in $H_2{}^{17}O$ (4% atom).

carbonyl oxygen and to a lesser extent those of the *gem*-diol grouping to shift to high field upon dilution.

The ^{17}O NMR spectra of 1 M ALA.HCl in ordinary water and in $H_2{}^{17}O$ (4% atom) [Fig. 3.2 (A) and Fig. 3.2 (B) respectively], were acquired after equilibrating the respective solutions of ALA.HCl in a thermostat at 37 °C for 10 minutes. The ^{17}O NMR spectrum of 1 M ALA.HCl in ordinary water reveals only the natural abundance $H_2{}^{17}O$ resonance at δ 0. The ^{17}O NMR spectrum of 1 M ALA.HCl in $H_2{}^{17}O$ (4% atom) however, reveals in addition to the $H_2{}^{17}O$ resonance at δ 0, the ^{17}O carbonyl resonance of ALA at δ 521.8 and a resonance at δ 252.1. The latter resonance is within the range characteristic of the carboxyl group and is therefore ascribed to the carboxyl group of ALA. This resonance, unlike the ketone resonance of ALA, was not observed immediately after a few scans, but rather increases with time, owing to the slow exchange of the carboxyl group. The rapid proton exchange in carboxylic acids between

leads to only one, time averaged ^{17}O NMR signal.

The signal due to the *gem*-diol oxygens of the hydrate form of ALA could not be detected, probably because of its low intensity and proximity to the strong water line. This was the case even with $H_2{}^{17}O$ (12% atom), and water suppression with 0.1 M manganese chloride. Greenzaid *et al* [13] have reported that acetone and monochloroacetone which exist over 99% in the unhydrated form exhibit only a single resonance due to the carbonyl oxygen at δ 523.0 and δ 528.0 respectively. No signal due to the *gem*-diol oxygens of the hydrate forms could be seen. However, the very fact

that the ^{17}O carbonyl oxygen of ALA shows up in the spectrum of ALA.HCl dissolved in $H_2{}^{17}O$ (4% atom) suggests that there is an isotope exchange reaction between ALA and the solvent $H_2{}^{17}O$, *via* the *gem*-diol or hydrate form (II) (Scheme 3.1) of ALA.

The mechanism of oxygen exchange at C_4 of ALA is probably through hydration and dehydration as illustrated in Scheme 3.2.

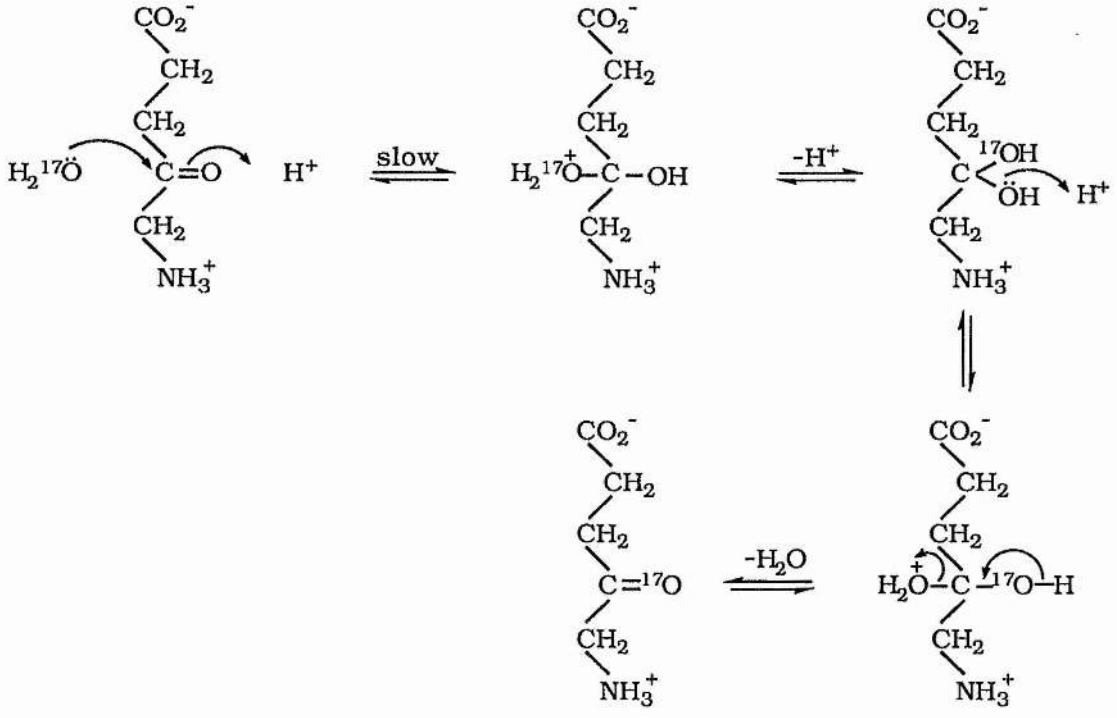

Similarly,

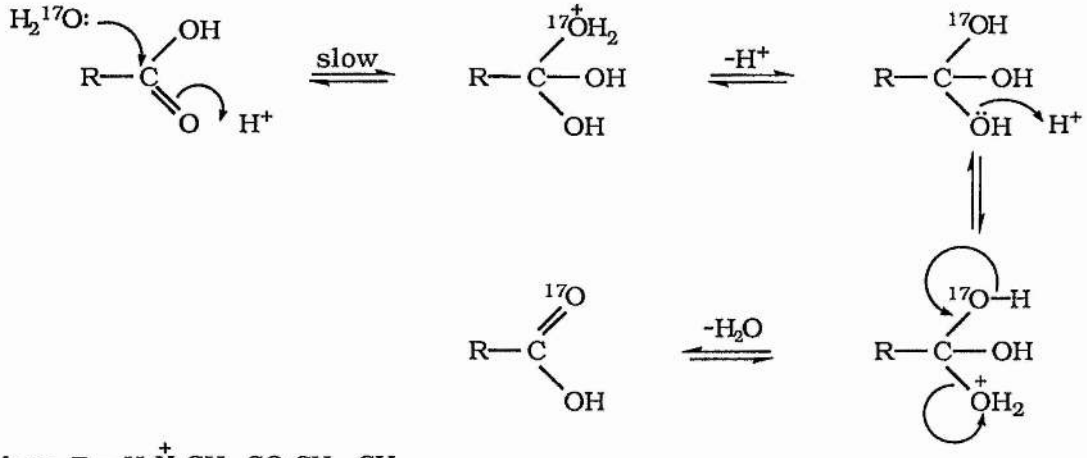

where R = $H_3\overset{+}{N}$-CH_2-CO-CH_2-CH_2

Scheme 3.2

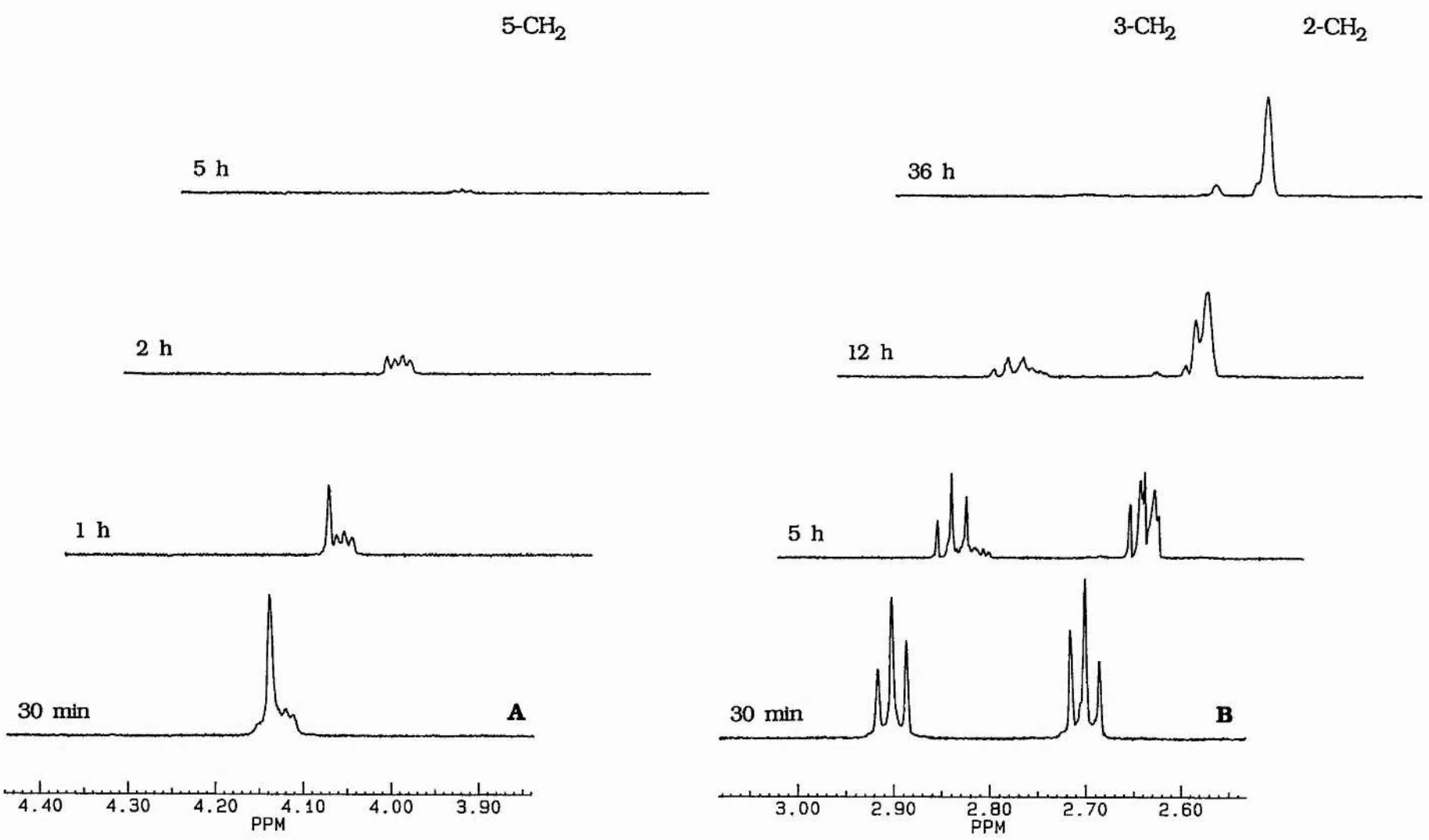

Figure 3.3 300.134 MHz ^{1}H NMR spectra of ALA.HCl (10 μmol) in 0.1 M lyophilised KPi buffer, pH 6.8, (99.8% D_2O), during deuterium exchange through enolisation at 37 °C. **(A)** Successive deuteration at C_5. **(B)** Successive deuteration at C_3.

3.3.4 Deuterium exchange to probe the existence of the enol tautomers of ALA.

ALA.HCl (10 μmol) was dissolved with one aliquot of 0.1 M lyophilised KPi buffer, pH 6.8, in 0.5 ml D_2O (99.8%). The time of ALA dissolution was defined as zero and the sample was immediately placed in a 5 mm NMR tube and inserted into the NMR probe which had been equilibrated at 37 °C. Spectra (Fig. 3.3) were acquired at appropriate time intervals to monitor the loss of protons at C_3 and C_5 and were processed using resolution enhancement.

The spectra (Fig. 3.3) reveal that at C_5, CH_2 is a singlet at 4.14 ppm and CHD is an isotope shifted 1:1:1 triplet at 4.12 ppm, J_{HD} = 2.62 Hz. For C_3, which is coupled to the methylene protons at C_2, the protons from the CH_2 species exhibit a 1:2:1 triplet line shape at 2.90 ppm, J_{HH} = 6.38 Hz; CHD is a 1:2:1 triplet of 1:1:1 triplets, which is difficult to decipher. Isotope exchange at C_3 can also be monitored by the structure of the signals from the C_2 protons. When adjacent to CH_2 the C_2 proton signal is a 1:2:1 triplet at 2.705 ppm, J_{HH} = 6.38 Hz. When adjacent to CHD, the C_2 proton signal is an isotope shifted doublet at 2.70 ppm, J_{HH} = 6.38 Hz, and the signal is slightly broadened by unresolved coupling to deuterium atoms. When adjacent to CD_2, the C_2 proton signal is a singlet at 2.69 ppm, substantially broadened by unresolved coupling to the deuterium atoms.

Thus the protons at C_3 and C_5 of ALA are labile to deuterium exchange through enolisation. The evolution from CH_2 to CD_2 can be monitored by ^1H NMR as total proton loss and by analysis of peak multiplicity.

Jaffe and Rajagopalan[14] have calculated the exchange rates of

protons at C_3 and C_5 of ALA under a variety of conditions. The most rapid exchange was observed at pH 6.8 in 0.1 M KPi buffer with the half-times for proton exchange at C_3 and C_5 being approximately 2 and 0.5 hours respectively. When the pH was lowered to 6.3, 50 mM KPi buffer, the half times for proton exchange at C_3 and C_5 were found to increase to 6.9 and 0.9 hours respectively. In all the zwitterionic buffers tested at 0.1 M, pH 6.8, (BES, HEPES, PIPES, MOPS and TES), proton exchange on ALA was substantially slower than in KPi.

Jaffe and Rajagopalan[14] have also found 5-chlorolevulinic acid and levulinic acid to undergo deuterium exchange at C_3 and C_5 which can be monitored by ^1H NMR. They found the half time for deuteration at C_5 of 5-chlorolevulinic acid to be almost identical to that for ALA and exchange of the C_3 protons to be about three times slower (in 0.1 M KPi buffer, pH 6.8, 37 °C). The half-times for deuteration of levulinic acid, which does not contain a C_5 substituent were calculated to be two orders of magnitude slower than for ALA, about 12 and 29 days for C_3 and C_5 respectively (in 0.1 M KPi buffer, pH 6.8, 37 °C). Thus both the amino group of ALA and the chloro group of 5-chlorolevulinic acid significantly enhance the enolisation rates of both C_3 and C_5.

In order to explain why this reaction is 12 fold slower for ALA in TES than in KPi buffer, Jaffe and Rajagopalan[14] have suggested that the phosphate buffer may act as a general base through electrostatic catalysis [Fig. 3.4(A)] and enhance the rate of enolisation at C_3 of ALA. In the case of 5-chlorolevulinic acid, the absence of such electrostatic catalysis at C_3 may account for the slower enolisation rate at C_3 relative to ALA. At C_5, the phosphate buffer may still act as a general base abstracting a proton as shown

in Fig. 3.4(B), but the rate of enolisation at C_5 is almost the same for ALA and 5-chlorolevulinic acid probably because of high kinetic acidities of the protons at C_5.

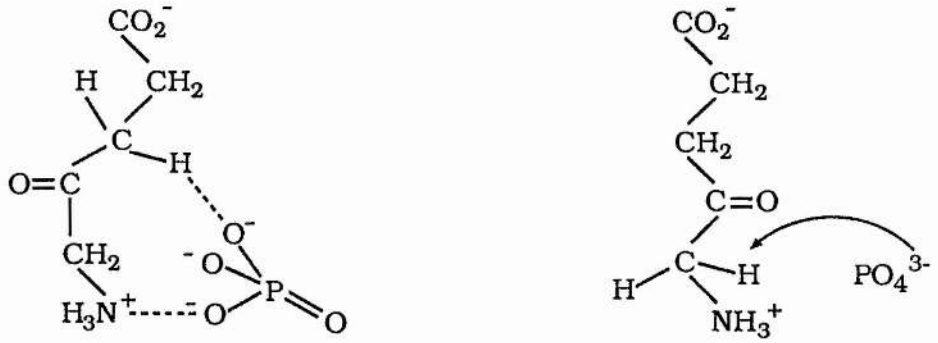

A **B**

Figure 3.4 Potential mechanism for KPi buffer catalysis of proton exchange **(A)** at C_3 and **(B)** at C_5 of ALA.

In TES buffer, the sulphonate group is too weak a base to abstract protons and the amino group is the only other general base. It has been previously observed[17] that proton exchange rates for aminoketones are enhanced approximately ten-fold by anionic bases such as carboxylate anion compared to neutral bases such as pyridine. This effect has been attributed to electrostatic catalysis by the oppositely charged buffer acting as the general base.

Simple ketones exhibit isomers analogous to I, II, III and IV at a ratio of about 10^5:200:1:1.[18] For ALA, the mole fraction of the hydrate is comparable to the value expected. The mole fractions of the enol forms of ALA maybe as low as 0.001% as in the case of simple ketones.

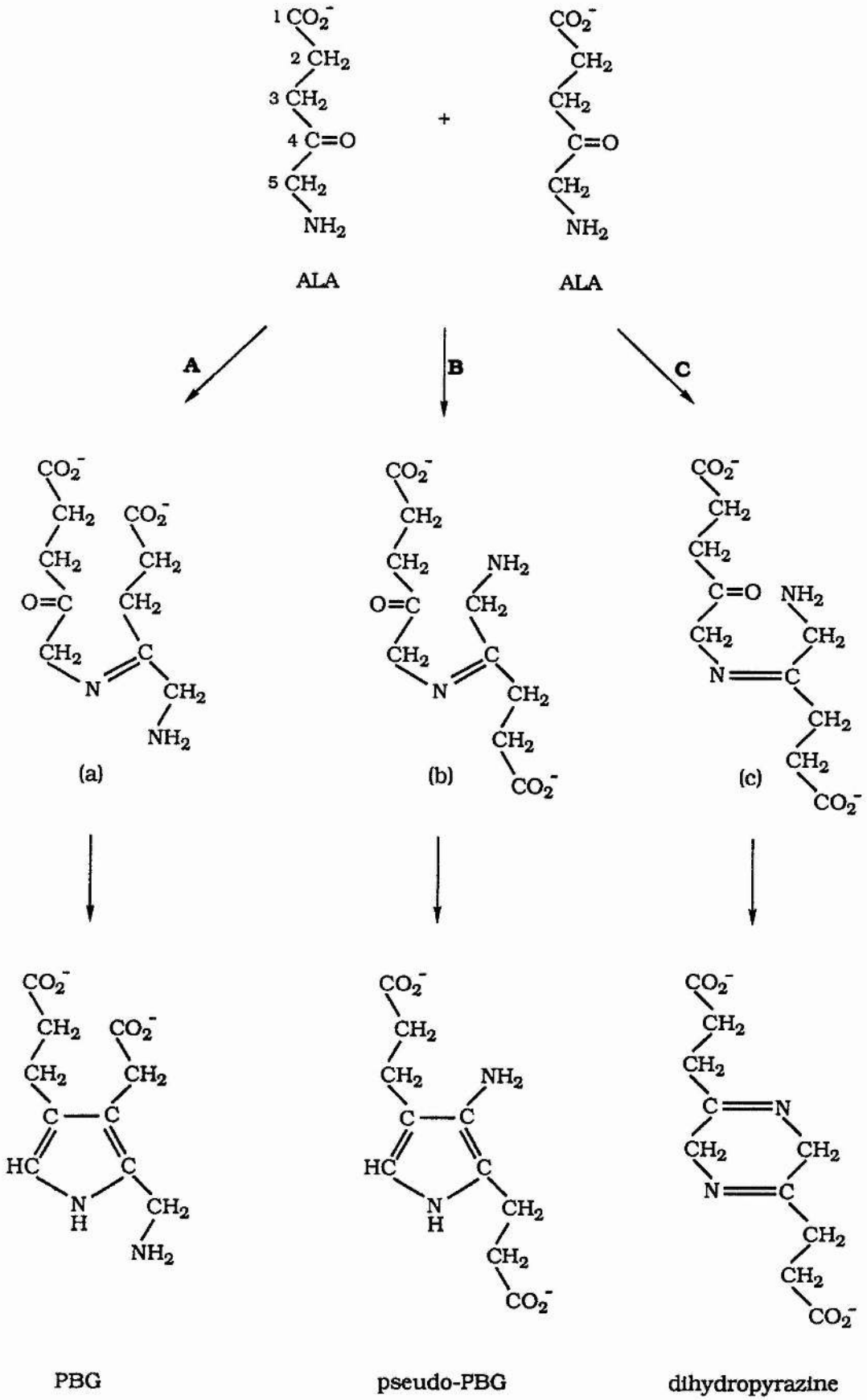

Scheme 3.3

3.3.5 Condensation Products of ALA.

The dimerisation of ALA to form a heterocyclic product can proceed *via* three different routes (Scheme 3.3). Enzymatic catalysis drives the reaction exclusively through route A. However, when the chemical dimerisation of ALA was studied, conflicting results were reported. Scott[19] reported that anaerobic treatment of ALA with aqueous alkali at 18 °C, gave PBG in 3% yield, after several days. Scott *et al*[20] were unable to substantiate that claim and found that the only product formed in over 70% yield was pseudo-PBG. The formation of pseudo-PBG differs from that of PBG by proceeding *via* the *Z*-form (b) of the intermediary Schiff-base and not *via* the *E*-form (a) as for PBG (Scheme 3.3). Scott *et al*[20] also reported that ALA was converted into PBG in 10% yield in the presence of Amberlite IR-45 after a 20 day incubation.

Granick and Mauzerall[21] found that at pH 6.8-8.0 and 40 °C, the dihydropyrazine was formed in 10% yield. This azomethine reaction is known for other α-aminoketones.

The formation of PBG by the enzyme ALA dehydratase, as well as the formation of pseudo-PBG in the chemical dimerisation of ALA, involve a Knorr type condensation. The difference between the two reactions lies in the mode of addition of the second molecule of ALA to the carbonyl carbon of the first molecule of ALA. In the formation of PBG, C_3 of the second molecule of ALA adds to the carbonyl carbon of the first molecule of ALA, whereas in the formation of pseudo-PBG, C_5 of the second molecule of ALA adds to the carbonyl carbon of the first molecule of ALA. Thus the difference with the enzymatic reaction lies in the lower acidity of the C_3 methylene protons compared with that of the C_5 methylene protons of ALA, which then has to be increased by the enzyme. The

greater acidity of the C_5 methylene protons of ALA was established in Section 3.3.4, where it was shown that they exchange about four times faster than the C_3 methylene protons in 0.1 M KPi buffer, pH 6.8 (99.8% D_2O), by ^1H NMR spectroscopy (Scheme 3.4).

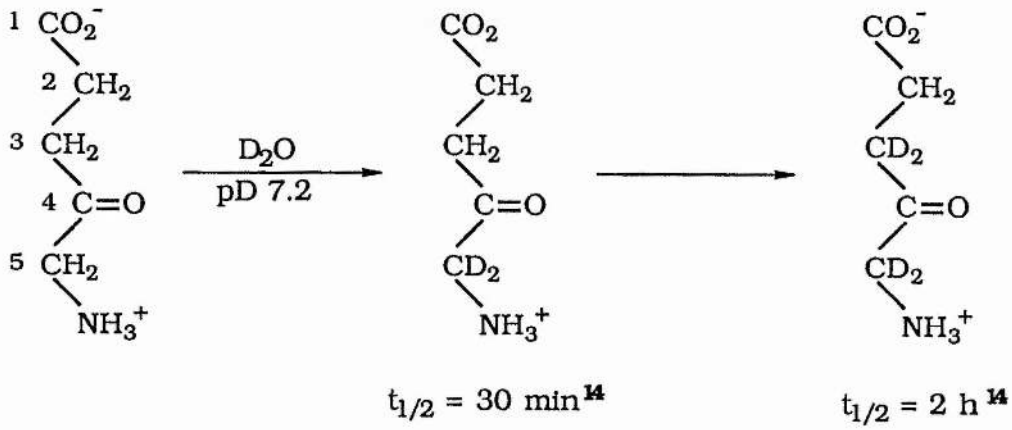

Scheme 3.4

The chemical dimerisation of ALA was investigated under a variety of pHs and it was found that only in strongly alkaline solution were two condensation products formed. This has been discussed in some detail in the following sections of the chapter.

3.3.5.1 Condensation of ALA in acetate, carbonate and phosphate buffers.

The condensation of ALA in acetate buffer, pH 4.6, carbonate buffer, pH 9.7 and phosphate buffer, pH 11.6, was investigated. In each case, ALA (0.25 mmol) was refluxed in 1 ml of the buffer for 6 hours. The solvent was then evaporated, D_2O (99.8%) added, and the reaction mixture analysed by NMR spectroscopy. The only condensation product formed in each of the above buffers was 2,5-bis(2-carboxyethyl)pyrazine (Scheme 3.5).

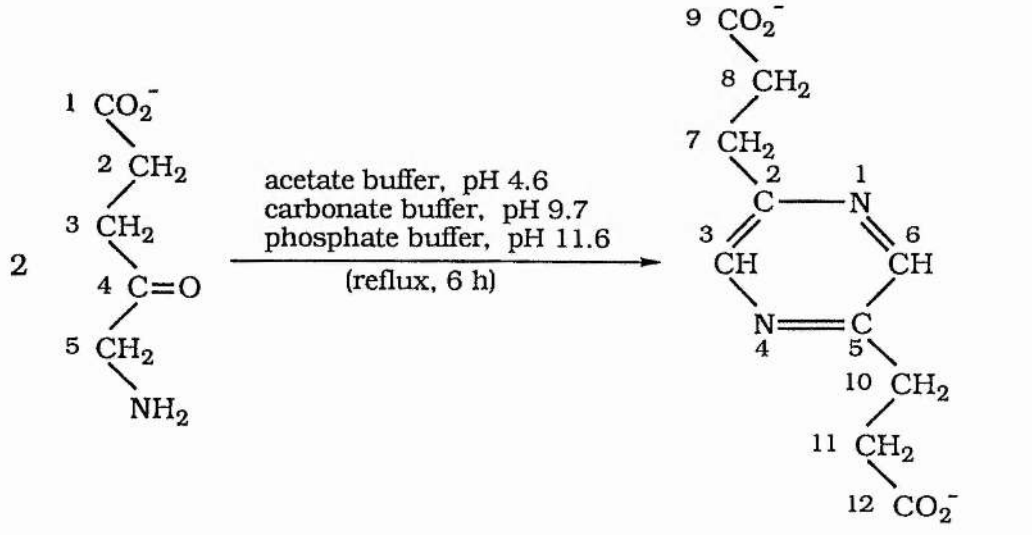

ALA

2,5-bis(2-carboxyethyl)pyrazine

Scheme 3.5

With acetate, carbonate and phosphate buffers respectively there was approximately 95, 15 and 20% conversion of ALA to the pyrazine product. Thus the cyclic dimerisation of ALA at moderate pH gives exclusively a pyrazine product, in a reaction favoured by acid. The proposed mechanism for this reaction is illustrated in Scheme 3.6. Although the amino group of ALA is substantially protonated in acetate buffer, pH 4.6, its pKa is such (8.9) that there will always be some of the free base. Nevertheless, the reaction is

favoured by acid because of the need to protonate the carbonyl group. Protonation will clearly increase the positive character of the carbonyl carbon atom and thereby facilitate nucleophilic attack upon it.

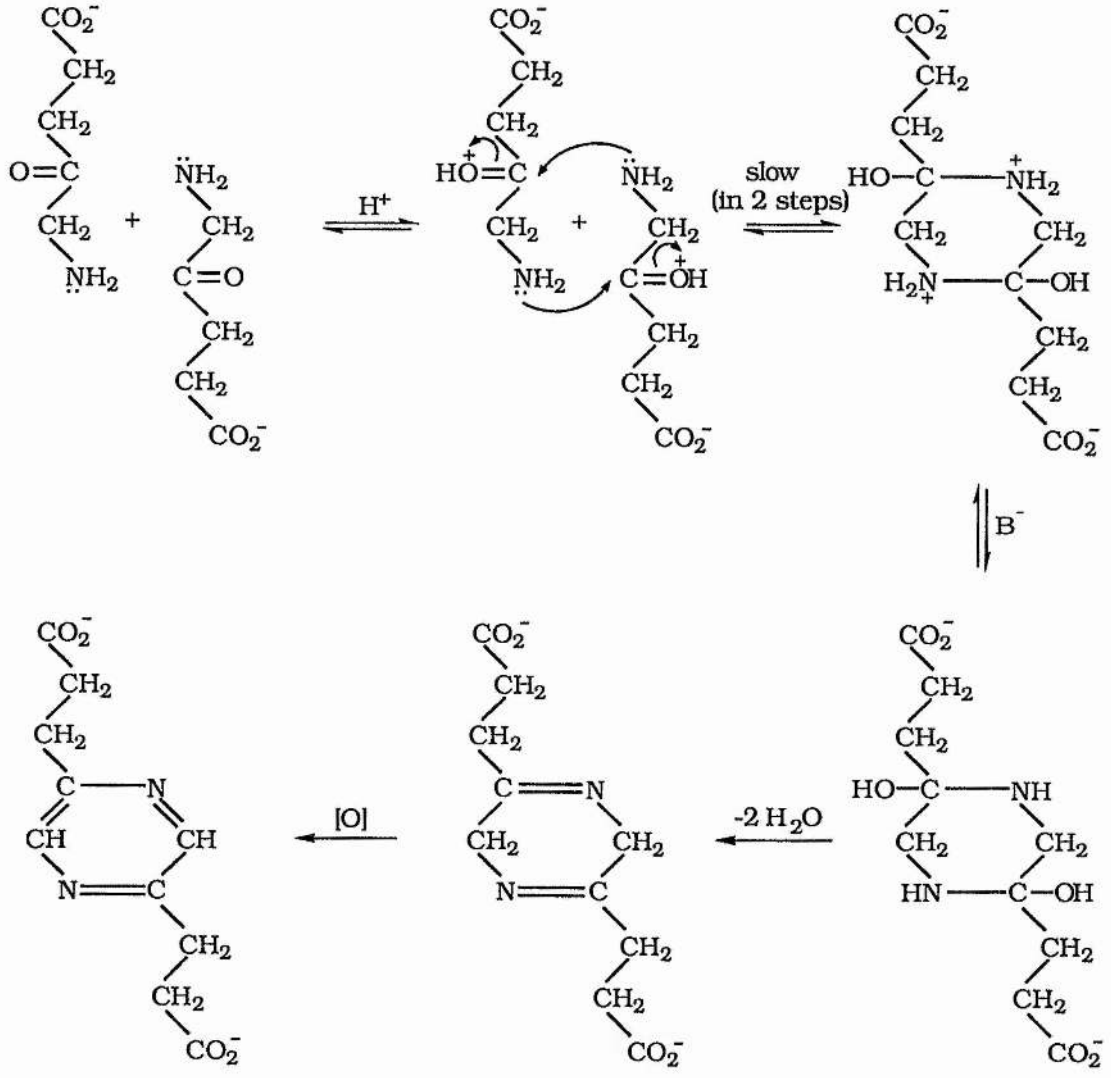

2,5-bis(2-carboxyethyl)-pyrazine

2,5-bis(2-carboxyethyl)-3,6-dihydropyrazine

where B^- is the conjugate base of the buffer under consideration.

Scheme 3.6

No intermediates were detected when the condensation of [4-^{13}C]ALA.HCl (50% enriched) (0.25 mmol), in acetate buffer,

pH 4.6, was probed by ^{13}C NMR spectroscopy, at 40 °C. This result supports the above mechanism (Scheme 3.6), which involves rapid pre-equilibrium proton transfer to the carbonyl oxygens of ALA followed by slow nucleophilic attack of the amino group of one molecule of ALA onto the carbonyl carbon of the second molecule of ALA.

The ^{13}C and ^{1}H NMR chemical shifts of ALA and 2,5-bis(2-carboxyethyl)pyrazine in each of the above buffers are listed in Table 3.2.

Table 3.2 ^{13}C and ^{1}H NMR assignments[a] of ALA and 2,5-bis(2-carboxyethyl)pyrazine in acetate, carbonate and phosphate buffers.

Compound	Carbon	^{13}C chemical shifts[b]			Proton	^{1}H chemical shifts[b]		
		acetate buffer	carbonate buffer	phosphate buffer		acetate buffer	carbonate buffer	phosphate buffer
ALA	C_1	undetected	179.4	179.4				
	C_2	28.6	30.0	30.0	2-CH_2	2.65 (t), J = 6.38 Hz	2.73 (t), J = 6.38 Hz	2.74 (t), J = 6.38 Hz
	C_3	37.2	37.0	37.0	3-CH_2	2.90 (t), J = 6.38 Hz	2.92 (t), J = 6.38 Hz	2.93 (t), J = 6.38 Hz
	C_4	undetected	206.8	206.7	5-CH_2	4.17 (s)	4.16 (s)	4.16 (s)
	C_5	49.1	49.7	49.7				
2,5-bis(2-carboxyethyl)-pyrazine	C_2,C_5	156.0	155.7	155.7				
	C_3,C_6	146.0	145.3	145.4	3,6-CH	8.47 (s)	8.69 (s)	8.65 (s)
	C_7,C_{10}	31.9	31.0	31.1	7,10-CH_2	3.10 (t), J = 7.29 Hz	3.23 (t), J = 6.83 Hz	3.21 (t), J = 6.83 Hz
	C_8,C_{11}	36.1	34.9	35.0	8,11-CH_2	2.79 (t), J = 7.29 Hz	2.91 (t), J = 6.83 Hz	2.92 (t), J = 6.83 Hz
	C_9,C_{12}	180.5	179.2	179.3				

(a) Obtained at room temperature. (b) In ppm downfield with respect to internal DSS set at δ 0.

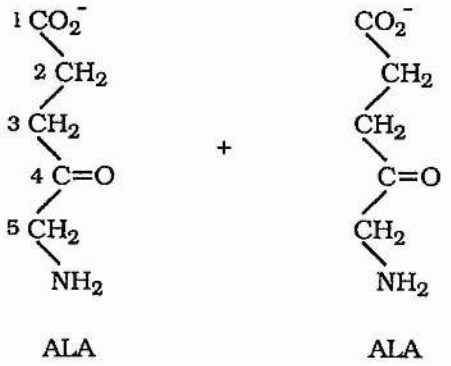

ALA ALA

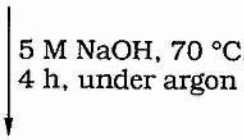

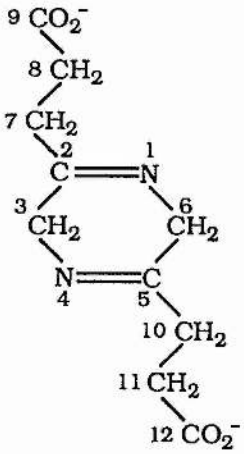

2,5-bis(2-carboxyethyl)-
3,6-dihydropyrazine

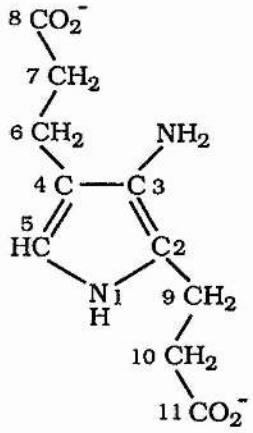

pseudo-PBG

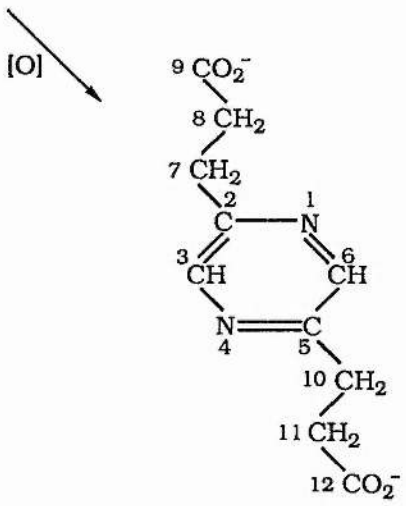

2,5-bis(2-carboxyethyl)pyrazine

Scheme 3.7

3.3.5.2 The anaerobic condensation of ALA in 5 M NaOH.

A deaerated solution of 5 M NaOH (0.5 ml) was added to a deaerated sample of ALA.HCl (0.25 mmol) under a stream of argon (using a vacuum line). The reaction mixture was well stirred at 70 °C in a water bath for 4 hours and then transferred into an evacuated 5 mm NMR tube under argon. It was found that this led to the quantitative conversion of ALA into a mixture of two condensation products. The major and minor products of the reaction, formed in a ratio of 2:1 were identified to be 2,5-bis(2-carboxyethyl)-3,6-dihydropyrazine and pseudo-PBG respectively (Scheme 3.7), on the basis of their ^{13}C and ^{1}H NMR chemical shifts (Table 3.3). The ^{13}C and ^{1}H NMR spectra of the reaction mixture are shown in Fig. 3.5 and 3.6 respectively. The spectra were acquired at a probe temperature of 21 °C, using a D_2O capillary insert and were referenced with respect to internal DSS (set at δ 0 for the ^{13}C and ^{1}H NMR spectra).

Franck and Stratmann[22] had previously incorrectly identified the minor product of this reaction to be PBG, on the basis of the positive Ehrlich test they obtained with this compound. The Ehrlich test is one in which a coloured condensation product, E, is produced by the condensation of an α-unsubstituted pyrrole, P, with *p*-N,N-dimethylaminobenzaldehyde (DMAB) in aqueous sulphuric or perchloric acids[23] (Scheme 3.8). Treibs and Herrman[24] produced a systematic study of the Ehrlich reaction and showed that the coloured salt E can further react with another molecule of P to form a colourless dipyrrylphenylmethane, M (Scheme 3.8). The above workers[24] have also shown that, contrary to what had been thought, a free α-position in the pyrrole is not obligatory for the formation of a coloured product. Electron-

donating (alkyl) substitutents, a free α-position in the pyrrole and also excess of the aldehyde reagent favour the reaction, whereas electronegative substituents or excess of the pyrrole hinder it. These and other aspects of the reaction have been discussed[25-28] in relation to the specificity and sensitivity of the Ehrlich colour reaction.

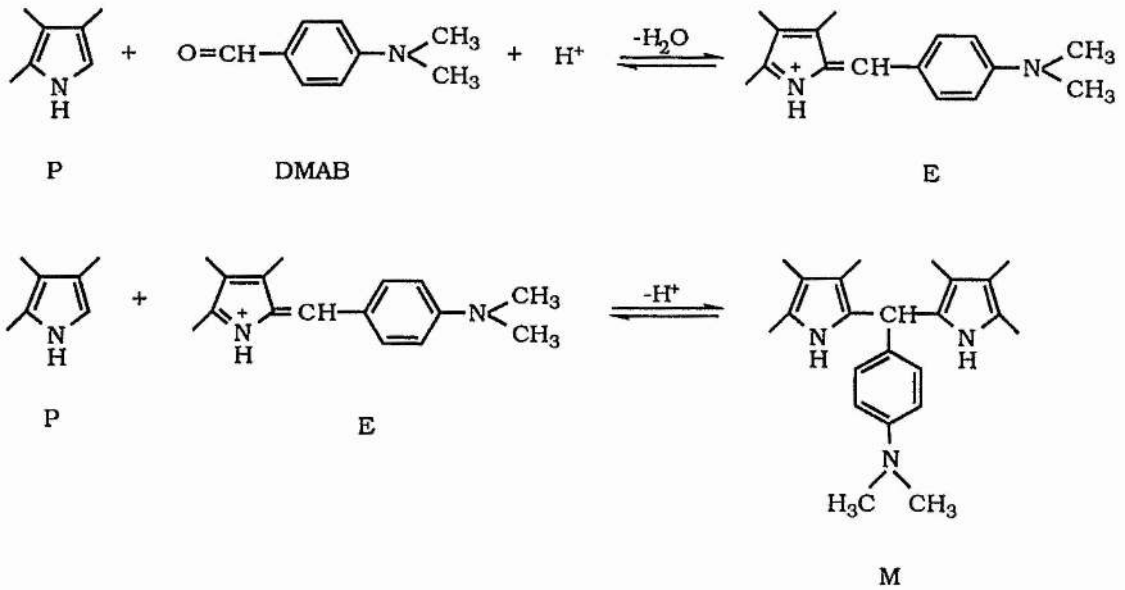

Scheme 3.8

Pseudo-PBG, like PBG has a free α-position and would also give a positive Ehrlich test. However, the two compounds can be readily differentiated from their ^1H NMR spectrum. As seen in Scheme 3.3, pseudo-PBG has two pairs of adjacent methylene groups which would appear as four triplets in its ^1H NMR spectrum. PBG on the other hand has 2 methylene groups adjacent to each other, each of which would appear as a triplet and two non-adjacent methylene groups each of which would appear as a singlet in its ^1H NMR spectrum. The former was what was observed in the case of the minor product formed as a result of the anaerobic condensation of ALA in 5 M NaOH. It was therefore unambiguously

identified as pseudo-PBG.

When the reaction mixture was exposed to air, there was slow and irreversible oxidation of 2,5-bis(2-carboxyethyl)-3,6-dihydropyrazine to 2,5-bis(2-carboxyethyl)pyrazine (Scheme 3.7). The ^{13}C and ^{1}H chemical shifts of the pyrazine product are listed in Table 3.4.

The ^{13}C NMR assignments of 2,5-bis(2-carboxyethyl)-3,6-dihydropyrazine, pseudo-PBG and 2,5-bis(2-carboxyethyl)pyrazine were confirmed by repeating the reaction using [4-^{13}C]ALA.HCl (20% enriched) (0.25 mmol) and exposing the reaction mixture to air. In the case of the dihydropyrazine, the C_2,C_5 resonance appears largely enhanced at 175.2 ppm, since these carbons are 20% enriched in ^{13}C. The C_3,C_6 and C_7,C_{10} methylene resonances at 53.0 ppm and 35.77 ppm respectively each has satellite peaks on either side of the parent signal and one eighth the intensity of the latter ($^{1}J_{C_2C_3}$ = 36.6 Hz; $^{1}J_{C_2C_7}$ = 47.7 Hz). The resonances at 35.71 and 183.7 ppm were assigned to the C_8,C_{11} and C_9,C_{12} carbons respectively, their intensities being greater than the remaining methylene and carboxyl resonances in the spectrum.

In the case of pseudo-PBG, two resonances, one at 117.3 ppm ($^{2}J_{C_2C_4}$ = 6.43 Hz) and the other at 120.4 ppm ($^{2}J_{C_2C_4}$ = 6.43 Hz), appear largely enhanced suggesting that these are resonances from carbons C_4 and C_2 which are 20% enriched in ^{13}C. However, these two resonances cannot be unambiguously assigned. The resonances at 114.3 and 125.1 ppm are assigned to the C_5 and C_3 carbons respectively ($^{1}J_{C_4C_5}$ = 56.1 Hz; $^{1}J_{C_2C_3}$ = 82.1 Hz and $^{1}J_{C_3C_4}$ = 58.8 Hz or vise versa). The resonances at 23.1 and 23.8 ppm each have satellite peaks on either side of the parent signal and about one eighth the intensity of the latter. These therefore correspond to

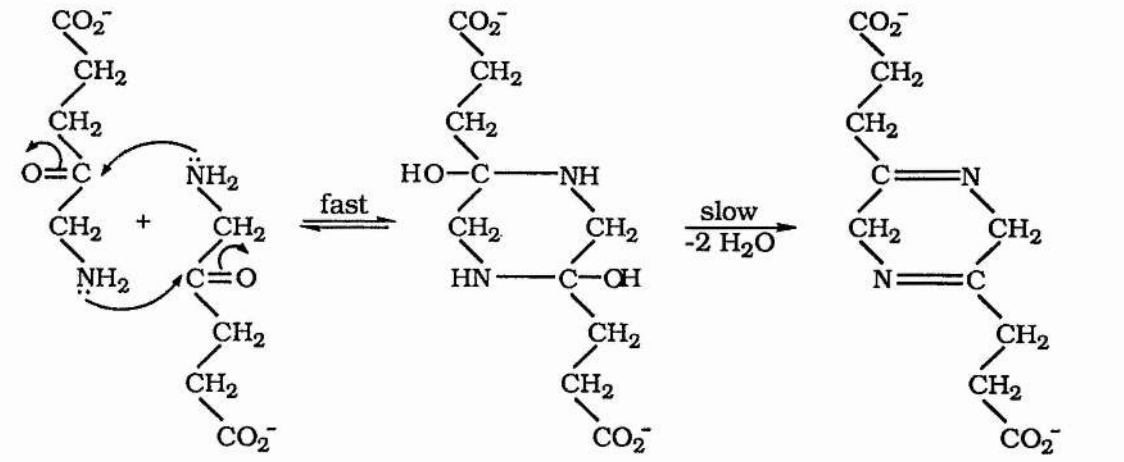

I

2,5-bis(2-carboxyethyl)-
3,6-dihydropyrazine

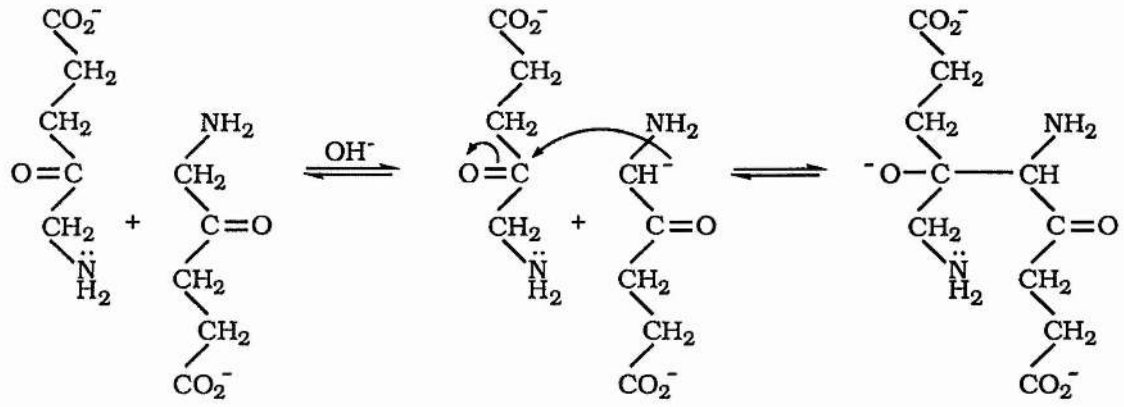

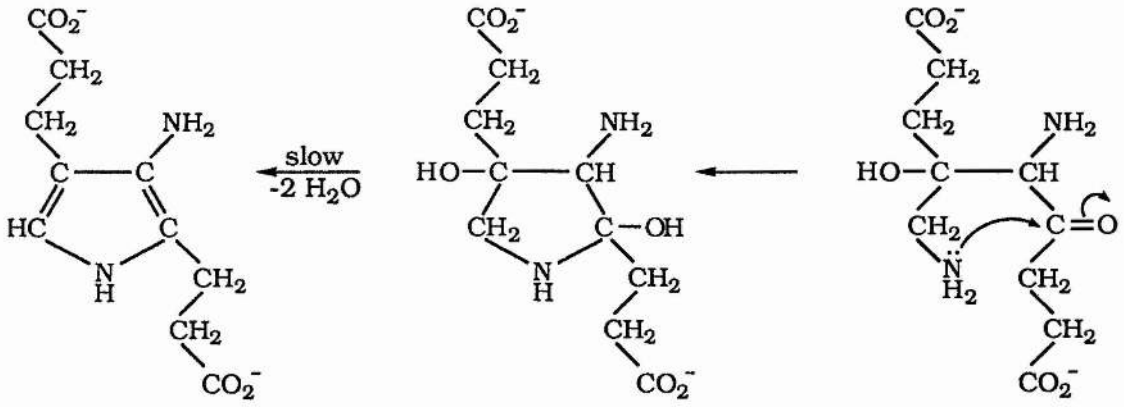

pseudo-PBG

II

Scheme 3.9

the C_6 and C_9 resonances although they cannot be unambiguously assigned. The resonance at 23.1 ppm has satellite peaks which lie 46.1 Hz apart and the resonance at 23.8 ppm has satellite peaks which lie 48.3 Hz apart. Resonances at 39.8 ppm and 40.3 ppm correspond to the methylene carbons C_7 and C_{10} or vice versa and the resonances at 184.6 and 185.2 ppm correspond to C_8 and C_{11} or vice versa.

In the case of the pyrazine which is formed by the slow irreversible oxidation of the dihydropyrazine, the C_2,C_5 resonance appears enhanced at 156.3 ppm, since these carbons are 20% enriched in ^{13}C. The resonances at 145.3 ($^1J_{C_2C_3}$ = 57.2 Hz) and 183.8 ppm were unambiguously assigned to the C_3,C_6 and C_9,C_{12} carbons respectively. Satellite peaks were observed on either side of the parent signal at 33.2 ppm, confirming this to be the C_7,C_{10} resonance ($^1J_{C_2C_7}$ = 48.9 Hz). The C_8,C_{11} methylene carbons have a chemical shift of 39.0 ppm.

The ^1H resonances of the dihydropyrazine, pseudo-PBG and pyrazine were assigned after performing a ^{13}C-^1H correlation on the partially oxidised reaction mixture.

It thus appears that the chemical dimerisation of ALA strongly favours its azomethine condensation to form 2,5-bis(2-carboxy-ethyl)-3,6-dihydropyrazine in comparison to pyrrole ring closure to form pseudo-PBG. The mechanism of the reaction in 5 M NaOH to give the dihydropyrazine is illustrated in Scheme 3.9. The reaction in 5 M NaOH to give pseudo-PBG probably involves the C_5 carbanion (Scheme 3.9) and it is reasonable to assume that the ease of carbanion formation (C_3 or C_5) will parallel the readiness with which the enol is formed (i.e. C_5 is more acidic than C_3). This explains why the formation of pseudo-PBG is always favoured over

that of PBG in the chemical dimerisation of ALA. In view of the ease of carbanion formation to give a strong nucleophile the formation of the dihydropyrazine is surprising.

When the condensation of [4-^{13}C]ALA.HCl (50% enriched) (0.1 mmol) in 5 M NaOH was probed by ^{13}C NMR spectroscopy (after the reaction mixture had been heated at 70 °C for one hour), three resonances in addition to those of the products were observed at 74.5, 82.2 and 83.4 ppm. The former resonance was approximately twice the intensity of the latter two. These resonances lie in a region characteristic of sp^3 rather than sp^2 hybridised carbons. Since carbinolamines invariably occur as intermediates in non-enzymic interconversions between carbonyl compounds and imines[29,30] it is reasonable to assign these three additional resonances to the carbinolamine carbon atoms of intermediates I and II (Scheme 3.9), formed in the course of the reaction. The carbinolamine carbon atoms of I and II are derived from the isotopically enriched C_4 carbon atom of ALA and are therefore also enriched in ^{13}C to the extent of 20%. As a result they are readily detected in the ^{13}C NMR spectrum of the reaction mixture. The resonance at 74.5 ppm corresponds to the carbinolamine carbon atoms of I, since it is twice the intensity of the other two resonances. The resonances at 82.2 ppm ($^2J_{C_2C_4}$ = 4.9 Hz) and 83.4 ppm ($^2J_{C_2C_4}$ = 4.9 Hz) correspond to the carbinolamine carbon atoms of II, although they cannot be unambiguously assigned.

Since intermediates I and II (Scheme 3.9) accumulate to such a level that they can be detected by ^{13}C NMR spectroscopy, the slow step of each reaction must be the dehydration of I and II to form the corresponding products.

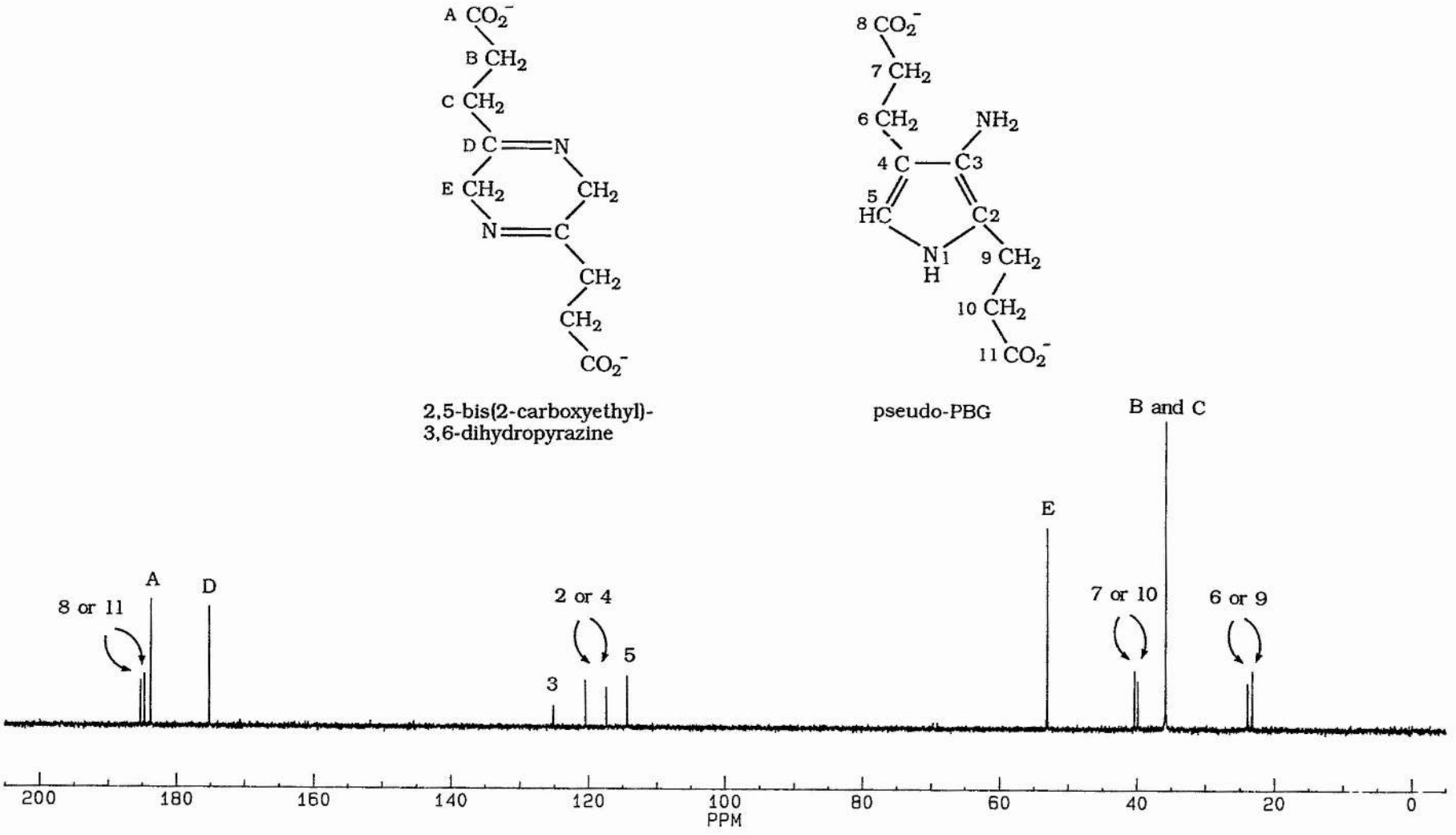

Figure 3.5 ^{1}H decoupled 75.469 MHz ^{13}C NMR spectrum of the anaerobic condensation products of ALA (0.25 mmol) in 5 M NaOH at 21 °C.

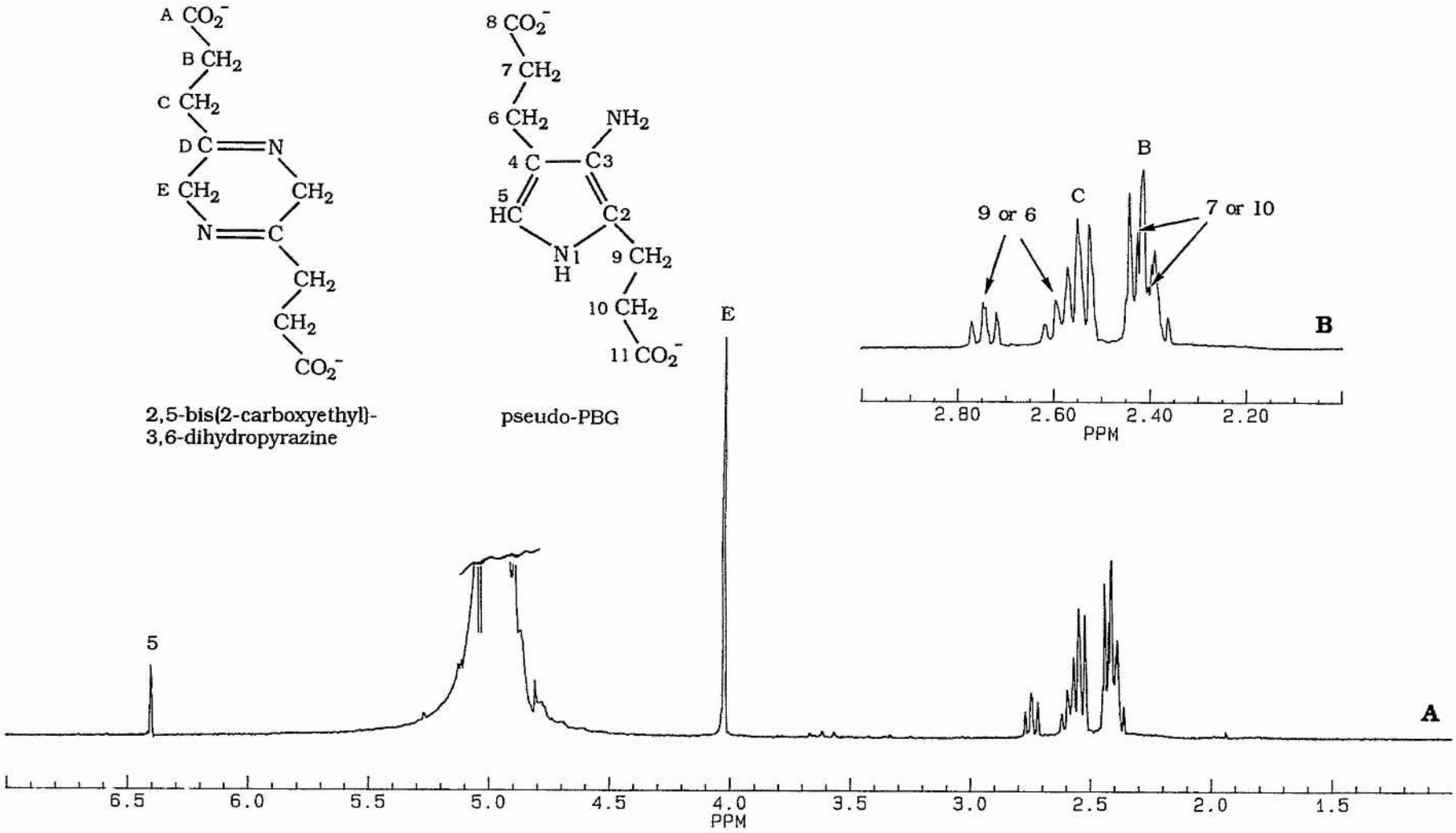

Figure 3.6 (A) 300.134 MHz ^{1}H NMR spectrum of the anaerobic condensation products of ALA (0.25 mmol) in 5 M NaOH at 21 °C. (The water line has been omitted for clarity). **(B)** 2-fold horizontal expansion of (A) between 2.0 and 3.0 ppm.

Table 3.3 ^{13}C and ^{1}H NMR assignments[a] of 2,5-bis(2-carboxyethyl)-3,6-dihydropyrazine and pseudo-PBG in 5 M NaOH.

Compound	Carbon	^{13}C chemical shifts[b],[c]	Proton	^{1}H chemical shifts[b],[c]
2,5-bis(2-carboxyethyl)-3,6-dihydropyrazine	C_2,C_5	175.2		
	C_3,C_6	53.0	3,6-CH_2	4.02 (s)
	C_7,C_{10}	35.77	7,10-CH_2	2.55 (t), J = 6.83 Hz
	C_8,C_{11}	35.71	8,11-CH_2	2.41 (t), J = 6.83 Hz
	C_9,C_{12}	183.7		
pseudo-PBG	C_2	[120.4]		
	C_3	125.1		
	C_4	[117.3]		
	C_5	114.3	5-CH	6.40 (s)
	C_6	{23.1}	6-CH_2	{2.60 (t), J = 6.83 Hz}
	C_7	(39.8)	7-CH_2	(2.40 (t), J = 6.83 Hz)
	C_8	*[184.6]*	9-CH_2	{2.75 (t), J = 6.83 Hz}
	C_9	{23.8}	10-CH_2	(2.43 (t), J = 6.83 Hz)
	C_{10}	(40.3)		
	C_{11}	*[185.2]*		

(a) Obtained at room temperature. (b) In ppm, downfield with respect to internal DSS set at δ 0. (c) Pairs of ambiguous assignments are placed within similar brackets.

Table 3.4 ^{13}C and ^{1}H NMR assignments[a] of 2,5-bis(2-carboxyethyl)pyrazine in 5 M NaOH.

Compound	Carbon	^{13}C chemical shifts[b]	Proton	^{1}H chemical shifts[b]
2,5-bis(2-carboxyethyl)-pyrazine	C_2,C_5	156.3		
	C_3,C_6	145.3	3,6-CH_2	8.41 (s)
	C_7,C_{10}	33.2	7,10-CH_2	3.03 (t), J = 7.33 Hz
	C_8,C_{11}	39.0	8,11-CH_2	2.73 (t), J = 7.33 Hz
	C_9,C_{12}	183.8		

(a) Obtained at room temperature. (b) In ppm, downfield with respect to internal DSS set at δ 0.

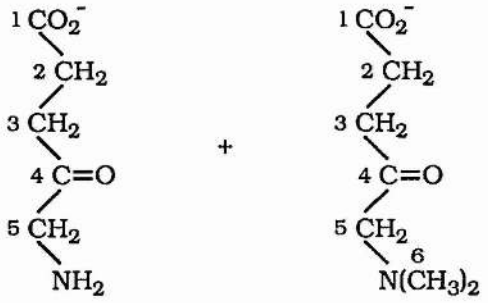

ALA + N,N-dimethyl-ALA

5 M NaOH, 70 °C,
6 h, under argon

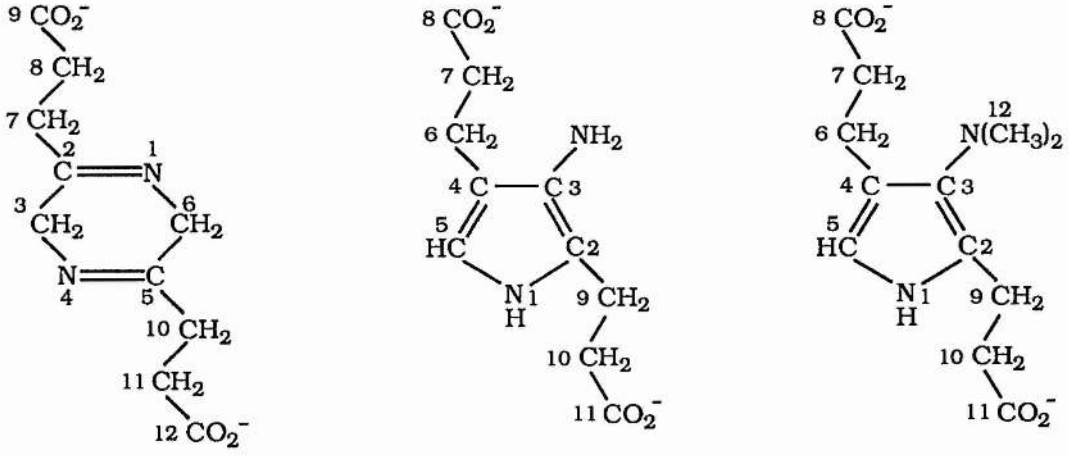

2,5-bis(2-carboxyethyl)-3,6-dihydropyrazine

pseudo-PBG

N,N-dimethyl-pseudo-PBG

[O]

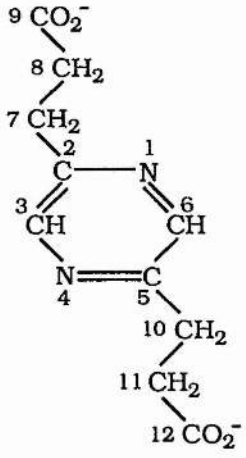

2,5-bis(2-carboxyethyl)pyrazine

Scheme 3.10

3.3.5.3 The anaerobic condensation of ALA with N,N-dimethyl-5-aminolevulinic acid in 5 M NaOH.

In an attempt to examine the possibility of favouring pyrrole ring closure in the chemical dimerisation of ALA, by protecting the amino group of one of the ALA molecules, N,N-dimethyl-5-aminolevulinic acid hydrochloride (N,N-dimethyl-ALA.HCl) was synthesised as described in Section 3.3.5.4.

To a well stirred deaerated solution of N,N-dimethyl-ALA.HCl (0.25 mmol) in 5 M NaOH (0.5 ml), maintained at 70 °C in a water bath, was added dropwise, a deaerated solution of ALA.HCl (0.25 mmol in 0.2 ml of water) under a stream of argon (using a vacuum line). After the addition was complete, the reaction mixture was left stirring at 70 °C for 6 hours and then transferred into a deaerated 5 mm NMR tube under argon.

It was found that ALA was quantitatively converted into a mixture of three condensation products in a ratio of 1:2:5. The products of the reaction were identified to be N,N-dimethylpseudo-PBG, 2,5-bis(2-carboxyethyl)-3,6-dihydropyrazine and pseudo-PBG respectively (Scheme 3.10), on the basis of their ^{13}C and ^{1}H NMR chemical shifts (Table 3.5). The N,N-dimethyl-ALA remained largely unreacted not as the hydrochloride, but as the free base. This was evident from the upfield shift of all its signals in the ^{1}H NMR spectrum of the reaction mixture compared with the shifts of the hydrochloride. The spectra were acquired at a probe temperature of 21 °C using a D_2O capillary insert and were referenced with respect to internal DSS (set at δ 0). Thus, protection of the amino group of one molecule of ALA, favours the formation of pyrrole, three times over that of the dihydropyrazine, in the chemical dimerisation of ALA under strongly alkaline conditions.

Table 3.5 ^{13}C and ^{1}H NMR assignments[(a)] of 2,5-bis(2-carboxyethyl)-3,6-dihydropyrazine, pseudo-PBG, N,N-dimethylpseudo-PBG and N,N-dimethyl-ALA in 5 M NaOH.

Compound	Carbon	^{13}C chemical shifts[(b),(c)]	Proton	^{1}H chemical shifts[(b),(c)]
2,5-bis(2-carboxyethyl)-3,6-dihydropyrazine	C_2,C_5	175.1		
	C_3,C_6	53.0	3,6-CH_2	4.02 (s)
	C_7,C_{10}	35.72	7,10-CH_2	2.55 (t), J = 6.83 Hz
	C_8,C_{11}	35.67	8,11-CH_2	2.41 (t), J = 6.83 Hz
	C_9,C_{12}	183.8		
pseudo-PBG	C_2	[120.3]		
	C_3	124.9		
	C_4	[117.2]		
	C_5	114.2	5-CH	6.40 (s)
	C_6	{23.1}	6-CH_2	{2.60 (t), J = 6.83 Hz}
	C_7	(39.8)	7-CH_2	(2.40 (t), J = 6.83 Hz)
	C_8	*[184.7]*	9-CH_2	{2.75 (t), J = 6.83 Hz}
	C_9	{23.7}	10-CH_2	(2.43 (t), J = 6.83 Hz)
	C_{10}	(40.3)		
	C_{11}	*[185.3]*		

Continued overleaf

Table 3.5 Continued

Compound	Carbon	^{13}C chemical shifts[(b),(c)]	Proton	^{1}H chemical shifts[(b),(c)]
N,N-dimethylpseudo-PBG	C_2	[124.4]		
	C_3	127.3		
	C_4	[118.3]		
	C_5	116.7	5-CH	6.60 (s)
	C_6	{24.0}	$6\text{-}CH_2$	{2.62 (t), J = 6.38 Hz}
	C_7	(40.5)	$7\text{-}CH_2$	(2.24 (t), J = 6.38 Hz)
	C_8	*[185.2]*	$9\text{-}CH_2$	{2.56 (t), J = 6.38 Hz}
	C_9	{24.2}	$10\text{-}CH_2$	(2.29 (t), J = 6.38 Hz)
	C_{10}	(40.8)	$12\text{-}CH_3$	2.20 (s)
	C_{11}	*[185.6]*		
	C_{12}	45.8		
N,N-dimethyl-ALA	C_1	183.7		
	C_2	33.4	$2\text{-}CH_2$	2.43 (t), J = 6.38 Hz
	C_3	39.1	$3\text{-}CH_2$	2.69 (t), J = 6.38 Hz
	C_4	213.7	$5\text{-}CH_2$	3.43 (s)
	C_5	69.3	$6\text{-}CH_3$	2.23 (s)
	C_6	46.9		

(a) Obtained at room temperature. (b) In ppm, downfield with respect to internal DSS set at δ 0. (c) Pairs of ambiguous assignments are placed within similar brackets.

3.3.5.4 Synthesis of N,N-dimethyl-ALA.HCl.

In view of the earlier success with the reductive alkylation of amino acids,[31] it seemed advisable to test the generality of this technique with ALA.HCl.

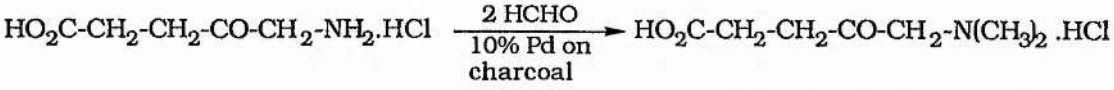

ALA.HCl N,N-dimethyl-ALA.HCl

Methylation was carried out by stirring a solution of ALA.HCl (0.08375 g, 0.5 mmol) in water (100 ml), containing formaldehyde (0.6 g, 0.02 mmol), with 10% palladised charcoal (0.8375 g) in an atmosphere of hydrogen at ordinary pressure and temperature until slightly more than the theoretical amount of hydrogen (260 cc) had been adsorbed. This required about 15 hours. The mixture was then heated to boiling and filtered over Celite. The filtrate was evaporated under reduced pressure and impurities of paraformaldehyde removed by reevaporation with water. The crude N,N-dimethyl-ALA.HCl was crystallised from acetone-ether as yellowish-brown crystals (0.69 g, 70.6%), m.p. 202-204 °C (Found: C, 43.3; H, 7.2; N, 7.2; Calculated for $C_7H_{14}NO_3Cl$: C, 43.0; H, 7.2; N, 7.2%); m/z 159 (M^+- HCl, 1%) 142 (1), 84 (2), 59 (97), 58 (100), 45 (8), 44 (16), 42 (20), 37 (16), 36 (27) and 28 (30); δ_H (D_2O/DSS) 2.72 (2 H, t, *J* 5.93, CH_2CO_2H), 2.87 (2 H, t, *J* 6.09, $CH_2CH_2CO_2H$), 2.93 (6 H, s, $N(CH_3)_2$), 4.40 (2 H, s, $CH_2N(CH_3)_2$) and 7.17 (1 H, t, $^1J_{^{14}NH}$ 52.2, $NH^+(CH_3)_2$); δ_C (D_2O/DSS) 30.1, 37.2, 46.5, 66.9, 179.2 and 205.5.

References.

1) P. A. Michini and E. K. Jaffe, *Fed. Proc., Fed. Am. Soc. Exp. Biol.*, 1987, **46**, 2246.

2) G. Kikuchi, A. Kumar, P. Talmage and D. Shemin, *J. Biol. Chem.*, 1958, **233**, 1214.

3) S. I. Beale, S. P Gough and S. Granick, *Proc. Nat. Acad. Sci. U.S.A.*, 1975, **72**, 2719.

4) L. Varticovski, J. P. Kushner and B. F. Burnham, *J. Biol Chem.*, 1980, **255**, 3742.

5) D. Gurne, J. Chen and D. Shemin, *Proc. Nat. Acad. Sci. U.S.A.*, 1977, **74**, 1383.

6) H. P. Monteiro, D. S. P. Abadalla, O. Augusto and E. J. H. Bechara, *Arch. Biochem. Biophys.*, 1989, **271**, 206.

7) H. A. Smith, *Dis. Abstr. Int. B.*, 1981, **42(6)**, 2347.

8) R. Lester and P. Klein, *J. Lab. Clin. Med.*, 1966, **67**, 1000.

9) C. L. Lerman and E. B. Whitacre, *J. Org. Chem.*, 1981, **46**, 468.

10) J. N. S. Evans, P. E. Fagerness, N. E. MacKenzie and A. I. Scott, *Magn. Res. Chem.*, 1986, **23**, 939.

11) R. M. Dawson, D. C. Elliot and K. M. Jones (eds.), 'Data for Biochemical Research', 2nd ed., Oxford University Press, London.

12) F. W. Wehrli and T. Wirthlin, 'Interpretation of Carbon-13 NMR Spectra', Heyden, New York, 1976.

13) P. Greenzaid, Z. Luz and D. Samuel, *J. Am. Chem. Soc.*, 1967, **89**, 749.

14) E. K. Jaffe and J. S. Rajagopalan, *Bioorg. Chem.*, 1990, **18**, 381.

15) J. M. Risley and R. L. Van Etten, *J. Am. Chem. Soc.*, 1980, **100**, 4609.

16) H. A. Christ, P. Diehl, H. R Schnieder and H. Dahn, *Helv. Chem. Acta.*, 1961, **44**, 865.

17) B. G. Cox, P. De Maria and A. Fini, *J. Chem Soc., Perkin Trans. II*, 1984, 1647.

18) D. Kemp and F. Vellacio, 'Organic Chemistry', Worth Publishers Inc., New York, 1980.

19) J. J. Scott, *Biochem J.*, 1955, **62**, 6P.

20) A. I. Scott, A. Townsend, K. Okada and M. Kajuwara, *Trans. N.Y. Acad. Sci.*, 1973, **35**, 72.

21) S. Granick and D. Mauzerall, *J. Biol. Chem.*, 1958, **232**, 1119.

22) B. Franck and H. Stratmann, *Heterocycles*, 1981, **15**, 919.

23) A. Treibs and R. Zimmer-Galler, *Annalen*, 1963, **664**, 140.

24) A. Treibs and E. Herrmann, *Z. Physiol. Chem.*, 1955, **299**, 168.

25) Q. H. Gibson and D. C. Harrison, *Biochem. J.*, 1950, **46**, 154.

26) D. Mauzerall and S. Granick, *J. Biol. Chem.*, 1956, **219**, 435.

27) F. T. G. Prunty, *Biochem. J.*, 1945, **39**, 446.

28) B. Vahlquist, *Z. Physiol. Chem.*, 1939, **239**, 213.

29) W. P. Jencks, *Prog. Phys. Org. Chem.*, 1964, **2**, 63.

30) W. P. Jencks, 'Catalysis in Chemistry and Enzymology', p. 463, McGraw-Hill, New York, 1969.

31) R. E. Bowman and H. H. Stroud, *J. Chem. Soc.*, 1950, 1342.

CHAPTER FOUR

THE KNORR AND FISCHER-FINK CONDENSATIONS OF ALA AND 5-METHYL-ALA

4.1 Introduction.

In 1886, Knorr[1] reported the preparation of 2,4-diethoxy-3,5-dimethylpyrrole (often called *Knorr's pyrrole*), by a zinc-dust reduction in acetic acid, of an equimolar mixture of ethyl α-oximinoacetoacetate and ethyl acetoacetate (Scheme 4.1). The equimolar mixture of ethyl α-oximinoacetoacetate and ethyl acetoacetate was prepared by dropwise treatment of an acetic acid solution of ethyl acetoacetate with a half equivalent of aqueous sodium nitrite.

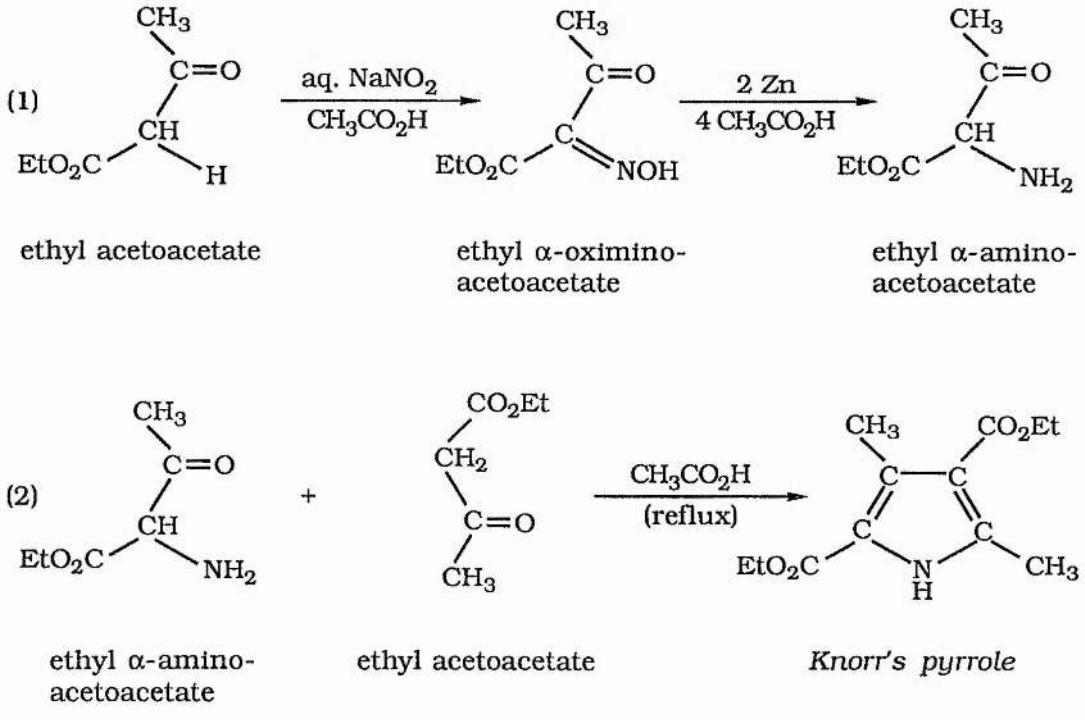

Scheme 4.1

Since then, the condensation of an α-aminoketone with a carbonyl compound having a reactive methylene group *alpha* to the carbonyl group has been referred to as the Knorr synthesis.[2] The latter has been widely exploited, particularly to prepare the necessary building blocks for the synthesis of tetrapyrroles. The utility of the reaction is limited by the tendency of α-aminoketones

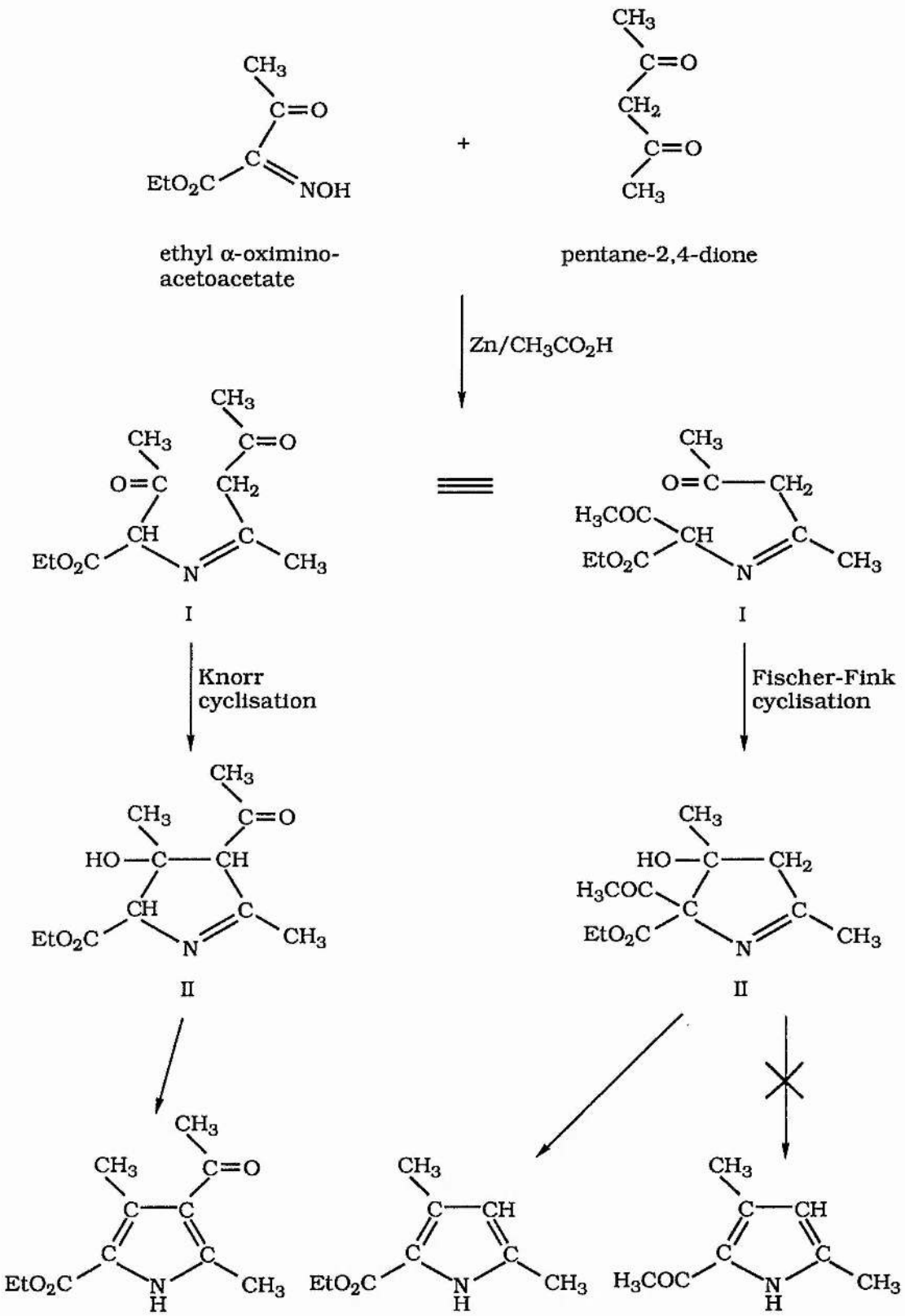
ethyl α-oximino-acetoacetate
pentane-2,4-dione
Zn/CH3CO2H
I
I
Knorr cyclisation
Fischer-Fink cyclisation
II
II
3-acetyl-2,4-dimethyl-5-ethoxycarbonylpyrrole
2,4-dimethyl-5-ethoxy-carbonylpyrrole
2-acetyl-3,5-dimethyl-pyrrole

Scheme 4.2

toward self-condensation. If the methylene ketone is not sufficiently reactive, the aminoketone will condense to form a pyrazine instead of a pyrrole. This condensation proceeds so readily that α-aminoketones are in general not capable of independent existence but must be isolated as hydrochlorides.

Many of the early examples of the Knorr synthesis have been discussed in the monograph by Fischer and Orth.[3] Corwin[4] has examined the limitations on the method and found that the yield of pyrrole is low unless there is a resonance stabilizing electron withdrawing substituent at the α-carbon of the carbonyl compound (e.g. COR, CO_2R, CN, aryl).

A number of very useful variations of the Knorr synthesis have been discovered since. Zanetti and Levi[5] found that pentane-2,4-dione reacted with ethyl α-oximinoacetoacetate in the Knorr fashion to give the expected Knorr product, 3-acetyl-2,4-dimethyl-5-ethoxycarbonylpyrrole (Scheme 4.2). Fifty years later, Fischer and Fink[6] isolated a very minor by-product, 2,4-dimethyl-5-ethoxy-carbonylpyrrole, which had arisen from an alternative mode of cyclisation of the intermediate Schiff's base, I (Scheme 4.2). The alternative reaction pathway is frequently referred to as a modified Knorr condensation or the Fischer-Fink synthesis.[6,7] This pathway is significant only when the carbonyl compound in the Knorr condensation is a β-diketone, since, in addition to the normal ring closure to give the Knorr product, the alternative condensation through the acyl group can lead to the formation of the Fischer-Fink product (Scheme 4.2). The preferential formation of 2,4-dimethyl-5-ethoxycarbonylpyrrole compared with 2-acetyl-3,5-dimethylpyrrole (Scheme 4.2) in the Fischer-Fink synthesis, reflects the greater ease of nucleophilic attack on the acetyl group

compared with the ester group.

Kleinspehn[8] deduced that this alternative mode could be forced to occur by the substitution of diethyl oximinomalonate for ethyl α-oximinoacetoacetate and indeed 2,4-dimethyl-5-ethoxy-carbonylpyrrole was obtained in 60% yield (Scheme 4.3).

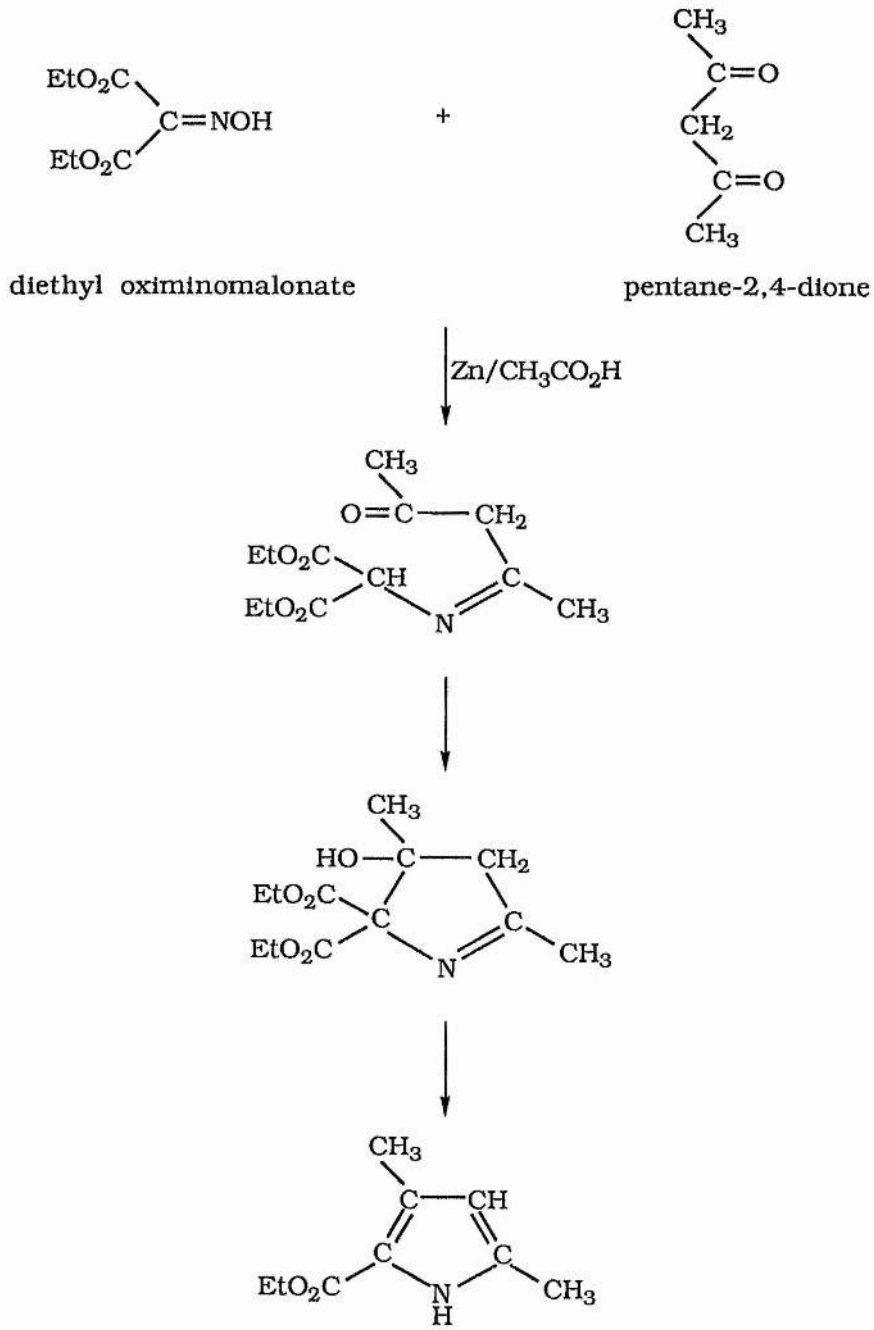

2,4-dimethyl-5-ethoxycarbonylpyrrole

Scheme 4.3

Via an identical mechanism, various 3-alkylpentane-2,4-diones (R = Et, $CH_2CH_2CO_2H$) were found to give excellent yields of 3-alkyl-2,4-dimethyl-5-ethoxycarbonylpyrroles (Scheme 4.4).

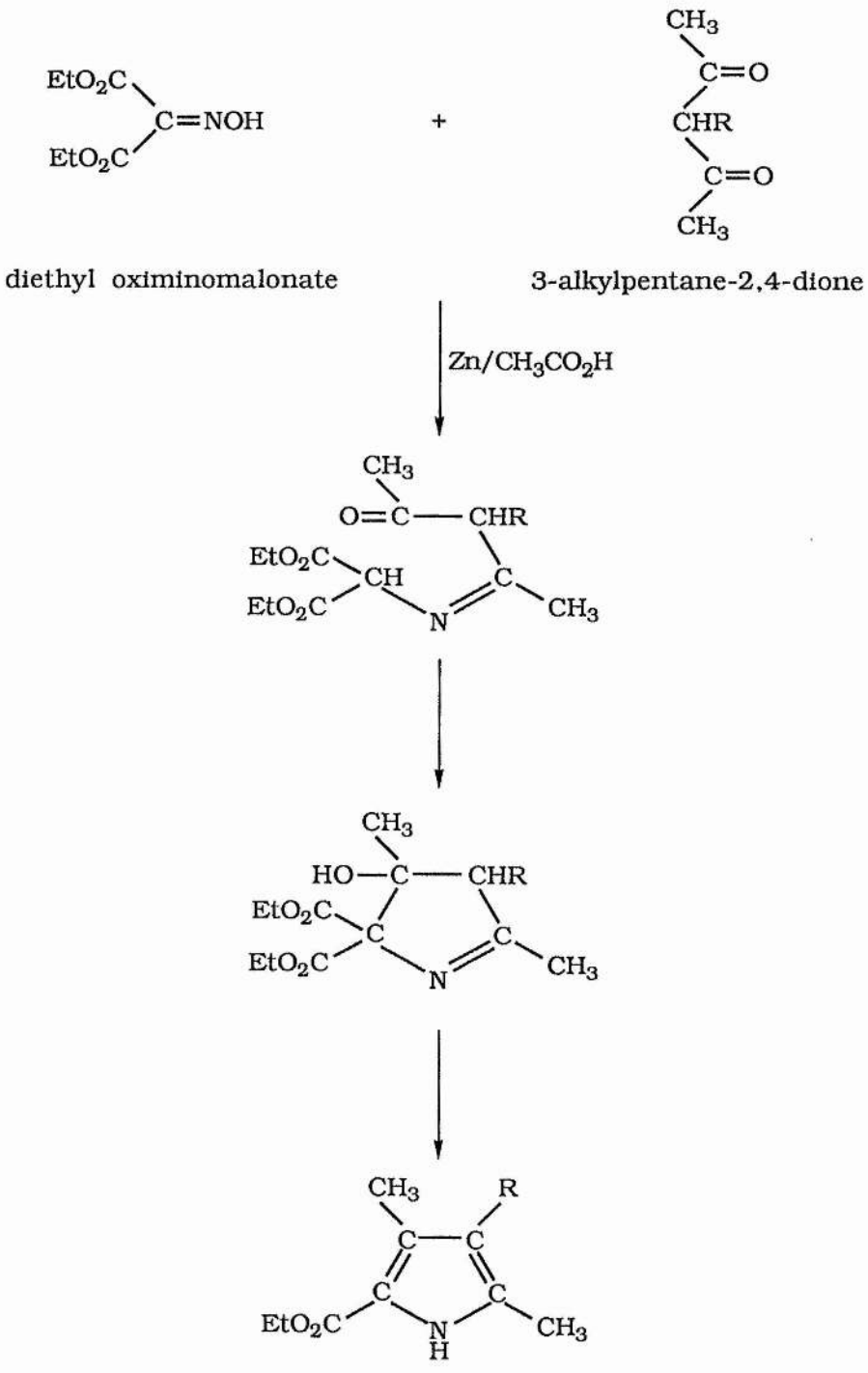

Scheme 4.4

Shortly thereafter Johnson *et al* [9] found that ethyl α-oximino-acetoacetate reacted under Knorr conditions with 3-alkylpentane-2,4-diones (R = CH_3, $CH_2CH_2CO_2Et$) to give similar products as were obtained from diethyl oximinomalonate i.e. 3-alkyl-2,4-dimethyl-5-ethoxycarbonylpyrroles (Scheme 4.5).

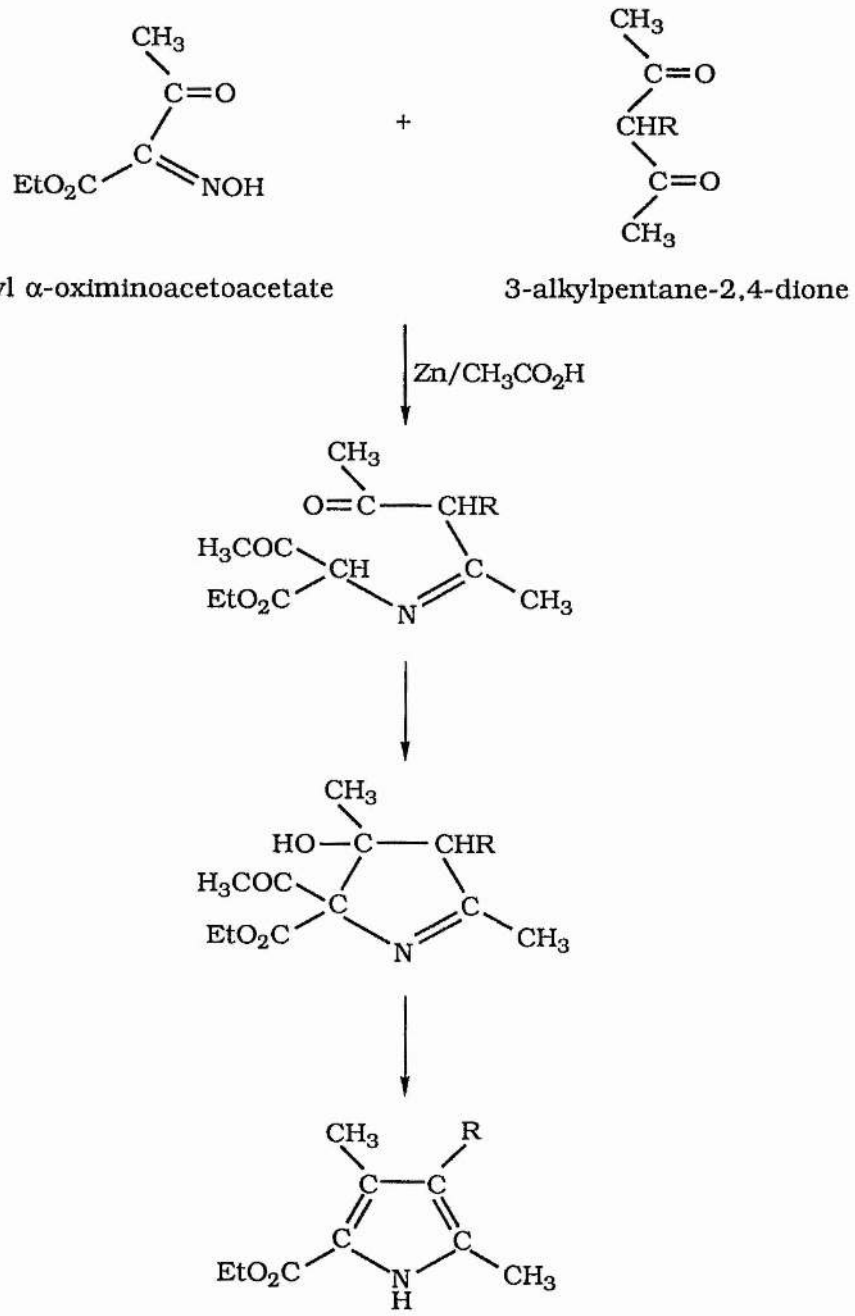

3-alkyl-2,4-dimethyl-5-ethoxycarbonylpyrrole

Scheme 4.5

It was shown by the use of other α-oximinoketoacetates[9] and by isotopic labelling[10] that the β-methyl substituent was derived exclusively from the pentanedione moiety.

Johnson's procedure affords somewhat lower yields than Kleinspehn's but has twin advantages of the more facile nitrosation of acetoacetates, compared with malonates, and the ability to introduce useful α-substituents such as tertiary butyl esters,[9] benzyl esters[11] or N,N-dialkylamides[12-15] by the substitution of *tert*-butyl or benzyl acetoacetates or N,N-dialkyl acetoacetamides for ethyl acetoacetate.

Kleinspehn's and Johnson's syntheses have been tried with unsymmetrical β-diketones and β-ketoaldehydes with various results. In Kleinspehn's procedure, whereas *meso*-alkylated unsymmetrical β-diketones (e.g. 3,5-disubstituted pentane-2,4-diones) show considerable selectivity toward Schiff's base formation at the less hindered carbonyl, thereby affording the 5-methyl-pyrrole isomer preferentially,[16-20] this is not the case with *meso*-unsubstituted unsymmetrical β-diketones. Hexane-2,4-dione favoured the formation of the 5-ethylpyrrole isomer[21] at least 2:1 over the 5-methylpyrrole. Ethyl 4,6-dioxoheptanoate[22] also gave a mixture of both possible isomers. In Johnson's procedure, the reaction of *tert*-butyl α-oximinoacetoacetate with 3-methyl- and 3-ethylhexane-2,4-dione resulted in low yields of pyrrole, with the 5-methylpyrrole isomer dominant but contaminated with the 3-methyl isomer to the extent of 30-40%.[23] Although ethyl α-oximinoacetoacetate and diethyl oximinomalonate afford the same pyrroles upon reductive condensation with 3-alkylpentane-2,4-diones (Schemes 4.4 and 4.5), this is not necessarily the case with unsymmetrical β-diketones. Anomalous results were found

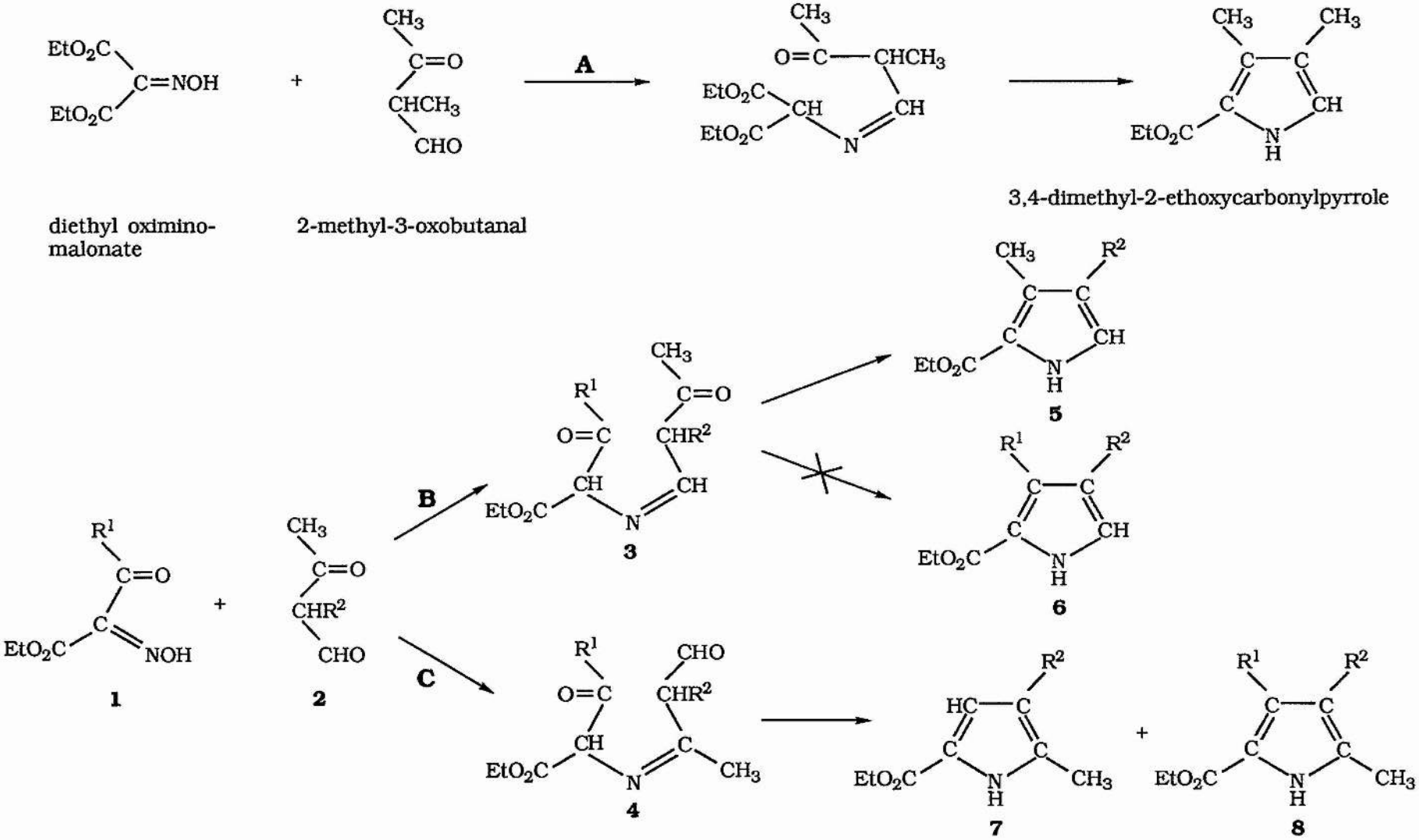
diethyl oximino-malonate
2-methyl-3-oxobutanal
3,4-dimethyl-2-ethoxycarbonylpyrrole
A
B
C
1
2
3
4
5
6
7
8

Scheme 4.6

with 2-methyl-3-oxobutanal. With diethyl oximinomalonate, Kleinspehn[8] obtained 3,4-dimethyl-2-ethoxycarbonylpyrrole [Scheme 4.6(A)] with condensation taking place between the reduced oxime and the formyl group of 2-methyl-3-oxobutanal. However, with ethyl α-oximinoacetoacetate Falk *et al*[24] have shown that condensation may occur between the reduced oxime and either carbonyl group. Examination of the reaction of ethyl α-oximinoketoacetates with a series of 2-substituted 3-oxobutanals has also shown that condensation may occur between the reduced oxime and either carbonyl group.[24] However, condensation with the formyl group leads only to 5 (~10%), the Fischer-Fink product, to the exclusion of 6, the Knorr product [Scheme 4.6 (B)]. On the other hand, condensation with the acetyl group results in the preferential formation of 7, the Fischer-Fink product (~30%) with lesser amounts of 8, the Knorr product (~5%)[24] [Scheme 4.6(C)].

Thus, as seen in Scheme 4.6(A), the use of diethyl oximinomalonate effectively eliminates the possibility of the formation of the Knorr product and the procedure has been used in the synthesis of a wide range of alkyl and aryl substituted 2-ethoxycarbonylpyrroles.[8,17,25-35]

It has also been reported that ethyl oxalylacetone condenses with α-aminoacetone at two sites to give either 3-acetyl-2-ethoxycarbonyl-4-methylpyrrole (2), the normal Knorr product, or 2-acetyl-3-ethoxycarbonyl-5-methylpyrrole (4), the Fischer-Fink product[36] (Scheme 4.7). The relative yields of the products depend upon the pH of the reaction medium.[36] Under alkaline conditions, condensation initially occurs at the oxalyl carbonyl group to give 1 and subsequently 2, whilst at pH 6, the acetyl group is sufficiently activated to give 3, leading to the Fischer-Fink product, 4 (Scheme 4.7).

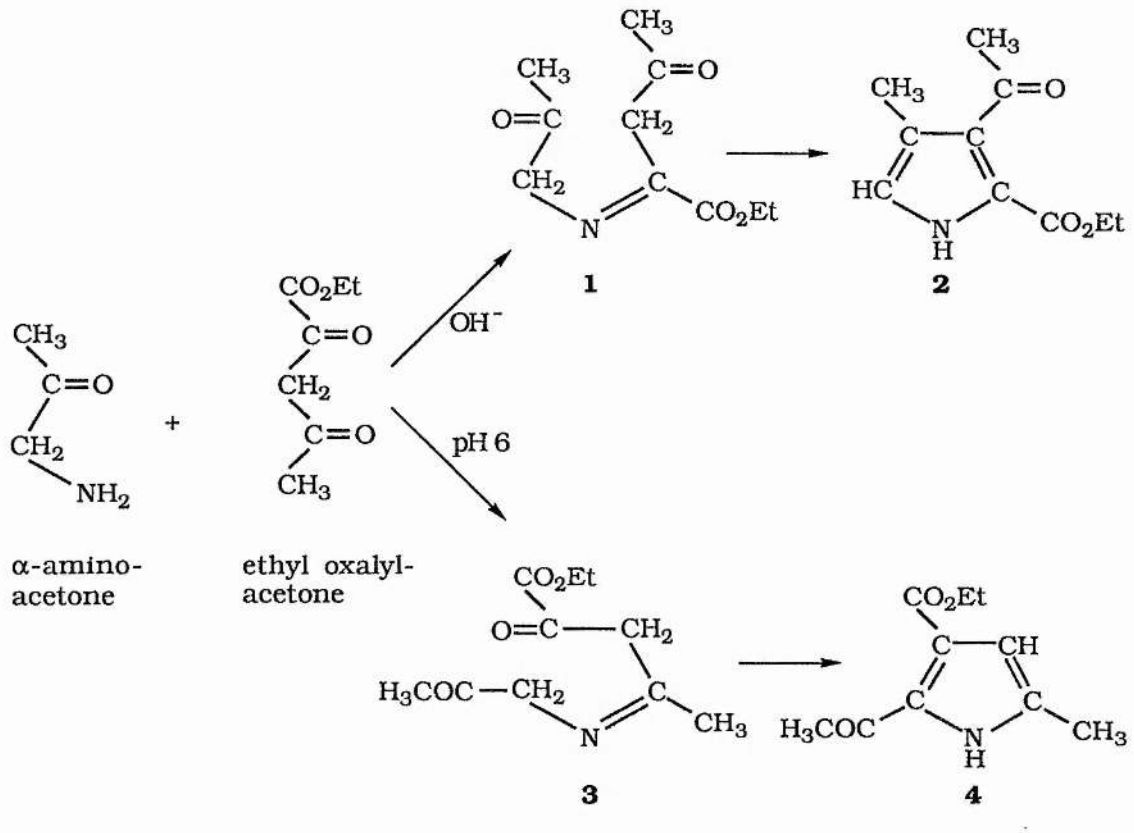

Scheme 4.7

The mechanism of the Knorr reaction has been inferred by the isolation of the enamine (or aminocrotonic ester) 3, (R^1 = H, R^2 = 3-chloro-2-nitrophenyl, R^3 = CO_2Et and R^4 = CH_3) when the

reaction was buffered at pH 4.0[37] (Scheme 4.8). The enamine 3, which in equilibrium with its tautomeric form 4, is believed to be an intermediate in the formation of pyrrole 6[37] (Scheme 4.8).

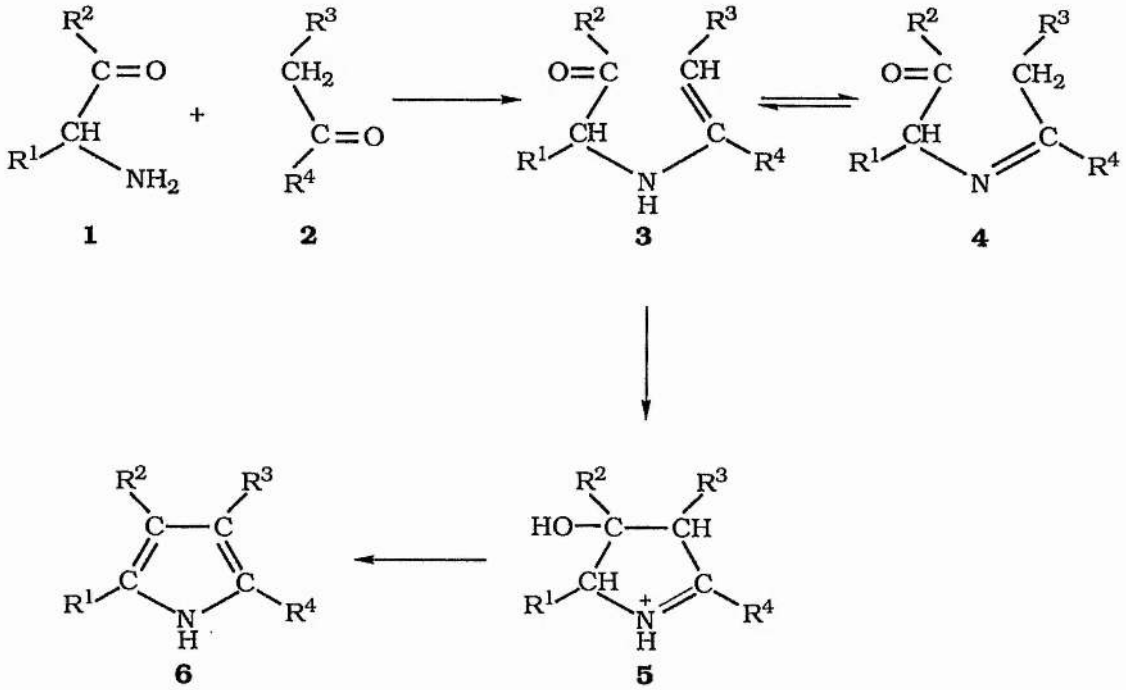

Scheme 4.8

Molecular orbital calculations using the AM1 method indicate that although the imine 4, is more stable than the enamine 3, when R^4 = H, for R^4 = CHO, the resonance stabilized imine is the more stable.[38]

4.2 Experimental.

4.2.1 Materials.

Butan-2-one, boron trifluoride-diacetic acid complex (BTDA), 3-methylbutan-2-one (BDH), acetic anhydride, Drierite, N-ethyl-urea, hexane-2,4-dione, 1,1,1,5,5,5-hexafluoropentane-2,4-dione, potassium phthalimide, sodium hydrogen carbonate, sodium nitrite, sodium sulphate (anhydrous), sodium hydroxide pellets, succinic anhydride, thionyl chloride, *p*-toluenesulphonic acid monohydrate (Aldrich), cupric acetate, ethyl acetoacetate, pentane-2,4-dione, potassium hydroxide pellets (AR), sodium acetate trihydrate (AR), (Fisons), methylene chloride (Ellis and Everard), 1,1,1-trifluoropentane-2,4-dione (Koch-Light Ltd.), absolute methanol, diethyl ether, glacial acetic acid, 37% hydrochloric acid, sulphuric acid (98% w/w), (Rhône Poulenc Ltd., analaR) and ALA.HCl (Sigma Chemical Company) were used as received unless otherwise specified. Molecular sieves Type 3A, 1-2 mm beads were purchased from Lancaster Synthesis. Deuteriated solvents for NMR were purchased from GOSS and used as received.

[4-^{13}C]ALA.HCl and [^{15}N]ALA.HCl were synthesised as described in Sections 2.2.3 and 2.2.4 respectively. 5-methyl-ALA.HCl, 3,3-dimethylpentane-2,4-dione and 3-methylpentane-2,4-dione were synthesised as described in Sections 4.2.5, 4.2.4 and 4.2.3 respectively.

4.2.2 Instrumentation and General Techniques.

Routine melting points, elemental analyses, mass spectra, ^{1}H, ^{13}C and ^{15}N NMR were obtained in exactly the same way as described in Section 2.2.2. Synthetic methanol was stored over molecular sieves Type 3A, and used as such.

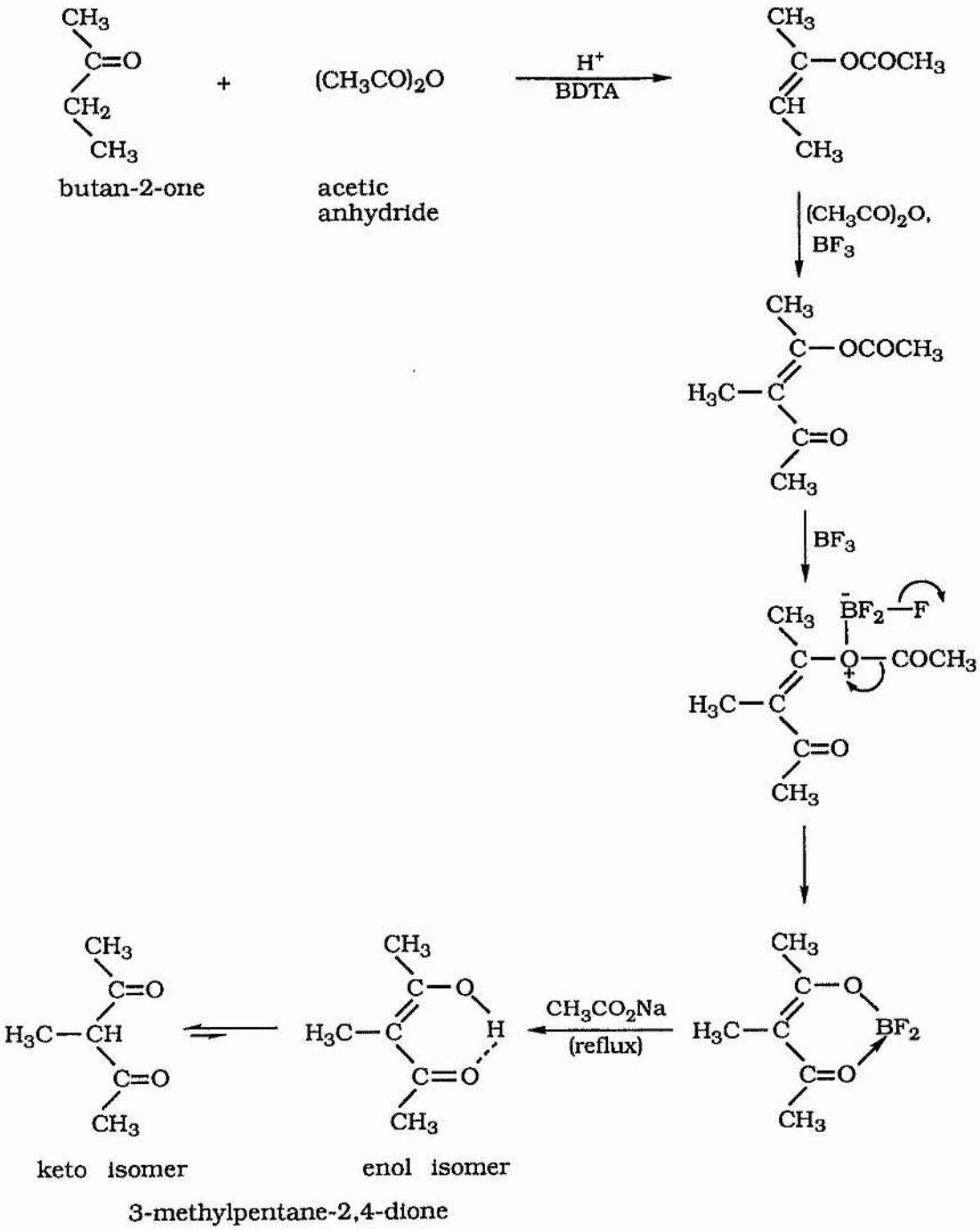

Scheme 4.9

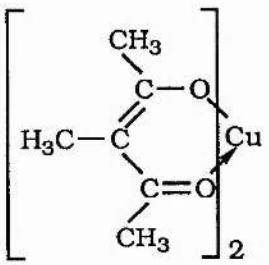

Figure 4.1 Structure of bis(3-methylacetylacetonato)copper (II) chelate.

4.2.3 Synthesis of 3-methylpentane-2,4-dione.

3-methylpentane-2,4-dione was prepared according to the method of Mao *et al.* [39] To a stirred solution of butan-2-one (28.8 g, 0.4 mol) and acetic anhydride (81.6 g, 0.8 mol) was added boron trifluoride-diacetic acid complex (BTDA) (150.2 g, 0.8 mol). After stirring overnight, the mixture was added to an aqueous solution of sodium acetate trihydrate [217.6 g, 1.6 mol, in water (1200 ml)] and refluxed for 3 hours (Scheme 4.9). The mixture was cooled, extracted with methylene chloride (3 x 400 ml) and the extracts combined. The extracts were washed free of acid with a saturated solution of sodium bicarbonate and dried over Drierite. The solution was filtered and the solvent removed under reduced pressure. The residual oil thus obtained was distilled and the fraction, b.p. 170-171 °C/760 mmHg (lit.,[40] 170-172 °C/760 mmHg) collected (29.45 g, 65%). The crude 3-methylpentane-2,4-dione containing trace impurities of unreacted butan-2-one and pentane-2,4-dione (formed by the self condensation of acetic anhydride[41]) was purified according to the method of Osborne[42] through the formation of its copper (II) salt, bis(3-methylacetylacetonato)-copper II chelate (Fig. 4.1).

The crude 3-methylpentane-2,4-dione (17.08 g, 0.15 mol) was dissolved in methanol (18 ml) and a hot filtered solution of copper acetate (45.4 g, 0.25 mol) in water (400 ml) added. The precipitated copper salt was dried and recrystallised several times from methanol to give the complex bis(3-methylacetylacetonato)-copper II chelate (Fig. 4.1) as greyish green plates, m.p. 208-230 °C (dec.), lit.,[43] m.p. 200-230 °C (dec.). The purified salt was shaken with dilute sulphuric acid (300 ml), extracted with methylene chloride and dried over Drierite. Removal of the solvent under

reduced pressure left pure 3-methylpentane-2,4-dione (7.81 g, 45.7%) as a yellow liquid; m/z 114 (M^+, 3%), 99 (9), 85 (11), 71 (3), 57 (4), 43 (100), 27 (8), 18 (46), 17 (26) and 15 (26); δ_H ($CDCl_3$) 1.33 (1.675 H, d, *J* 7.71, central Me keto), 1.85 (1.325 H, s, central Me enol), 2.12 (2.74 H, s, terminal Me enol), 2.20 (3.26 H, s, terminal Me keto), 3.70 (0.54 H, q, *J* 7.07, CH keto) and 16.42 (0.46 H, s, OH enol); δ_C ($CDCl_3$) 12.6, 12.6, 23.4, 28.7, 61.8, 104.9, 190.5 and 205.2.

4.2.4 Synthesis of 3,3-dimethylpentane-2,4-dione.

3,3-dimethylpentane-2,4-dione was also prepared according to the method of Mao *et al* .[39] To a stirred solution of 3-methyl-butan-2-one (34.45 g, 0.4 mol), acetic anhydride (81.6 g, 0.8 mol) and *p*-toluenesulphonic acid monohydrate (3.8 g, 0.02 mol) was added BTDA (150.2 g, 0.8 mol). After stirring overnight, the mixture was added to an aqueous solution of sodium acetate trihydrate [217.6 g, 1.6 mol, in water (1200 ml)] and refluxed for 3 hours. The mixture was cooled, extracted with methylene chloride (3 x 400 ml) and the extracts combined. The extracts were washed free of acid with a saturated solution of sodium bicarbonate and dried over Drierite. The solution was filtered and the solvent evaporated under reduced pressure. The residual oil was then twice distilled and the fraction, b.p. 170-174 °C/760 mmHg (lit.,[44] b.p. 172-174 °C/760 mmHg) collected (23.0 g, 45%); m/z 128 (M^+ 2%), 86 (59), 71 (70), 59 (5), 43 (100) and 28 (80); δ_H ($CDCl_3$) 1.35 (6 H, s, $C(CH_3)_2$) and 2.15 (6 H, s, 2 x $COCH_3$); δ_C($CDCl_3$) 21.2, 26.1, 62.4 and 207.7.

4.2.5 Synthesis of 5-methyl-ALA.HCl.

The route adopted for the synthesis of 5-methyl-5-amino-levulinic acid hydrochloride (5-methyl-ALA.HCl) (V) (Scheme 4.10) was that of Lartillot and Baron.[45]

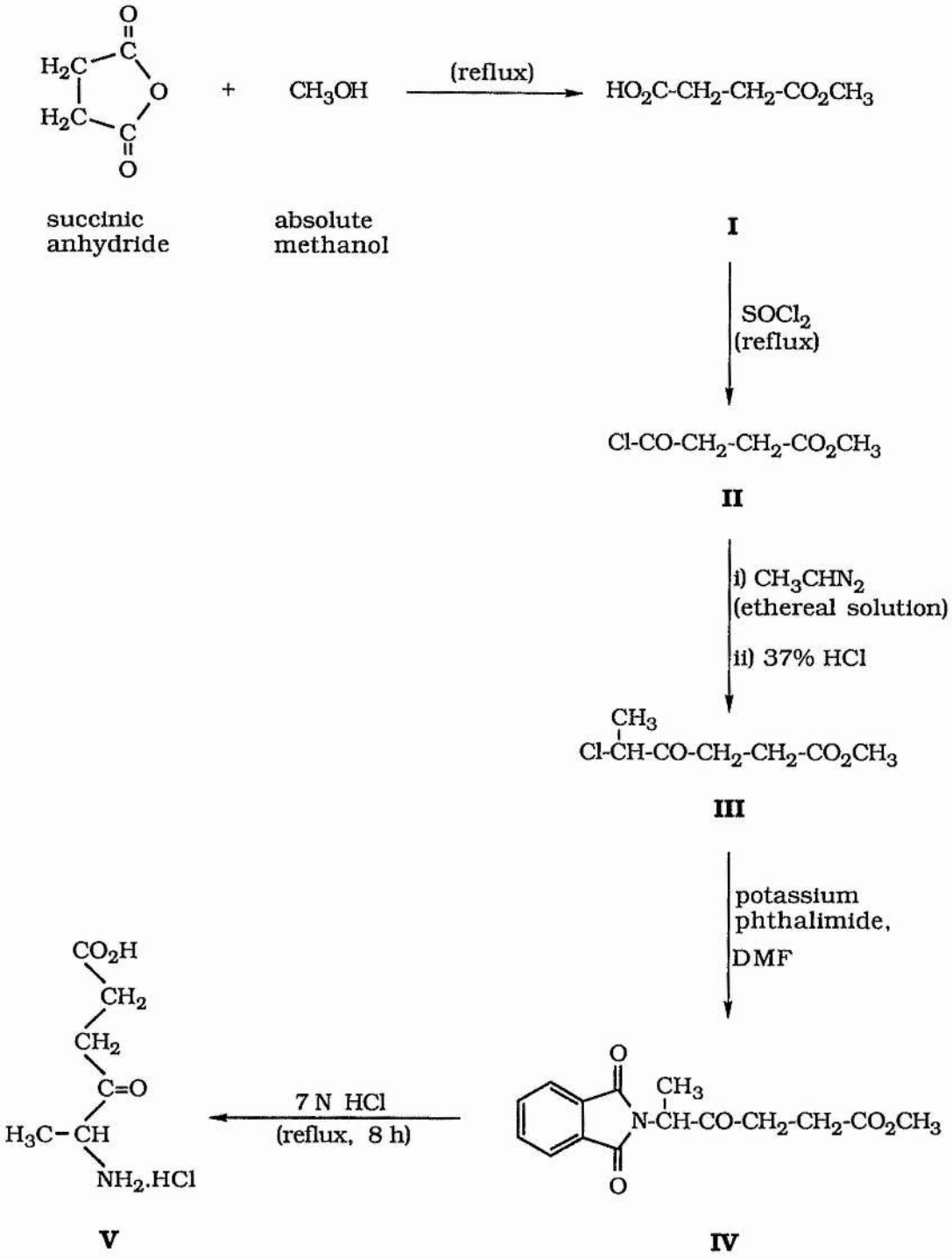

Scheme 4.10

4.2.5.1 Synthesis of methyl hydrogen succinate (I).

Methyl hydrogen succinate was prepared in exactly the same way and in the same scale as described in Section 2.2.4.1 and will therefore not be repeated here.

4.2.5.2 Synthesis of methyl 3-chloroformylpropanoate (II).

Methyl 3-chloroformylpropanoate was prepared in exactly the same way and in the same scale as described in Section 2.2.4.2 and will therefore not be repeated here.

4.2.5.3 Synthesis of methyl 5-chloro-5-methyllevulinate (III).

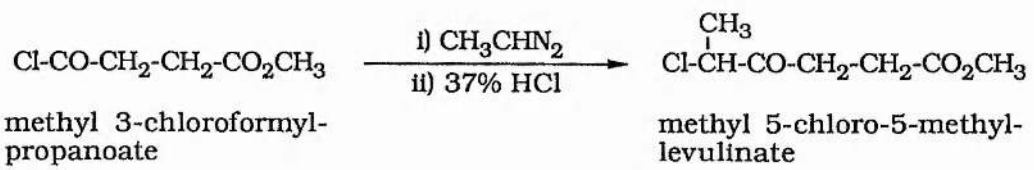

Methyl 5-chloro-5-methyllevulinate was prepared according to the method of Lartillot and Baron.[45] To a solution of diazoethane in dry ether (500 ml) (preparation described below), cooled to 0 to -5 °C in an ice-salt mixture was added dropwise with mechanical stirring, a solution of methyl 3-chloroformylpropanoate (7.3 g, 0.049 mol) in ether (22 ml). When the addition was complete, the orange colour of the diazoethane solution was permanently replaced by the yellow colour of the diazoketone. The mixture was then left standing at room temperature overnight.

An equivalent amount of 37% HCl (4.17 ml) was gradually added with stirring to the ethereal solution of the diazoketone. This resulted in a rapid evolution of nitrogen, after which the solution was practically colourless. The ethereal solution was washed three times with water to remove HCl and the combined

aqueous fractions were then washed six times with small amounts of ether. The combined ether extracts were dried over anhydrous Na_2SO_4 and the solvent removed under reduced pressure. The residual material was Kugelrohr distilled to give methyl 5-chloro-5-methyllevulinate (3.85 g, 40%) as a yellow liquid, b.p. 64 °C/0.2 mmHg (lit.,[46] b.p. 64 °C/0.2 mmHg) (Found: C, 46.8, H, 6.35. $C_7H_{11}ClO_3$ requires C, 47.1; H, 6.2%); m/z 147 (M^+- OMe, 45%), 115 (70), 91 (8), 87 (45), 63 (38), 73 (7), 59 (63), 56 (38), 55 (73) and 28 (100); δ_H ($CDCl_3$) 1.64 (3 H, d, *J* 6.84, $CHCH_3$), 2.64 (2 H, t, *J* 6.84, $CH_2CO_2CH_3$), 2.65 (2 H, t, *J* 6.84, $COCH_2$), 3.68 (3 H, s, CO_2CH_3) and 4.43 (1 H, q, *J* 6.84, $CHCH_3$); δ_C ($CDCl_3$) 20.2, 28.0, 33.2, 51.9, 58.6, 172.9 and 204.0.

4.2.5.3.1 Synthesis of diazoethane from N-nitroso-N-ethyl urea.

The synthesis of N-nitroso-N-ethyl urea and its subsequent treatment with 70% KOH to form diazoethane were carried out according to the method of Werner.[47]

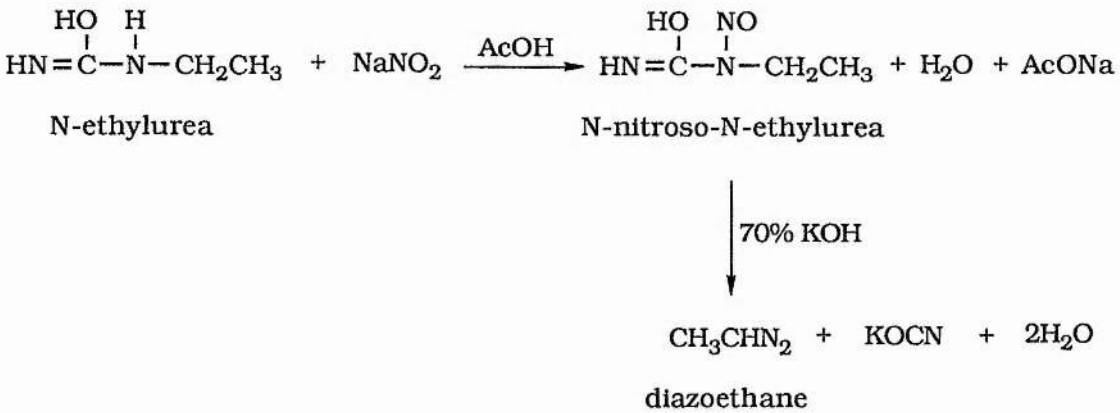

N-ethyl urea (63.3 g, 0.719 mol) and $NaNO_2$ (49.6 g, 0.719 mol) were dissolved in water (430 ml) contained in a 1 litre volumetric flask immersed in melting ice. A cold solution of glacial acetic acid (43.2 g, 0.719 mol) in water (160 ml) was gradually

added, the liquid being well stirred. The reaction mixture was left standing for 24 hours and the pale buff-yellow crystals of N-nitroso-N-ethyl urea were filtered and dried to a constant weight in a vacuum desiccator. The total yield of product was 40.13 g, 47.7%, m.p. 102 °C (lit.,[47] 103-104 °C).

A conical flask with a side arm was fitted with a short length of plastic tubing, the other end of which passes below the surface of ether in a round bottomed flask, placed in an ice-salt mixture. In the conical flask are placed dry ether (170 ml), 70% aqueous KOH (68 ml) and the Teflon coated bar of a magnetic stirrer. The conical flask was placed on melting ice, the stirrer started and a solution of N-nitroso-N-ethyl urea (40.13 g, 0.343 mol), in dry ether (400 ml) added at a regular rate by means of a syringe inserted into the stopper of the conical flask. The ethereal solution of diazoethane thus produced, was then dried over KOH pellets for 3 hours.

4.2.5.4 Synthesis of methyl 5-methyl-5-phthalimidolevulinate (IV).

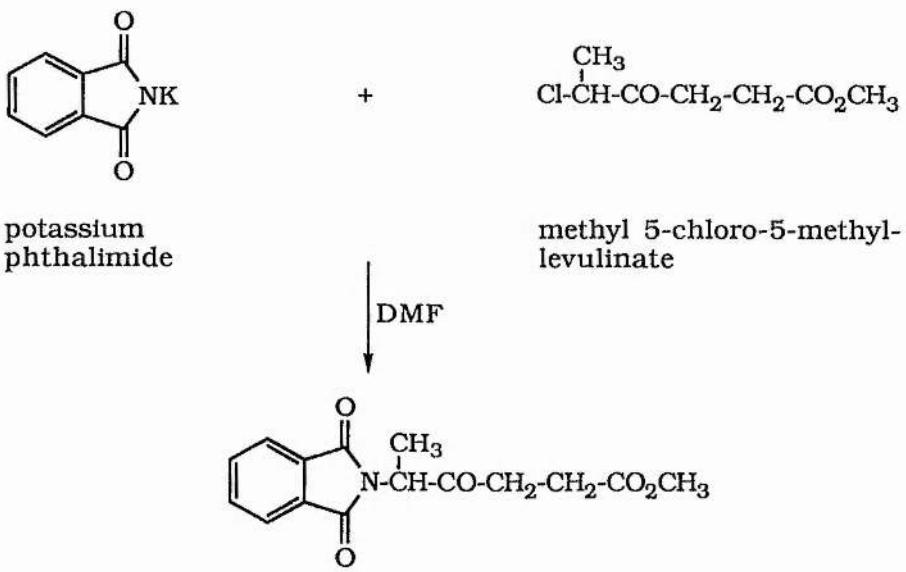

methyl 5-methyl-5-phthalimidolevulinate

Methyl 5-methyl-5-phthalimidolevulinate was prepared

according to the method of Lartillot and Baron.[45] To a suspension of potassium phthalimide (3.7 g, 0.02 mol) in DMF (25 ml) was added methyl 5-chloro-5-methyllevulinate (3.5 g, 0.0196 mol). The reaction mixture was stirred for 21/2 hours and left stirring at 60 °C for 1/2 an hour. The deep brown reaction mixture was filtered to remove KCl and any unreacted potassium phthalimide, and the filtrate shaken with methylene chloride (40 ml) and water (120 ml). The aqueous phase was decanted and washed twice with methylene chloride (12 ml). The methylene chloride extracts were then washed with 0.2 M NaOH (15 ml) and then repeatedly with water until the washings were colourless. The solution was dried over anhydrous Na_2SO_4 and the solvent removed under reduced pressure. Methyl 5-methyl-5-phthalimidolevulinate (2.99 g, 52.5%) was obtained as a thick viscous oil which could not be purified by crystallisation; m/z 289 (M^+, 2%), 258 (7), 230 (21), 174 (100), 160 (7), 147 (10), 130 (33), 115 (91), 104 (11), 84 (34), 76 (18), 59 (13), 55 (27), 49 (32) and 28 (24); δ_H ($CDCl_3$) 1.68 (3 H, d, *J* 7.33, $CHCH_3$), 2.62 (2 H, t, *J* 6.92, $CH_2CO_2CH_3$), 2.82 (2 H, t, *J* 6.92, $CH_2CH_2CO_2CH_3$), 3.67 (3 H, s, CO_2CH_3), 4.89 (1 H, q, *J* 7.33, $CHCH_3$), 7.83 (4 H, m, Ar*H*); δ_C ($CDCl_3$) 14.3, 27.9, 33.6, 51.9, 54.4, 123.6, 131.9, 134.3, 167.7, 172.8 and 203.7.

4.2.5.5 Synthesis of 5-methyl-ALA.HCl (V).

5-methyl-ALA.HCl was prepared according to the method of Lartillot and Baron.[45] Methyl 5-methyl-5-phthalimidolevulinate (2.99 g, 0.0103 mol) was refluxed with 7 N HCl (30 ml) for 8 hours after which the reaction mixture was left to cool overnight. The phthalic acid that separated out was filtered and the filtrate evaporated under vacuum.

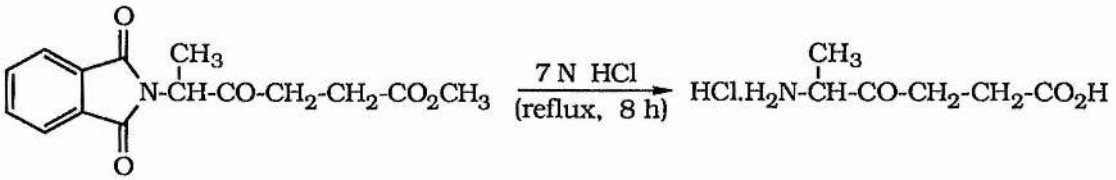

methyl 5-methyl-5-phthalimidolevulinate

5-methyl-5-aminolevulinic acid hydrochloride

+

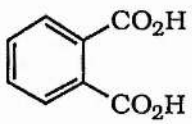

phthalic acid

The residual oil thus obtained was recrystallised from a mixture of dry methanol and ethyl acetate in the form of very fine white crystals (1.56 g, 83.4%), m.p. 142 °C (lit.,[46] 140-142 °C) (Found: C, 39.4, H, 6.8; N, 7.4. $C_6H_{12}NO_3Cl$ requires C, 39.7; H, 6.7; N, 7.7%); m/z 129 (M^+- NH_2- HCl, 2%), 101 (3), 84 (7), 73 (8), 69 (24), 55 (17), 45 (23), 44 (100), 36 (38) and 28 (79); δ_H (D_2O) 1.60 (3 H, d, *J* 7.07, $CHCH_3$), 2.72 (2 H, t, *J* 6.36, CH_2CO_2H), 2.97 (2 H, m, *J* 6.36, $CH_2CH_2CO_2H$), 4.33 (1 H, q, *J* 7.0 $CHCH_3$); δ_C (D_2O) 17.4, 30.2, 35.9, 57.4, 179.6 and 209.9.

4.3 Results and Discussion.

The condensation of ALA with pentane-2,4-dione and with ethylacetoacetate (Knorr type condensations) have long been used as a means of assay for ALA in biological material.[48] The condensation of ALA with pentane-2,4-dione is known to form 3-acetyl-4-(2-carboxyethyl)-2-methylpyrrole which has a free α-carbon. The quantitative determination of ALA is based on the reaction of a solution of this pyrrole with an equal volume of modified Ehrlich's reagent[48] to form a coloured compound.

The Knorr and Fischer-Fink condensations of ALA and its 5-methyl analogue with a variety of carbonyl compounds is described in Sections 4.3.1 to 4.3.9. The pyrrole products isolated from these reactions have been characterised by their melting points, elementary analyses, mass spectra and NMR spectra. The condensation reactions of ALA with pentane-2,4-dione and with 1,1,1-trifluoropentane-2,4-dione have both been shown to proceed *via* an enaminoketone intermediate when they were probed by ^{13}C and ^{15}N NMR spectroscopy. The kinetics of these reactions are discussed in detail in Chapter 5. No intermediates were detected in the reactions of [^{15}N]ALA.HCl (50% enriched) with ethylaceto-acetate, hexane-2,4-dione or 3-methylpentane-2,4-dione when they were probed by ^{15}N NMR spectroscopy. The same was true for the reactions of 5-methyl-ALA.HCl with pentane-2,4-dione and with 3-methylpentane-2,4-dione, when they were probed by ^{13}C NMR spectroscopy. This probably suggests that the enaminoketone intermediate in each of the above reactions is formed slowly, *via* a rate determining step. As a result, a significant amount of intermediate does not accumulate at any given time and its detection is therefore not possible by NMR spectroscopy. Although

not detected, the enaminoketone has been implicated as the reaction intermediate in all the above reactions.

It should be noted that a by-product detected in trace amounts, in the mother liquor of all the reactions of ALA with carbonyl compounds was 2,5-bis(2-carboxyethyl)pyrazine, formed by the chemical dimerisation of ALA. Similarly, trace amounts of 2,5-bis(2-carboxyethyl)-3,6-dimethylpyrazine was detected in the mother liquor of the reactions of 5-methyl-ALA with pentane-2,4-dione and with 3-methylpentane-2,4-dione, formed by the chemical dimerisation of 5-methyl-ALA.

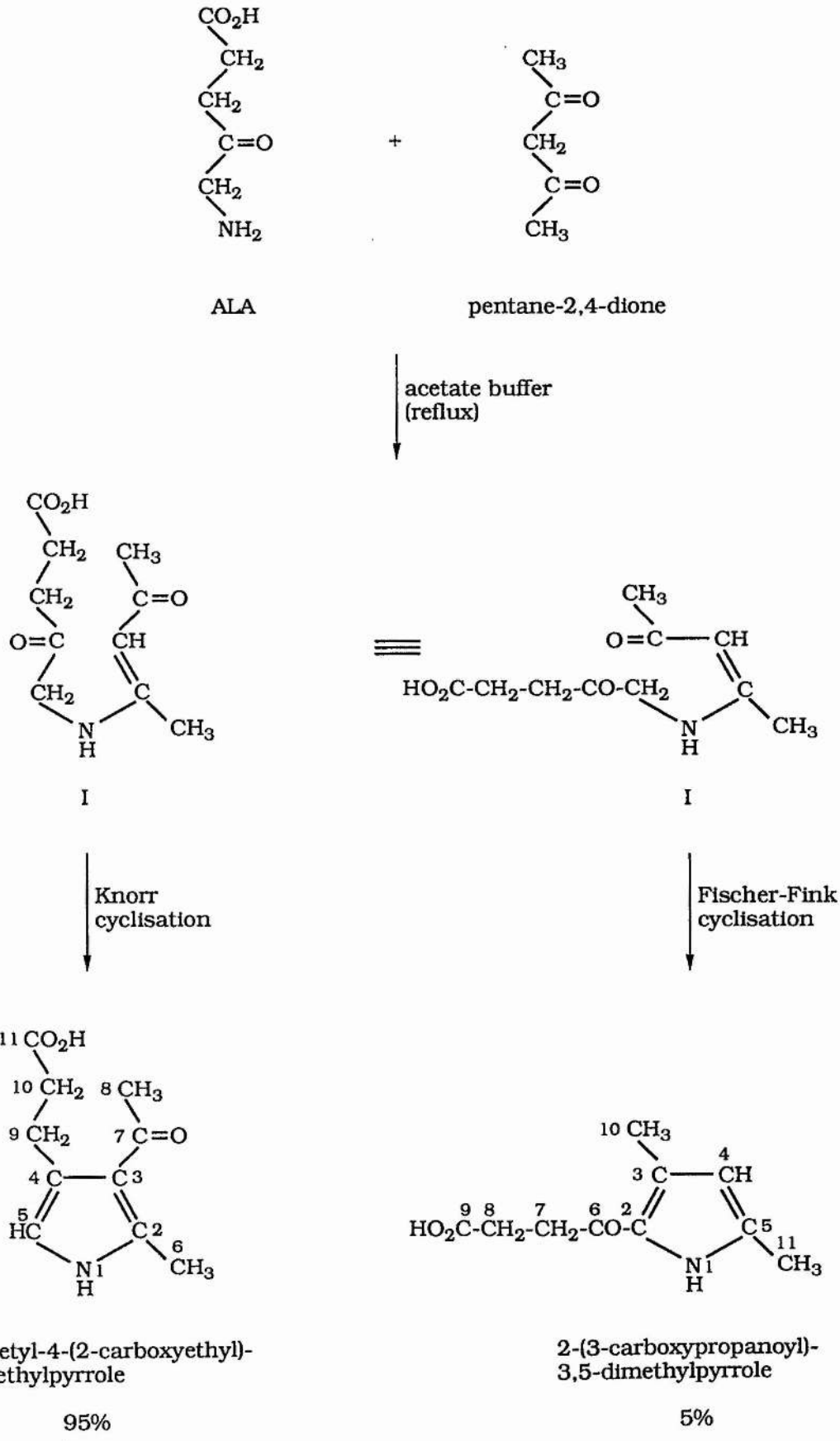
ALA
pentane-2,4-dione
acetate buffer
(reflux)
I
I
Knorr
cyclisation
Fischer-Fink
cyclisation
3-acetyl-4-(2-carboxyethyl)-
2-methylpyrrole
95%
2-(3-carboxypropanoyl)-
3,5-dimethylpyrrole
5%

Scheme 4.11

4.3.1 Condensation of ALA with pentane-2,4-dione.

A solution of ALA.HCl (0.08375 g, 0.5 mmol) and pentane-2,4-dione (0.05 g, 0.5 mmol) in acetate buffer (2 ml), pH 4.6, was heated under reflux for half an hour. The reaction mixture was cooled, and the product formed, filtered and washed thoroughly with cold water on a filter funnel. It was then dried to a constant weight (0.0605 g, 62%), over phosphorus pentoxide in a vacuum desiccator, m.p. 191 °C (Found: C, 61.5; H, 6.7; N, 7.1. $C_{10}H_{13}NO_3$ requires C, 61.5; H, 6.7; N, 7.2%).

Analysis of the product by NMR spectroscopy as well as GCMS revealed that it was a mixture of two products of identical molecular mass. The major product of the reaction constituting 95% of the total product is the expected Knorr product, 3-acetyl-4-(2-carboxyethyl)-2-methylpyrrole (Scheme 4.11). The minor product of the reaction, constituting 5% of the total product is the Fischer-Fink product, 2-(3-carboxypropanoyl)-3,5-dimethyl-pyrrole, formed by the alternative mode of cyclisation of the enaminoketone intermediate, I (Scheme 4.11). The ^{13}C and ^{1}H NMR data of the two products are listed in Table 4.1. The ^{13}C assignments of the pyrrole carbons of the Knorr product were confirmed from the ^{13}C NMR spectrum of the material labelled at the 4-position with 50% ^{13}C [prepared from equimolar amounts of [4-^{13}C]ALA.HCl (50% enriched) and pentane-2,4-dione]. Both the C_3 and C_5 resonances had satellite peaks on either side of the parent signal ($^{1}J_{C_4C_5}$ = 69.6 Hz; $^{1}J_{C_3C_4}$ = 53.7 Hz) and C_2 was assigned by default. Similarly the C_9 resonance had satellite peaks on either side of the parent signal ($^{1}J_{C_4C_9}$ = 48.8 Hz) and C_{10} was assigned by default. In the case of the Fischer-Fink product, with the ^{13}C label at C_6, satellite peaks were observed on either side of the C_7

resonance ($^1J_{C_6C_7}$ = 41.5 Hz) and C_8 was assigned by default. However, because of the very small intensities of the pyrrole carbons, satellite peaks were not observed on either side of the C_2 resonance. The ^{13}C resonances of C_2, C_3, C_5, C_{10} and C_{11} of the Fischer-Fink product were therefore assigned from a comparison of the ^{13}C resonances of similar pyrroles.[49] The ^1H NMR assignments of the Knorr and the Fischer-Fink products were made from a ^{13}C-^1H correlation.

The Knorr product and the Fischer-Fink product were separated by gas chromatography and their fragment ions obtained in the mass spectrometer are listed below.

3-acetyl-4-(2-carboxyethyl)-2-methylpyrrole: m/z 195 (M^+, 15%), 177 (20), 152 (21), 138 (45), 134 (61), 120 (20), 108 (40), 93 (22), 77 (34), 82 (22), 65 (35), 43 (100), 39 (50) and 28 (55).

2-(3-carboxypropanoyl)-3,5-dimethylpyrrole: m/z 195 (M^+, 10%), 166 (19), 150 (15), 136 (50), 134 (44), 122 (29), 108 (34), 94 (11), 93 (14), 77 (21), 65 (22), 59 (14), 45 (7), 43 (47), 39 (20) and 28 (100).

Table 4.1 ^{13}C and ^{1}H NMR data of 3-acetyl-4-(2-carboxyethyl)-2-methylpyrrole (A) and 2-(3-carboxypropanoyl)-3,5-dimethylpyrrole (B) (Scheme 4.11) in CD_3OD with reference to TMS.

Compound	Carbon	^{13}C chemical shift (ppm)	Proton	^{1}H chemical shift (ppm)
A	C_2	138.0		
	C_3	121.0		
	C_4	125.8	5-CH	6.40 (s)
	C_5	116.2	6-CH_3	2.47 (s)
	C_6	15.4	8-CH_3	2.40 (s)
	C_7	197.6	9-CH_2	2.94 (t), J = 7.42 Hz
	C_8	30.7	10-CH_2	2.53 (t), J = 7.42 Hz
	C_9	24.2		
	C_{10}	35.9		
	C_{11}	177.6		
B	C_2	129.0		
	C_3	131.0		
	C_4	113.4	4-CH	5.80 (s)
	C_5	136.4	7-CH_2	3.01 (t), J = 6.60 Hz
	C_6	189.2	8-CH_2	2.64 (t), J = 6.60 Hz
	C_7	35.0	10-CH_3	2.21 (s)
	C_8	27.1	11-CH_3	2.32 (s)
	C_9	176.9		
	C_{10}	12.8		
	C_{11}	14.6		

4.3.2 Condensation of ALA with ethyl acetoacetate.

A solution of ALA.HCl (0.08375 g, 0.5 mmol) and ethyl-acetoacetate (0.065 g, 0.5 mmol) in acetate buffer (2 ml), pH 4.6, was heated under reflux for half an hour. The reaction mixture was cooled and the product formed, filtered and washed thoroughly with cold water on a filter funnel. It was then dried to a constant weight (0.0665 g, 59.1%), over phosphorus pentoxide in a vacuum desiccator, m.p. 163 °C (Found: C, 59.0; H, 6.7; N, 6.2. $C_{11}H_{14}NO_4$ requires C, 58.7; H, 6.7; N, 6.2.%); m/z 226 (M^++ 1, 4%), 225 (M^+, 56), 207 (8), 196 (1), 179 (54), 166 (10), 152 (28), 151 (91), 138 (100), 134 (88), 122 (38), 106 (34), 93 (21), 77 (32), 65 (32), 42 (26) and 39 (16).

Analysis of the product by NMR spectroscopy revealed that the only product formed in this reaction was the expected Knorr product, 3-(2-carboxyethyl)-4-ethoxycarbonyl-5-methyl-pyrrole (Scheme 4.12).

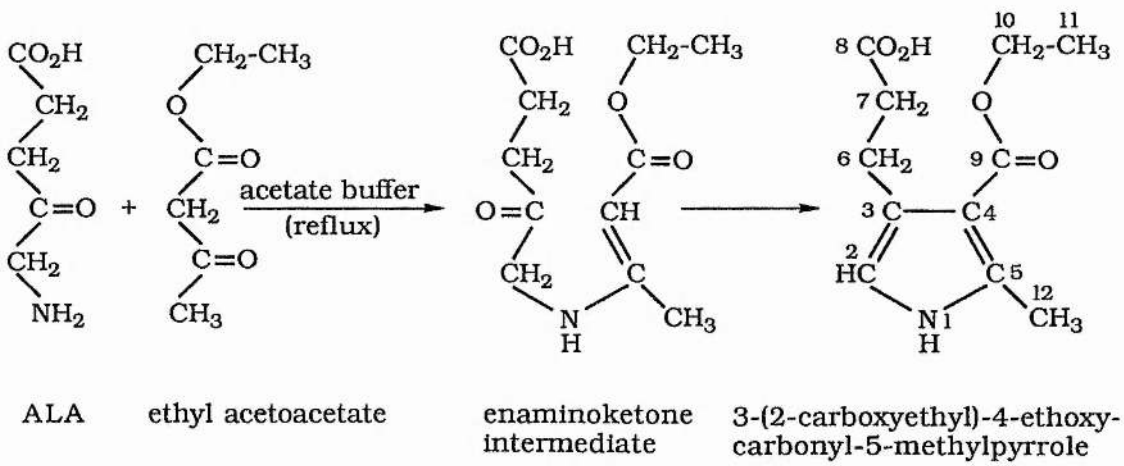

ALA ethyl acetoacetate enaminoketone intermediate 3-(2-carboxyethyl)-4-ethoxy-carbonyl-5-methylpyrrole

Scheme 4.12

The ^{13}C and ^{1}H NMR data for 3-(2-carboxyethyl)-4-ethoxy-carbonyl-5-methylpyrrole are listed in Table 4.2.

Table 4.2 ^{13}C and ^{1}H NMR data of 3-(2-carboxyethyl)-4-ethoxycarbonyl-5-methylpyrrole (A) (Scheme 4.12) in CD_3OD with reference to TMS.

Compound	Carbon	^{13}C chemical shift (ppm)	Proton	^{1}H chemical shift (ppm)
A	C_2	115.7		
	C_3	125.2		
	C_4	110.1	2-CH	6.36 (s)
	C_5	138.0	6-CH_2	2.92 (t), J = 7.70 Hz
	C_6	23.7	7-CH_2	2.56 (t), J = 7.70 Hz
	C_7	36.4	10-CH_2	4.22 (q), J = 7.15 Hz
	C_8	176.0	11-CH_3	1.33 (t), J = 7.15 Hz
	C_9	168.0	12-CH_3	2.41 (s)
	C_{10}	60.2		
	C_{11}	(14.8)[a]		
	C_{12}	(13.9)[a]		

(a) Ambiguous assignments are bracketed.

4.3.3 Condensation of ALA with 3-methylpentane-2,4-dione.

A solution of ALA.HCl (0.08375 g, 0.5 mmol) and 3-methylpentane-2,4-dione (0.057 g, 0.5 mmol) in acetate buffer (2 ml), pH 4.6, was heated under reflux for one hour. The reaction mixture was cooled and the product formed, filtered and washed thoroughly with cold water on a filter funnel. It was then dried to a constant weight (0.0174 g, 16.7%), over phosphorus pentoxide in a vacuum desiccator, m.p. 218 °C (Found: C, 63.2; H, 7.2; N, 6.7. $C_{11}H_{15}NO_3$ requires C, 63.1; H, 7.2; N, 6.7.% ; m/z 209 (M^+, 35%), 164 (19), 136 (100), 109 (25), 108 (10), 93 (14), 78 (23), 65 (13), 64 (63), 45 (70) and 39 (25)).

Analysis of the product by NMR spectroscopy revealed that only the Fischer-Fink product, 2-(3-carboxypropanoyl)-3,4,5-trimethylpyrrole (Scheme 4.13) was formed in this reaction.

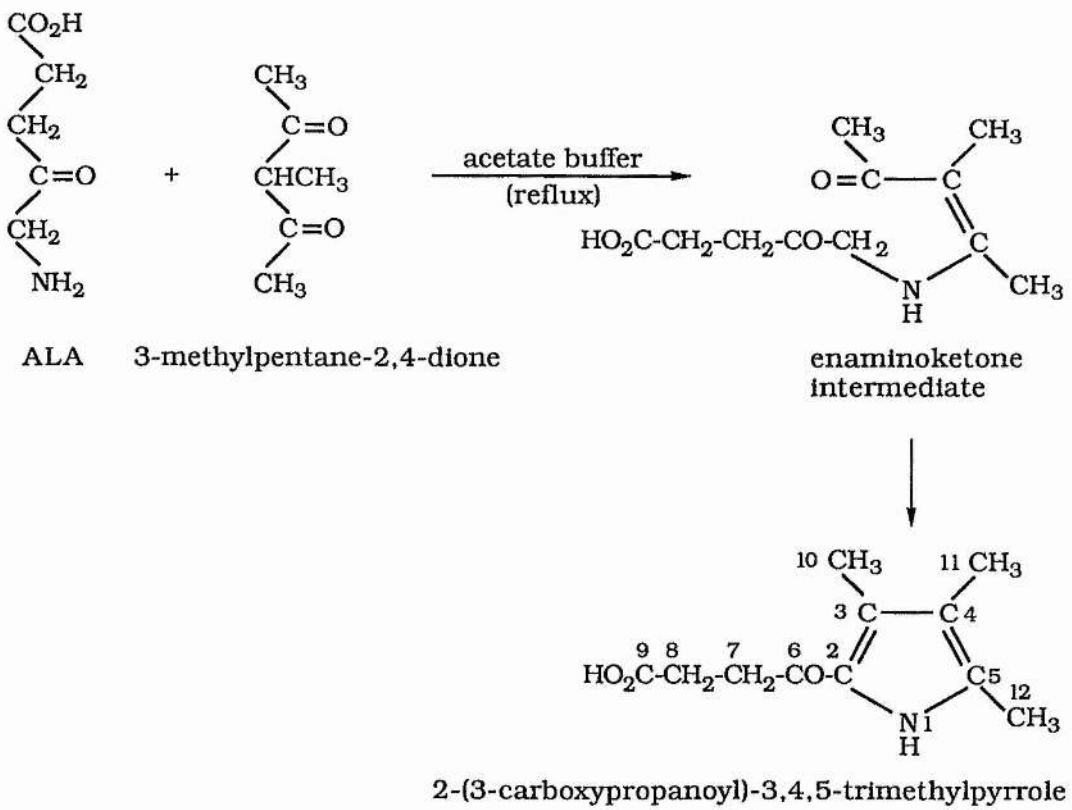

Scheme 4.13

The ^{13}C and ^{1}H NMR data for 2-(3-carboxypropanoyl)-3,4,5-trimethylpyrrole are listed in Table 4.3.

Table 4.3 ^{13}C and ^{1}H NMR data of 2-(3-carboxypropanoyl)-3,4,5-trimethylpyrrole (A) (Scheme 4.13) in $(CD_3)_2SO$ with reference to TMS.

Compound	Carbon	^{13}C chemical shift (ppm)	Proton	^{1}H chemical shift (ppm)
A	C_2	125.6 } a		
	C_3	126.2		
	C_4	116.4		
	C_5	131.1	7-CH_2	2.90 (t), J = 6.60 Hz
	C_6	186.4	8-CH_2	2.50 (t), J = 6.60 Hz
	C_7	33.5	10-CH_3	2.13 (s) } a
	C_8	27.8	11-CH_3	1.85 (s)
	C_9	174.0	12-CH_3	2.19 (s)
	C_{10}	10.9 } a		
	C_{11}	8.4		
	C_{12}	11.3		

(a) Not necessarily respectively.

4.3.4 Condensation of ALA with 3-isopropylpentane-2,4-dione.

A solution of ALA.HCl (0.08375 g, 0.5 mmol) and 3-isopropyl-pentane-2,4-dione (0.071 g, 0.5 mmol) in acetate buffer (2 ml), pH 4.6, was heated under reflux for one hour. The reaction mixture was cooled and the product formed, filtered and washed thoroughly with cold water on a filter funnel. It was then dried to a constant weight (0.0119 g, 10%), over phosphorus pentoxide in a vacuum desiccator, m.p. 178 °C (Found: C, 65.8; H, 8.0; N, 5.8. $C_{13}H_{19}NO_3$ requires C, 65.8; H, 8.1; N, 5.9.%); m/z 219 (M^+- H_2O, 53%), 204 (100), 190 (19), 176 (42), 147 (67), 148 (39), 134 (11), 120 (17), 91 (17), 77 (25), 67 (17), 43 (8) and 39 (28).

Analysis of the product by NMR revealed that only the Fischer-Fink product, 2-(3-carboxypropanoyl)-3,5-dimethyl-4-isopropylpyrrole (Scheme 4.14) was formed in this reaction.

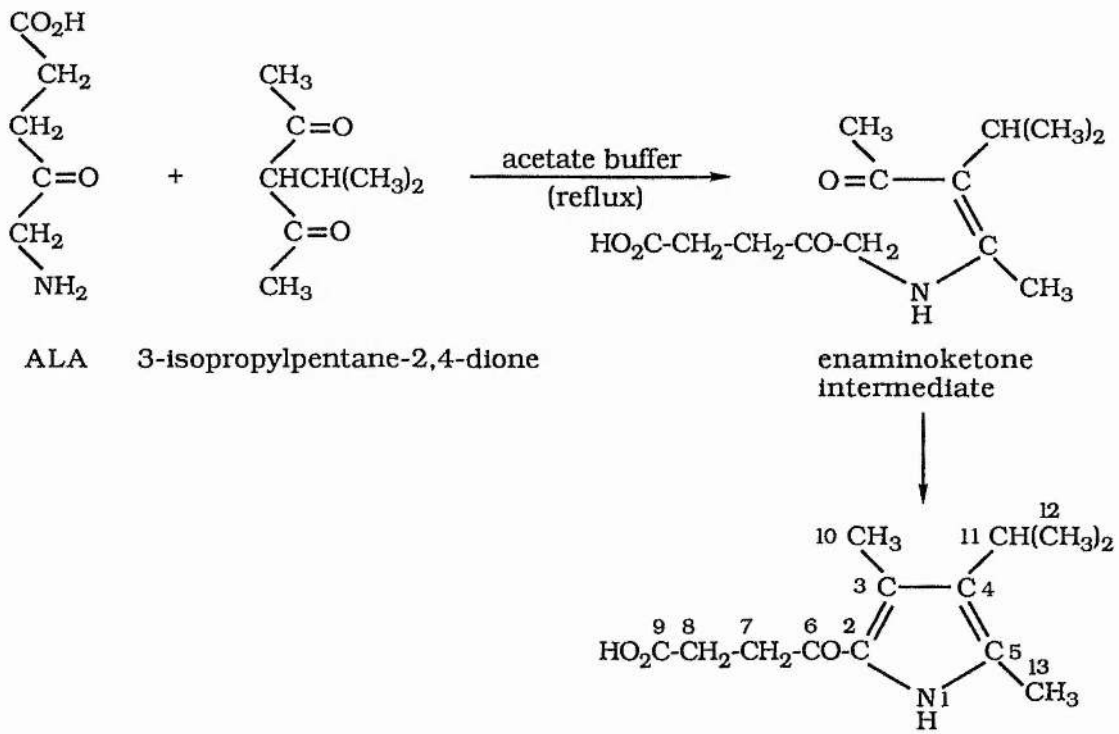

Scheme 4.14

The ^{13}C and ^{1}H NMR data for 2-(3-carboxypropanoyl)-3,5-dimethyl-4-isopropylpyrrole are listed in Table 4.4.

Table 4.4 ^{13}C and ^{1}H NMR data of 2-(3-carboxypropanoyl)-3,5-dimethyl-4-isopropylpyrrole (A) (Scheme 4.14) in $(CD_3)_2SO$ with reference to TMS.

Compound	Carbon	^{13}C chemical shift (ppm)	Proton	^{1}H chemical shift (ppm)
A	C_2	126.0 } a		
	C_3	126.5		
	C_4	124.7		
	C_5	129.7	7-CH_2	2.84 (t), J = 6.95 Hz
	C_6	187.9	8-CH_2	2.39 (t), J = 6.95 Hz
	C_7	34.7	10-CH_3	[2.20 (s)][b]
	C_8	29.8	11-CH	2.87 (m), J = 6.95 Hz
	C_9	174.8	12-CH_3	1.18 (d), J = 6.95 Hz
	C_{10}	[11.4][b]	13-CH_3	[2.25 (s)][b]
	C_{11}	24.3		
	C_{12}	22.4		
	C_{13}	[12.2][b]		

(a) Not necessarily respectively.

(b) Ambiguous assignments are bracketed.

4.3.5 Condensation of ALA with 3,3-dimethylpentane-2,4-dione.

A solution of ALA.HCl (0.08375 g, 0.5 mmol) and 3,3-dimethylpentane-2,4-dione (0.064 g, 0.5 mmol) in acetate buffer (2 ml), pH 4.6, was heated under reflux for one hour. The reaction mixture was cooled and analysed by NMR spectroscopy. The only product detected in the reaction mixture was 2,5-bis(2-carboxyethyl)pyrazine formed by the dimerisation of ALA (Scheme 4.15). 3,3-dimethylpentane-2,4-dione remained unreacted and there was no evidence for the formation of a carbinolamine or an imine species, by the condensation of the amino group of ALA with the carbonyl carbon of 3,3-dimethylpentane-2,4-dione. This could be due to steric factors with the two methyl groups at the 3-position of the latter, preventing the approach of the amino group of ALA onto either of its carbonyl carbons. Another reason that maybe considered, is the fact that reaction of an amine with a carbonyl compound will only take place when an enol grouping is available in the latter. 3,3-dimethylpentane-2,4-dione exists 100% in the keto form and therefore does not react with ALA.

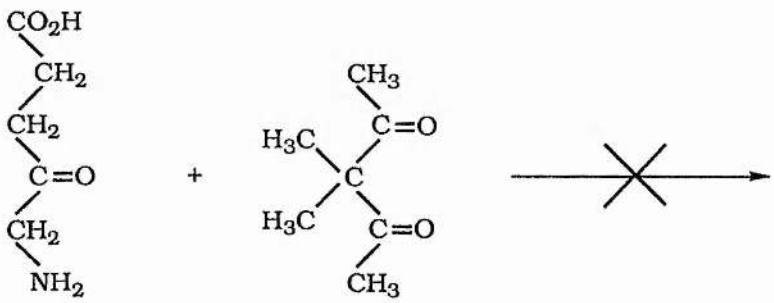

ALA 3,3-dimethylpentane-2,4-dione

dimerisation

2,5-bis(2-carboxyethyl)pyrazine

Scheme 4.15

During extensive investigations of β-diketones, Combes[50] carried out the following series of reactions (Scheme 4.16).

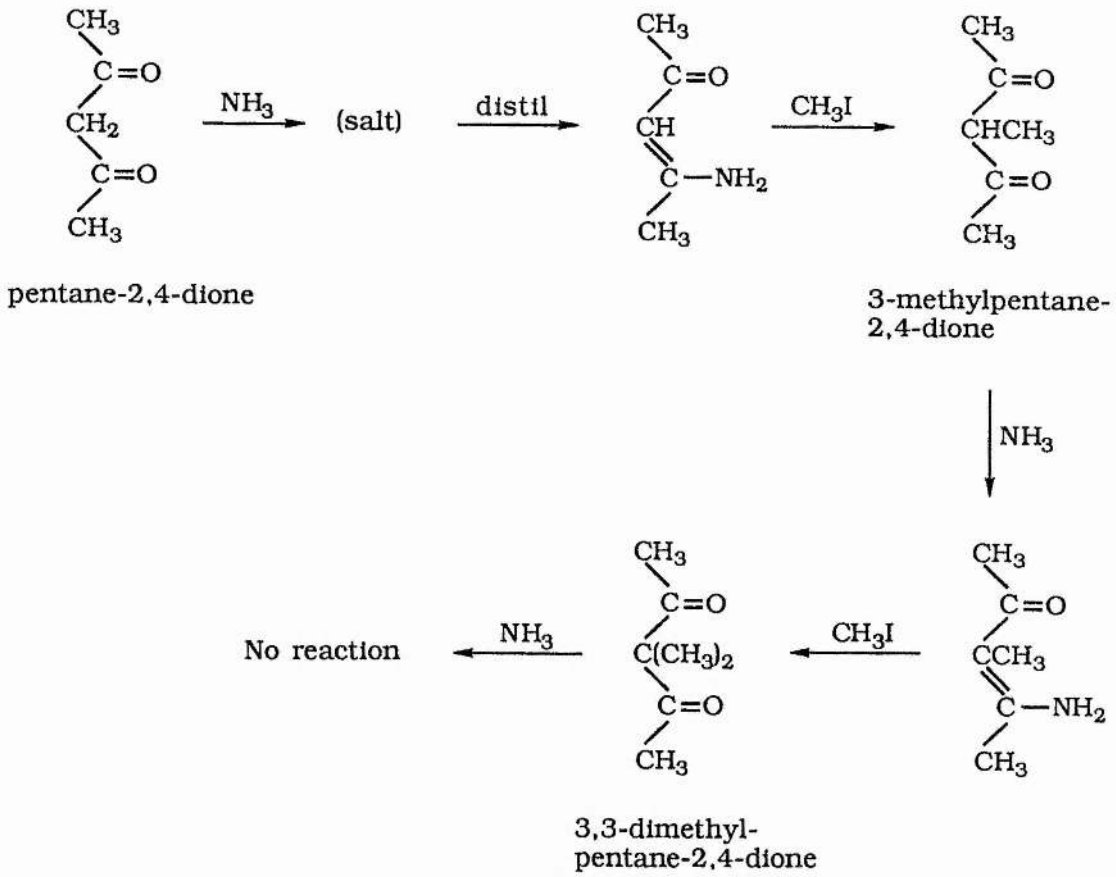

Scheme 4.16

Since 3,3-dimethylpentane-2,4-dione gave no reaction with ammonia, Combes interpreted this as meaning that an enol grouping in the carbonyl compound is essential for the reaction to take place.

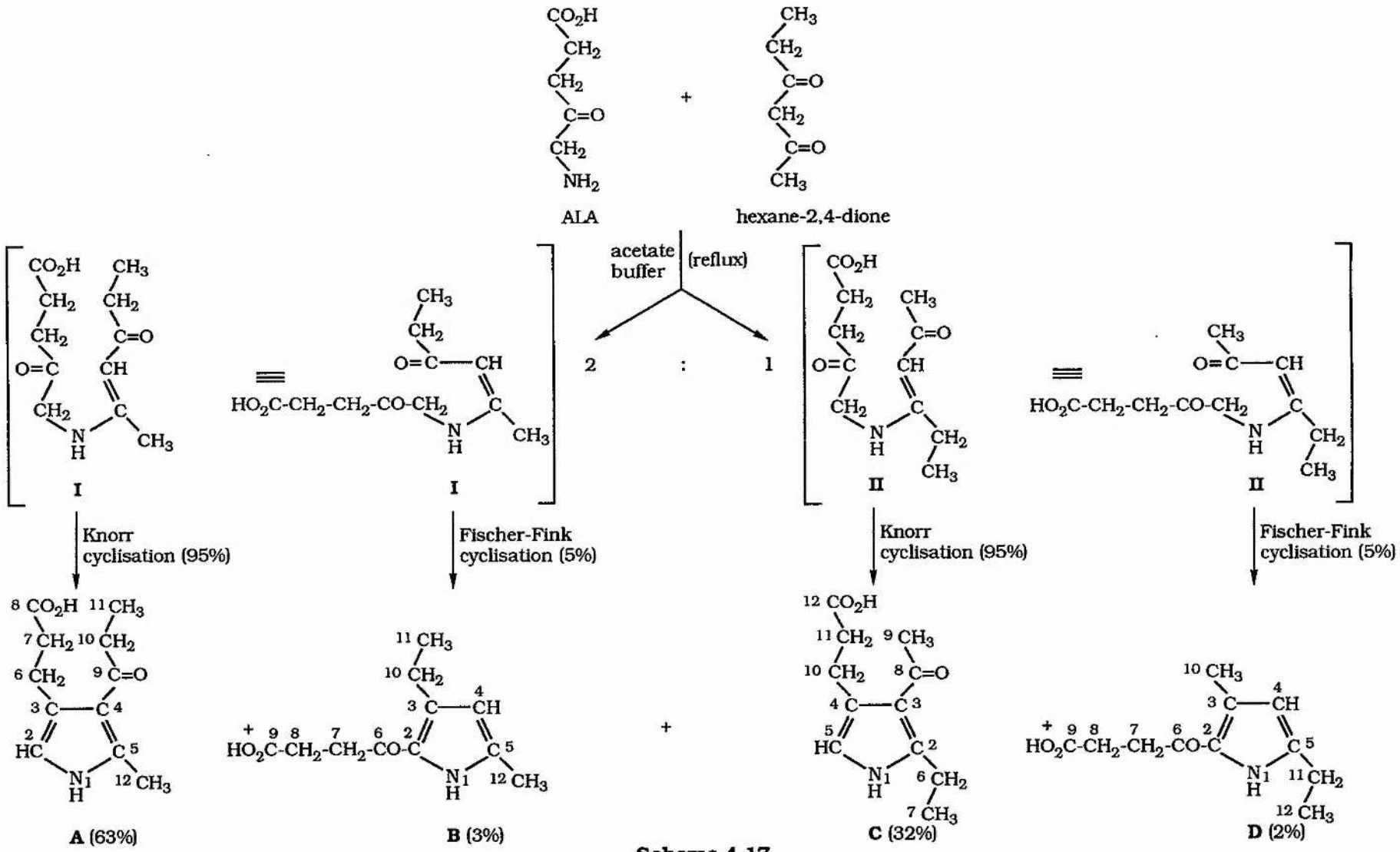
ALA
hexane-2,4-dione
acetate buffer
(reflux)
2 : 1
I
I
II
II
Knorr cyclisation (95%)
Fischer-Fink cyclisation (5%)
Knorr cyclisation (95%)
Fischer-Fink cyclisation (5%)
A (63%)
B (3%)
C (32%)
D (2%)

Scheme 4.17

4.3.6 Condensation of ALA with hexane-2,4-dione.

A solution of ALA.HCl (0.08375 g, 0.5 mmol) and hexane-2,4-dione (0.057 g, 0.5 mmol) in acetate buffer (2 ml), pH 4.6, was heated under reflux for half an hour. The reaction mixture was cooled and the product formed, filtered and washed thoroughly with cold water on a filter funnel. It was then dried to a constant weight (0.0624 g, 59.7%), over phosphorus pentoxide in a vacuum desiccator, m.p. 161 °C (Found: C, 62.9; H, 7.2; N, 6.6. $C_{11}H_{15}NO_3$ requires C, 63.1; H, 7.2; N, 6.7.%).

Analysis of the product by NMR spectroscopy as well as GCMS revealed it to be a mixture of four products of identical molecular mass. As illustrated in Scheme 4.17, the amino group of ALA can condense with either carbonyl group of the unsymmetrical β-diketone, hexane-2,4-dione. Condensation preferentially takes place at the less hindered carbonyl with the formation of the enaminoketone intermediates I and II in a ratio of 2:1 (Scheme 4.17). 95% of each of the intermediate forms I and II, cyclises to form the Knorr products, 3-(2-carboxyethyl)-5-methyl-4-propanoyl-pyrrole, (A) and 3-acetyl-4-(2-carboxyethyl)-2-ethylpyrrole, (C) respectively, while the remaining 5% of the intermediates I and II cyclises *via* the alternative mode to form the Fischer-Fink products, 2-(3-carboxypropanoyl)-3-ethyl-5-methylpyrrole, (B) and 2-(3-carboxypropanoyl)-3-methyl-5-ethylpyrrole, (D) respectively (Scheme 4.17). The percentage of each pyrrole formed is indicated in Scheme 4.17. The ^{13}C and ^{1}H NMR data of the products are listed in Table 4.5.

The four pyrrole products were separated by gas chromatography and their fragment ions obtained in the mass spectrometer are listed below.

3-(2-carboxyethyl)-5-methyl-4-propanoylpyrrole (A): m/z 209 (M^+, 9%), 180 (7), 152 (9), 138 (100), 134 (23), 120 (12), 106 (14), 93 (9), 77 (18), 65 (21), 57 (20), 42 (17), 39 (24), 27 (46), 28 (48) and 18 (28).

2-(3-carboxypropanoyl)-3-ethyl-5-methylpyrrole (B): m/z 209 (M^+, 8%), 191 (7), 180 (6), 162 (40), 148 (4), 134 (31), 120 (14), 106 (16), 93 (9), 77 (24), 65 (29), 57 (18), 55 (12), 42 (24), 39 (32), 29 (48), 28 (94) and 18 (100).

3-acetyl-4-(2-carboxyethyl)-2-ethylpyrrole (C): m/z 209 (M^+, 6%), 191 (7), 166 (33), 152 (18), 148 (37), 134 (29), 122 (16), 120 (15), 106 (31), 93 (16), 77 (30), 65 (22), 59 (5), 43 (100), 39 (33), 29 (14), 28 (82) and 18 (78).

2-(3-carboxypropanoyl)-3-methyl-5-ethylpyrrole (D): m/z 210 (M^++ 1, 2%), 180 (14), 164 (2), 150 (10), 134 (11), 122 (8), 106 (9), 78 (8), 65 (7), 57 (7), 43 (34), 39 (12) and 28(100).

Table 4.5 ^{13}C and ^{1}H NMR data of 3-(2-carboxyethyl)-5-methyl-4-propanoyl-pyrrole (A) and 3-acetyl-4-(2-carboxyethyl)-2-ethylpyrrole (C) (Scheme 4.17) in CD_3OD with reference to TMS.

Compound	Carbon	^{13}C chemical shift (ppm)	Proton	^{1}H chemical shift (ppm)
A	C_2	116.1	2-CH	6.40 (s)
	C_3	125.7	6-CH_2	2.95 (t), J = 7.29 Hz
	C_4	120.6	7-CH_2	2.54 (t), J = 7.53 Hz
	C_5	116.1	10-CH_2	2.75 (q), J = 7.53 Hz
	C_6	24.3	11-CH_3	1.13 (t), J = 7.29 Hz
	C_7	35.9	12-CH_3	2.47 (s)
	C_8	177.6		
	C_9	200.8		
	C_{10}	36.0		
	C_{11}	9.0		
	C_{12}	15.5		
C	C_2	143.8	5-CH	6.43 (s)
	C_3	120.1	6-CH_2	2.89 (q), J = 7.53 Hz
	C_4	125.4	7-CH_3	1.23 (t), J = 7.29 Hz
	C_5	116.3	9-CH_3	2.42 (s)
	C_6	22.8	10-CH_2	2.95 (t), J = 7.29 Hz
	C_7	14.2	11-CH_2	2.55 (t), J = 7.53 Hz
	C_8	197.8		
	C_9	30.5		
	C_{10}	24.2		
	C_{11}	35.8		
	C_{12}	177.5		

Table 4.5 Cont... ^{13}C and ^{1}H NMR data of 2-(3-carboxypropanoyl)-3-ethyl-5-methylpyrrole (B) and 2-(3-carboxypropanoyl)-3-methyl-5-ethylpyrrole (D) (Scheme 4.17) in CD_3OD with reference to TMS.

Compound	Carbon	^{13}C chemical shift (ppm)	Proton	^{1}H chemical shift (ppm)
B	C_2	116.2		
	C_3	136.5		
	C_4	111.2	4-CH	5.87 (s)
	C_5	137.3	7-CH_2	3.023 (t), J = 6.60 Hz
	C_6	189.1	8-CH_2	2.65 (t), J = 6.60 Hz
	C_7	34.7	10-CH_2	3.48 (q), J = 7.29 Hz
	C_8	29.2	11-CH_3	1.17 (t), J = 7.29 Hz
	C_9	176.9	12-CH_3	2.23 (s)
	C_{10}	66.9		
	C_{11}	(15.1)[a]		
	C_{12}	(12.9)[a]		
D	C_2	116.5		
	C_3	138.3		
	C_4	111.8	4-CH	5.84 (s)
	C_5	144.6	7-CH_2	3.017 (t), J = 6.60 Hz
	C_6	189.3	8-CH_2	2.651 (t), J = 6.60 Hz
	C_7	35.0	10-CH_3	2.33 (s)
	C_8	29.2	11-CH_2	2.76 (q), J = 7.29 Hz
	C_9	176.0	12-CH_3	1.19 (t), J = 7.53 Hz
	C_{10}	(14.7)[a]		
	C_{11}	22.2		
	C_{12}	(14.0)[a]		

(a) Ambiguous assignments are bracketed.

4.3.7 Condensation of ALA with 1,1,1-trifluoropentane-2,4-dione.

A solution of ALA.HCl (0.08375 g, 0.5 mmol) and 1,1,1-trifluoropentane-2,4-dione (0.077 g, 0.5 mmol) in acetate buffer (2 ml), pH 4.6, was left standing overnight. The fine white crystals that formed were filtered and washed thoroughly with cold water on a filter funnel. They were dried to a constant weight (0.054 g, 40.4%), over phosphorus pentoxide in a vacuum desiccator, m.p. 154 °C (Found: C, 45.0; H, 4.2; N, 5.1. $C_{10}H_{12}NO_4F_3$ requires C, 45.0; H, 4.5; N, 5.2.%; m/z 267 (M^+, 2%), 249 (2), 198 (1), 166 (17), 101 (3), 96 (3), 69 (11), 55 (5), 45 (9), 44 (11) and 28 (100)).

Analysis of the product by NMR spectroscopy revealed that it was a hydrogen-bonded enaminoketone (Scheme 4.18).

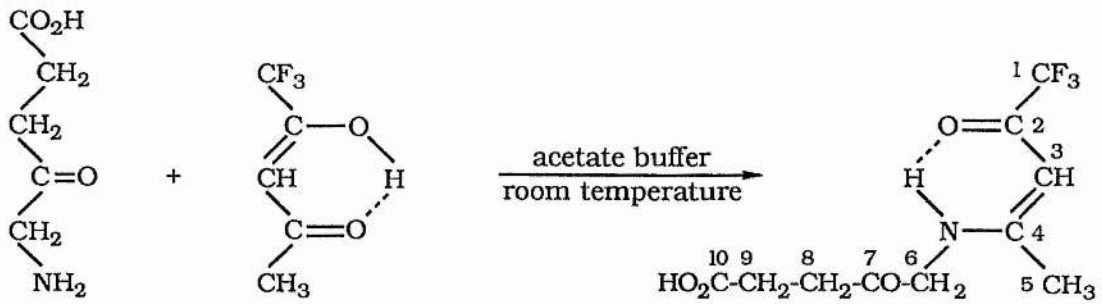

ALA 1,1,1-trifluoropentane-2,4-dione enaminoketone

Scheme 4.18

The ^{13}C and ^{1}H NMR data of the enaminoketone are listed in Table 4.6. The presence of the hydrogen-bonded chelate ring was inferred from the large paramagnetic shift (δ 11.3), of the N-H proton. Hydrogen bonding leads to deshielding and to an increase in the frequency of the NMR signal of the hydrogen-bonded proton. The structure of the enaminoketone was further confirmed from the following evidence. The low field proton signal of the enaminoketone, 50% enriched in ^{15}N [synthesised from equimolar

amounts of [^{15}N]ALA.HCl (50% enriched) and 1,1,1-trifluoro-pentane-2,4-dione], appears as a broad resonance at δ 11.3, which is the ^{14}NH resonance and a doublet one on either side of the broad resonance, due to a one bond ^{15}N-H coupling ($^{1}J_{^{15}NH}$ = 92.5 Hz). (Fig. 4.2). Each signal of this doublet is further split into a triplet due to coupling with the protons of the α-CH_2 group attached to the nitrogen atom ($^{3}J_{HH}$ = 5.47 Hz) (Fig. 4.2). The splitting of the α-CH_2 protons into a doublet, due to coupling with the NH proton however, could not be resolved.

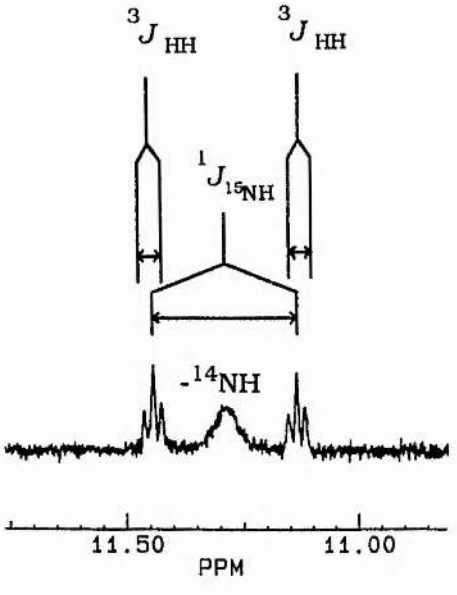

Figure 4.2 300.134 MHz ^{1}H NMR spectrum of the enaminoketone (50% enriched with ^{15}N) indicating the broad ^{14}NH resonance at 11.3 ppm, the one bond ^{15}N-H coupling constant, $^{1}J_{^{15}NH}$ = 92.5 Hz and the three bond H-H coupling constant, $^{3}J_{HH}$ = 5.47 Hz. The solvent was CD_3OD and the spectrum referenced with respect to TMS.

Further evidence that the product of the above reaction is an enaminoketone and not an imine, was obtained from the ^{15}N chemical shift (δ 120.5) of the latter, 50% enriched in ^{15}N. This lies well outside the ^{15}N chemical shift range for imines (δ 305 to δ 365)[51] but within the ^{15}N chemical shift range for enaminoketones (δ 80 to δ 125).[51]

From these findings it can be concluded that the product exists > 95% in the enaminoketone form in solution. There was no evidence to suggest the presence of the other tautometric forms of the product: the enimine and ketimine forms (Fig. 4.3) in solution.

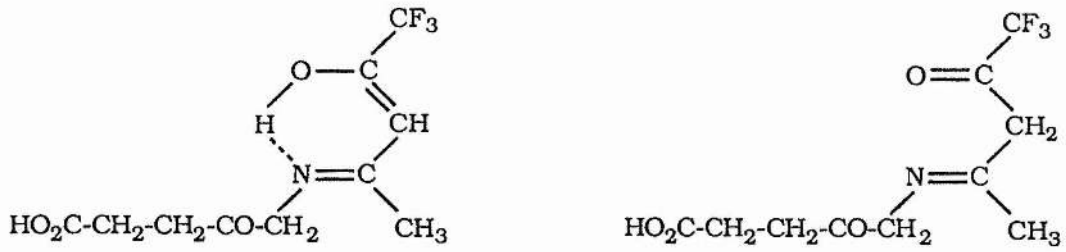

Figure 4.3 Tautometric forms of the enaminoketone - the enimine and ketimine forms.

Previous investigation into the keto-enol tautomerisation of Schiff bases prepared from monoamines and aliphatic dicarbonyl compounds have indicated that only one isomer, the enamino-ketone is present in solution.[52,53] Dudek and Holm[58] have ascribed the preferential existence of the enaminoketone form, over that of the enimine and ketimine to greater stabilisation through resonance and hydrogen bonding. The above authors[58] have also proposed that the resonance interaction in the enaminoketone is intrinsically more stabilizing,

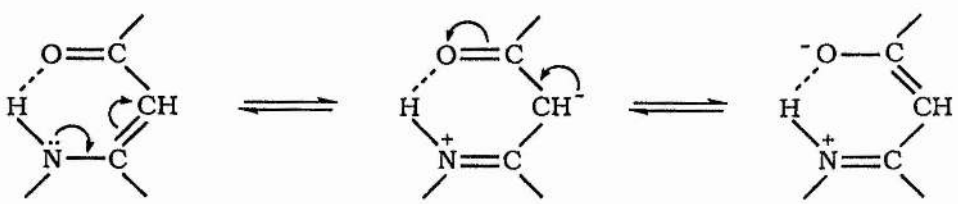

than that in the enimine in which the negative change cannot be delocalised on oxygen.

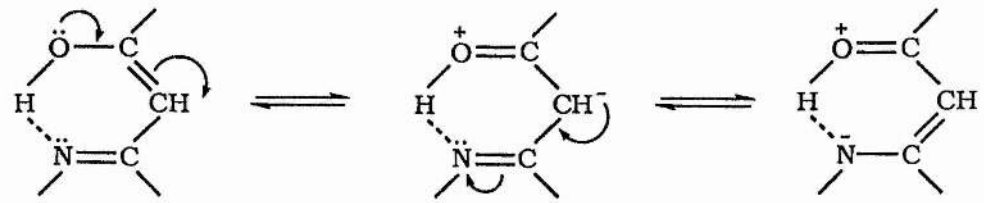

The existence of the enol form (II) of the enaminoketone, in rapid equilibrium with its keto form (I) was indirectly demonstrated by monitoring hydrogen exchange at the C_6 methylene group of I (50% enriched in ^{15}N) by ^1H NMR in CD_3OD.

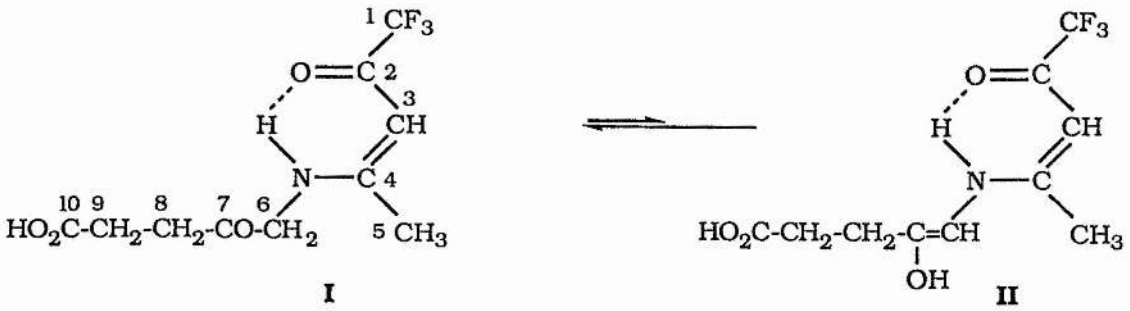

Hydrogen exchange at C_6 led to the gradual evolution of I to Ib *via* Ia.

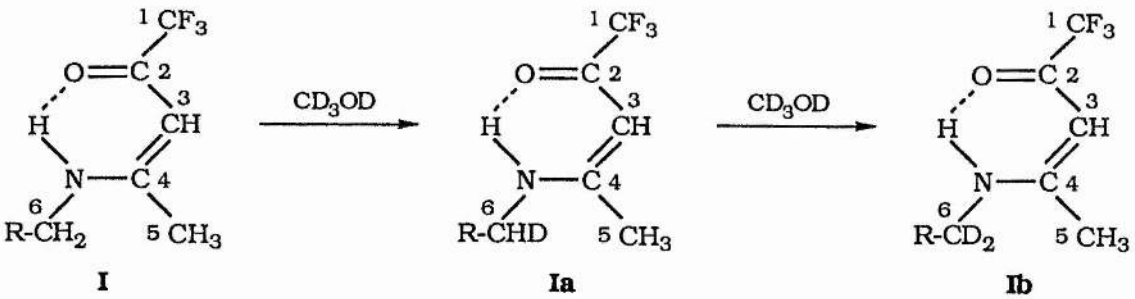

where R = HO_2C-CH_2-CH_2-CO

The 6-CHD proton of Ia appears as a 1:1:1 triplet at 4.50 ppm while its ^{15}N-H resonance appears as a doublet, each signal of which is further split into a doublet due to coupling with the proton of the α-CHD group attached to the nitrogen atom. The ^{15}N-H resonance of Ib appears as a doublet, one on either side of its ^{14}N-H resonance at 11.3 ppm.

Table 4.6 ^{13}C and ^{1}H NMR data of the enaminoketone (Scheme 4.18) in CD_3OD with reference to TMS.

Compound	Carbon	^{13}C chemical shift (ppm)	Proton	^{1}H chemical shift (ppm)
enaminoketone	C_1	125.0, 121.2, 117.4, 113.6 (quartet, $^{1}J_{CF}$ = 287.6 Hz)		
	C_2	176.8, 176.4, 176.0, 175.6 (quartet, $^{2}J_{CF}$ = 32.3 Hz)	3-CH	5.43 (s)
			5-CH_3	2.10 (s)
	C_3	90.3	NH	11.3 (s)
	C_4	172.4	6-CH_2	4.52 (s)
	C_5	20.0	8-CH_2	2.77 (t), J = 6.36 Hz
	C_6	53.7	9-CH_2	2.65 (t), J = 6.36 Hz
	C_7	204.1		
	C_8	35.3		
	C_9	28.7		
	C_{10}	176.1		

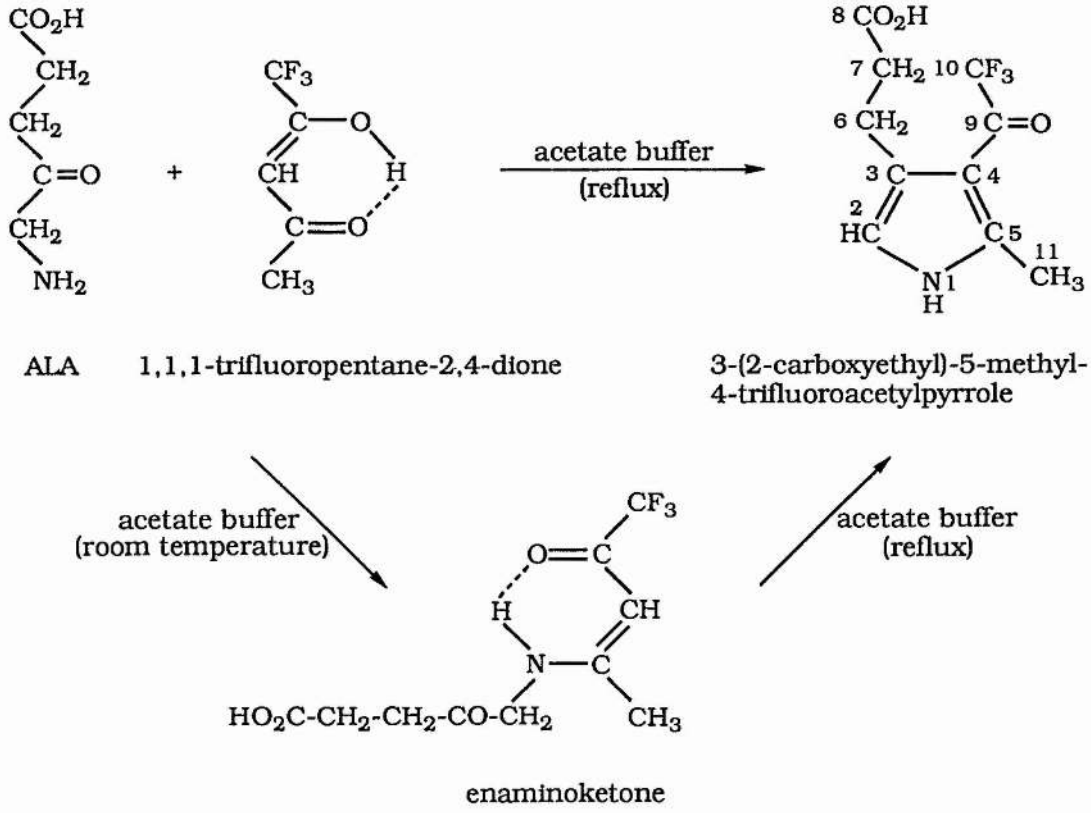
CO2H
CH2
CH2
C=O
CH2
NH2
+
CF3
C
O
CH
H
C=O
CH3
acetate buffer
(reflux)
8 CO2H
7 CH2
10 CF3
6 CH2
9 C=O
3 C
C 4
2
HC
C 5
11
CH3
N 1
H
ALA
1,1,1-trifluoropentane-2,4-dione
3-(2-carboxyethyl)-5-methyl-
4-trifluoroacetylpyrrole
acetate buffer
(room temperature)
acetate buffer
(reflux)
CF3
O=C
H
CH
N
C
HO2C-CH2-CH2-CO-CH2
CH3
enaminoketone

Scheme 4.19

4.3.8 Condensation of ALA with 1,1,1-trifluoropentane-2,4-dione in refluxing acetate buffer.

A solution of ALA.HCl (0.08375 g, 0.5 mmol) and 1,1,1-trifluoropentane-2,4-dione (0.077 g, 0.5 mmol) in acetate buffer (2 ml), pH 4.6, was heated under reflux for half an hour. The reaction mixture was cooled and the product formed, filtered and washed thoroughly with cold water on a filter funnel. It was then dried to a constant weight (0.0272 g, 23.4%), over phosphorus pentoxide in a vacuum desiccator, m.p. 187 °C (Found: C, 48.2; H, 3.5; N, 5.6. $C_{10}H_{10}NO_3F_3$ requires C, 48.2; H 4.0; N, 5.6.% ; m/z 250 (M^++ 1, 17%), 249 (M^+, 10), 232 (1), 204 (9), 191 (7), 180 (3), 153 (7), 139 (34), 134 (11), 108 (7), 94 (3), 81 (2), 69 (5), 66 (6), 44 (8) and 28 (100).

Analysis of the product by NMR spectroscopy revealed that the only product formed in this reaction was the Knorr product, 3-(2-carboxyethyl)-5-methyl-4-trifluoroacetylpyrrole, (Scheme 4.19). This was inferred from the ^1H chemical shift (δ 6.53), corresponding to an α-CH proton of a pyrrole ring, which is what is present in the Knorr product. There was however no evidence for the formation of the Fischer-Fink product. The same product, 3-(2-carboxyethyl)-5-methyl-4-trifluoroacetylpyrrole was also formed when the enaminoketone (described in Section 4.3.7) was refluxed in acetate buffer, pH 4.6, (Scheme 4.19). It is therefore concluded that the enaminoketone is an intermediate in the formation of 3-(2-carboxyethyl)-5-methyl-4-trifluoroacetylpyrrole. The ^{13}C and ^1H NMR data of the latter are listed in Table 4.7.

Table 4.7 ^{13}C and ^{1}H NMR data of 3-(2-carboxyethyl)-5-methyl-4-trifluoroacetyl-pyrrole (A) (Scheme 4.19) in CD_3OD with reference to TMS.

Compound	Carbon	^{13}C chemical shift (ppm)	Proton	^{1}H chemical shift (ppm)
A	C_2	117.7		
	C_3	127.9		
	C_4	114.2		
	C_5	140.6		
	C_6	23.7		
	C_7	35.4	2-CH	6.53 (s)
	C_8	177.4	6-CH_2	2.94 (t), J = 7.53 Hz
			7-CH_2	2.54 (t), J = 7.53 Hz
	C_9	176.5, 177.0, 177.4, 177.9 quartet $^{2}J_{CF}$ = 34.8 Hz	11-CH_3	2.46 (q), $J_{H_{11}F}$ = 1.52 Hz
	C_{10}	112.5, 116.4, 120.2, 124.0 quartet $^{2}J_{CF}$ = 34.8 Hz		
	C_{11}	14.29, 14.35, 14.40, 14.46 quartet $J_{C_{11}F}$ = 4.48 Hz		

4.3.9 Condensation of ALA with 1,1,1,5,5,5-hexafluoropentane-2,4-dione.

A solution of ALA.HCl (0.08375 g, 0.5 mmol) and 1,1,1,5,5,5-hexafluoropentane-2,4-dione(0.104 g, 0.5 mmol) in acetate buffer (2 ml), pH 4.6, was heated under reflux for one hour. The reaction mixture was cooled and analysed by NMR spectroscopy. The only product detected in the reaction mixture was 2,5-bis(2-carboxy-ethyl)pyrazine formed by the dimerisation of ALA (Scheme 4.20). The highly enolised (100%) 1,1,1,5,5,5-hexafluoropentane-2,4-dione remained unreacted, partly as a solid and partly in solution as its dihydrate (Scheme 4.20). There was no evidence for any reaction between ALA and 1,1,1,5,5,5-hexafluoropentane-2,4-dione.

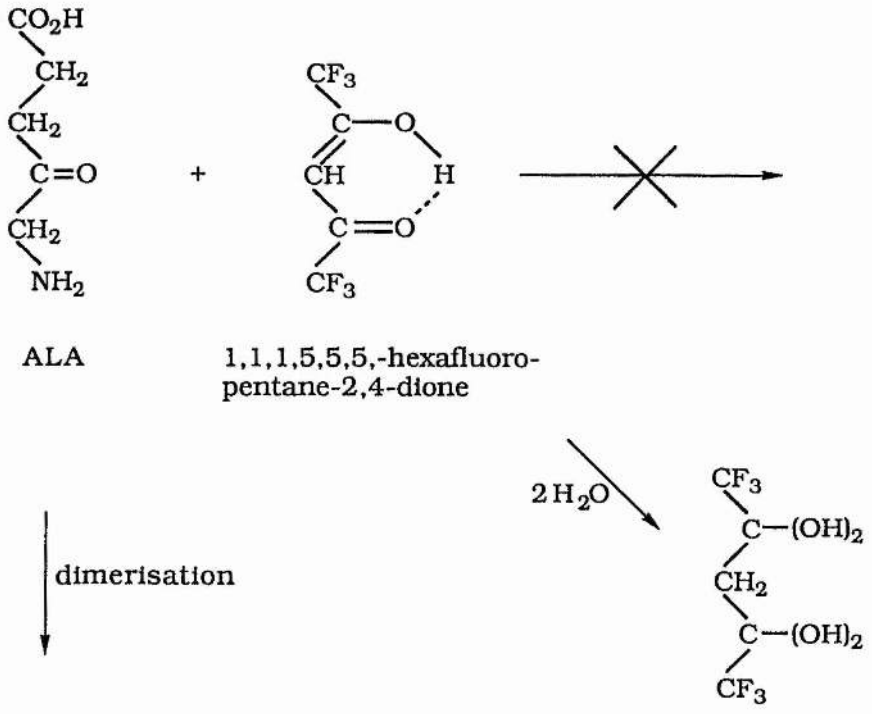

Scheme 4.20

4.3.10 Condensation of 5-methyl-ALA with pentane-2,4-dione.

A solution of 5-methyl-ALA.HCl (0.0908 g, 0.5 mmol) and pentane-2,4-dione(0.05 g, 0.5 mmol) acetate buffer (2 ml), pH 4.6, was heated under reflux for half an hour. The reaction mixture was cooled and the product formed, filtered and washed thoroughly with cold water on a filter funnel. It was then dried to a constant weight (0.0174 g, 16.7%), over phosphorus pentoxide in a vacuum desiccator, m.p. 222-224 °C (Found: C, 61.7; H, 7.6; N, 6.4. $C_{11}H_{15}NO_3$ requires C, 62.1; H, 7.7; N, 6.7.% ; m/z 209 (M^+, 24%), 180 (7), 166 (18), 150 (49), 122 (13), 55 (13), 43 (39) and 28 (100).

Analysis of the product by NMR spectroscopy revealed that the only product formed in this reaction was the Knorr product, 3-acetyl-4-(2-carboxyethyl)-2,5-dimethylpyrrole (Scheme 4.21). The alternative mode of cyclisation through the acyl group of pentane-2,4-dione does not lead to aromatisation with the formation of the Fischer-Fink product. The ^{13}C and ^{1}H NMR data for 3-acetyl-4-(2-carboxyethyl)-2,5-dimethylpyrrole are listed in Table 4.8.

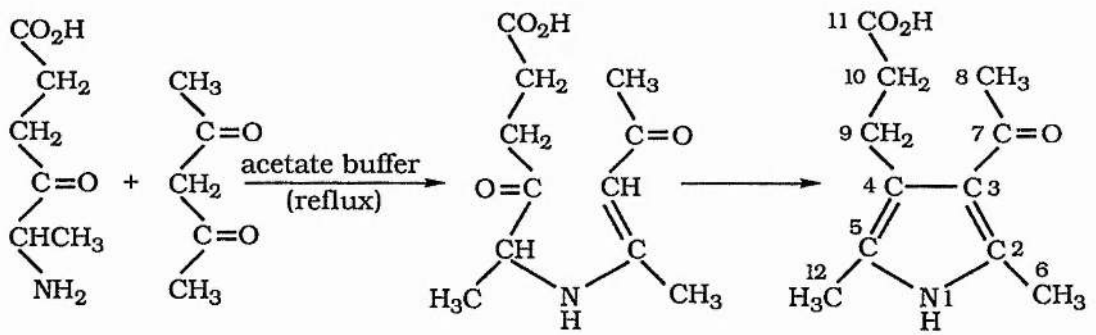

5-methyl-ALA | pentane-2,4-dione | enaminoketone intermediate | 3-acetyl-4-(2-carboxyethyl)-2,5-dimethylpyrrole

Scheme 4.21

Table 4.8 ^{13}C and ^{1}H NMR data of 3-acetyl-4-(2-carboxyethyl)-2,5-dimethyl-pyrrole (A) (Scheme 4.21) in $(CD_3)_2SO$ with reference to TMS.

Compound	Carbon	^{13}C chemical shift (ppm)	Proton	^{1}H chemical shift (ppm)
A	C_2	133.1		
	C_3	119.7		
	C_4	122.8		
	C_5	118.3	6-CH_3	2.38 (s)
	C_6	14.8	8-CH_3	2.27 (s)
	C_7	193.3	9-CH_2	2.72 (t), J = 7.74 Hz
	C_8	30.4	10-CH_2	2.29 (t), J = 7.74 Hz
	C_9	20.8	12-CH_3	2.03 (s)
	C_{10}	35.1		
	C_{11}	174.5		
	C_{12}	9.7		

4.3.11 Condensation of 5-methyl-ALA with 3-methylpentane-2,4-dione.

A solution of 5-methyl-ALA.HCl (0.0908 g, 0.5 mmol) and 3-methylpentane-2,4-dione (0,057 g, 0.5 mmol) in acetate buffer (0.5 ml), pH 4.6, was incubated at 40 °C for a week and then analysed by NMR spectroscopy. The reaction mixture was found to contain 3-(2-carboxyethyl)-2,4,5-trimethylpyrrole, formed by the Knorr condensation of 5-methyl-ALA with 3-methylpentane-2,4-dione together with a smaller amount of 2,5-bis(2-carboxyethyl)-3,6-dimethylpyrazine formed by the dimerisation of 5-methyl-ALA (Scheme 4.22).

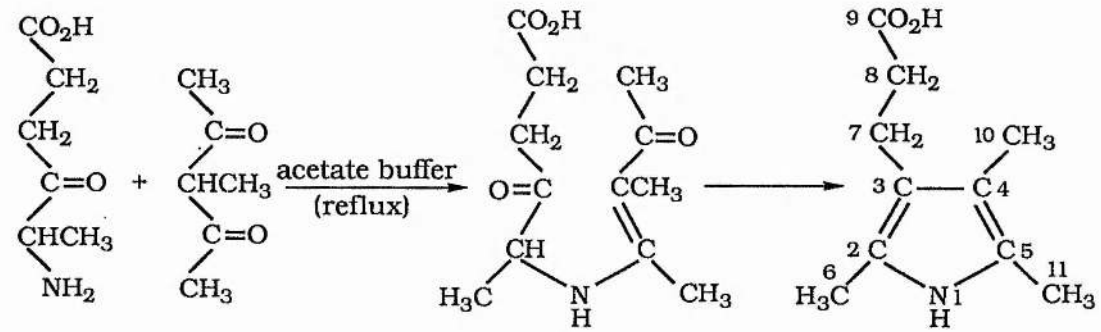

5-methyl-ALA | 3-methylpentane-2,4-dione | enaminoketone intermediate | 3-(2-carboxyethyl)-2,4,5-trimethylpyrrole

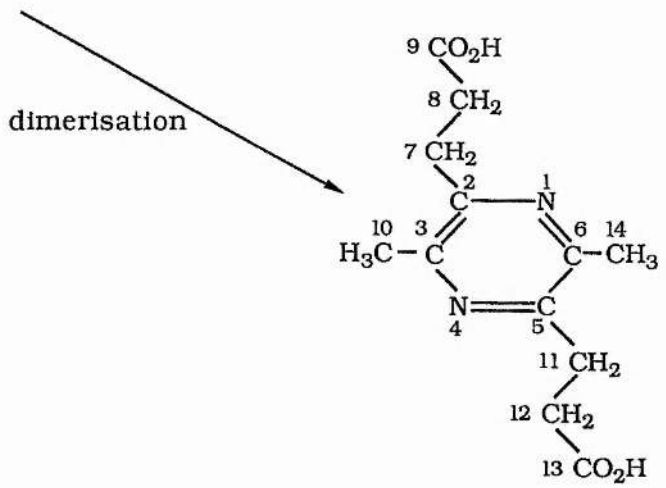

2,5-bis(2-carboxyethyl)-3,6-dimethylpyrazine

Scheme 4.22

The products remained in solution and were not characterised in any other way. The Fischer-Fink product is not formed in this reaction, since such a mode of cylisation does not lead to aromatisation. The ^{13}C and ^{1}H NMR data of the products are listed in Table 4.9.

Table 4.9 ^{13}C and ^{1}H NMR data of 3-(2-carboxyethyl)-2,4,5-trimethylpyrrole (A) and 2,5-bis(2-carboxyethyl)-3,5-dimethylpyrazine (B) (Scheme 4.22) in CD_3OD with reference to CD_3OD set at 49.04 ppm.

Compound	Carbon	^{13}C chemical shift (ppm)[a]	Proton	^{1}H chemical shift (ppm)[a]
A	C_2	(122.4)		
	C_3	116.6		
	C_4	112.6		
	C_5	(122.1)	6-CH_3	[2.10 (s)]
	C_6	[10.8]	7-CH_2	2.63 (t), J = 8.25 Hz
	C_7	21.1	8-CH_2	2.38 (t), J = 8.25 Hz
	C_8	37.0	11-CH_3	[2.09 (s)]
	C_9	179.2	10-CH_3	1.88 (s)
	C_{10}	9.1		
	C_{11}	[10.7]		
B	C_2, C_5	(151.5)		
	C_3, C_6	(149.5)		
	C_7, C_{11}	29.7	7, 11-CH_2	3.05 (t), J = 7.15 Hz
	C_8, C_{12}	34.1	8, 12-CH_2	2.70 (t), J = 7.15 Hz
	C_9, C_{13}	178.7	10, 14-CH_3	2.26 (s)
	C_{10}, C_{14}	20.4		

(a) Pairs of ambiguous assignments are placed within similar brackets.

From the experimental results obtained, the following observations can be made. ALA reacts with 3-unsubstituted alkane-2,4-diones (e.g. pentane-2,4-dione and hexane-2,4-dione) to form a mixture of the Knorr and Fischer Fink products in a ratio of 95:5 or 19:1. With 3-alkyl substituted pentane-2,4-diones (e.g. 3-methyl-pentane-2,4-dione and 3-isopropylpentane-2,4-dione), the reaction proceeds to form only the Fischer-Fink product to the exclusion of the Knorr product.

5-methyl-ALA on the otherhand, reacts with pentane-2,4-dione to form the expected Knorr product and it also reacts with 3-methylpentane-2,4-dione to form only the Knorr product and not the expected Fischer-Fink product. The implications of this anomaly and the mechanistic details of pyrrole formation will be discussed in Chapter 5.

With the exception of 3,3-dimethylpentane-2,4-dione and 1,1,1,5,5,5-hexafluoropentane-2,4-dione which exist 100% in the keto and enol forms respectively as neat liquids, all the other carbonyl compounds with which the condensation of ALA and 5-methyl-ALA were investigated, exhibit keto-enol tautomerism. The keto-enol equilibrium is however very largely solvent dependent.

In the case of the unsymmetrical β-diketone, 1,1,1-trifluoro-pentane-2,4-dione, which is very largely enolised (92.5% as a neat liquid),[54] evidence from ^{13}C NMR data has been shown that enolisation on the methyl side is only slightly favoured.[55] A hydrogen bond with a fluorine atom in both the *cis* and *trans* conformations of the enol form of 1,1,1-trifluoropentane-2,4-dione was invoked to explain the very high enol content of the latter.

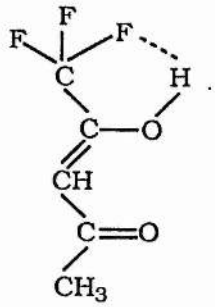

cis

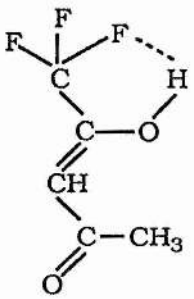

trans

The condensation of the amino group of ALA with 1,1,1-trifluoropentane-2,4-dione was shown in Section 4.3.7 to occur exclusively at the carbonyl carrying the methyl substituent, to form a hydrogen bonded enaminoketone in a chelated ring. This evidence then, is indication of the fact that condensation of the amino group accurs preferentially at the keto carbonyl of a keto-enol tautomer. This could then explain the absence of any reaction between ALA and 1,1,1,5,5,5-trifluoropentane-2,4-dione which is 100% enolised as a neat liquid and is completely hydrated in aqueous medium. Décombe[56] in his studies with β-keto esters and amines has chosen the keto form as the reactant in such condensations. His investigation indicated that the pure enolic form of acetoacetic ester did not react immediately with dry ammonia, while the equilibrium mixtures in dry ether at 0 °C gave an immediate crystalline enamine compound. The absence of any reaction of ALA with 3,3-dimethylpentane-2,4-dione which exists 100% in the keto form, would then be largely due to steric factors.

On the basis of the results obtained, the mechanism for the formation of the enaminoketone intermediate is proposed to be as illustrated in Scheme 4.23. The water molecule might split from intermediate I either according to course A to form the imine intermediate II, which then tautomerises to the more stable

enaminoketone intermediate III, or according to course B directly to form III. Course A would be possible only when a hydrogen atom was available on nitrogen and would be impossible when secondary amines are used in these reactions. In order to determine if III could be formed exclusively *via* course B, an attempt was made at monoalkylating ALA, to form a secondary amine. ALA, being a primary amino acid, could not be monoalkylated. All attempts at monoalkylation only lead to the formation of the N,N-dialkyl compound. It is to be recalled that ALA gave no reaction with 3,3-dimethylpentane-2,4-dione which has no α-hydrogen atoms in it. This latter reaction might be expected if the mechanism of such condensation were expected to follow course B. This is strong negative evidence for such a mechanism.

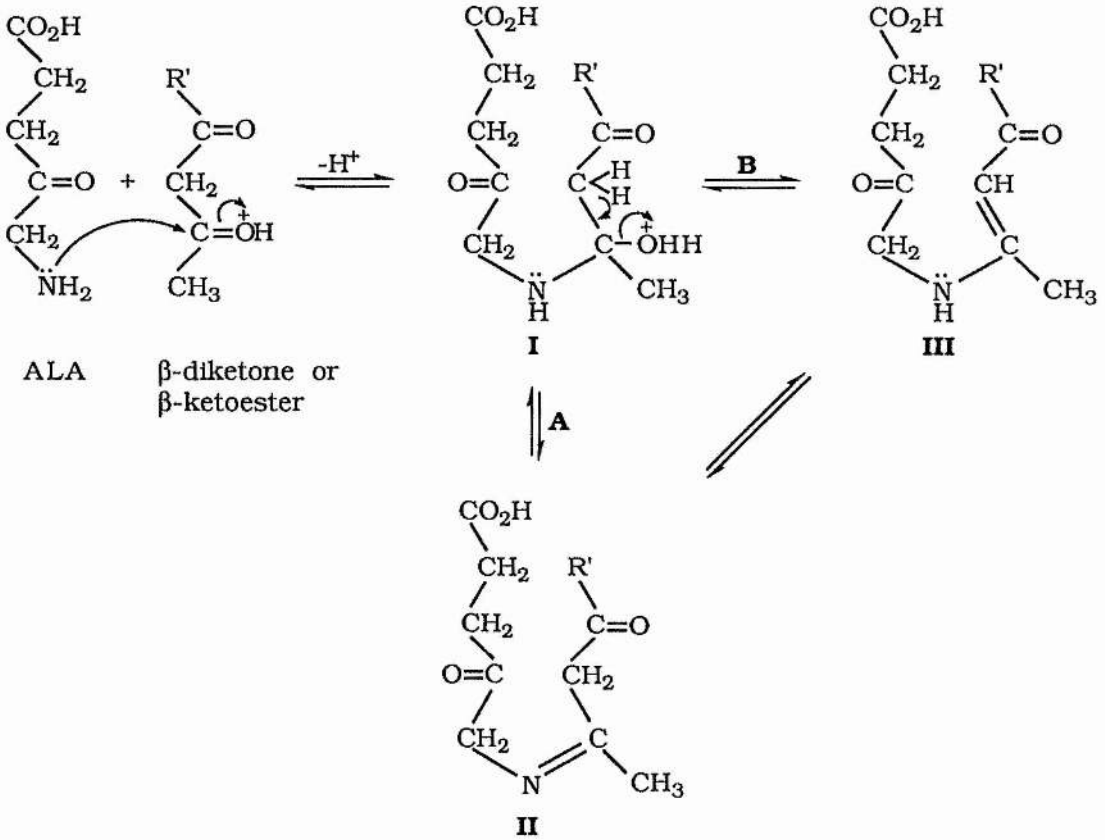

Scheme 4.23

References.

1. L. Knorr, *Annalen*, 1886, **236**, 290.
2. L. Knorr and H. Lange, *Ber.*, 1902, **35**, 2998.
3. H. Fischer and H. Orth, 'Die Chemie des Pyrroles', Vol. I, Akad. Verlagsges., Leipzig, 1934.
4. A. H. Corwin, 'Heterocyclic Chemistry', Vol. I, Wiley, New York, 1950.
5. C. U. Zanetti and E. Levi, *Gazz. Chim. Ital.*, 1894, **24**, 546.
6. H. Fischer and E. Fink, *Hoppe-Seyler's Z. Physiol. Chem.*, 1944, **280**, 123.
7. H. Fischer and E. Fink, *Hoppe-Seyler's Z. Physiol. Chem.*, 1948, **283**, 152.
8. G. G. Kleinspehn, *J. Am. Chem. Soc.*, 1955, **77**, 1546.
9. E. Bullock, A. W. Johnson, E. Markham, and K. B. Shaw, *J. Chem. Soc.*, 1958, 1430.
10. H. Rapoport and J. W. Harbuck, *J. Org. Chem.*, 1971, **36**, 853.
11. A. W. Johnson, E. Markham, R. Price and K. B. Shaw, *J. Chem. Soc.*, 1958, 4254.
12. J. B. Paine III and D. Dolphin, *Can. J. Chem.*, 1975, **12**, 1317.
13. J. B. Paine III and D. Dolphin, *Can. J. Chem.*, 1976, **54**, 411.
14. J. B. Paine III, R. B. Woodward and D. Dolphin, *J. Org. Chem.*, 1976, **41**, 2826.
15. T. T. Howarth, A. H. Jackson and G. W. Kenner, *J. Chem. Soc., Perkin Trans. I*, 1974, 502.
16. E. Samuels, R. Shuttleworth and T. S. Stevens, *J. Chem. Soc.*, 1968(C), 145.
17. H. Plieninger, P. Hess and J. Ruppert, *Chem Ber.*, 1968, **101**, 240.

18. P. S. Clezy, C. J. R. Fookes and T. T. Hai, *Aust. J. Chem.*, 1978, **31**, 365.
19. P. S. Clezy and V. Diakiw, *Aust. J. Chem.*, 1973, **26**, 2697.
20. J. A. P. Baptista De Almeida, G. W. Kenner, J. Rimmer and K. M. Smith, *Tetrahedron*, 1976, **32**, 1793.
21. A. Treibs and A. Ohorodnik, *Annalen*, 1958, **611**, 139.
22. A. Treibs and K. Hintermeier, *Chem. Ber.*, 1954, **87**, 1163.
23. J. B. Paine III and D. Dolphin, *J. Org. Chem.*, 1985, **50**, 5598.
24. H. Falk, O. Hofer and H. Lehner, *Monatsh.*, 1973, **104**, 925.
25. G. G. Kleinspehn and A. H. Corwin, *J. Org. Chem.*, 1960, **25**, 1048.
26. Y. Joh, *Seikagaku*, 1961, **33**, 787; *Chem. Abstr.*, 1962, **57**, 11143.
27. A. M. Fargali, R. P. Evstigneeva, T. N. Khandii and N. A. Preobrazhenskii, *Zhur. Obshchei. Khim.*, 1964, **34**, 893; *Chem. Abstr.*, 1964, **60**, 15812.
28. Belgian Patent 670428; *Chem. Abstr.*, 1966, **65**, 13661.
29. Japanese Patent 6800703; *Chem. Abstr.*, 1968, **69**, 51990.
30. Japanese Patent 6814947; *Chem. Abstr.*, 1969, **70**, 57631.
31. Japanese Patent 6814699; *Chem. Abstr.*, 1969, **70**, 87560.
32. Japanese Patent 7018653; *Chem. Abstr.*, 1970, **73**, 77039.
33. Japanese Patent 7023141; *Chem. Abstr.*, 1970, **73**, 98792.
34. Japanese Patent 7033649; *Chem. Abstr.*, 1971, **74**, 53510.
35. G. E. Weigand, V. J. Bauer, S. R. Safir, D. A. Blickens and S. J. Riggi, *J. Med. Chem.*, 1971, **14**, 214.
36. H. Fischer, H. Beyer and E. Zaucker, *Annalen*, 1931, **486**, 55.
37. H. Nakano, S. Umio. K. Kariyone, K. Tanaka, T. Kishimoto, H. Noguchi, I. Ueda, H. Nakamura and Y. Morimoto, *Tetrahedron Lett.*, 1966, 737.

38. G. P. Bean, (unpublished observations).

39. C.- L. Mao, F. C. Frontick, Jr., E. H. Man, R. M. Manyik, R. L. Wells and C. R. Hauser, *J. Org. Chem.*, 1969, **34**, 1425.

40. A. W. Johnson, E. Markham and R. Price, *Org. Syn.*, 1962, **42**, 75.

41. H. Meerwein and D. Vossen, *J. prakt. Chem.*, 1934, **141**, 149.

42. A. G. Osborne, *Tetrahedron*, 1983, **39**, 2831.

43. D. P. Graddon and R. A. Schulz, *Aust. J. Chem.*, 1965, **18**, 1731.

44. C. R. Hauser and J. T. Adams, *J. Am. Chem. Soc.*, 1944, **66**, 345.

45. S. Lartillot and C. Baron, *Bull. Chim. Soc. Fr.*, 1964, **1**, 783.

46. C. C. Price and T. Padmanathan, *J. Org. Chem.*, 1965, **30**, 2064.

47. E. A. Warner, *J. Chem Soc.*, 1919, **115**, 1093.

48. D. Mauzerall and S. Granick, *J. Biol. Chem.*, 1956, **219**, 435.

49. R. J. Abraham, R. D. Leeper, K. M. Smith and J. F. Unsworth, *J. Chem. Soc., Perkin Trans. II*, 1974, 1004.

50. A. Combes and C. Combes, *Bull. Soc. Chim.*, 1892, **7**, 778.

51. G. J. Martin, M. L. Martin and J. P. Goursnard, '^{15}N NMR Spectroscopy', Springer-Verlag, Berlin, 1981.

52. G. O. Dudek, and R. H. Holm, *J. Am. Chem. Soc.*, 1961, **83**, 2099.

53. G. O. Dudek, and R. H. Holm, *J. Am. Chem. Soc.*, 1962, **84**, 2691.

54. J. D. Park, H. A. Brown and J. R. Lacher, *J. Am. Chem. Soc.*, 1953, **75**, 4753.

55. K. I. Lazaar and S. H. Bauer, *J. Phys. Chem.*, 1983, **87**, 2411.

56. J. Décombe, *Ann. Chim.*, 1932, **18**, 81.

CHAPTER FIVE

KINETIC INVESTIGATIONS OF THE KNORR AND FISCHER-FINK PYRROLE SYNTHESES

5.1 Introduction.

The Knorr condensation of ALA with 1,1,1-trifluoropentane-2,4-dione to form 3-(2-carboxyethyl)-5-methyl-4-trifluoroacetyl-pyrrole was shown in Chapter 4 to proceed *via* an enaminoketone intermediate (Scheme 5.1), similar to those postulated as intermediates in the Knorr synthesis.[1-4]

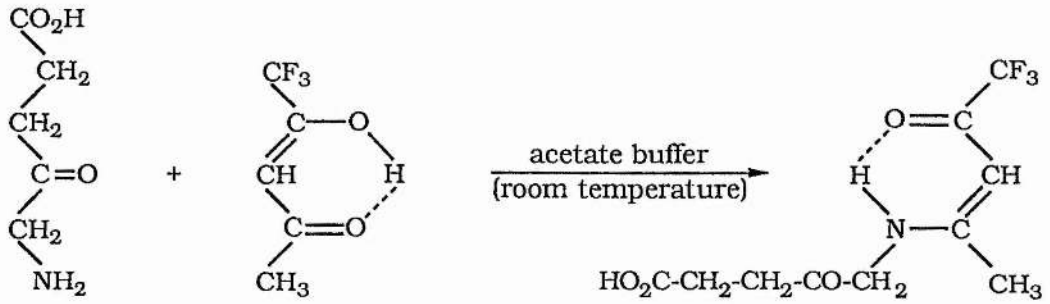

ALA 1,1,1-trifluoropentane-2,4-dione enaminoketone

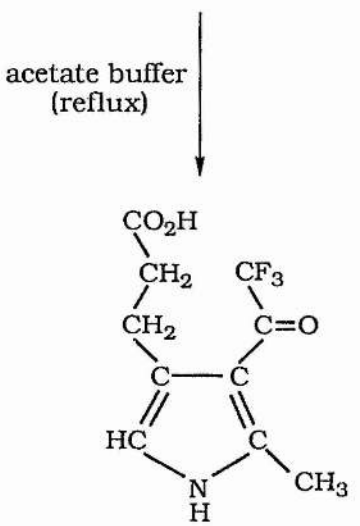

3-(2-carboxyethyl)-5-methyl-4-trifluoroacetylpyrrole

Scheme 5.1

The enzyme ALA dehydratase, catalyses a similar Knorr reaction; the dimerisation of two molecules of ALA to form PBG, the monopyrrolic precursor of a wide spectrum of tetrapyrroles.[5] The ε-amino group of a lysine residue of the human[6] and bovine[7] zinc

metalloenzyme, forms a Schiff base with one molecule of ALA which becomes the P-side of PBG[7,8] (Scheme 5.2). It is now presumed that this enzyme bound species then reacts with a second molecule of ALA to form an enamine intermediate (with the C-C double bond between C_3 and C_4 of the second molecule of ALA), which cyclises and eventually yields PBG with release of the lysine residue[6, 9-12] (Scheme 5.2).

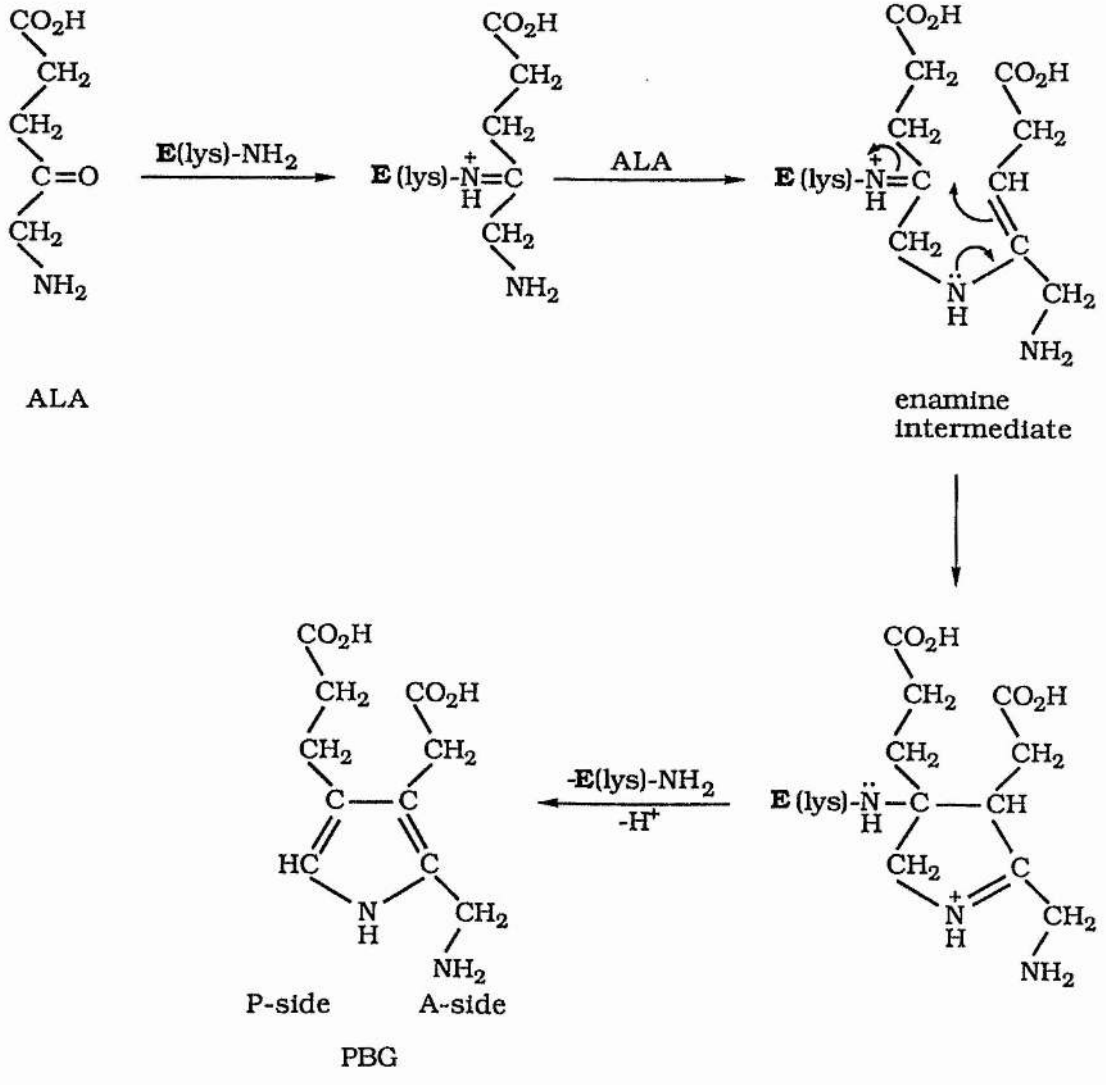

Scheme 5.2

The mechanism postulated for the ALA dehydratase reaction (Scheme 5.2), is similar to that proposed for the Knorr pyrrole

synthesis[13-16] (Scheme 5.3).

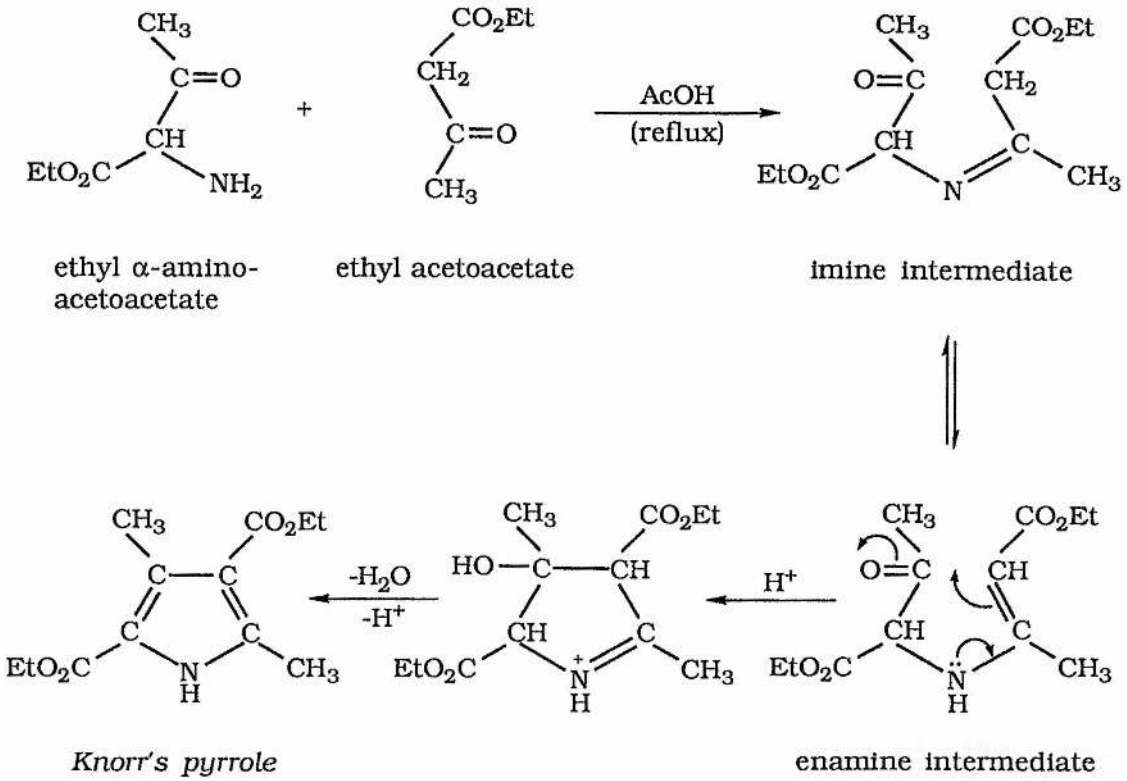

Scheme 5.3

In order to explore the validity of this analysis and to gain further insight into the ALA dehydratase reaction, the mechanism of a comparable or 'model' reaction, that of ALA with pentane-2,4-dione was examined by high field NMR. Besides serving as a model for the ALA dehydratase reaction, the condensation of ALA with pentane-2,4-dione is an excellent probe for the Knorr reaction. Although a mechanism for the Knorr reaction is readily proposed, to date there appear to be few detailed mechanistic and kinetic studies.

5.2 Experimental.

5.2.1 Materials.

Acetic acid (deuteriated), pentane-2,4-dione, potassium chloride, sodium acetate (anhydrous), sodium acetate trihydrate and 1,1,1-trifluoropentane-2,4-dione, were purchased from Aldrich Chemical Company. ALA.HCl was purchased from Sigma Chemical Company, glacial acetic acid (analaR) from Rhône Poulenc Ltd. and deuteriated methanol (99.8%) from GOSS. [4-^{13}C]ALA.HCl (50% enriched) and [^{15}N]ALA.HCl (50% enriched) were synthesised as described in Sections 2.2.3 and 2.2.4 respectively.

Acetic acid-sodium acetate buffer solutions used for NMR experiments were prepared as listed in Table 5.1.

Table 5.1 pH of acetic acid-sodium acetate buffer solutions. 10 ml mixtures of x ml 1 M AcOH and y ml 1 M NaOAc.3H_2O.

Sample	AcOH (x ml of 1 M)	NaOAc.3H_2O (y ml of 1 M)	pH at 21 °C	pH at 21 °C after the addition of 40% CD_3OD
5.1 (A)	1.0	9.0	5.86	6.45
5.1 (B)	3.0	7.0	5.23	5.87
5.1 (C)	5.0	5.0	4.76	5.40
5.1 (D)	7.0	3.0	4.44	5.07
5.1 (E)	9.0	1.0	3.94	4.59

5.2.2 Instrumentation and General Techniques.

^{13}C NMR kinetics were performed at 300.134 MHz on a Bruker AM 300 spectrometer using the kinetics program AU KINETICS.AUR. Spectra were acquired using 32 K data points, a pulse width of 2.0 μs (3.9 μs for a 90 ° flip angle), a recycle time of

1.82 s and a spectral width of 20,000 Hz. The probe temperature was maintained at 21 °C. Each accumulation, with a scan time of 15 minutes and 21 seconds was preceeded by 4 dummy scans (9 seconds) and followed by a delay time of 4 minutes and 20 seconds. Thus, the time between the start of successive accummulations was 20 minutes. Spectra were referenced with respect to internal CD_3OD set at δ 49.04. They were processed after the peak intensities of the first spectrum were normalised, by setting the absolute intensity parameter to unity before the spectrum was transformed. This ensured that peak intensites of each successive spectrum were in relation to those of the first. The data from the spectra were analysed on an Apple MacIntosh Computer using a BASIC ^{13}C datahanding program devised by Broan.[17]

^{15}N NMR spectra were obtained in exactly the same way as described in Section 2.2.2D.

The kinetics of cyclisation of the enaminoketone intermediate formed in the reaction between ALA and 1,1,1-trifluoropentane-2,4-dione, were followed spectrophotometrically with a Philips PU 8732 U.V./Visible scanning spectrophotometer, fitted with a PU 8732 cell programmer. The latter was equipped with a thermostated multi-cell compartment in which the temperature was maintained at 40 ± 0.1 °C by circulating water from a constant temperature water bath. The reaction was followed by monitoring the gradual disappearance of the absorption of the enaminoketone intermediate at λ = 317.6 nm, and infinity values in all cases were recorded at 10 half-lives. Both reaction and reference cells were filled with buffer solutions and sufficient time (half an hour) was allowed for temperature equilibration. Reaction was

initiated by addition of the substrate (enaminoketone intermediate) (5 μl of a 0.025 M solution in methanol), to acetate buffer (3 ml), maintained at 40 °C in a quartz cell and shaking vigorously to effect solution. In all cases, the reactions were run under pseudo first-order conditions in which the hydrogen ion concentration of the buffer solution was in great excess over the concentration of the substrate. First-order kinetic plots were constructed using conventional first-order kinetics employing an infinity reading of the absorbance and plotting $\ln(A_t-A_\infty)$ versus time.

All pH measurements were made at 40 °C with a Griffin digital pH meter equipped with a PHP-100-030C glass electrode. A correction of 0.40 pH unit was added to the pH meter reading to obtain pD readings.[18] The pH meter was checked against a standard of known pH, before each measurement.

5.2.3 Mechanistic investigation of the condensation of ALA with pentane-2,4-dione by ^{13}C NMR spectroscopy.

The condensation of ALA with pentane-2,4-dione in refluxing acetate buffer, pH 4.6, forms the Knorr product, 3-acetyl-4-(2-carboxyethyl)-2-methylpyrrole (95%) and the Fischer-Fink product, 2-(3-carboxypropanoyl)-3,5-dimethylpyrrole (5%) as illustrated in Scheme 5.4.

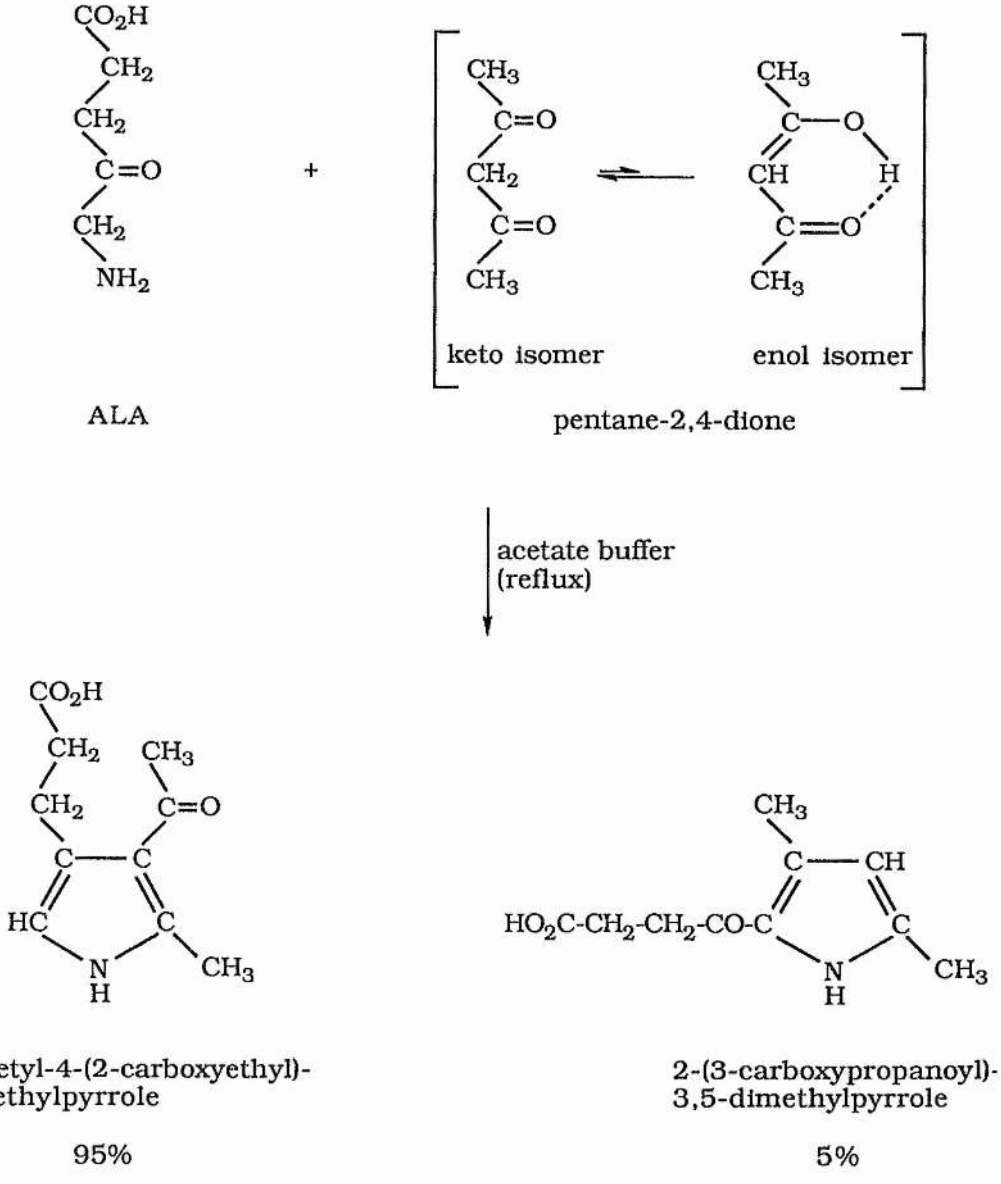

Scheme 5.4

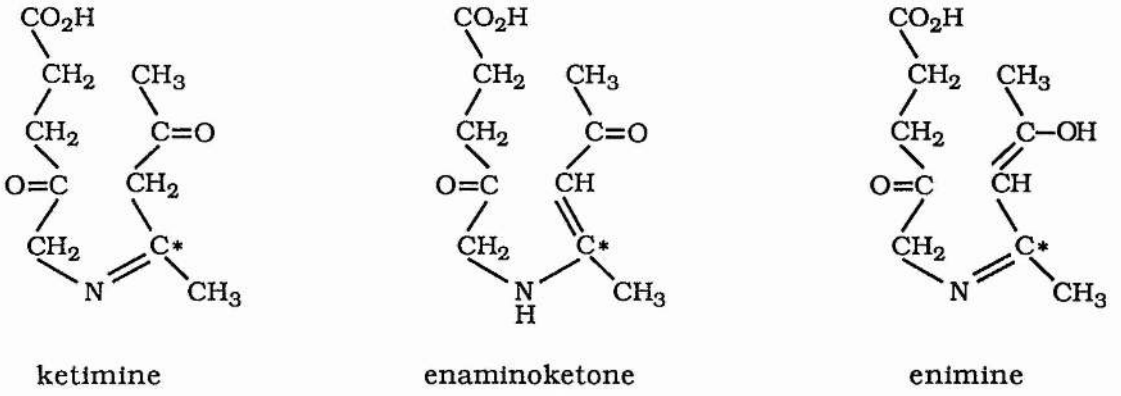

Figure 5.1 Tautomeric structures of the intermediate species formed in the reaction between ALA and pentane-2,4-dione. * denotes the carbon atom with a ^{13}C chemical shift of δ 167.1.

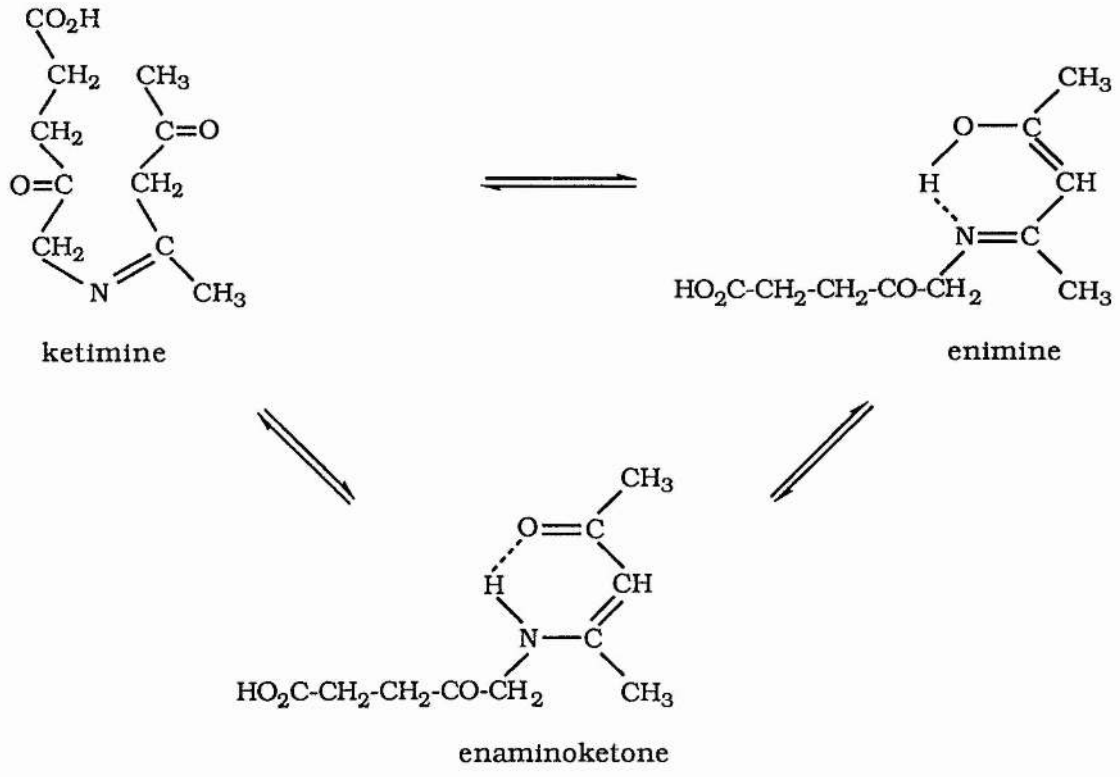

Figure 5.2 Possible solution structures of the intermediate species formed in the reaction between ALA and pentane-2,4-dione.

In principle, reaction mechanisms can be studied by following the evolution of reactants by high field NMR. ^{1}H and ^{13}C NMR spectroscopy have often been used to identify intermediates and/or to determine kinetic parameters by means of line intensity measurements as a function of time. In order to investigate the mechanism of the ALA : pentane-2,4-dione reaction, its progress was followed by monitoring the conversion of reactants to products by ^{13}C NMR spectroscopy.

The reaction of a 1:1 mixture of [4-^{13}C]ALA.HCl (5% enriched) and pentane-2,4-dione in acetate buffer, 5.1(A) [Table 5.1] was monitored over six hours and a spectrum recorded every 20 minutes. A careful examination of the spectra revealed that, apart from the reactant peaks which diminish in intensity with time, and the product peaks which increase in intensity with time, there are a cluster of peaks which grow to a maximum and gradually diminish to zero intensity with time. The latter peaks were all assigned to a single intermediate species formed in the above reaction, since they all appear, grow to a maximum and disappear from the spectra at the same time.

A clue to the nature of the intermediate species formed in the ALA : pentane-2,4-dione reaction was a peak at δ 167.1 which lies in the ^{13}C NMR chemical shift range for the imines and enamines.[19] On the basis of the above evidence, three tautomeric structures may be considered as possible intermediates, formed in the course of the above reaction: the keto-imine or ketimine intermediate, the keto-enamine or enaminoketone intermediate and the enol-imine or enimine intermediate (Fig. 5.1).

The enaminoketone and enimine intermediates probably exist in solution as the more stable hydrogen bonded forms, as

illustrated in Fig. 5.2.

Numerous tautomeric equilibria are fast with respect to the NMR time scale and the observed chemical shifts represent weighted averages over the δ values of the individual species. ^{13}C NMR spectroscopy alone does not give any conclusive evidence as to which of the above three tautomeric possibilities is the predominant one in solution, nor does it specify the favoured tautomeric equilibrium. The determination that the enaminoketone is the favoured tautomeric form of the intermediate species was greatly facilitated by the use of ^{15}N NMR spectroscopy. This is discussed in detail in Section 5.2.4.

The ^{13}C spectral changes of the reactants, intermediate and product with time are illustrated in Fig. 5.3(a and b), Fig. 5.4 and Fig. 5.5 respectively. It should be noted that the short accumulation time of 15 minutes and 31 seconds for each spectrum was not sufficient to detect the peaks of the minor product of the reaction, the Fischer-Fink product. The ^{13}C spectral changes were recorded over a period of 6 hours only, although the reaction was not complete at this stage, because the products saturate the reaction mixture and come out of solution as a solid. As a result, uniform shimming could not be attained over the entire reaction mixture and no significant spectral changes were noted after this time.

As illustrated in Fig. 5.3(a and b), the intensities of the reactant peaks, that of ALA and the keto and enol isomers of pentane-2,4-dione respectively, decrease gradually with time. The intensities of the peaks of the enaminoketone intermediate grow to a maximum and then gradually decrease in intensity with time (Fig. 5.4). The intensities of the peaks of the Knorr product,

3-acetyl-4-(2-carboxyethyl)-2-methylpyrrole are zero or almost zero to start with, and then increase steadily in intensity until 21/2 hours after mixing the reactants. At this stage, the products saturate or possibly supersaturate the solution and come out as a solid. From then on, the concentration of the products in solution decreases and this is illustrated in Fig. 5.5.

The above ^{13}C NMR experiment was repeated in four more acetic acid-sodium acetate buffer solutions [5.1(B) to 5.1(E)] whose pHs at 40 °C are listed in Table 5.1. No intermediate other than the enaminoketone intermediate was detected at these different pHs, although the reaction between ALA and pentane-2,4-dione was found to get progressively slower with increasing hydrogen ion concentration. This is anticipated, since with increasing acidity of the reaction mixture, the amino group of ALA is progressively converted into its protonated form. A protonated amino group is not nucleophilic and as a result, the rate of condensation of ALA with pentane-2,4-dione decreases as the pH of the reaction mixture is lowered.

The above ^{13}C NMR experiment was also repeated using a 1:1 mixture of [4-^{13}C]ALA.HCl (50% enriched) and pentane-2,4-dione in acetate buffer, 5.1(A) [Table 5.1]. Even at this enrichment of ALA.HCl, no intermediate other than the enaminoketone intermediate was detected in the course of the reaction. The very fact that the enaminoketone intermediate accumulates to such a level, that it can be detected by NMR spectroscopy suggests that the next step must be the rate limiting step of the reaction.

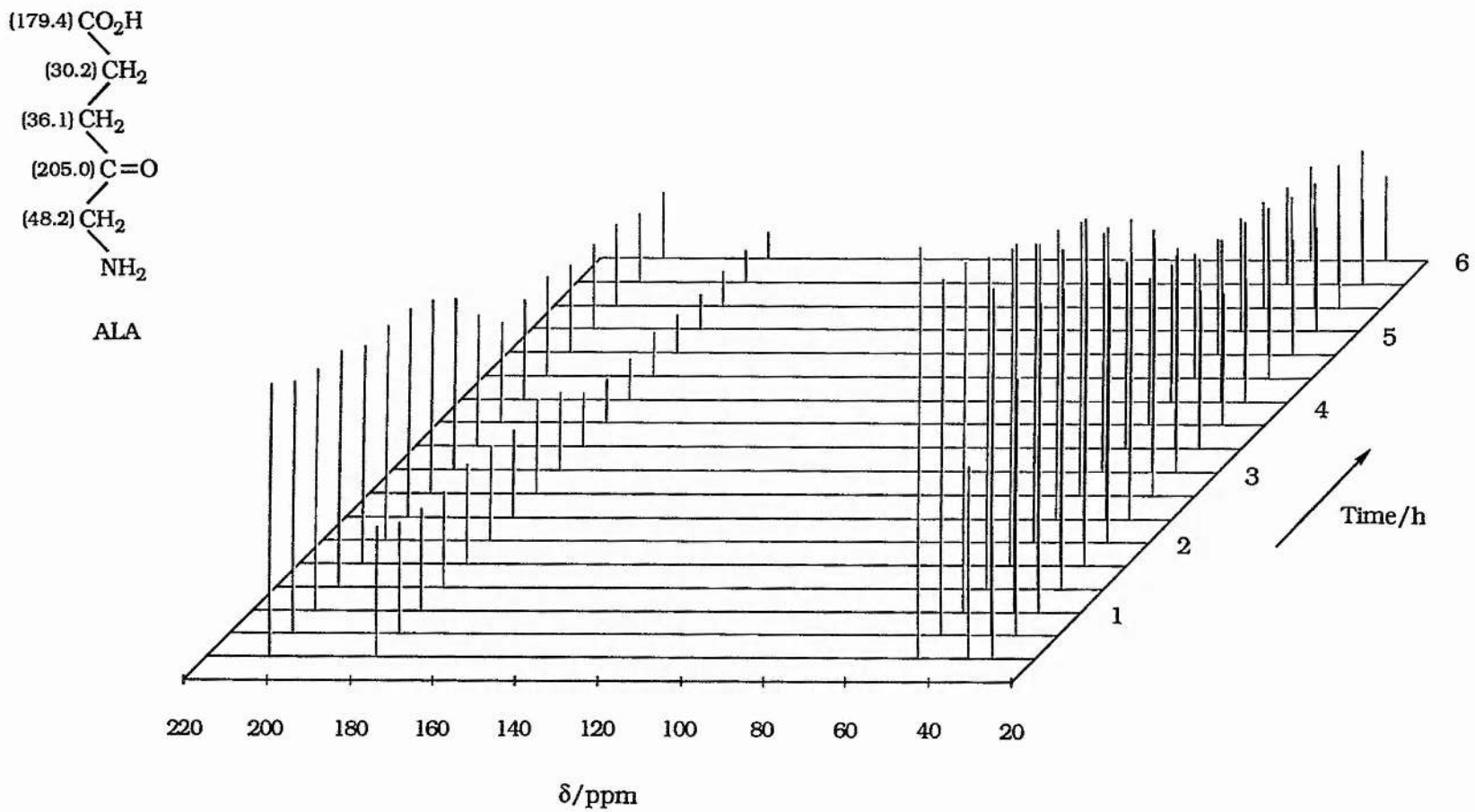

Figure 5.3 (a) ^{13}C spectral changes of ALA during the first 6 hours of the reaction of ALA with pentane-2,4-dione, in acetate buffer, pH 5.86, at 30 °C. Figures in parentheses represent the ^{13}C chemical shift of the respective carbon atoms of ALA.

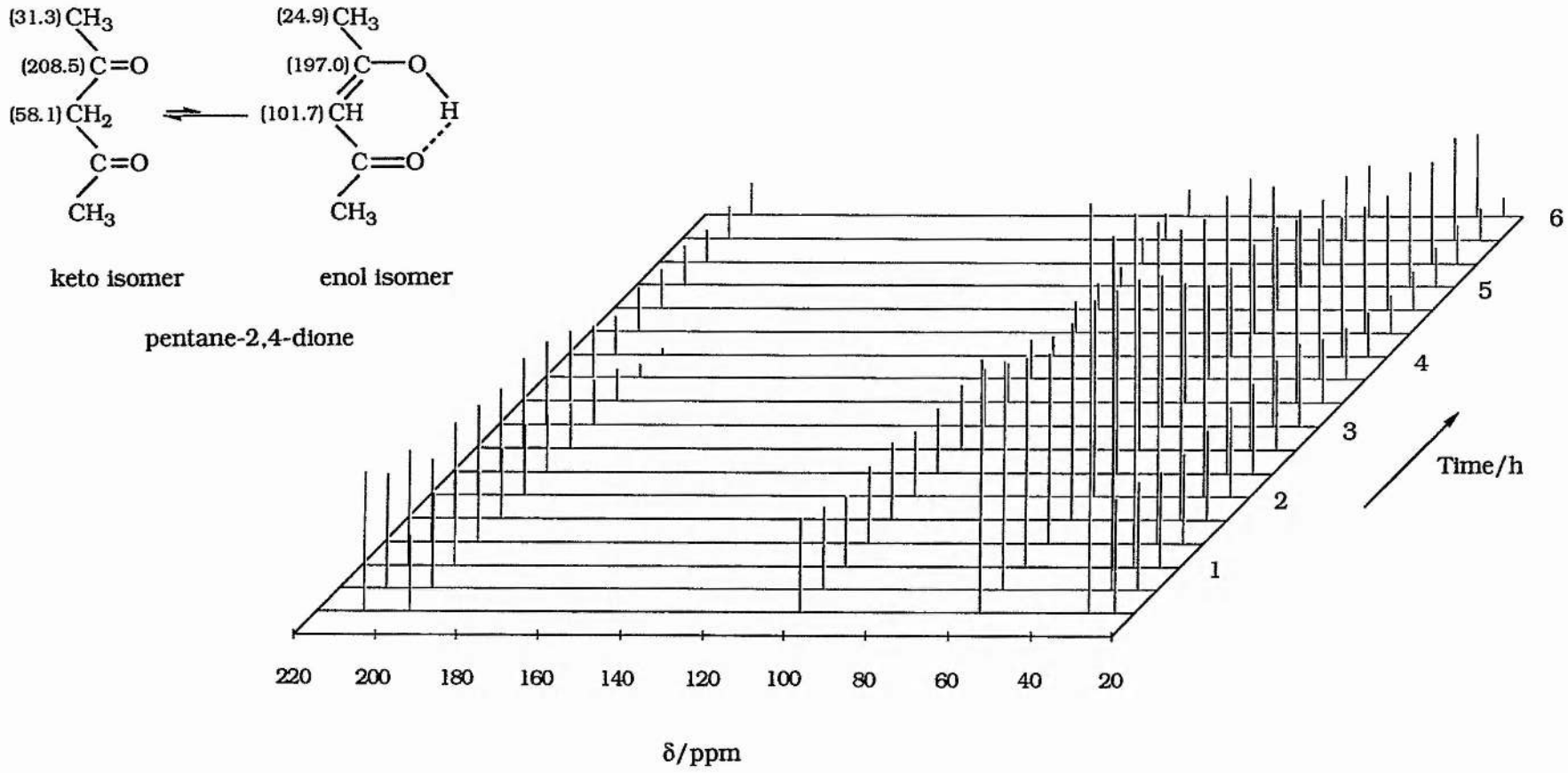

Figure 5.3 (b) ^{13}C spectral changes of pentane-2,4-dione during the first 6 hours of the reaction of ALA with pentane-2,4-dione, in acetate buffer, pH 5.86, at 30 °C. Figures in parentheses represent the ^{13}C chemical shift of the respective carbon atoms of pentane-2,4-dione.

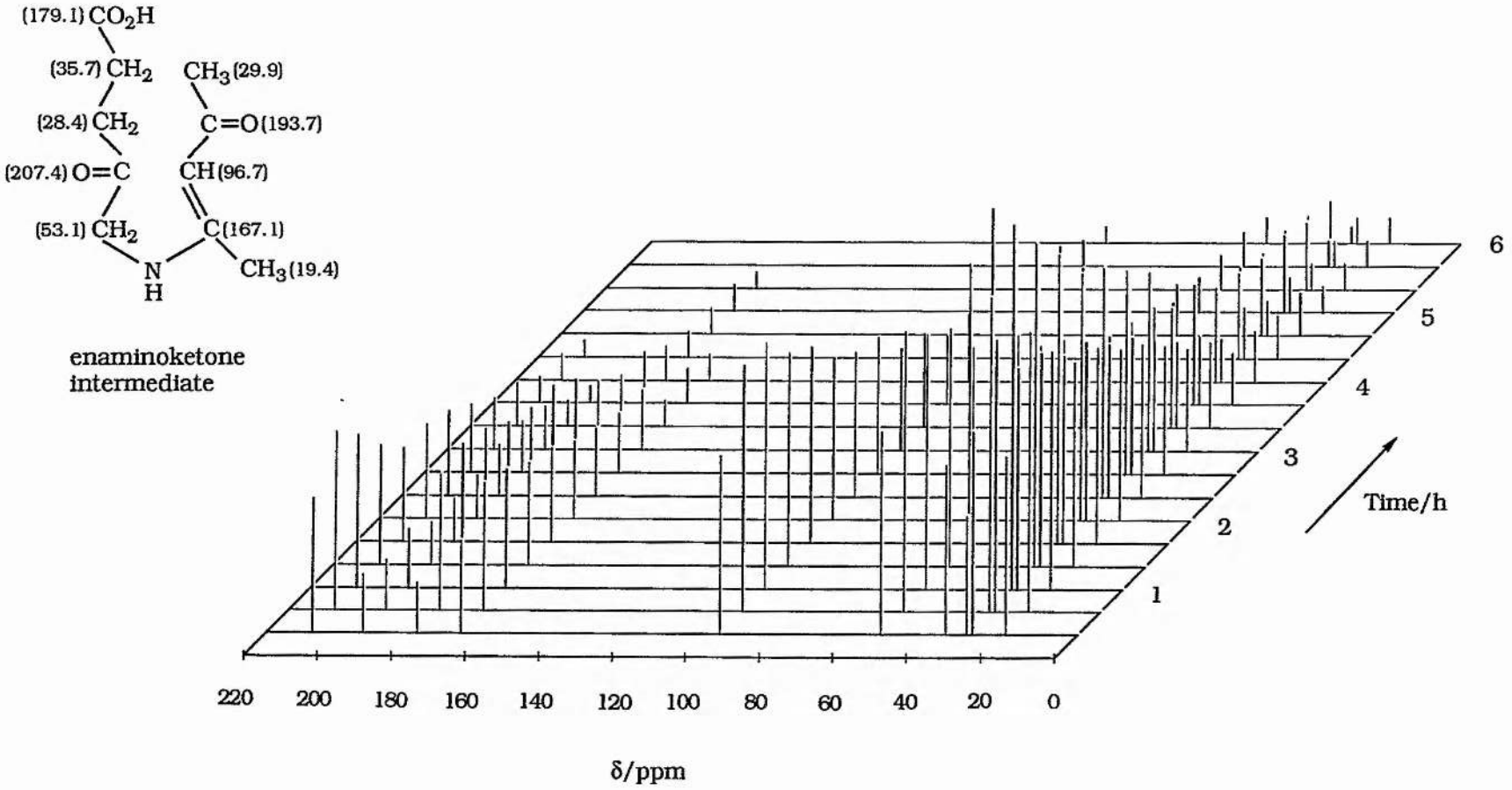

Figure 5.4 ^{13}C spectral changes of the enaminoketone intermediate during the first 6 hours of the reaction of ALA with pentane-2,4-dione, in acetate buffer, pH 5.86, at 30 °C. Figures in parentheses represent the ^{13}C chemical shift of the respective carbon atoms of the enaminoketone intermediate.

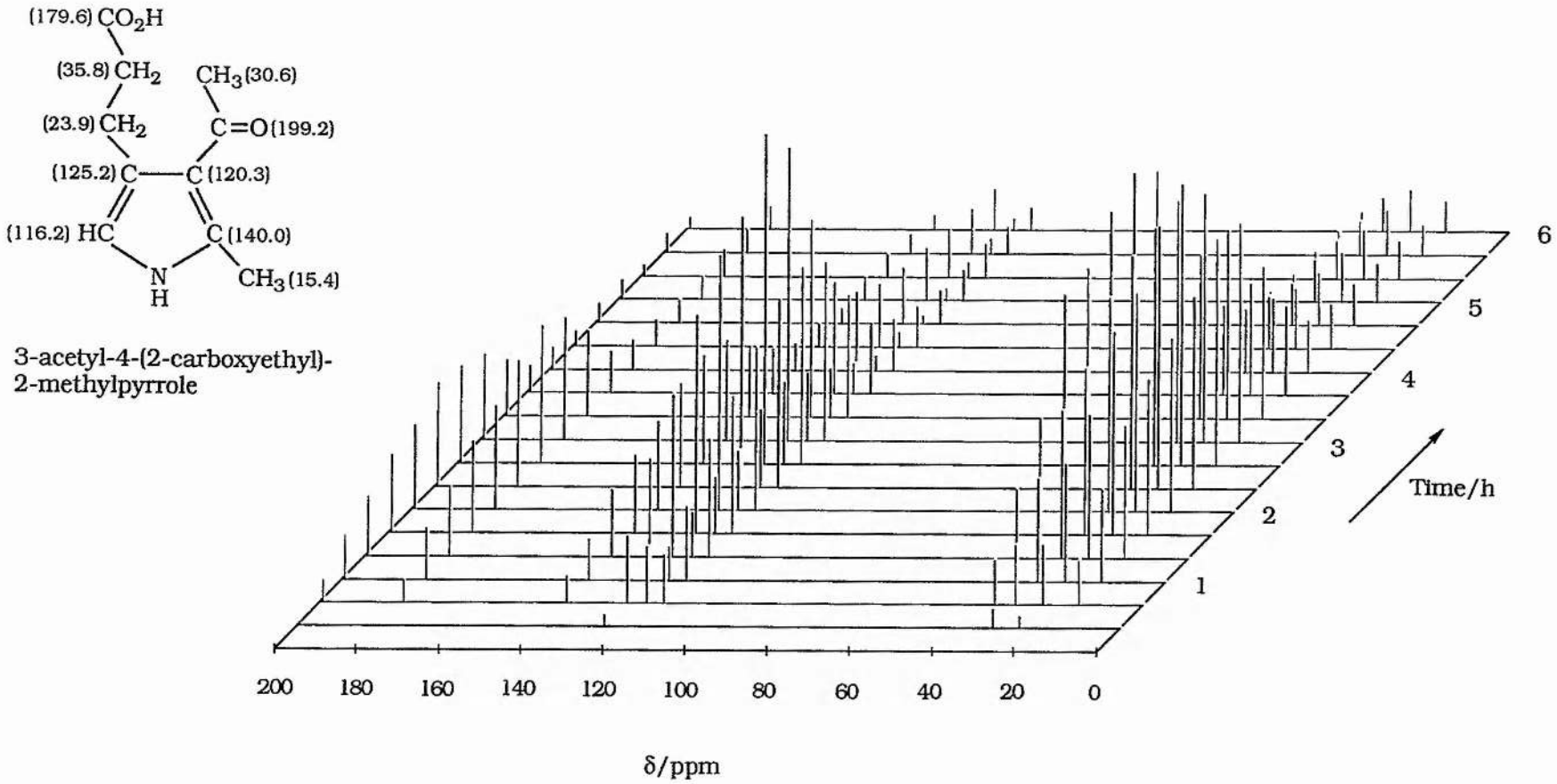

Figure 5.5 ^{13}C spectral changes of 3-acetyl-4-(2-carboxyethyl)-2-methylpyrrole during the first 6 hours of the reaction of ALA with pentane-2,4-dione, in acetate buffer, pH 5.86, at 30 °C. Figures in parentheses represent the ^{13}C chemical shift of the respective carbon atoms of 3-acetyl-4-(2-carboxyethyl)-2-methylpyrrole.

5.2.4 Mechanistic investigation of the condensation of ALA with pentane-2,4-dione by ^{15}N NMR spectroscopy.

To the extent that ^{15}N NMR constitutes a good method of structure elucidation, it can be of much help in the identification of intermediates and final products of various reactions.

A schematic representation of the ^{15}N NMR chemical shifts[20,21] of amine hydrochlorides, enaminoketones, pyrroles and imines with respect to external nitromethane (neat), set at δ 380.23 is illustrated in Fig. 5.6.

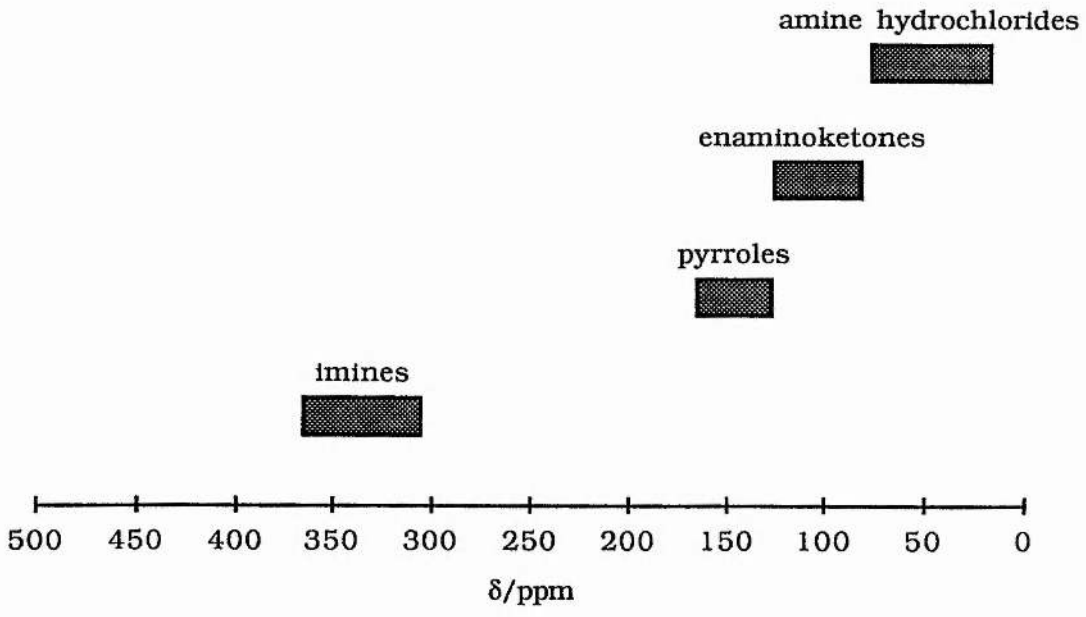

Figure 5.6 Schematic representation of the ^{15}N NMR chemical shifts of amine hydrochlorides, enaminoketones, pyrroles and imines with respect to external nitromethane (neat) set at δ 380.23.

The ^{15}N chemical shift range for amine hydrochlorides, enaminoketones, pyrroles and imines lies between 15 and 75 ppm, 80 and 125 ppm, 125 amd 165 ppm and 305 and 365 ppm respectively. Since the ^{15}N chemical shift range of enaminoketones and imines lie approximately 200 ppm apart, ^{15}N NMR spectroscopy can readily distinguish between an enaminoketone

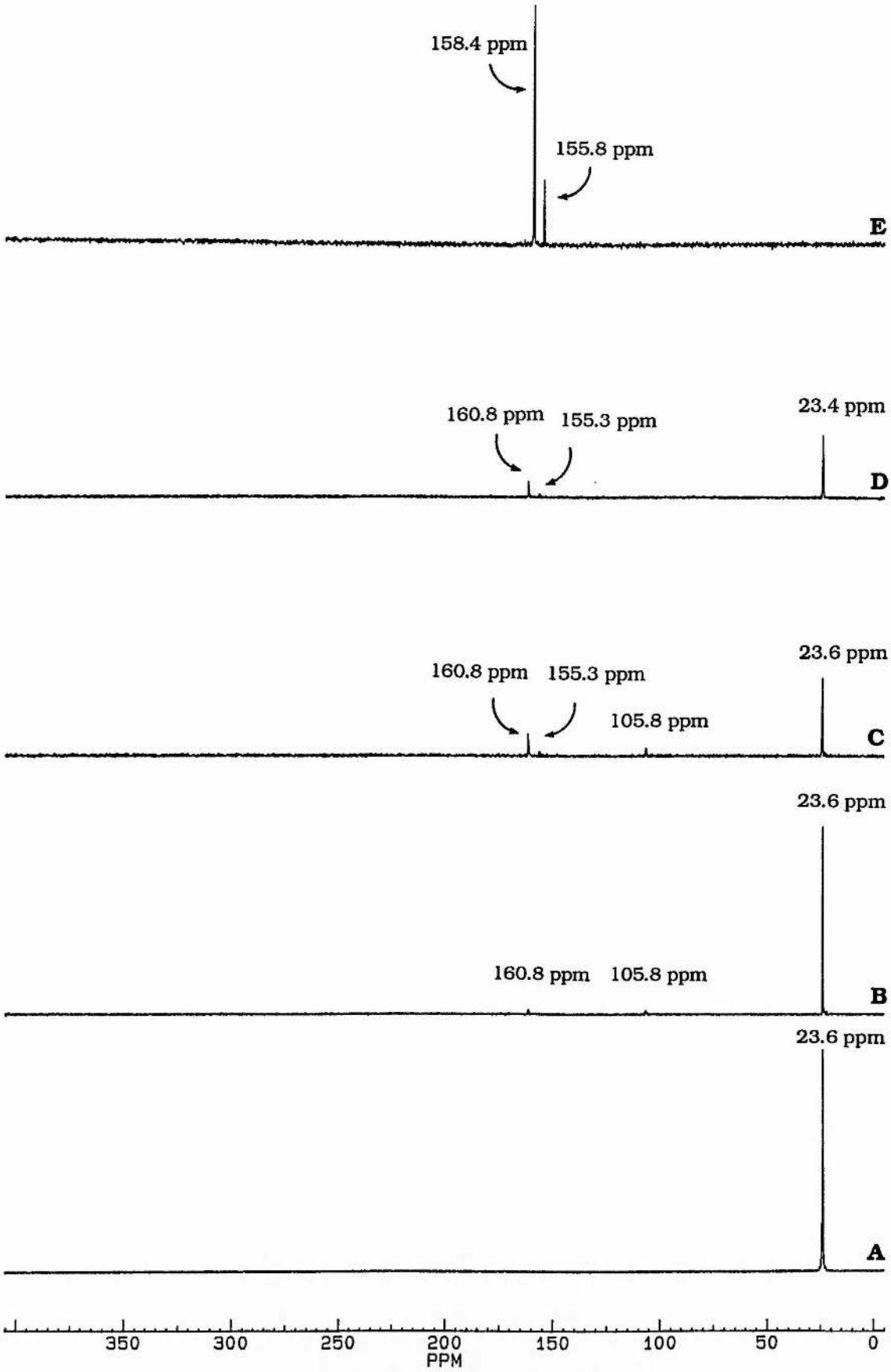

Figure 5.7 ^{1}H decoupled 30.412 MHz ^{15}N NMR spectra: **(A)** [^{15}N]ALA.HCl (50% enriched) (1.5 mmol) in acetate buffer, pH 5.86. **(B-D)** [^{15}N]ALA.HCl (50% enriched) (1.5 mmol) and pentane-2,4-dione (1.5 mmol) in acetate buffer, pH 5.86, 7, 25 and 105 minutes respectively after mixing the two reactants. **(E)** A saturated solution of the Knorr and Fischer-Fink products of the above reaction in methanol. All spectra were acquired using a CD_3OD capillary insert.

and an imine species. It thus seems possible that ^{15}N NMR can unambiguously determine the nature of the intermediate species or at least specify the favoured tautomeric equilibrium of the possible intermediates, in the reaction between ALA and pentane-2,4-dione.

To investigate the above possibility, the reaction of a 1:1 mixture of [^{15}N]ALA.HCl (50% enriched) and pentane-2,4-dione in acetate buffer, 5.1(A) [Table 5.1], was monitored by ^{15}N NMR spectroscopy over 2 hours and a spectrum recorded at definite intervals of time. Fig. 5.7(A) is the spectrum of [^{15}N]ALA.HCl (50% enriched) (1.5 mmol) in acetate buffer, 5.1(A) [Table 5.1], with the resonance of the amino group of ALA at δ 23.6. Fig. 5.7(B), (C) and (D) are the spectra of [^{15}N]ALA.HCl (50% enriched) (1.5 mmol) and pentane-2,4-dione (1.5 mmol), 7, 25 and 105 minutes after mixing the two reactants. Two peaks which can be attributed to an enaminoketone and a pyrrole nitrogen appear at δ 105.8 and δ 160.8 respectively. The intensity of the former grows to a maximum and decreases to zero with time. It is therefore assigned to the resonance of an enaminoketone intermediate formed during the course of the reaction. The intensity of the resonance at δ 160.8 increases gradually with time and is assigned to the nitrogen atom of the Knorr product, 3-acetyl-4-(2-carboxyethyl)-2-methylpyrrole, formed in the above reaction. As mentioned in Section 5.2.3, the ^{15}N resonance of the Fischer-Fink product, 2-(3-carboxy-propanoyl)-3,5-dimethylpyrrole is not readily detected in any spectrum of the reaction mixture, because of its low intensity. Fig. 5.7(E) is the spectrum of a saturated solution of the Knorr and Fischer-Fink products of the above reaction in methanol (using a CD_3OD insert) after they were isolated from the reaction mixture, washed and dried. The resonance of the Knorr product appears at

δ 158.4 and that of the Fischer-Fink product at δ 155.8.

Thus, the intervention of the enaminoketone as the predominant intermediate species (> 95%) in the reaction between ALA and pentane-2,4-dione is confirmed. This however, does not altogether rule out the existence of the ketimine and enimine species in solution. They may also have been formed during the course of the reaction, but tautomerise to the more stable enaminoketone form. As previously mentioned, resonance and hydrogen bonding are attributed to the greater stability of the enaminoketone intermediate.

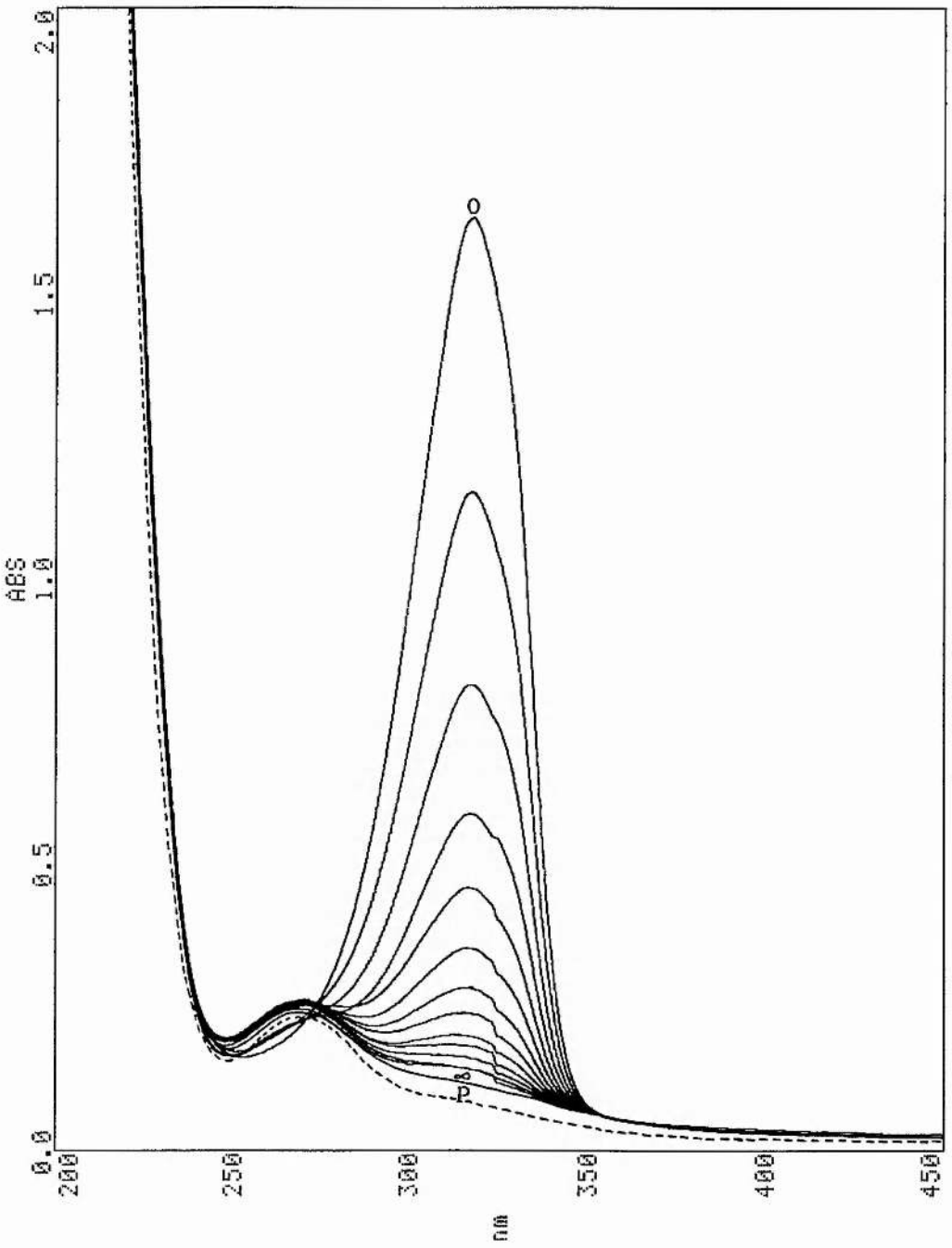

Figure 5.8 U.V. spectral changes of the enaminoketone, S, (0.25 μmol) (Scheme 5.1), added to acetate buffer (3 ml), pH 3.86, at 40 °C. 0 is the trace of S obtained at zero time, ∞ that at 10 half-lives and P that of 3-(2-carboxyethyl)-5-methyl-4-trifluoroacetylpyrrole, P, (0.375 μmol) (Scheme 5.1), added to acetate buffer (3 ml), pH 3.86, at 40 °C.

5.2.5 Kinetic investigation of the formation of 3-(2-carboxyethyl)-5-methyl-4-trifluoroacetylpyrrole.

It was mentioned at the beginning of this chapter, that ALA condenses with 1,1,1-trifluoropentane-2,4-dione in acetate buffer, at room temperature, to form an enaminoketone intermediate, S, which cyclises to 3-(2-carboxyethyl)-5-methyl-4-trifluoroacetyl-pyrrole, P, when refluxed in the same buffer (Scheme 5.1). Since S was readily isolated from the reaction mixture as a solid, the mechanism of its cyclisation to P in acetate buffer was investigated.

A solution of S in acetate buffer has an intense U.V. absorption at λ = 317.6 nm, whereas an equilvalent molecular amount of P in acetate buffer has a much weaker absorption at λ = 268.0 nm. In order to determine if the cyclisation of S to P proceeded at 40 °C, the U.V. spectral changes of S (10 µl of a 0.025 M solution of S in methanol) added to acetate buffer (3 ml, pH 3.86, ionic strength, I = 0.05 M) were monitored regularly. The results of a plot of absorption over a spectral width of λ = 200 nm to λ = 450 nm are displayed in Fig. 5.8. The first trace (marked 0 in Fig. 5.8) was obtained at zero time, immediately after adding S to acetate buffer contained in a quartz cell, which was thermostated at 40 °C for half an hour previously. Each successive trace thereafter, was obtained at hourly intervals of time, with the last trace (marked ∞ in Fig. 5.8) having been obtained at 10 half-lives. The traces from zero to 10 half-lives show a steady decrease in their maximum absorption at λ = 317.6 nm and a gradual increase in a second absorption, at λ = 268.0 nm. This corresponds to the conversion of S (with an absorption at λ = 317.6 nm) to P (with an absorption at λ = 268.0 nm) in acetate buffer at 40 °C. This was further confirmed by a comparison of the absorption of S at 10 half-lives with the dotted

line trace (Fig. 5.8). The latter is the absorption of P (15 μl of a 0.025 M solution in methanol) added to acetate buffer (3 ml, pH 3.86, ionic strength, I = 0.05) contained a quartz cell which had been thermostated at 40 °C for half an hour previously. P has an absorption maximum at λ = 268.0 nm and its absorption spectrum is similar to that of S in acetate buffer obtained at 40 °C at 10 half-lives.

5.2.5.1 Effect of hydrogen ion concentration on the rate of formation of 3-(2-carboxyethyl)-5-methyl-4-trifluoroacetyl-pyrrole.

In order to investigate the mechanism of cyclisation of S to P (Scheme 5.1), the above reaction was probed at different hydrogen ion concentrations, by monitoring the disappearance of the absorption of S at different pHs. Acetate buffers of five different pHs, but of constant ionic strength, I = 0.05 M, were prepared as listed in Table 5.2.

Table 5.2 pH of acetic acid-sodium acetate buffer solutions. 10 ml mixtures of x ml 1 M AcOH and y ml 1 M $NaOAc.3H_2O$.

Sample	AcOH (x ml of 1 M)	$NaOAc.3H_2O$ (y ml of 1 M)	pH at 40 °C	$[NaOAc.3H_2O]$/M	[KCl]/M
5.2 (A)	9.0	1.0	3.86	0.01	0.04
5.2 (B)	8.0	2.0	4.16	0.02	0.03
5.2 (C)	7.0	3.0	4.43	0.03	0.02
5.2 (D)	6.0	4.0	4.61	0.04	0.01
5.2 (E)	5.0	5.0	4.74	0.05	0.00

A stock solution of 0.025 M S in methanol was prepared.

5 μl of this solution was added to 3 ml of each acetate buffer solution, 5.2(A) to 5.2(E) (Table 5.2), thermostated at 40 °C in a quartz cell and absorbances recorded at regular intervals of time at a fixed wavelength of λ = 317.6 nm. A plot of $3 + \ln(A_t - A_\infty)$ versus time for the cyclisation of S to P in each of the above acetate buffer solutions, was found to be linear and the results are displayed in Fig. 5.9. The slopes of these straight lines are the experimental pseudo first-order rate constants, k^H_{obs}, for the transformation of S to P in the respective buffer solutions.

Figure 5.9 Plot of $3 + \ln(A_t - A_\infty)$ versus time for the cyclisation of S to P in acetate buffers 5.2(A) to 5.2(E) (Table 5.2).

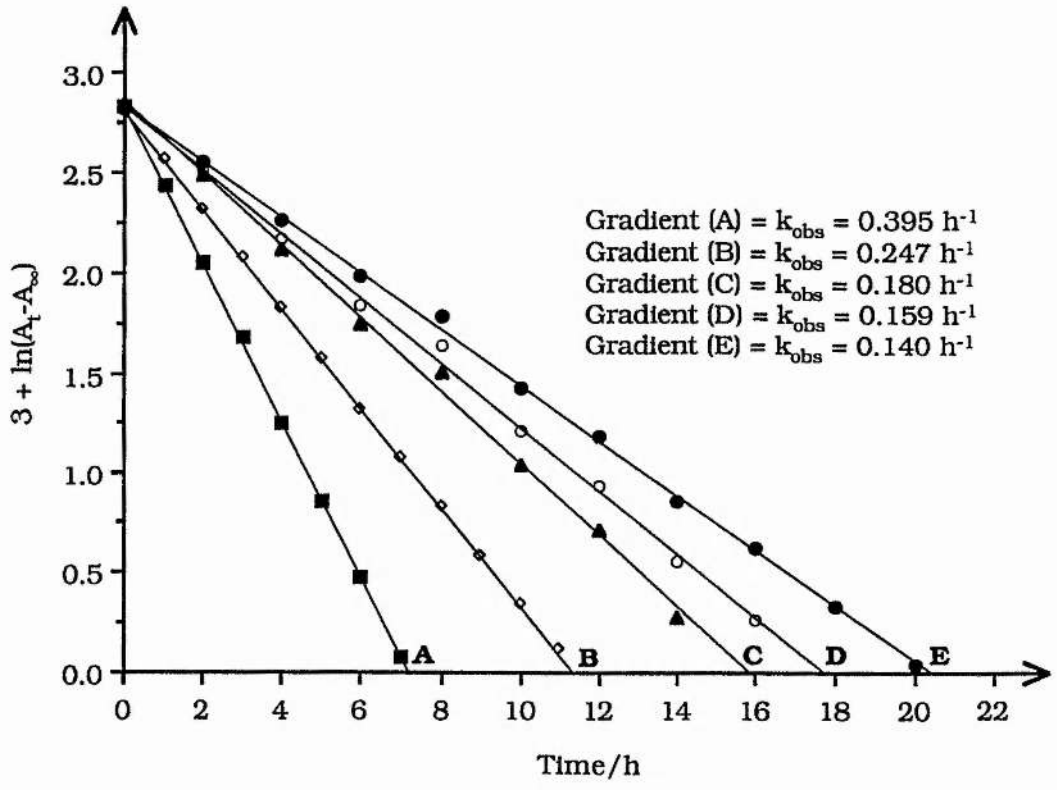

The pH, hydronium ion concentration, $[H_3O^+]$ and the experimental pseudo first-order rate constant, k^H_{obs}, for the cyclisation of S to P in acetate buffers 5.2(A) to 5.2(E) (Table 5.2) are listed in Table 5.2(A).

Table 5.2(A) The experimental pseudo first-order rate constants, k^{H}_{obs} for the cyclisation of S to P in acetate buffers 5.2(A) to 5.2(E) (Table 5.2).

Sample	pH at 40 °C	$[H_3O^+]$ = antilog[-pH]	$10^5 \times [H_2O^+]/M$	$10^2 \times k^{H}_{obs}/h^{-1}$
5.2 (A)	3.86	1.38×10^{-4}	13.80	39.5
5.2 (B)	4.16	6.92×10^{-5}	6.92	24.7
5.2 (C)	4.43	3.72×10^{-5}	3.72	18.0
5.2 (D)	4.61	2.45×10^{-5}	2.45	15.9
5.2 (E)	4.74	1.82×10^{-5}	1.82	14.0

A plot of $10^2 \times k^{H}_{obs}$ versus $10^5 \times [H_3O^+]$ (Fig 5.10) is a straight line, suggesting that in aqueous acidic solution, k^{H}_{obs}, for the cyclisation of S to P is linearly dependent upon $[H_3O^+]$.

Figure 5.10 Rate of cyclisation of S to P in aqueous acidic solution, at 40 °C.

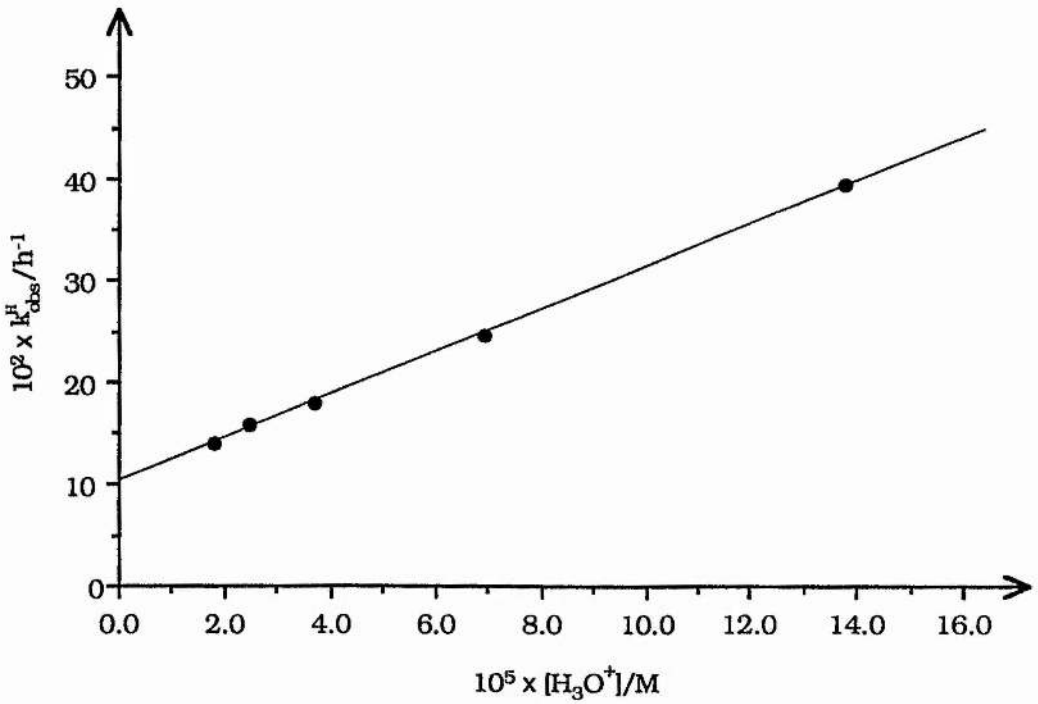

The slope of the straight line gives k_H, which is the second order catalytic constant for the reaction catalysed by $[H_3O^+]$.

Extrapolation of the straight line reveals, that for this

particular transformation, when $[H_3O^+] = 0$, $k^H_{obs} = k^H_o = 0.103\ h^{-1}$, suggesting that there is a significant amount of 'background' or 'spontaneous' reaction, uncatalysed by hydronium ions. k^H_o is the first order rate constant for the uncatalysed reaction.

Thus from the above graph,

$$k^H_{obs} = k^H_o + k_H[H_3O^+],$$

$$\text{slope} = k_H = 2.15 \times 10^3\ l\ mol^{-1}\ h^{-1},$$

$$\text{intercept} = k^H_o = 0.103\ h^{-1}.$$

The rate law for the above transformation is given by the following equations,

$$\frac{-d[S]}{dt} = k^H_o[S] + k_H[H_3O^+][S]$$

or, at constant pH,

$$\frac{-d[S]}{dt} = k^H_{obs}[S]$$

where,

$$k^H_{obs} = k^H_o + k_H[H_3O^+]$$

The source of the protons contributing to the total hydronium ion concentration is acetic acid, and it contributes to an extent determined by the magnitude of its dissociation constant. The catalytic effect of the unionised weak acid, acetic acid however, must be assessed separately.

The acidity constant K_{AcOH} of acetic acid,

$$AcOH + H_2O \rightleftharpoons H_3O^+ + AcO^-$$

is given by

$$K_{AcOH} = \frac{[H_3O^+][AcO^-]}{[AcOH]}$$

It follows from this that,

$$[H_3O^+] = K_{AcOH}\frac{[AcOH]}{[AcO^-]}$$

therefore,

$$pH = -\log[H_3O^+] = pK_{AcOH} - \log\frac{[AcOH]}{[AcO^-]}$$

or,

$$pH = pK_{AcOH} - \log r$$

where

$$r = \frac{[AcOH]}{[AcO^-]} = \text{the buffer ratio.}$$

It is therefore possible to vary the absolute value of [AcOH] i.e. the buffer concentration, at constant pH, provided the buffer ratio, r, and the ionic strength, I, are kept constant.

5.2.5.2 Effect of buffer concentration on the rate of formation of 3-(2-carboxyethyl)-5-methyl-4-trifluoroacetylpyrrole.

In order to investigate what effect if any, acetic acid had on the rate of cyclisation of S, a series of two experiments were conducted, using buffers of constant buffer ratio, r, in each case. The ionic strength, I, of the buffer solutions were maintained at 0.1 M by the addition of KCl (Tables 5.3 and 5.4).

Table 5.3 Acetic acid-sodium acetate buffer solutions of pH 3.87; r = 9, I = 0.1.

Sample	AcOH (x ml of 0.5 M)	$NaOAc.3H_2O$ (y ml of 0.5 M)	[AcOH]/M	[$NaOAc.3H_2O$]/M	[KCl]/M in 10 ml
5.3 (A)	90.0	10.0	0.45	0.05	0.05
5.3 (B)	8 ml of sample 5.3(A) diluted to 10 ml		0.36	0.04	0.06
5.3 (C)	6 ml of sample 5.3(A) diluted to 10 ml		0.27	0.03	0.07
5.3 (D)	4 ml of sample 5.3(A) diluted to 10 ml		0.18	0.02	0.08
5.3 (E)	2 ml of sample 5.3(A) diluted to 10 ml		0.09	0.01	0.09

Table 5.4 Acetic acid-sodium acetate buffer solutions of pH 4.20; r = 4, I = 0.1.

Sample	AcOH (x ml of 0.5 M)	$NaOAc.3H_2O$ (y ml of 0.5 M)	[AcOH]/M	[$NaOAc.3H_2O$]/M	[KCl]/M in 10 ml
5.4 (A)	90.0	10.0	0.40	0.10	0.00
5.4 (B)	8 ml of sample 5.4(A) diluted to 10 ml		0.32	0.08	0.02
5.4 (C)	6 ml of sample 5.4(A) diluted to 10 ml		0.24	0.06	0.04
5.4 (D)	4 ml of sample 5.4(A) diluted to 10 ml		0.16	0.04	0.06
5.4 (E)	2 ml of sample 5.4(A) diluted to 10 ml		0.08	0.02	0.08

As in the previous experiments, S (5 μl of a 0.025 M solution of S in methanol) was added to acetate buffer (3 ml), thermostated at 40 °C and absorbances recorded at regular intervals of time, at a fixed wavelength of λ = 317.6 nm. A plot of $3 + \ln(A_t - A_\infty)$ versus time for the cyclisation of S to P in each of the acetate buffer solutions, 5.3(A) to 5.3(E) (Table 5.3), of pH 3.87 and buffer ratio 9 was found to be linear. The slopes of the straight lines, k^H_{obs}, were calculated to be 0.413 h^{-1}, 0.415 h^{-1}, 0.418 h^{-1}, 0.415 h^{-1} and 0.414 h^{-1} respectively. A similar plot for the cyclisation of S to P in each of the acetate buffer solutions, 5.4(A) to 5.4(E) (Table 5.4), of pH 4.20 and buffer ratio 4 was also found to be linear. The slopes of the straight lines, k^H_{obs}, were calculated to be 0.278 h^{-1}, 0.280 h^{-1}, 0.280 h^{-1}, 0.280 h^{-1}, and 0.280 h^{-1} respectively.

Thus, the experimental pseudo first-order rate constants, k^H_{obs}, for the cyclisation of S to P in acetic acid-sodium acetate buffer solutions at a constant buffer ratio, r, and pH, were found to be independent of the acetic acid concentration. The results of the plot of $10^2 \times k^H_{obs}$ versus [AcOH] for buffer solutions of pH 3.87, r = 9 and of pH 4.20, r = 4 are displayed in Fig. 5.11.

Figure 5.11 Plot of $10^2 \times k^H_{obs}$ versus [AcOH] for the cyclisation of S.

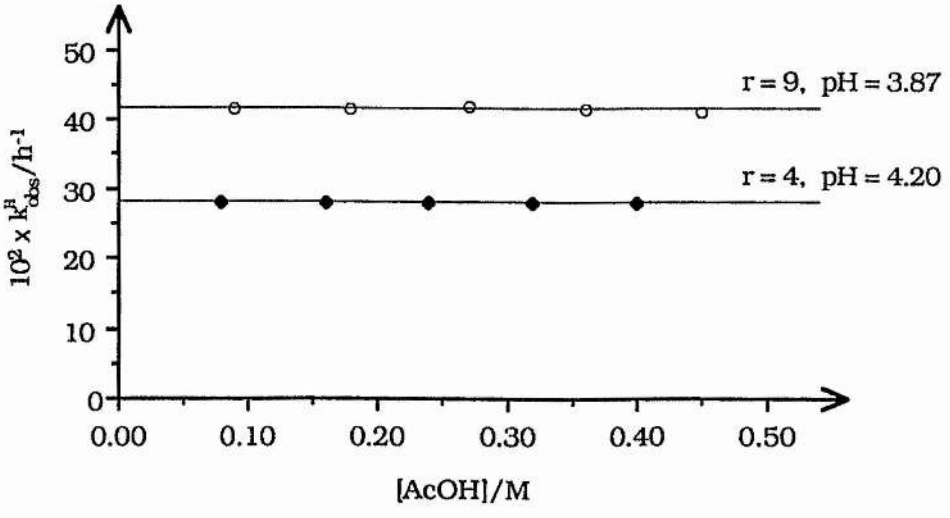

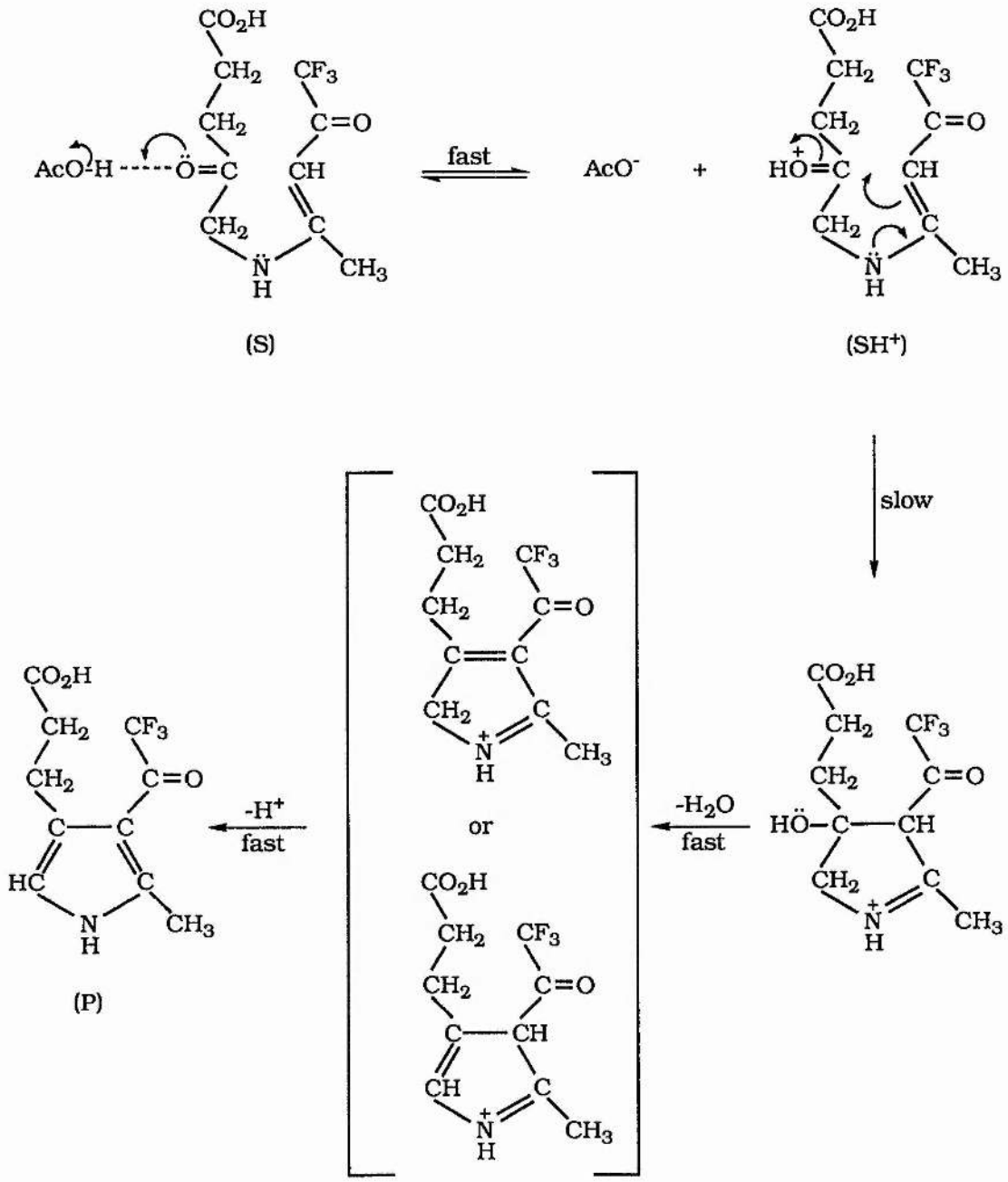

Scheme 5.5

The cyclisation of S to P is therefore catalysed by hydronium ions but not by undissociated weak Brønsted acids such as acetic acid. i.e. the above transformation is specific acid catalysed.

5.2.5.3 Proposed mechanism for the hydronium ion catalysed formation of 3-(2-carboxyethyl)-5-methyl-4-trifluoro-acetylpyrrole.

From the foregoing kinetic evidence, it can be concluded that the transition state in the hydronium ion catalysed cyclisation of S to P comprises a molecule of S plus proton.

The proposed mechanism for the hydronium ion catalysed cyclisation of S to P is illustrated in Scheme 5.5, where for convenience, S is written as the non-hydrogen bonded structure.

Thus by this route,

$$S + AcOH \underset{}{\overset{fast}{\rightleftharpoons}} SH^+ + AcO^- \; ; \; K = \frac{[SH^+][AcO^-]}{[S][AcOH]}$$

$$SH^+ \xrightarrow[r.d.s]{k} P$$

Therefore,

$$\frac{d[P]}{dt} = k[SH^+]$$

$$= kK\frac{[S][AcOH]}{[AcO^-]}$$

But,

$$AcOH + H_2O \overset{fast}{\rightleftharpoons} H_3O^+ + AcO^-$$

$$K_{AcOH} = \frac{[H_3O^-][AcO^-]}{[AcOH]}$$

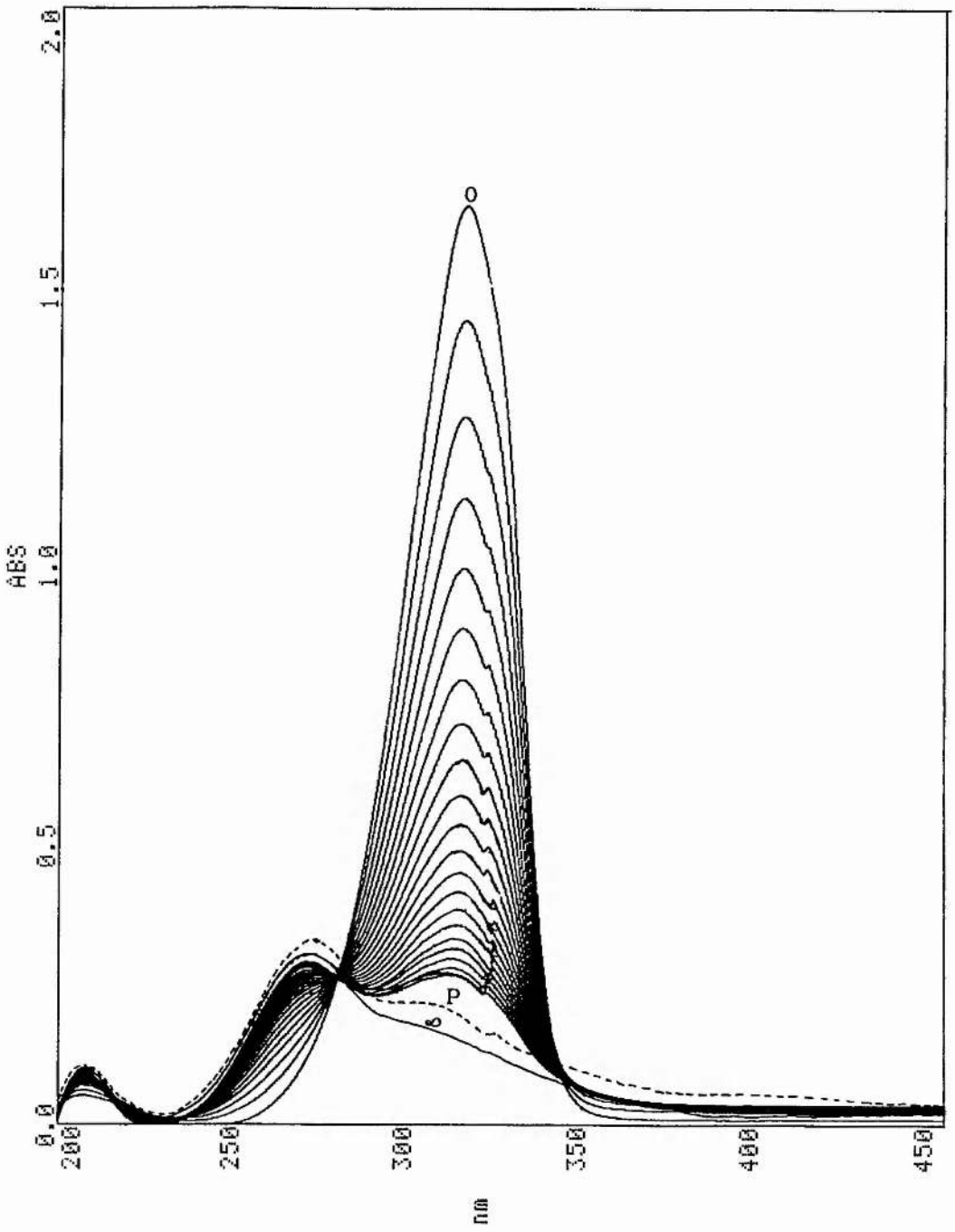

Figure 5.12 U.V. spectral changes of the enaminoketone, S, (0.25 μmol) (Scheme 5.1), added to water (3 ml), at 40 °C. 0 is the trace of S obtained at zero time, ∞ that at 10 half-lives and P that of 3-(2-carboxyethyl)-5-methyl-4-trifluoroacetylpyrrole, P, (0.375 μmol) (Scheme 5.1), added to water (3 ml), at 40 °C.

Therefore, by this route,

$$\frac{d[P]}{dt} = \frac{kK[S][H_3O^+]}{K_{AcOH}}$$

$$= k_H[S][H_3O^+]$$

Thus the above mechanism which involves rapid protonation of the substrate, S, as a pre-equilibrium, followed by the rate determining step, not involving proton transfer, leads to a specific acid-catalysis rate law, even when the undissociated weak acid, acetic acid, contributes directly in the pre-equilibrium.

5.2.5.4 The water catalysed formation of 3-(2-carboxyethyl)-5-methyl-4-trifluoroacetylpyrrole.

The cyclisation of S to P (Scheme 5.1) in aqueous acidic solution, was shown in Section 5.2.5.2 to involve a significant amount of 'spontaneous' reaction, uncatalysed by hydronium ions. In order to investigate if this 'spontaneous' reaction is due to neutral water catalysis, the U.V. spectral changes of S (10 μl of a 0.025 M solution of S in methanol) added to water (3 ml) were monitored at hourly intervals of time. The results of a plot of absorption over a spectral width of λ = 200 nm to λ = 450 nm (Fig. 5.12) were similar to that obtained in acetate buffer, pH 3.86, (Fig. 5.8) although as anticipated, the former reaction was found to be slower than the latter. This then suggests that the spontaneous cyclisation of S to P is a water catalysed reaction.

In order to determine the rate of cyclisation of S in water, S (5 μl of a 0.025 M solution in methanol) was added to water (3 ml), thermostated at 40 °C in a quartz cell and absorbances recorded at

regular intervals of time, at a fixed wavelength of λ = 317.6 nm. A plot of $3 + \ln(A_t - A_\infty)$ versus time for the cyclisation of S to P in water was found to be linear and the result is displayed in Fig. 5.13.

Figure 5.13 Plot of $3 + \ln(A_t - A_\infty)$ versus time for the cyclisation of S to P in water at 40 °C.

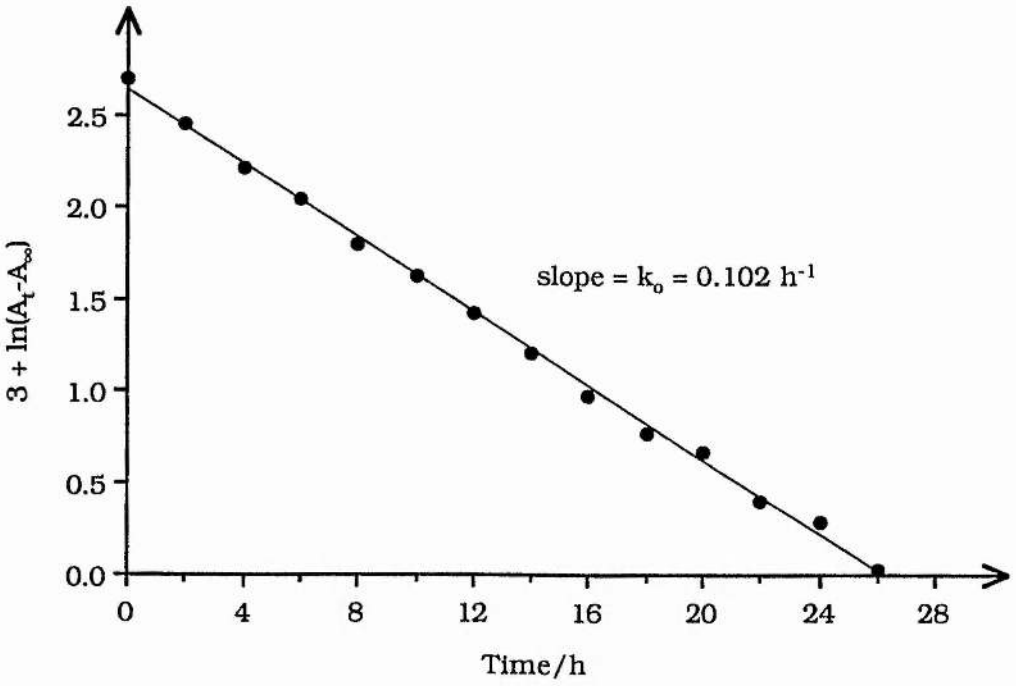

The slope of this straight line is the first-order rate constant, k_o^H, for the water catalysed reaction. The value of k_o^H, calculated from the above graph was found to be 0.102 h^{-1}. This is identical to the value of the intercept in Fig. 5.10, which was shown to be the first-order rate constant, k_o^H, for the 'spontaneous' reaction. The above evidence confirms the fact, that the mode that was previously described as 'spontaneous', is indeed a water-induced cyclisation of the substrate, S.

5.2.5.5 Solvent kinetic isotope effect on the rate of formation of 3-(2-carboxyethyl)-5-methyl-4-trifluoroacetylpyrrole.

In order to determine if the water catalysed cyclisation of S exhibited any solvent kinetic isotope effect, the above reaction was repeated using D_2O (3 ml) in the quartz cell instead of H_2O. A plot of $3 + \ln(A_t - A_\infty)$ versus time for the cyclisation of S to P in D_2O (Fig. 5.14) was found to be linear. The slope of this straight line is the first order rate constant, k^D_{obs}, for the deuterium oxide catalysed reaction, the value of which was calculated to be 0.052 h^{-1}.

Figure 5.14 Plot of $3 + \ln(A_t - A_\infty)$ versus time for the cyclisation of S to P in deuterium oxide at 40 °C.

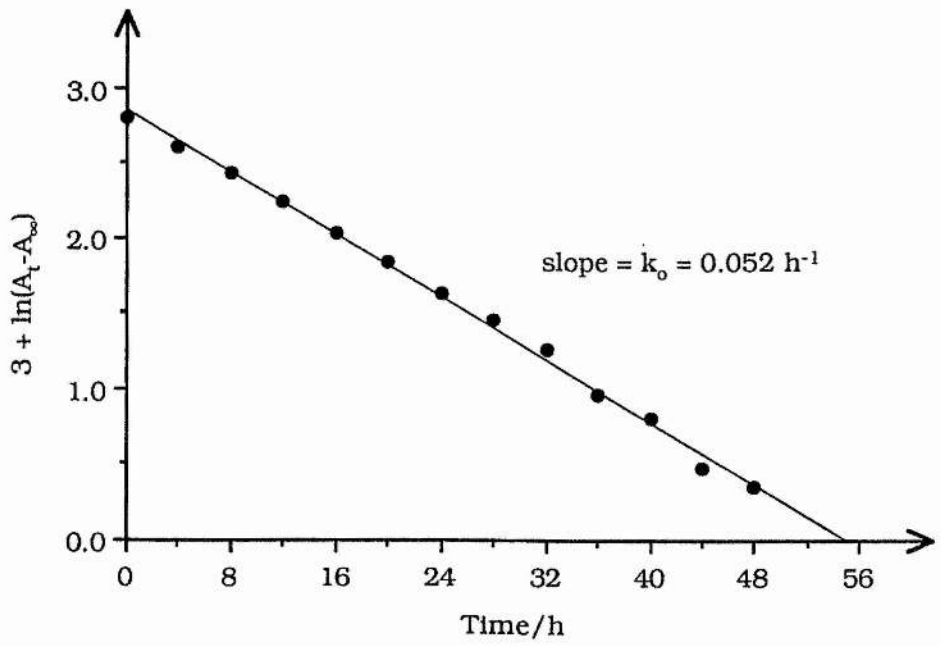

Thus the solvent isotope effect for the neutral water reaction is given by,

$$\frac{k_o^H}{k_o^D} = \frac{0.103}{0.052} = 1.98$$

The very fact that the water catalysed cyclisation of S to P exhibits a deuterium isotope effect with a substantial primary

contribution, suggests that the rate determining step of the reaction involves protonation of the substrate by the solvent.

In order to explain the water-induced reaction, a mechanism is proposed in which water itself acts as a general acid, with proton transfer from a molecule of water to the substrate occuring in the rate limiting step of the reaction (Scheme 5.6).

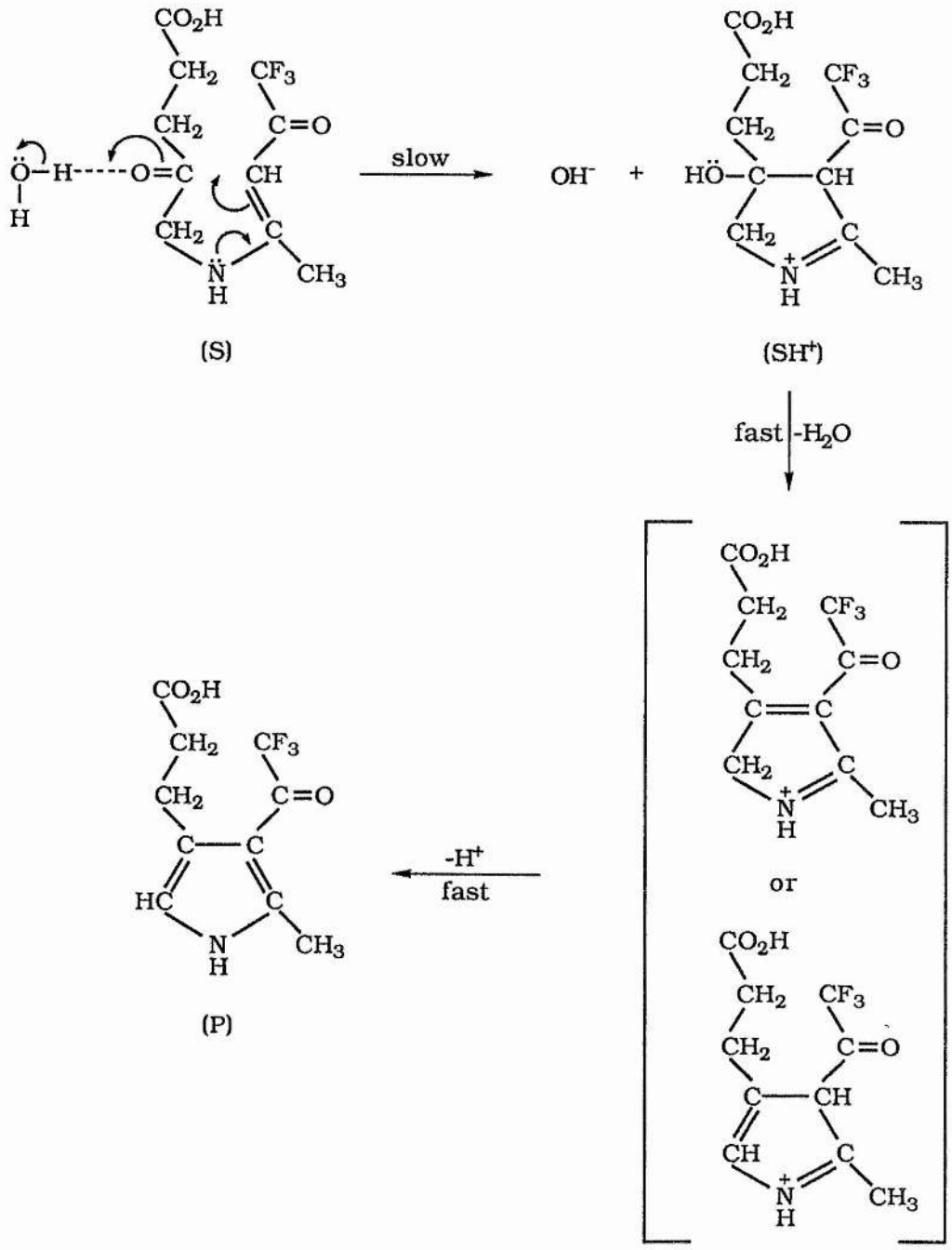

Scheme 5.6

Thus by this route,

$$S + H_2O \xrightarrow[r.d.s]{k} SH^+ + OH^-$$

$$SH^+ \xrightarrow{fast} P$$

Therefore,

$$\frac{d[P]}{dt} = k[S][H_2O]$$

$$= k_o^H [S]$$

where k_o^H is the first-order rate constant for the water catalysed cyclisation of S.

Thus according to the mechanisms illustrated in Schemes 5.5 and 5.6, for the hydronium ion and water catalysed cyclisations of S to P respectively, the overall forward rate for the cyclisation of S is given by,

$$\frac{-d[S]}{dt} = k_o^H[S] + k_H[H_3O^+][S]$$

or, at constant pH,

$$\frac{-d[S]}{dt} = k_{obs}^H[S]$$

where,

$$k_{obs}^H = k_o^H + k_H[H_3O^+]$$

Since the acid catalysed cyclisation of S to P involves transfer of a proton from one species to another (Scheme 5.5), it is anticipated that the substitution of H_2O by D_2O will affect both the rate and equilibrium constant of the above process.

Thus, the experiment described in Section 5.2.5.1 was repeated using deuteriated equivalents of all solvents and anhydrous sodium acetate instead of its hydrated form. Stock solutions of 0.1 M AcOD in D_2O (99.8%) and 0.1 M NaOAc in D_2O (99.8%) were prepared and appropriately mixed, to give three different acetic acid-sodium acetate buffers, whose pD values at 40 °C are listed in Table 5.5. The ionic strength of each of these buffer solutions were maintained at 0.05 M by the addition of KCl.

Table 5.5 pD of acetic acid-sodium acetate buffer solutions. 10 ml mixtures of x ml 1 M AcOD and y ml 1 M NaOAc.

Sample	AcOD (x ml of 1 M)	NaOAc (y ml of 1 M)	pD at 40 °C	[NaOAc]/M	[KCl]/M
5.5 (A)	9.0	1.0	4.34	0.01	0.04
5.5 (B)	8.0	2.0	4.69	0.02	0.03
5.5 (C)	7.0	3.0	4.90	0.03	0.02

As in the previous experiments, S (5 µl of a 0.025 M solution in methanol) was added to acetate buffer, (3 ml), thermostated at 40 °C, and absorbances recorded at regular intervals of time at a fixed wavelength of λ = 317.6 nm. A plot of $3 + \ln(A_t - A_\infty)$ versus time for the cyclisation of S to P in each of the acetate buffer solutions 5.5(A) to 5.5(C) (Table 5.5) was found to be linear and the results are displayed in Fig. 5.15. The slopes of these straight lines are the

experimental pseudo first-order rate constants, k^{D}_{obs}, for the cyclisation of S to P in the respective deuteriated acetate buffer solutions.

Figure 5.15 Plot of $3 + \ln(A_t - A_\infty)$ versus time for the cyclisation of S to P in deuteriated acetate buffers 5.5(A) to 5.5(C) (Table 5.5).

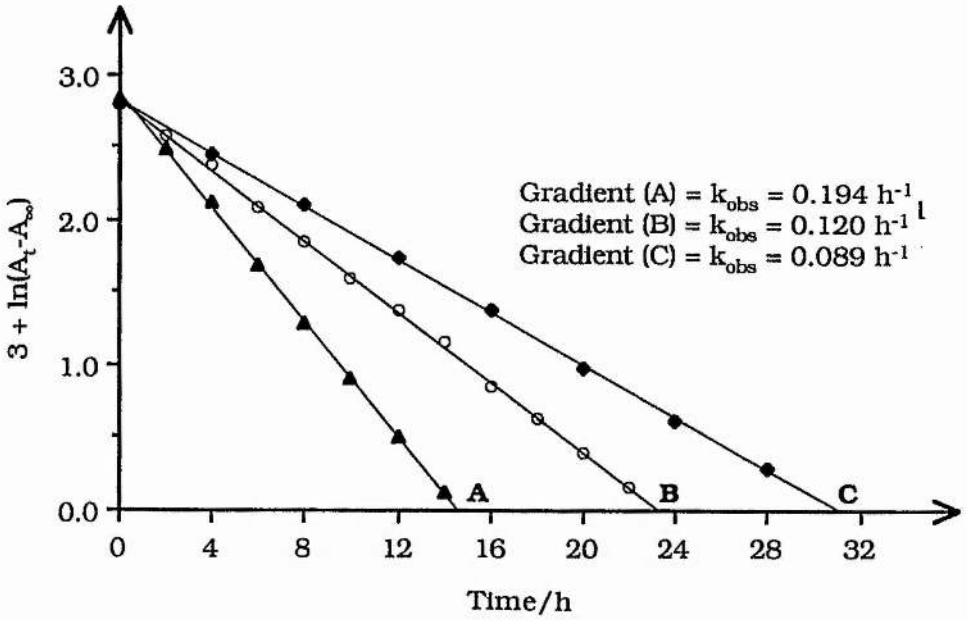

The pD, deuteronium ion concentration, $[D_3O^+]$ and the experimental pseudo first-order rate constant, k^{D}_{obs}, for the cyclisation of S to P in the deuteriated acetate buffer solutions 5.5(A) to 5.5(C) are listed in Table 5.5(A).

Table 5.5(A) The experimental pseudo first order rate constants, k^{D}_{obs} for the cyclisation of S to P in deuteriated acetate buffers 5.5(A) to 5.5(C) (Table 5.5).

Sample	pD at 40 °C	$[D_3O^+]$ = antilog [-pD]	$10^5 \times [D_3O^+]/M$	$10^2 \times k^{D}_{obs}/h^{-1}$
5.5 (A)	4.34	4.57×10^{-5}	4.57	19.4
5.5 (B)	4.69	2.04×10^{-5}	2.04	12.0
5.5 (C)	4.90	1.26×10^{-5}	1.26	8.9

A plot of $10^2 \times k^D_{obs}$ versus $10^5 \times [D_3O^+]$ (Fig.5.16) is a straight line, the slope of which gives k_D, which is the second order catalytic constant for the reaction catalysed by $[D_3O^+]$. The value of k_D, calculated from the graph is 3.11×10^3 l mol^{-1} h^{-1}. Extrapolation of the straight line reveals that when $[D_3O^+] = 0$, $k^D_{obs} = k^D_o = 0.052$ h^{-1}. This in fact was the rate obtained for the cyclisation of S to P in deuterium oxide.

Figure 5.16 Rate of cyclisation of S to P in deuteriated acidic solution, at 40 °C.

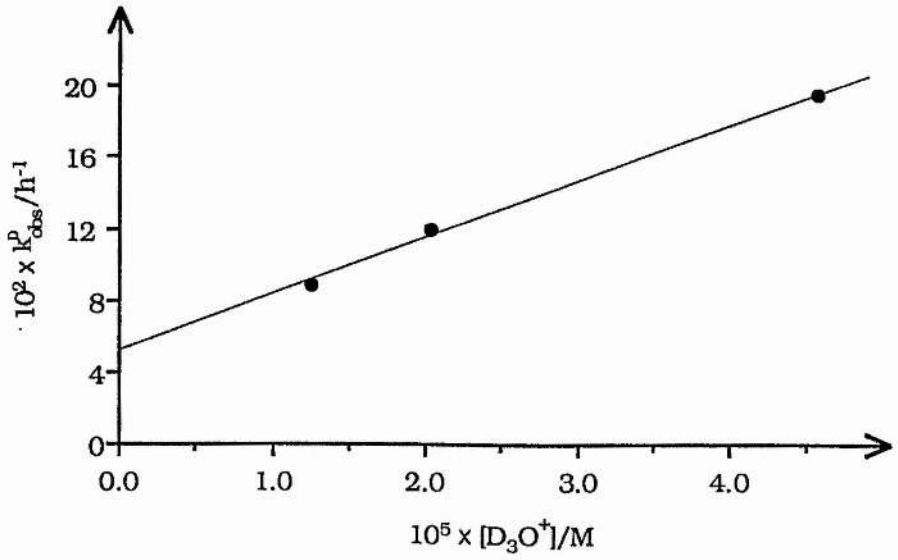

The solvent isotope effect for the reaction catalysed by oxonium ions is given by,

$$\frac{k_H}{k_D} = \frac{2.15 \times 10^3}{3.11 \times 10^3} = 0.69$$

Thus the acceleration of rate by oxonium ions due to the use of D_2O as solvent is 1.45.

For the autoprotolysis (dissociation) of water itself, the overall equilibrium effect is a complex term.[22-24]

$$2\ H_2O \rightleftharpoons H_3O^+ + OH^-$$

$$K_{AP} = [H_3O^+][OH^-]$$

K^H_{AP}/K^D_{AP} = 7.47(0.24), where D = ^2H.

Since deuterium oxide has a smaller autoprotolysis constant than water, it is believed to be less basic than water.[25] The apparent lower basicity of deuterium oxide is caused at least in part by the decrease in the H-O stretching force constant in going from water to oxonium ion which is observed in the I.R. spectrum.[26] Thus, the zero point energies of H-O and D-O bonds are closer in the ion than in water, making equilibrium toward the ion less favourable in D_2O than in H_2O.

Because of the lower basicity of deuterium oxide compared with ordinary water, the substrate, S, is able to compete with the solvent for the deuteron in D_2O more effectively than for the proton in H_2O. Since the concentration of the conjugate acid of the substrate, SH^+, will then be higher in D_2O, the rate of cyclisation of S due to oxonium ions will be higher in D_2O than in H_2O.

The water induced reaction on the otherhand is slower in D_2O than in H_2O, because the bond from oxygen to one of the isotopically substituted atoms is broken in the rate determining step of the reaction, as a result of which there is a primary contribution to the solvent isotope effect.

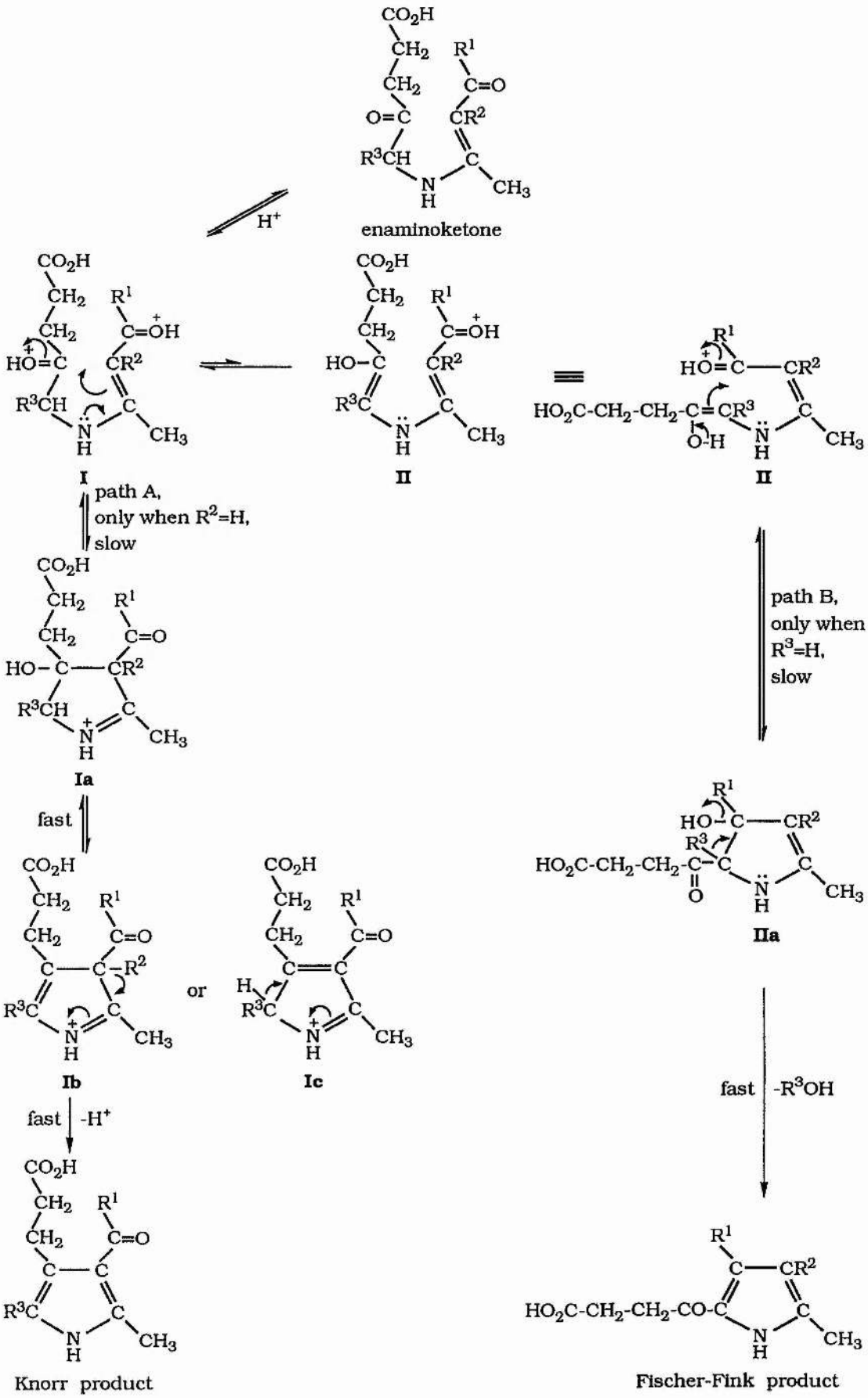
enaminoketone
H+
I
II
path A,
only when R2=H,
slow
path B,
only when
R3=H,
slow
Ia
IIa
fast
Ib
Ic
or
fast -H+
fast -R3OH
Knorr product
Fischer-Fink product

Scheme 5.7

5.2.5.6 Proposed mechanism for the condensation of ALA and 5-methyl-ALA with carbonyl compounds.

The condensation of ALA with 1,1,1-trifluoropentane-2,4-dione and with pentane-2,4-dione have both been shown to proceed *via* the corresponding enaminoketone intermediate. Although not detected, the condensation of ALA with the carbonyl compounds discussed in Chapter 4 and the condensation of 5-methyl-ALA with pentane-2,4-dione and with 3-methylpentane-2,4-dione are all assumed to proceed *via* an enaminoketone intermediate. The proposed mechanism for the formation of the enaminoketone intermediate has been discussed in Chapter 4.

On the basis of the kinetic evidence obtained for the cyclisation of the enaminoketone intermediate, S, in the reaction between ALA and 1,1,1-trifluoropentane-2,4-dione, (Scheme 5.1) the general mechanism proposed for the cyclisation of the enaminoketone intermediate is illustrated in Scheme 5.7.

It is reasonable to assume that in aqueous acidic solution, there is a rapid pre-equilibrium proton transfer to the free carbonyl oxygens of the enaminoketone intermediate, to form its conjugate acid (I) (Scheme 5.7). The degree to which the two carbonyl oxygens of the enaminoketone are protonated however, depends to a large extent on the nature of the substituent R^1. The intermediate I exists in solution, in equilibrium with its enol form, (II) (Scheme 5.7). I and II undergo separate cyclisation pathways (path A and path B) to form the Knorr and the Fischer-Fink products respectively. Path A however, is followed only when R^2 = H because only then can intermediate I aromatise to form the Knorr product. I, in a slow step undergoes a shift of its nitrogen lone pair to form the cyclic intermediate Ia. Ia in subsequent fast steps loses a

molecule of water to form either Ib or Ic which then loses a proton to form the Knorr product.

The first step in the cyclisation of intermediate II, is the loss of its enolic proton in a slow step to form IIa, which then loses a molecule of water (R^3 = H) in a fast step to form the Fisher-Fink product.

The course followed by the individual reactions, depends to a large extent, on the nature of the substituents, R^1, R^2 and R^3 of the enaminoketone intermediate. When R^2 = H, R^3 = H and R^1 = CF_3 or OEt, i.e. for the condensation of ALA with 1,1,1-trifluoropentane-2,4-dione and with ethyl acetoacetate respectively, the reaction follows path A to form the Knorr product exclusively. This is believed to be the result of the electron-withdrawing effect of the CF_3 and OEt groups which reduces electron density on the adjacent carbonyl oxygen. Consequently, the latter becomes less susceptible to protonation and path B is hindered.

When R^2 = H, R^3 = H and R^1 = CH_3 or Et, i.e. for the condensation of ALA with pentane-2,4-dione and with hexane-2,4-dione, 95% of the enaminoketone follows path A to form the Knorr product and 5% the enaminoketone follows path B to form the Fischer-Fink product. This then suggests that the equilibrium between I and II lies in favour of I. A possible explanation of the above fact, is that the cyclisation of I to Ia is faster relative to its enolisation to form II as a result of which most of the reaction is driven along path A. An alternative explanation is the lower basicity of the R^1CO carbonyl oxygen, which lies in conjugation with an electron withdrawing carbon-carbon double bond, compared with the other carbonyl group of the enaminoketone, which is flanked by two methylene groups (R^3 = H). As a result, the former is less

susceptible to protonation than the latter, the equilibrium is shifted to the left-hand side and path A is favoured.

When $R^1 = CH_3$, $R^3 = H$ and R^2 = alkyl, e.g. CH_3 or $CH(CH_3)_2$, i.e. for the condensation of ALA with 3-methylpentane-2,4-dione and with 3-isopropylpentane-2,4-dione respectively, the reaction follows path B to form the Fischer-Fink product exclusively. Path A in these reactions is disfavoured because intermediate Ia (Scheme 5.7) loses a molecule of water to form intermediate Ib which then cannot aromatise to form the Knorr product. Aromatisation is therefore the driving force favouring path B in the above reactions, leading to the exclusive formation of the Fischer-Fink product.

When $R^1 = CH_3$, $R^2 = H$ and $R^3 = CH_3$, i.e. for the condensation of 5-methyl-ALA with pentane-2,4-dione, the reaction follows path A to form the Knorr product exclusively. Path B is hindered because intermediate IIa (Scheme 5.7) formed in this reaction, cannot aromatise to form the Fischer-Fink product. When $R^1 = CH_3$, $R^2 = CH_3$ and $R^4 = CH_3$, i.e. for the condensation of 5-methyl-ALA with 3-methylpentane-2,4-dione, path B is hindered for precisely the same reason explained for the reaction between 5-methyl-ALA and pentane-2,4-dione. The reaction follows path A to form intermediate Ia. Ia loses a molecule of acetic acid to form Id (Scheme 5.8), which then aromatises to form the Knorr product.

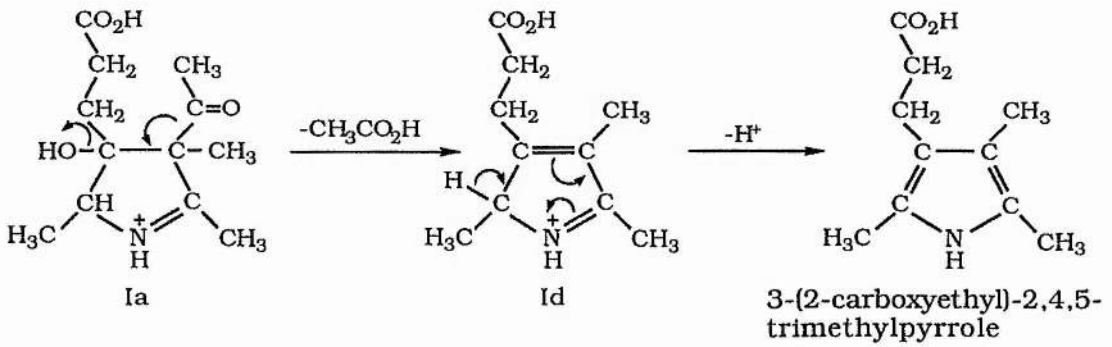

Ia Id 3-(2-carboxyethyl)-2,4,5-trimethylpyrrole

Scheme 5.8

References.

1) J. B. Hendrickson and R. Rees, *J. Amer. Chem. Soc.*, 1961, **83**, 1250.

2) D. S. James and P. E. Fanta, *J. Org. Chem.*, 1962, **27**, 3346.

3) J. B. Henrickson, R. Rees and J. F. Templeton, *J. Amer. Chem. Soc.*, 1964, **86**, 107.

4) S. K. Khetan, J. G. Hiriyakkanavar and M. V. George, *Tetrahedron*, 1968, **24**, 1567.

5) A. M. Cheh and J. B. Neilands, *Struct. Bond.*, 1976, **29**, 123.

6) P. N. B. Gibbs and P. M. Jordan, *Biochem. J.*, 1986, **236**, 447.

7) P. M. Jordan and J. S. Seehra, *FEBS Lett.*, 1980, **114**, 283.

8) P. M. Jordan and P. N. B. Gibbs, *Biochem. J.*, 1985, **227**, 1015.

9) S. S. Hasnain, E. M. Wardell, C. D. Garner, M. Schlosser and D. Beyersmann, *Biochem. J.*, 1985, **230**, 625.

10) E. K. Jaffe and D. Hanes, *J. Biol. Chem.*, 1986, **261**, 9348.

11) E. K. Jaffe and G. D. Markham, *Biochemistry.*, 1987, **26**, 4258.

12) E. K. Jaffe and G. D. Markham, *Biochemistry.*, 1988, **27**, 4475.

13) A. H. Jackson *in* 'Comprehensive Organic Chemistry', (P. G. Sammes, ed.), Vol. 4, Ch. 17.1, Pergamon Press, Oxford, 1979.

14) A. Gossauer, 'Die Chimie der Pyrrole', p. 213ff, Springer-Verlag, Berlin.

15) R. A. Jones and G. P Bean *in* 'The Chemistry of Pyrroles', (A. T. Blomquist and H. H.Wasserman, eds.), Ch. 3, Academic Press, London, 1977.

16) R. A. Jones (ed.), 'Pyrroles, Chemistry of Heterocyclic Compounds', Wiley-Interscience, 1990.

17) C. J. Broan, Ph.D Thesis, University of St. Andrews, 1988.

18) B. Zerner and M. L. Bender, *J. Am. Chem. Soc.*, 1961, **83**, 2267.

19) G. C. Levy , 'Topics in Carbon-13 Nuclear Magnetic Resonance Spectroscopy', Vol. 2, Wiley-Interscience, New York, 1976.

20) G. C. Levy and R. L. Lichter, 'Nitrogen-15 Nuclear Magnetic Resonance Spectroscopy', Wiley-Interscience, New York, 1979.

21) G. J . Martin, M. L. Martin and J. P. Goursnard, '^{15}N NMR Spectroscopy', Vol. 18, Springer-Verlag, Berlin, 1981.

22) R. P. Bell, 'The Proton in Chemistry', 2nd ed., Chapman and Hall, London, 1973.

23) P. Saloman, *Acta Chem. Scand.*, 1971, **25**, 367.

24) M. Goldblatt and W. M. Jones, *J. Chem. Phys.*, 1969, **51**, 1881.

25) K. Wiberg, *Chem. Rev.*, 1955, **55**, 713.

26) D. E. Bethell and N. Sheppard, *J. Chem. Phys.*, 1953, **50**, C72.

CHAPTER SIX

ON THE MECHANISM OF PORPHOBILINOGEN BIOSYNTHESIS

6.1 Introduction.

The enzyme ALA dehydratase (EC 4.2.1.24) has been isolated from many bacterial, plant, avian and mammalian sources. These include the bacteria *Rhodopseudomonas spheroids,*[1-3] and *Rhodopseudomonas capsulata,*[4] the fungus *Ustilago sphaerogena,*[5] yeast (*Saccharomyces cerevisiae*),[6] spinach,[7] tobacco[8] and wheat[9] leaves, soyabean callus tissues,[10] chicken erythrocytes,[11] bovine[12-15] and mouse[16,17] liver, rat harderian gland,[18] rabbit[11] and human erythrocytes,[19-22] and guinea pig liver and erythrocytes.[23]

Although the enzymes from different sources have not been purified to the same degree, an analysis of the published data reveals that the specific activities of the enzyme vary widely. It appears that the bacterial enzymes are more active than those from eukaryotic organisms. It is also of interest to note that fetal mouse liver enzyme is twice as active as adult mouse liver enzyme.[17]

The K_m values for various preparations are similar. The K_m at pH 6.8 and 37 °C is 0.4 mM for the mouse liver enzyme.[17] This may be compared with 0.15 mM for the bovine liver enzyme[13,15] and 0.5 mM for the enzyme prepared from chicken and rabbit erythrocytes.[11] A value of 0.083 mM for the enzyme prepared from human erythrocytes was found in the complete absence of haem, while 0.32 mM was obtained for similar preparations in the presence of haem.[20] The K_m at pH 8.5 and 37 °C for the enzyme from *Rhodopseudomonas spheroids* has been reported to be 0.7 mM.[2]

With the exception of the enzyme from *Rhodopseudomonas spheroids,* a plot of enzymic activity versus substrate concentration for the enzymes from all the other sources gives a hyperbolic saturation curve. A similar curve is also obtained with the enzyme

from *Rhodopseudomonas spheroids* in the presence of K^+ ions.[2] However, in the absence of K^+ ions, with this enzyme, a sigmoidal curve is obtained, demonstrating the cooperative homotropic effect of the substrate. Under the latter conditions, the maximum velocity found at a substrate concentration of 0.05 M is only about one-half that found in the presence of K^+ ions.

The properties of the partially purified enzymes have been tabulated.[24] It appears that at least 1000-fold purification of a crude homogenate of the mammalian liver ALA dehydratase is required to achieve homogeneity.

Nandi and Shemin,[25] working on the enzyme from *Rhodopseudomonas spheroids*, demonstrated that a Schiff's base forms between ALA and the enzyme at the active site lysine residue. These workers[25] showed that ALA could be irreversibly bound to the enzyme by $NaBH_4$ reduction of the Schiff base to a secondary amine. This led to concomitant loss of enzyme activity, and if ^{14}C-labelled substrate is used, the inactivation is accompanied by the incorporation of label into the enzyme protein. Schiff base formation with the active site lysine residue was also demonstrated with other γ-keto acids, such as levulinic acid, ethyl levulinate, N-acetyl-ALA, but not with 4-ketoglutaric acid[25] (Fig. 6.1).

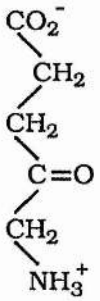

ALA

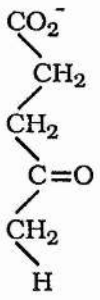

levulinic acid

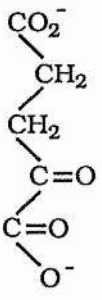

4-ketoglutaric acid

Figure 6.1 Comparison of the structures of some 4-ketoacids.

These findings show that the site occupied by the amino methyl group of ALA, covalently linked to the enzyme, is unable to accomodate a carboxyl group. Nandi and Shemin[25] also demonstrated that although both levulinic acid and ethyl levulinate form Schiff bases with the enzyme, only the free acid acts as a competitive inhibitor. Lack of inhibition by ethyl levulinate was also consistent with the findings of Nandi and Shemin[26] that the ethyl ester of ALA is a poor substrate for the enzyme. Nandi and Shemin therefore implied that the degree of substrate affinity is determined both by the formation of a Schiff base and by the formation of an ionic bond between a positively charged group on the enzyme and the carboxylate ion in β-position to the carbonyl group of the substrate.

Work with the bovine liver enzyme has shown that the mammalian enzyme also forms a covalent Schiff base linkage with one of the substrate molecules.[27,28] Jordan and Seehra[29] and Jordan and Gibbs[30] have used stopped-flow techniques to establish that a Schiff's base forms between the enzyme and the first ALA which binds to its active site. Labelling with [5-^{13}C]ALA and [5-^{14}C]ALA and using the single-turnover enzyme reaction technique, these authors[29,30] demonstrated that this ALA becomes the P-side of PBG in the case of the bovine liver and the human red blood cell enzyme respectively. Subsequent addition of the second substrate molecule to the A-side of the catalytic site eventually leads to the formation of PBG. This mechanism first proposed by Jordan and Seehra,[28,29] differs substantially from Nandi and Shemin's conclusion, in which the converse order of addition of the two molecules of ALA to the enzyme was favoured. The approach by these latter workers involved the use of levulinic acid, which

together with ALA yielded a 'mixed' pyrrole with the dehydratase from *Rhodopseudomonas spheroids*. Since levulinic acid was also shown to form a Schiff base with the enzyme, it was suggested that the formation of the 'mixed' pyrrole can only occur if the β-methylene carbon atom of levulinic acid condensed with the carbonyl carbon atom of ALA [Fig. 6.2(A)], for if condensation were to occur between the β-methylene carbon atom of ALA and the carbonyl carbon of levulinic acid [Fig. 6.2(B)], pyrrole formation would not be possible.

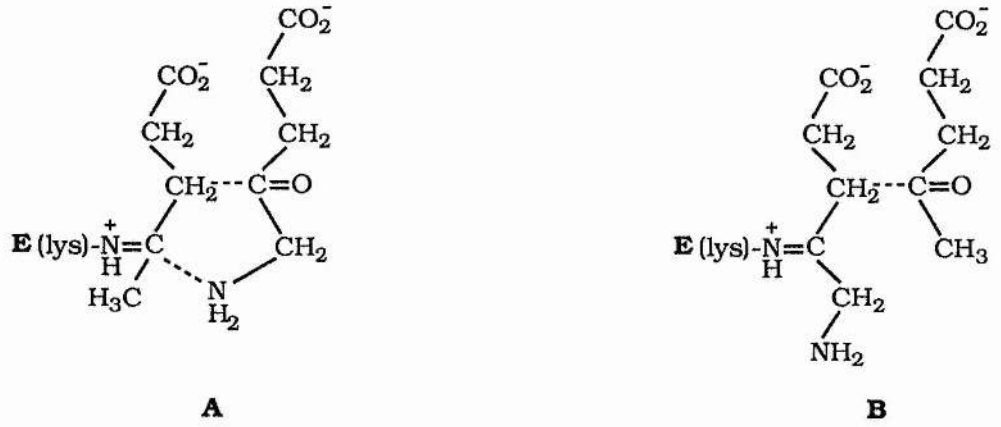

Figure 6.2 Schemes for the formation of heterologous pyrroles from ALA and levulinic acid.

The conclusion therefore was that levulinic acid is in Schiff base linkage with the enzyme and formed the A-side of the 'mixed' pyrrole. It was therefore argued that in PBG synthesised from two molecules of ALA, the side carrying the acetic acid side chain is the molecule of ALA which was attached to the enzyme through a Schiff base.

The above reasoning, however, does not take into account the fact that levulinic acid could interact with both substrate binding sites, acting as a substrate at the A-site, but since it has no amino group like the true substrate, acting as an inhibitor at the P-site.

The findings of Jordan and Seehra[28,29] and Jordan and Gibbs,[30] that the first molecule of ALA which is covalently linked to the enzyme in the form of an enzyme-substrate Schiff base complex becomes the P-side of PBG, suggest that the enzyme inactivation which occurs when the enzyme is allowed to react with $NaBH_4$ in the presence of levulinic acid,[25] is as a result of the binding of the latter to the P-site.

Gibson *et al* [12] have shown that the bovine liver enzyme does not act on aminoacetone, 6-amino-5-ketohexanoic acid and 2,5-diaminolevulinic acid. The formation of 'mixed' pyrroles, formed from ALA in the presence of any of the above compounds, has however not been looked into.

In an elegant study of the inactivation of crude rat liver ALA dehydratase by 4,6-dioxoheptanoic acid (succinylacetone), Tschudy *et al* [31] demonstrated that the latter is a highly active irreversible inhibitor of the enzyme. Succinylacetone is an analogue of ALA in which the amino group of the latter is replaced by an acetyl group. The structural similarity to ALA suggests that succinylacetone reacts with the enzyme at the catalytic site. This is further confirmed by the fact that succinylacetone prevented the formation of a secondary amine, produced by reduction of the labelled enzyme-substrate complex by $NaBH_4$.[31] The above workers[31] also demonstrated that of the compounds which have previously been known to inhibit ALA dehydratase, including EDTA,[12,32] 3-amino-1,2,4-triazole,[33-35] levulinic acid,[25] and hemin,[17,20,23,36] succinylacetone is by far the most effective inhibitor of the enzyme.

In order to determine the specificity of the second binding site or the A-site of the enzyme from bovine liver, the formation of 'mixed' pyrroles was investigated, using the single-turnover enzyme

reaction technique. In this method, stoichiometric equivalents of [4-^{13}C]ALA.HCl (50% enriched) and homogeneous bovine ALA dehydratase were initially mixed for approximately 5 seconds, the reasoning being that all of the labelled substrate would be covalently bound to the enzyme at the P-site, in the form of an enzyme-substrate Schiff base complex. Subsequent addition of a large excess of an unlabelled substrate analogue was used to determine if the bound labelled substrate had been carried over to product, thus completing a single-turnover with respect to the labelled substrate.

6.2 Experimental.

6.2.1 Materials.

ALA dehydratase, ALA.HCl, ALA.HCl (methyl ester), dithioerythreitol (DTT) and GAL-PAC powder were purchased from Sigma Chemical Company. *p*-N,N-dimethylaminobenzaldehyde, mercuric chloride, methanol, 70% perchloric acid, trichloroacetic acid and zinc chloride were purchased from Aldrich. [4-^{13}C] ALA.HCl, N,N-dimethyl-ALA.HCl and 5-methyl-ALA.HCl were synthesised as described in Sections 2.2.3, 3.3.5.4 and 4.2.5 respectively. Glacial acetic acid was purchased from Rhône Poulenc Limited and Sephadex G-50 from Pharmacia Fine Chemicals.

6.2.2 Methods.

A. Desalting of ALA dehydratase.

The bovine liver ALA dehydratase which was purchased as an ammonium sulphate suspension (5 units), was desalted by gel filtration on a 10 cm long Sephadex G-50 column which had been equilibrated at 4 °C with 0.1 M KPi buffer, pH 6.8. The most active fractions were pooled, flash frozen in liquid nitrogen and stored at 0 °C. A dehydratase unit is defined as the amount of enzyme that catalyses the formation of 1 micromole of PBG, per hour, at 37 °C. Specific activity is defined as the micromoles of PBG formed, per milligram of protein, per hour, at 37 °C.

B. Protein determination.

Protein concentrations were determined by reading U.V. absorbances at 280 nm. Values of $A^{1\%} = 11.8$,[37] have been reported using the protein determination of Lowry.[38]

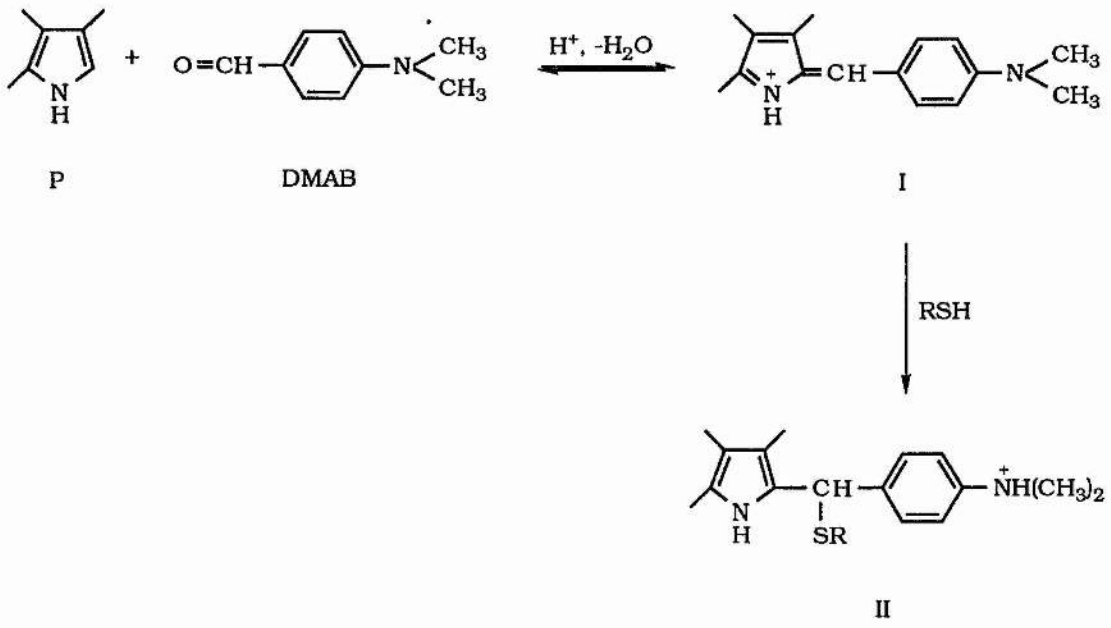

P DMAB I II

Scheme 6.1

C. ALA dehydratase activity determination.

The identification of PBG in biological material depends primarily upon the coloured complex it forms with Ehrlich's reagent[39-41] (DMAB). The desalted enzyme (3.75 mg, 5 units) was made upto 1 ml in 0.1 M KPi buffer, pH 6.8. 0.01 ml of this enzyme solution was preincubated in 0.6 ml of 0.1 M KPi buffer, pH 6.8, containing 10 mM DTT and 10 μM Zn^{2+} for one hour at 37 °C. Reaction was initiated by the addition of ALA.HCl (0.2 ml of an appropriate concentration) and incubation continued for definite periods of time. Reaction was then terminated by the addition of 0.8 ml of 0.1 M mercuric chloride in 20% trichloroacetic acid. After centrifugation, the supernatant solution was removed and mixed with an equal volume of modified Ehrlich's reagent. The resulting colour density was measured at 555 nm, 15 minutes after mixing, against a blank made from equal volumes of the reagent and water. Under these conditions, PBG has an apparent molar extinction coefficient of 6.1×10^4.

As mentioned in Chapter 3, on allowing a pyrrole, P, with a free α-position to react with DMAB in acid solution, a coloured Ehrlich colour salt, I arises (Scheme 6.1), which is decolourised by thiol compounds. Nucleophilic reagents such as sulphydryl compounds add to the methine carbon to produce the colourless compound, II (Scheme 6.1), which is protonated in acid solution. The method of choice to overcome sulphydryl interference is to form a tight complex with a heavy metal such as Hg^{2+}.

D. Preparation of modified Ehrlich reagent.

The modified Ehrlich reagent of Mauzerall and Granick[42] is less convenient for general use than the regular Ehrlich's reagent

(2% w/v DMAB in 6 N HCl), since it must be made freshly each day. It is more sensitive however, and is useful when smaller amounts of PBG are to be determined. It is made as follows. For the reagent, 2 N with respect to perchloric acid, 1 g of DMAB (recrystallised from aqueous methanol) is dissolved in 30 ml of glacial acetic acid, 8.0 ml of 70% perchloric acid added and the solution diluted to 50 ml with glacial acetic acid.

E. Single-turnover enzyme experiments.

For the single-turnover enzyme experiments, desalted ALA dehydratase (5.68 nmol), was dissolved in 0.5 ml of 0.1 M KPi buffer, pH 6.8, containing 10 mM DTT and 10 μM Zn^{2+}, and activated at 37 °C for one hour. Assuming 4 active sites per mole of enzyme, of which only 70% remain unoccupied,[43] a stoichiometric amount of [4-^{13}C]ALA.HCl (50% enriched) (15.9 nmol in 0.1 ml of 0.1 M KPi buffer, pH 6.8) was then mixed with the enzyme for approximately 5 seconds. The resulting solution was then flushed with a 1000-fold excess of a second unlabelled substrate analogue in 0.1 ml of the same buffer and incubated for a further 20 minutes. It was then transferred into a 5 mm NMR tube with a D_2O capillary insert and ^{13}C NMR spectral acquisition started.

6.2.3 Instrumentation and General Techniques.

^{1}H decoupled, ^{13}C NMR spectra were obtained at 75.469 MHz on a Bruker AM 300 spectrometer using 32 K data points. They were acquired at 37 °C, using a pulse width of 2.0 μs (3.9 μs for a 90 ° flip angle), a recycle time of 5.8 s and a spectral width of 20,000 Hz. The thermal stability of ALA dehydratase enabled the use of elevated temperatures (37 °C) for spectral acquisition, which

provides a mechanism for reducing the sample viscosity. Spectra were processed using an exponential line broadening of 2 Hz unless otherwise specified and were referenced with respect to external dioxane set at δ 67.4.

Colorimetric measurements were made at room temperature, with a Philips PU 8732 UV/Visible scanning spectrophotometer fitted with a PU 8732 cell programmer. Quartz cells of 1 cm path length were used for all measurements.

6.3 Results and Discussion.

6.3.1 Formation of [3,5-^{13}C]PBG from [4-^{13}C]ALA.

^{13}C NMR was used to monitor the formation of [3,5-^{13}C]PBG from [4-^{13}C]ALA (50% enriched), in order to compare the ^{13}C chemical shift of the labelled carbon of P-side PBG with the corresponding carbon of possible 'mixed' pyrroles formed by the enzyme, ALA dehydratase. The reaction is illustrated in Scheme 6.2.

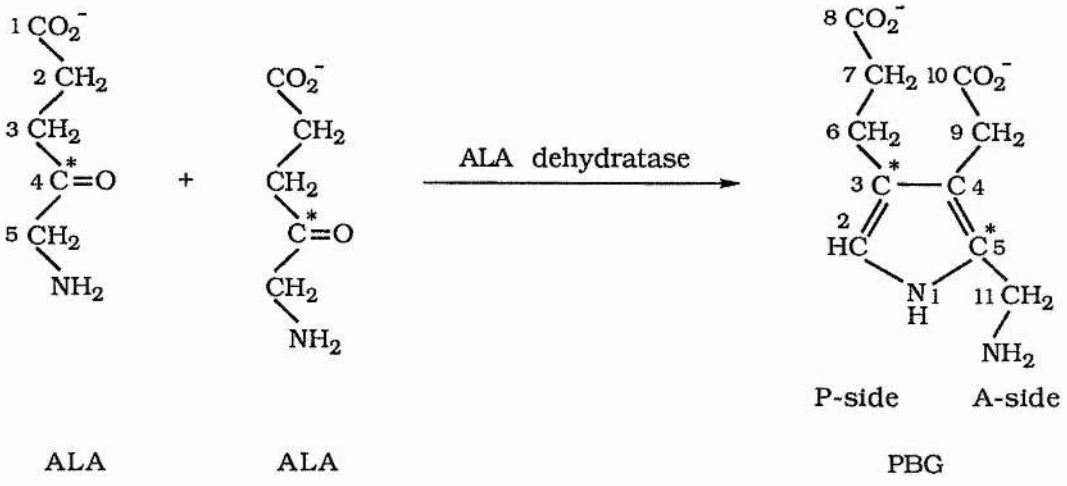

Scheme 6.2 Formation of [3,5-^{13}C]PBG from [4-^{13}C]ALA (50% enriched). * denotes ^{13}C labelled positions.

The ^{13}C NMR spectrum of [4-^{13}C]ALA.HCl (50% enriched) (7.2 μmol), in 0.1 M KPi buffer (0.5 ml), pH 6.8, revealed only a sharp singlet at δ 204.7 (200 transients), which is attributed to the C_4 carbonyl carbon of ALA. After a six hour incubation of the above solution of labelled ALA.HCl with activated ALA dehydratase (3.75 mg, 5 units), in 0.1 M KPi buffer (0.5 ml), pH 6.8, containing 10 mM DTT and 10 μM Zn^{2+}, there arose two resonances of equal intensity at 122.2 and 121.1 ppm. These resonances are attributed to C_3 and C_5 of PBG respectively, on the basis of assignments made in the literature.[44]

6.3.2 Single-turnover enzyme experiments.

6.3.2.1 Single-turnover reaction with [4-^{13}C]ALA.HCl (50% enriched) and levulinic acid.

The ^{13}C NMR spectrum (96,000 transients) of the reaction mixture, containing stoichiometric equivalents of ALA dehydratase and [4-^{13}C]ALA.HCl (50% enriched) together with a 1000-fold excess of levulinic acid, revealed a minor peak at 124.3 ppm, suggesting that the labelled substrate had been carried over to product, as illustrated in Scheme 6.3.

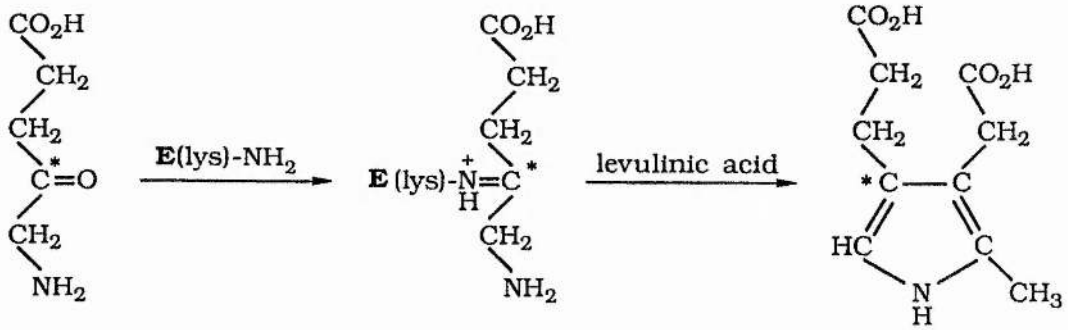

ALA

P-side enzyme-substrate Schiff-base

* denotes ^{13}C-labelled positions.

Scheme 6.3

The single-turnover with levulinic acid, suggests that the latter binds to the A-side binding site of ALA dehydratase like the true substrate, ALA.

6.3.2.2 Single-turnover reaction with [4-^{13}C]ALA.HCl (50% enriched) and N,N-dimethyl-ALA.HCl.

The ^{13}C NMR spectrum (36,000 transients) of the reaction mixture, containing stoichiometric equivalents of ALA dehydratase and [4-^{13}C]ALA.HCl (50% enriched) together with a 1000-fold

excess of N,N-dimethyl-ALA.HCl, revealed no peaks in the aromatic spectral region, suggesting that the labelled substrate had not been carried over to product as illustrated in Scheme 6.4.

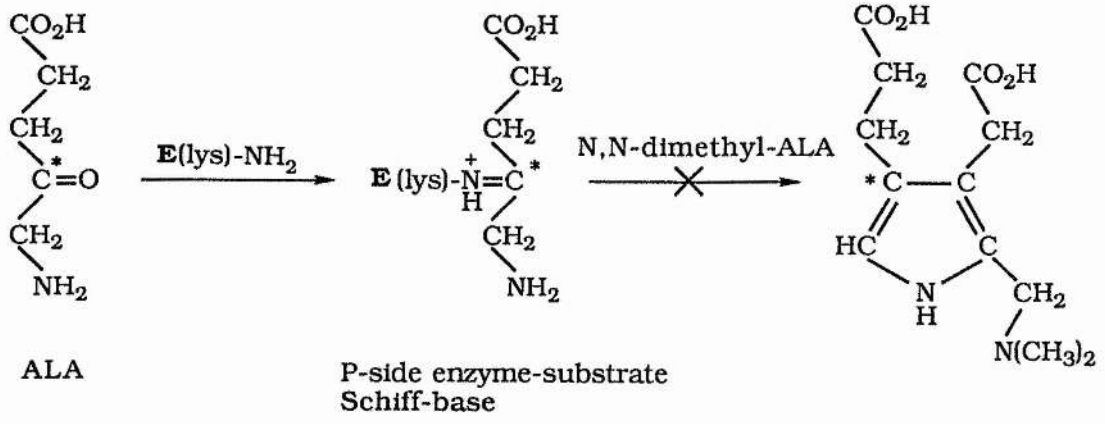

* denotes ^{13}C-labelled positions.

Scheme 6.4

The absence of any turnover with N,N-dimethyl-ALA, suggests that it does not bind to the A-side binding site of ALA dehydratase and is therefore not a suitable substrate for the enzyme.

6.3.2.3 Single-turnover reaction with [4-^{13}C]ALA.HCl (50% enriched) and 5-methyl-ALA.HCl.

The ^{13}C NMR spectrum (36,000 transients) of the reaction mixture, containing stoichiometric equivalents of ALA dehydratase and [4-^{13}C]ALA.HCl (50% enriched) together with a 1000-fold excess of 5-methyl-ALA.HCl, revealed no peaks in the aromatic spectral region, suggesting that the labelled substrate had not been carried over to product as illustrated in Scheme 6.5.

The absence of any turnover with the 5-methyl-ALA suggests that it does not bind to the A-side binding site of ALA dehydratase and is therefore not a suitable substrate for the enzyme.

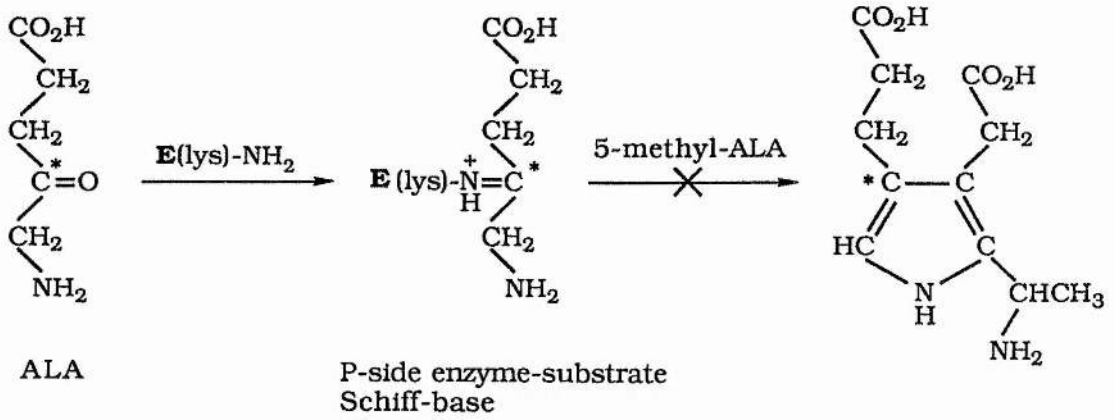

* denotes ^{13}C-labelled positions.

Scheme 6.5

6.3.2.4 Single-turnover reaction with [4-^{13}C]ALA.HCl (50% enriched) and the methyl ester of ALA.HCl.

The ^{13}C NMR spectrum (72,000 transients) of the reaction mixture, containing stoichiometric equivalents of ALA dehydratase and [4-^{13}C]ALA.HCl (50% enriched) together with a 1000-fold excess of ALA.HCl (methyl ester), revealed no peaks in the aromatic spectral region, suggesting that the labelled substrate had not been carried over to product as illustrated in Scheme 6.6.

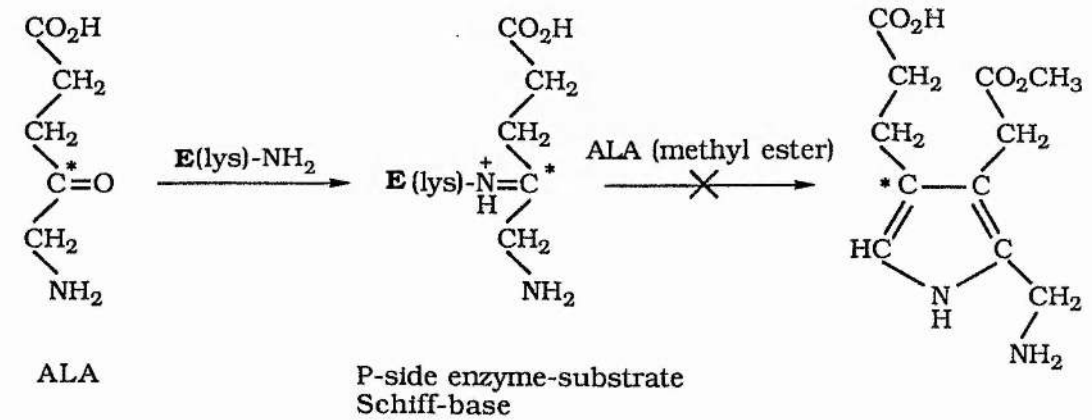

* denotes ^{13}C-labelled positions.

Scheme 6.6

The absence of any turnover with the methyl ester of ALA

suggests that it does not bind to the A-side binding site of ALA dehydratase and is therefore not a suitable substrate for the enzyme.

In order to determine what effect if any, the four analogues of ALA discussed above had on the rate of production of PBG, enzyme kinetics were carried out and this is discussed in detail in the following sections of the Chapter.

6.3.3 Enzyme kinetics.

6.3.3.1 Substrate concentration and initial velocity.

The progress curves of PBG production at pH 6.8 and 37 °C, from four concentrations of ALA (Fig. 6.3), were obtained with a highly purified preparation of ALA dehydratase which had been previously desalted. The amount of PBG formed per ml of the final solution was found to be proportional to time, within the limits of experimental error.

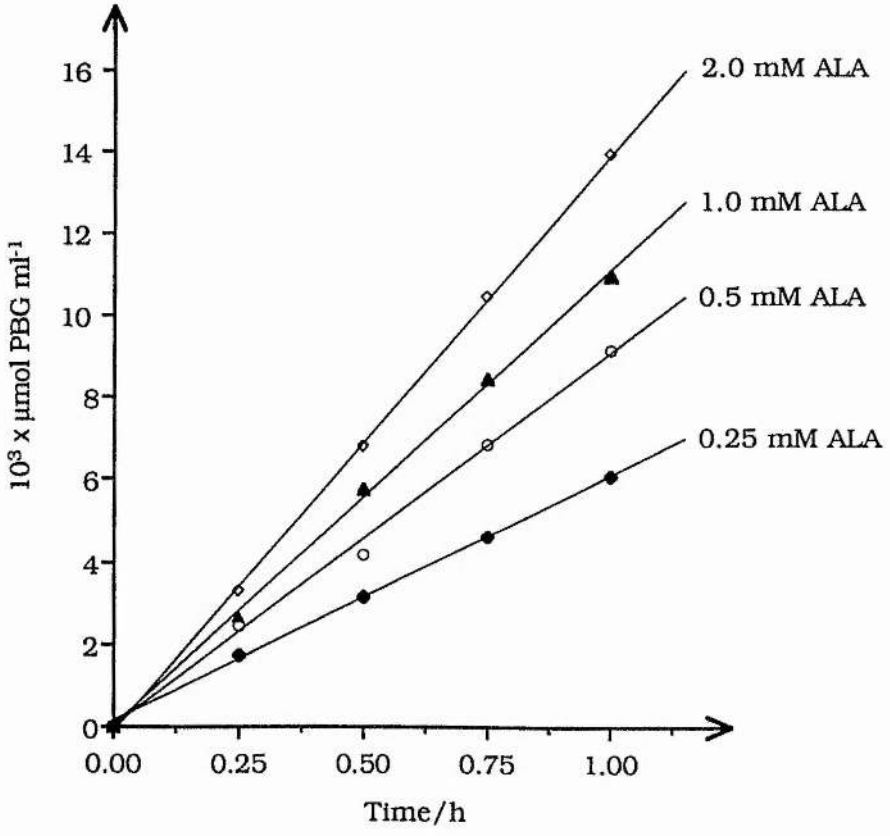

Figure 6.3 Progress curves showing the amount of PBG formed per ml of final solution. Each point represents a separate incubation, employing 0.0375 mg of ALA dehydratase.

Figure 6.4 is a plot of the reciprocol of the initial velocity of ALA dehydratase against the reciprocol of the concentration of ALA, at pH 6.8 and 37 °C.

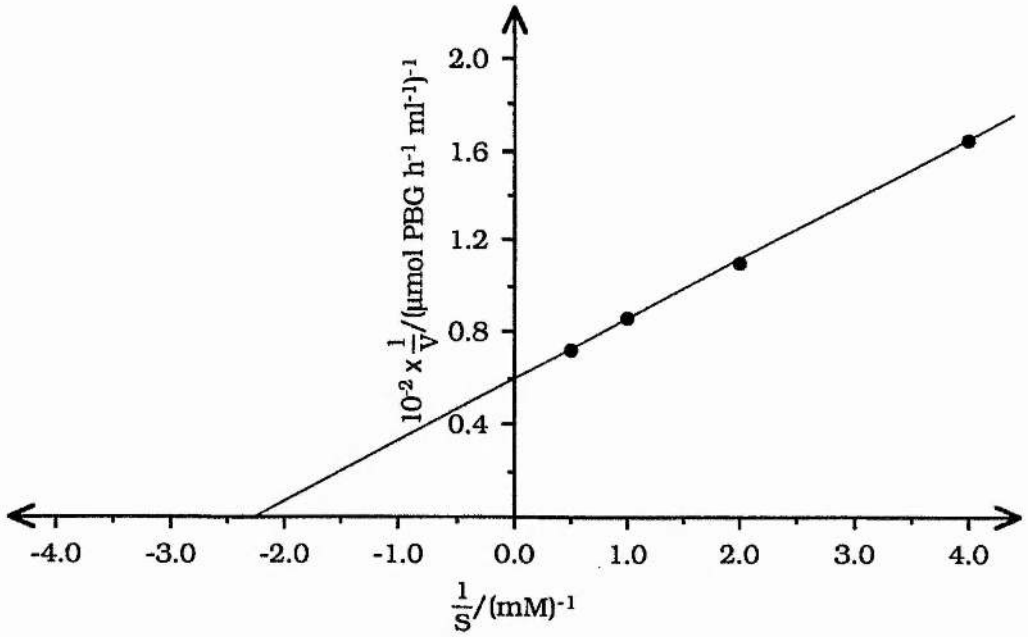

Figure 6.4 Plot of $10^{-2} \times 1/V$ versus 1/S, showing enzyme activity as a function of substrate concentration.

The value of K_m for this enzyme preparation, determined from the intercept on the abscissa is 0.44 mM. The maximum initial velocity, V_{max}, (determined from the ordinal intercept) was 1.33 mmol PBG/h/mg under these conditions.

6.3.3.2 Effect of levulinic acid on the initial velocity of ALA dehydratase.

The progress curves of PBG production from four concentrations of ALA, each in the presence of 0.25 mM levulinic acid are shown in Fig. 6.5.

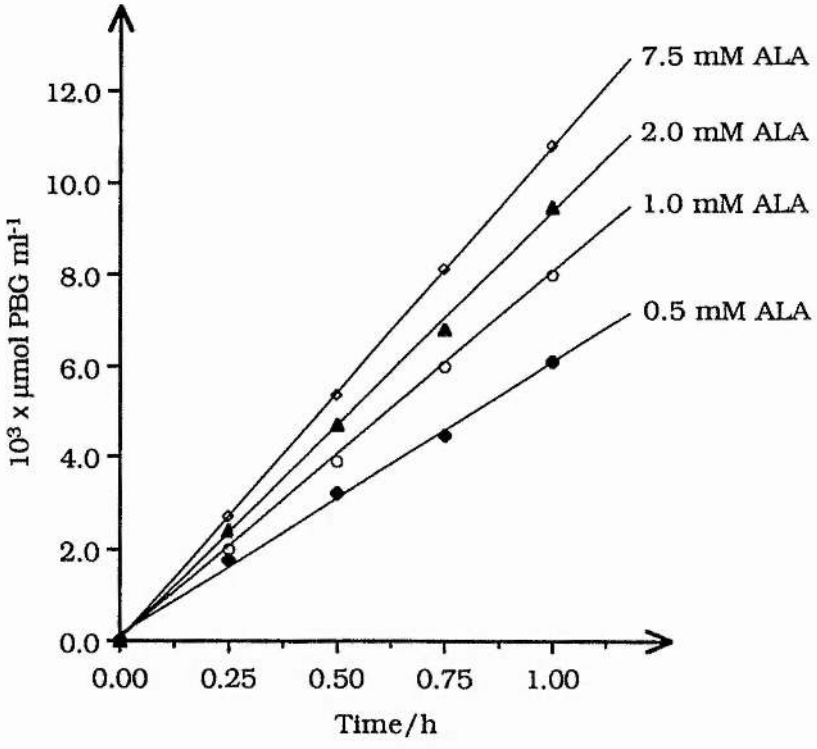

Figure 6.5 Progress curves showing the amount of PBG formed per ml of final solution in the presence of 0.25 mM levulinic acid. Each point represents a separate incubation, employing 0.0375 mg of ALA dehydratase.

A comparison of the initial velocities obtained in the presence and in the absence of levulinic acid, clearly suggest that levulinic acid inhibits the enzyme reaction.

In order to determine the nature of this inhibition, a plot of the reciprocol of the initial velocity of ALA dehydratase against the reciprocol of the concentration of ALA in the presence and in the absence of levulinic acid was made, and this is show in Fig. 6.6.

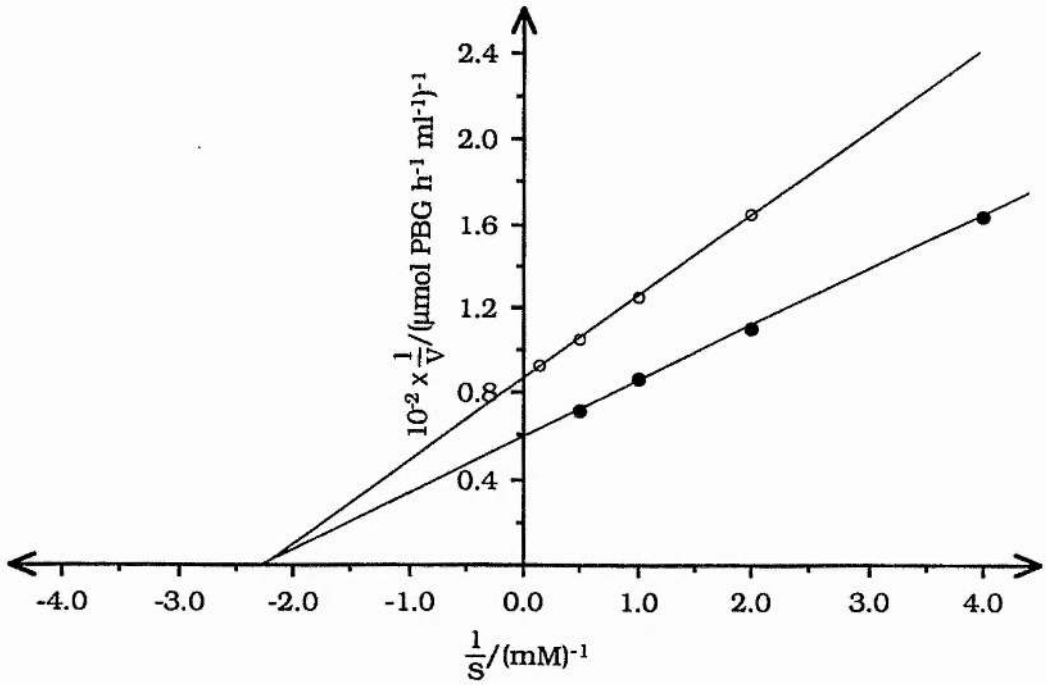

Figure 6.6 Plot of $10^{-2} \times 1/V$ versus $1/S$, showing enzyme activity as a function of substrate concentration in the presence (o) and in the absence (•) of levulinic acid.

The plot clearly shows that levulinic acid behaves as a non-competitive inhibitor, competing with the natural substrate, ALA, for the enzyme to form an enzyme-inhibitor complex, EI, as well as binding to the enzyme-substrate complex, ES, to form an enzyme-substrate-inhibitor complex, ESI. This is schematically represented below.

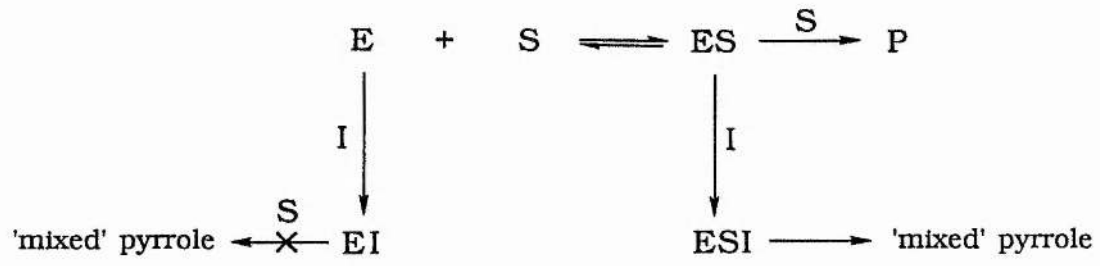

Since levulinic acid is known to form a Schiff base with the bovine liver enzyme, it must be competing with the substrate for the P-side binding site of the enzyme and acting as an inhibitor

because it lacks an amino group for pyrrole ring formation. The fact that levulinic acid forms an enzyme-substrate-inhibitor complex, does not altogether rule out the formation of product, since a 'mixed' pyrrole was detected in the single-turnover reaction, described in Section 6.3.2.1. The rate of formation of the 'mixed' pyrrole however, must be slower than the rate of dimerisation of the natural substrate, ALA, to form PBG. The fact that levulinic acid behaves as a non-competitive inhibitor of the bovine liver enzyme is in direct contrast to its action as a competitive inhibitor of the enzyme from *Rhodopseudomonas spheroids*.

6.3.3.3 Effect of N,N-dimethyl-ALA.HCl on the initial velocity of ALA dehydratase.

No change in the initial velocity of ALA dehydratase was observed with four different concentrations of ALA (0.25 mM, 0.5 mM, 1 mM, and 2 mM), each in the presence of 0.25 mM N,N-dimethyl-ALA.HCl. This suggests that the latter is not a substrate for the enzyme and therefore does not bind to either of its binding sites. The above result explains why no 'mixed' pyrrole was formed in the single-turnover reaction with equimolar amounts of ALA dehydratase and [4-^{13}C]ALA.HCl (50% enriched) and a large excess of N,N-dimethyl-ALA.HCl.

6.3.3.4 Effect of 5-methyl-ALA.HCl on the initial velocity of ALA dehydratase.

No change in the initial velocity of ALA dehydratase was observed with four different concentrations of ALA (0.25 mM, 0.5 mM, 1 mM, and 2 mM), each in the presence of 0.25 mM 5-methyl-ALA.HCl. This suggests that the latter is not a substrate for

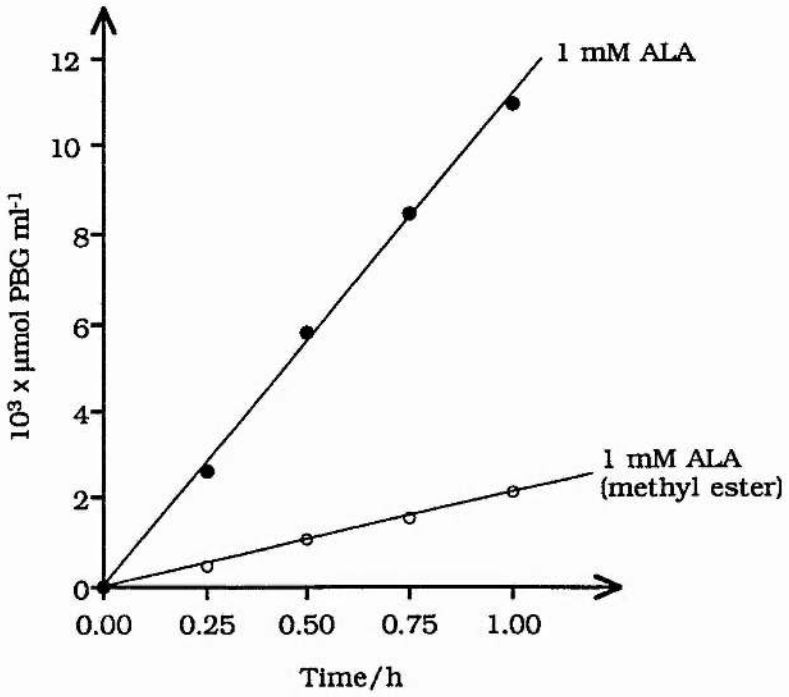

Figure 6.7 Progress curves showing the amount of PBG formed per ml of final solution. Each point represents a separate incubation, employing 0.0375 mg of ALA dehydratase.

the enzyme and therefore does not bind to either of its binding sites. The above result explains why no 'mixed' pyrrole was formed in the single-turnover reaction with equimolar amounts of ALA dehydratase and [4-^{13}C]ALA.HCl (50% enriched) together with a large excess of 5-methyl-ALA.HCl.

6.3.3.5 Effect of ALA.HCl (methyl ester) on the initial velocity of ALA dehydratase.

The progress curves of PBG production from four concentrations of ALA (0.25 mM, 0.5 mM, 1 mM, and 2 mM), each in the presence of 0.25 mM ALA.HCl (methyl ester), showed that the methyl ester has virtually no effect on the inital velocity of ALA dehydratase.

A comparison of the progress curves of PBG production using 1 mM ALA.HCl and 1 mM ALA.HCl (methyl ester) as substrates (Fig. 6.7), suggests that the latter is only a poor substrate for the enzyme. This explains why no 'mixed' pyrrole was formed in the single-turnover reaction with equimolar amounts of ALA dehydratase and [4-^{13}C]ALA.HCl (50% enriched) together with a large excess of ALA.HCl (methyl ester).

The only difference between ALA and its methyl ester is that the latter lacks a free carboxyl group which possibly plays an important role in binding the substrate to the enzyme. The *Rhodopseudomonas spheroids* enzyme is known to bind the methyl ester of ALA in the form of an enzyme-substrate Schiff base complex, at the P-site as it does the natural substrate, ALA. The free carboxyl group of the substrate must therefore be essential for binding to the A-site of the enzyme.

These findings imply the existence of a positively charged

group at the A-side binding site of the enzyme, which not only increases the affinity of the substrate, ALA, to the enzyme but also plays a role in orienting the molecule in such a manner that PBG rather than its isomer, pseudo-PBG, is formed. If one assumes that pyrrole formation proceeds *via* an enamine intermediate, then in the absence of an orienting group, pseudo-PBG would be formed (Fig. 6.8).

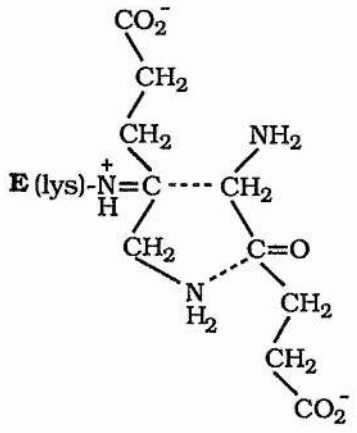

Figure 6.8 Formation of pseudo-PBG.

This is because the C_5 protons of ALA are more acidic than the C_3 protons and therefore the carbon-carbon double bond of the enamine would be formed between C_4 and C_5 of A-side ALA.

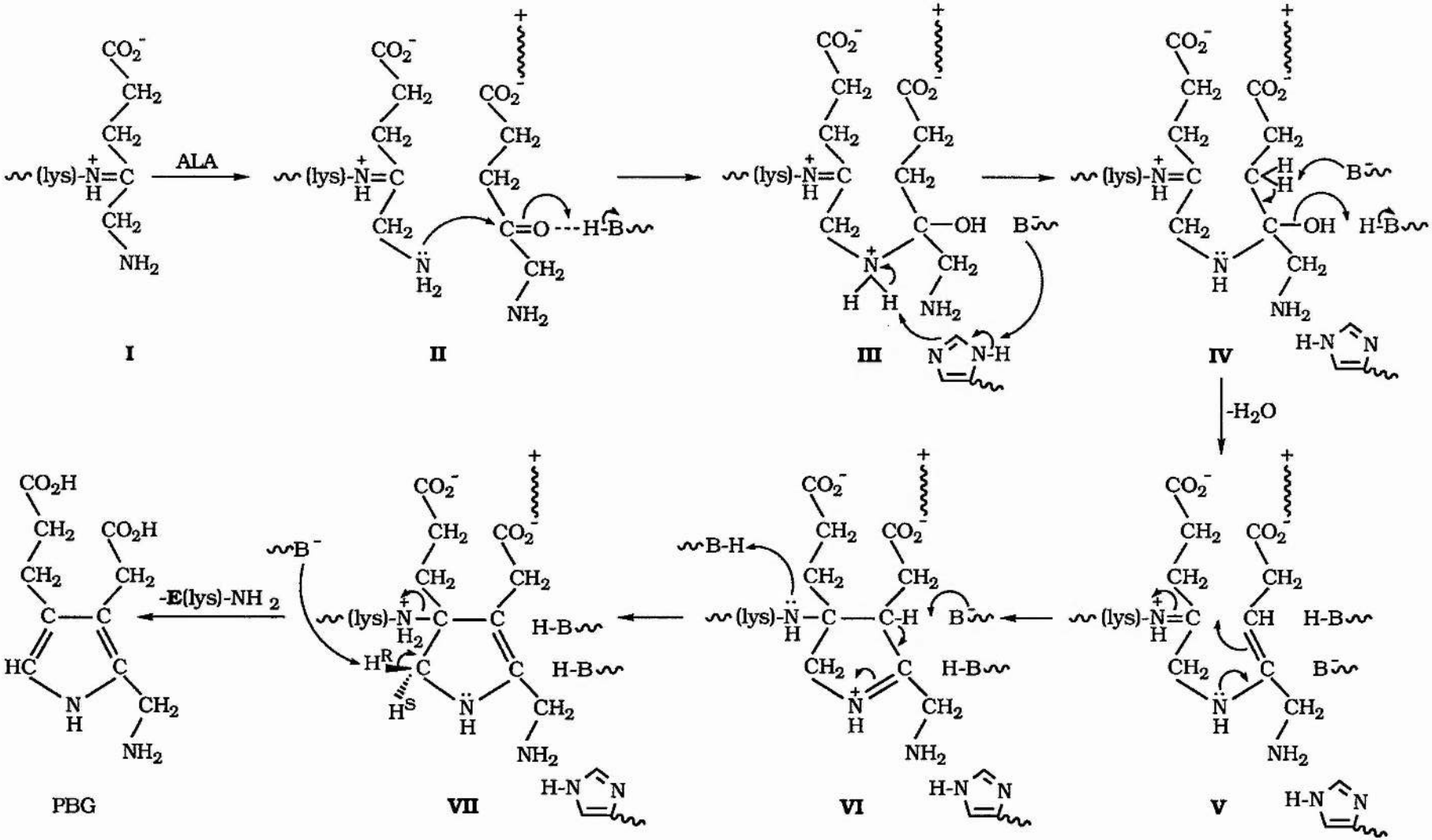

Scheme 6.7 Postulated mechanism for the ALA dehydratase catalysed dimerisation of ALA. **E** = enzyme.

6.3.4 Postulated mechanism for the ALA dehydratase catalysed dimerisation of ALA.

On the basis of the results obtained for the 'model' reaction,- the condensation of ALA with pentane-2,4-dione, it is reasonable to assume that PBG formation, which is also a Knorr-type condensation, proceeds *via* an enamine intermediate. Assuming the existence of a minimal functional dimer, involving adjacent alignment of two ALA binding sites on separate subunits,[45] a mechanism has been postulated for the ALA dehydratase catalysed dimerisation of ALA (Scheme 6.7). This mechanism suggests the requirement of several protonation/deprotonation sequences catalysed by particular residues at the active site of the enzyme.

The finding that cysteinyl residues at the active site are of high reactivity, suggests that these residues may participate in the necessary acid/base catalysis by the enzyme. In order to participate throughout the catalysis as depicted in Scheme 6.7, each group (B^- or BH) must alternate in acid/base status. A convenient means of achieving this is to interpose an imidazole bridge for regeneration of the required state. Consistent with this suggestion is the observation that a histidinyl residue is essential for ALA dehydratase catalysis.[47]

The mechanism in Scheme 6.7 involves the initial formation of a Schiff base between the carbonyl group of P-side ALA and a lysine residue in subunit 1 (I). This is followed by the alignment of A-side ALA in subunit 2, by a positively charged group, possibly an arginine or a lysine residue (II). A hydrogen bond between the carbonyl oxygen of A-side ALA and BH (possibly thiol) in subunit 2, polarises the former and facilitates nucleophilic attack upon it by the amino group of P-side ALA. The starting BH status is

regenerated by mediation of a histidine residue and leads to the formation of a carbinolamine intermediate (IV).

This is followed by a second protonation/deprotonation sequence, with the elimination of a molecule of water across C_3 and C_4 of A-side ALA resulting in the formation of an enamine intermediate (V). The latter then undergoes a shift of its nitrogen lone pair to form a cyclic intermediate (VI). (The alternation of the B/BH status from V to VI *via* the imidazole bridge has not been shown in Scheme 6.7, for clarity).

It has been reported, that the C_5 *pro*-S proton of P-side ALA is stereospecifically retained during the aromatisation process.[48] This implies, that the removal of the *pro*-R proton from an intermediate of type VII occurs while the species is enzyme-bound and not after its release into the medium. The subsequent steps including transamination and proton transfer from BH residues to the carboxylate groups of VII with the mediation of the imidazole bridge system, complete PBG formation and regenerate the initial state of the enzyme.

References.

1) B. F. Burnham and J. Lascelles, *Biochem. J.*, 1963, **87**, 462.

2) D. L. Nandi, K. F. Baker-Cohen and D. Shemin, *J. Biol. Chem.*, 1968, **243**, 1224.

3) S. van Heyningen and D. Shemin, *Biochemistry*, 1971, **10**, 4676.

4) D. L. Nandi and D. Shemin, *Arch. Biochem. Biophys.*, 1973, **158**, 305.

5) H. Komai and J. B. Neilands, *Biochim. Biophys. Acta*, 1969, **171**, 311.

6) O. L. Clara de Barriero, *Biochim. Biophys. Acta*, 1967, **139**, 479.

7) W. Leidgens, C. Lutz and H. A. W. Schneider, *Eur. J. Biochem.*, 1983, **135**, 75.

8) A. S. Shetty and G. U. Miller, *Biochem. J.*, 1969, **114**, 331.

9) D. L. Nandi and E. R. Waygood, *Can. J. Biochem.*, 1967, **45**, 327.

10) H. A. Tigier, A. M. del C. Battle and G. Locascio, *Biochim. Biophys. Acta*, 1968, **151**, 300.

11) S. Granick and D. Mauzerall, *J. Biol. Chem.*, 1958, **232**, 1119.

12) K. D. Gibson, A. Neuberger and S. Scott, *J. Biochem. Soc.*, 1955, **61**, 618.

13) E. L. Wilson, P. E. Burger and E. B. Dowdle, *Eur. J. Biochem.*, 1972, **29**, 563.

14) P. E. Gurba, R. E. Sennett, and R. D. Kobes, *Arch. Biochem. Biophys.*, 1972, **150**, 130.

15) A. M. del C. Battle, A. M. Ferramola and M. Grinstein, *Biochem. J.*, 1967, **104**, 244.

16) D. L. Coleman, *J. Biol. Chem.*, 1966, **241**, 5511.

17) D. Doyle and R. T. Schimke, *J. Biol. Chem.*, 1969, **244**, 5449.

18) J. M. Tomio, V. Tuzman and M. Grinstein, *Eur. J. Biochem.*, 1968, **6**, 84.

19) P. Calissano, C. Cartesegna and M. Mattein, *Ital. J. Biochem.*, 1966, **15**, 18.

20) P. Calissano, D. Bonsignore and C. Cartesegna, *Biochem. J.*, 1966, **101**, 550.

21) P. N. B. Gibbs, A. G. Chaudhry and P. M. Jordan, *Biochem. J.*, 1985, **230**, 25.

22) P. M. Anderson and R. J. Desnick, *J. Biol. Chem.*, 1979, **254**, 6924.

23) J. B. Weissberg and P. E. Voytek, *Biochim. Biophys. Acta*, 1974, **364**, 304.

24) D. Shemin *in* 'The Enzymes', (P. D. Boyer, ed.), 3rd ed., Vol. 7, p. 323, New York, Academic Press, 1972.

25) D. L. Nandi and D. Shemin, *J. Biol. Chem.*, 1968, **243**, 1236.

26) D. L. Nandi and D. Shemin, *J. Biol. Chem.*, 1968, **243**, 1224.

27) D. L. Nandi, *Z. Naturforsch. C. Biosci.*, 1978, **33**, 799.

28) P. M. Jordan and J. S. Seehra, *J. Chem. Soc., Chem. Commun.*, 1980, 240.

29) P. M. Jordan and J. S. Seehra, *FEBS Lett.*, 1980, **114**, 283.

30) P. M. Jordan and P. N. B. Gibbs, *Biochem. J.*, 1985, **227**, 1015.

31) D. P. Tschudy, R. A. Hess and B. C. Frykholm, *J. Biol. Chem.*, 1981, **256**, 9915.

32) G. H. Taite *in* 'Heme and Hemoproteins', (F. De Matteis and W. N. Aldridge, eds.), Vol. 44, p. 1, Springer-Verlag, New York, 1978.

33) D. P. Tschudy and A. Collins, *Science*, 1957, **126**, 168.

34) J. Baron and T. R. Tephly, *Mol. Pharmacol.*, 1969, **5**, 10.

35) J. Baron and T. R. Tephly, *Biochem. Biophys. Res. Commun.*, 1969, **36**, 526.

36) R. Satyanarayana, G. Padmanaban, S. Muthukrishnan and P. S. Sharma, *Ind. J. Biochem.*, 1970, **7**, 132.

37) D. Shemin, *Philos. Trans. R. Soc. Lond. B.*, 1976, **273**, 109.

38) O. H. Lowry, N. J. Rosebrough, A. L. Farr and R. J. Randall, *J. Biol. Chem.*, 1951, **193**, 265.

39) A. Rossi-Fanelli, E. Antonini and A. Caputo, *Biochim. Biophys. Acta*, 1958, **30**, 608.

40) B. Vahlquist, *Z. Physiol. Chem.*, 1939, **259**, 213.

41) C. J. Watson and S. Schwartz, *Proc. Soc. Exptl. Biol. Med.*, 1941, **47**, 393.

42) D. Mauzerall and S. Granick, *J. Biol. Chem.*, 1956, **219**, 435.

43) E. K.Jaffe and P. A. Michini, (unpublished observations).

44) E. K. Jaffe and G. D. Markham, *Biochemistry*, 1987, **26**, 4258.

45) A. M. del C. Battle, A. M. Stella, A. M. Ferramola, E. Wider de Xifrae and H. A. Sancovich, *Int. J. Biochem.*, 1978, **9**, 401.

46) M. M. Abboud and M. Akhtar, *J. Chem. Soc., Chem. Commun.*, 1976, 1007.

47) I. Tsukamoto, T. Yoshinaga and S. Sano, *Biochem. Biophys. Res. Commun.*, 1975, **67**, 294.

48) A. G. Chaudhry and P. M. Jordan, *Biochem. Soc. Trans.*, 1976, **4**, 760.

CHAPTER SEVEN

KINETIC INVESTIGATIONS OF THE VAN DEN BERGH REACTION

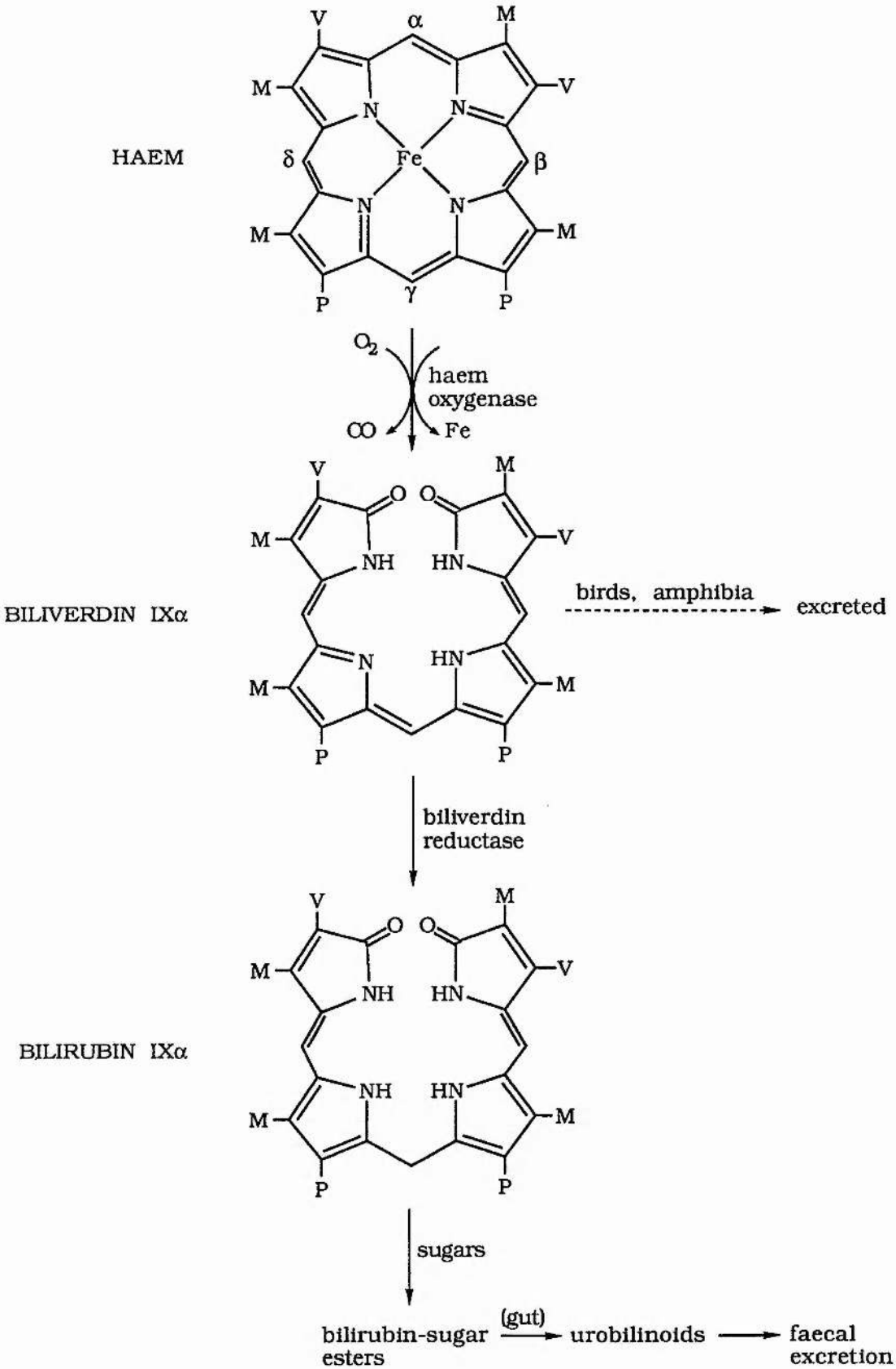

Scheme 7.1 The metabolic degradation of haem to bile pigments in mammals and other vertebrates (M = CH_3; V = $CH{=}CH_2$; P = $CH_2CH_2CO_2H$).

7.1 Introduction.

Because of their extensive highly delocalised electron systems, haems and porphyrins are relatively stable molecules as far as the macrocycle ring system is concerned. Nevertheless degradation of haem and porphyrin macrocycles does occur in biological and non-biological systems.

Haem, in association with various proteins, plays a remarkably versatile set of roles in biology. In haemoglobin and myoglobin, which are concerned with oxygen transport and storage, it is essential that the iron atom of haem is maintained in the +2 oxidation state in order that the haem may bind oxygen. In the cytochromes which are concerned with electron transport, the iron atom of haem must shuttle between the +2 and +3 oxidation states. Cytochrome P450, which is concerned with hydroxylation and drug metabolism, must permit its iron to oscillate between the +2 and +3 oxidation states and it must accomodate the binding of oxygen while the iron is in the +2 oxidation state. Other haemoproteins include catalase, peroxidase and tryptophan dioxygenase which are concerned with decomposition of H_2O_2, oxidations by H_2O_2 and dioxygenation respectively. Although haemoproteins carry out a variety of functions, in mammals, by far the great majority of the haem resides in the haemoglobin contained in the circulating erythrocytes.

The most important functional pathway by which haem is broken down in living systems is its conversion to the bile pigment biliverdin IXα as shown in Scheme 7.1. In human beings and many animals, the further conversion of biliverdin to the yellow bile pigment, bilirubin IXα occurs (Scheme 7.1).

Although theoretically the porphyrin ring of haem may be

broken at any of the four carbon bridges, leading to a series of tetrapyrroles,[1] in living organisms, only one isomer, bilirubin IXα is derived from haem degradation. This compound results from the iron protoporphyrin ring opening at the α-bridge of the IX isomer.

Oxidation of haem at the α-bridge by haem oxygenase (an enzyme located in the microsomal fraction of a variety of tissues such as spleen, liver, bone marrow and kidney), produces carbon monoxide and an unstable iron complex that loses iron to give the green pigment, biliverdin IXα. The iron is retained as ferritin and reutilised and bilverdin is reduced enzymatically to bilirubin IXα (Scheme 7.1). Detailed mechanistic analyses of haem degradation have been presented in earlier reviews.[2-4]

Catabolism of haem is the only known source of bilirubin IXα and 300 to 500 mg of the pigment are produced per day in adult human beings.[5] The high degree of hydrogen bonding present in bilirubin renders it highly insoluble in water at physiological pH. In order to be transported in plasma, bilirubin binds strongly to certain proteins, particularly serum albumin. Although serum albumin is the major carrier, other proteins such as α and β globulins have also been found to associate with bilirubin.[6] Protein bound bilirubin is not easily excreted and cannot efficiently pass out of the circulation across either of the selective barriers, kidney and liver, into urine or bile.[7] This problem is circumvented in nature by conjugation of bilirubin, that is, by attaching polar substances such as glucuronic acid to the carboxylic acid groups of bilirubin. A glucuronyl transferase enzyme esterifies the carboxylic acid groups of bilirubin giving a mixture of mono- and di-glucuronides. These glucuronides (sugars), which are synthesised mainly in the liver are more polar than bilirubin and can be readily excreted in bile.

Conjugated bilirubin exists mainly in serum as the diglucuronide, a form in which it is water-soluble and non-toxic. The glucuronides are then secreted *via* the bile duct into the intestinal tract where they undergo further reductive transformation to urobilinoids before their final excretion in the faeces. Bilirubin appears to have no specific function other than participation in a pathway for the elimination of unwanted haem from the organism.

The bilirubin concentration in plasma is at most 15 μM.[8] This amount can be dealt with efficiently by healthy liver, but diseased liver, in which one or more of the processes between bilirubin production and excretion is disrupted, leads to the development of elevated levels of bilirubin in the serum, known as hyperbilirubinemia. The increased amounts of pigment result in the characteristic yellow colouring of the skin, referred to as jaundice. Jaundice and hyperbilirubinemia are not diseases in themselves but symptoms of a number of liver disorders which result in abnormally high levels of serum bilirubin. Hyperbilirubinemia is particularly prevalent amongst newborn babies where levels of the glucuronyl transferase enzyme involved in the formation of bilirubin diglucuronide are very low. In the fetus this is not a problem because the lipophilic bilirubin can pass readily across the placenta from the fetal to the maternal circulation where is it glucuronidated and excreted by the mother's liver. This cannot occur in the newborn however, so after birth, levels of bilirubin in serum begin to rise, resulting in hyperbilirubinemia. Usually within 7-14 days the baby is able to synthesise and excrete bilirubin glucuronides with complete efficiency. However while hyperbilirubinemia lasts, the toxicity of bilirubin may lead to irreversible cell damage, even brain damage if bilirubin crosses the blood-brain barrier.

The most usual and effective form of treatment of hyperbilirubinemia in newborns is phototherapy. The patient is exposed to ultra-violet light for several hours or even days, until the jaundiced yellow colouring disappears. The way in which phototherapy works to reduce free bilirubin is not entirely clear although studies have been undertaken to investigate possible mechanisms.[9] Evidence has established that bilirubin undergoes rapid reversible carbon-carbon double bond configurational isomerism to unstable 4*E* and 15*E* isomers when irradiated in solution[10] and it seems likely that photoisomerisation of bilirubin, disrupting hydrogen bonds and forming a more soluble configuration, increases the efficiency of transportation and excretion of the pigment. McDonagh *et al* [10] also note that binding of bilirubin to albumin does not inhibit photoisomerisation. Indeed, in human albumin the rates of structural and configurational isomerisation are higher than in the presence of organic solvents.

The clinical diagnostic test for serum bilirubin is based on a method devised by van den Bergh. In the van den Bergh method[11,12] for the colorimetric determination of bilirubin in biological fluids, bilirubin reacts with arenediazonium ions (diazotised sulphanilic acid) in acid solution, to form stable red to violet azo pigments and this reaction enables its presence in blood and urine to be demonstrated and its content determined. The structures of the azo pigments derived from diazotised ethyl anthranilate and aniline have been established[13] and the reaction with diazotised ethyl anthranilate has been used in the determination of the structures of bilirubin conjugates.[14] Overbeek *et al* [15] showed, on the basis of kinetic measurements that bilirubin couples with two equivalents of a diazonium ion in two stages with

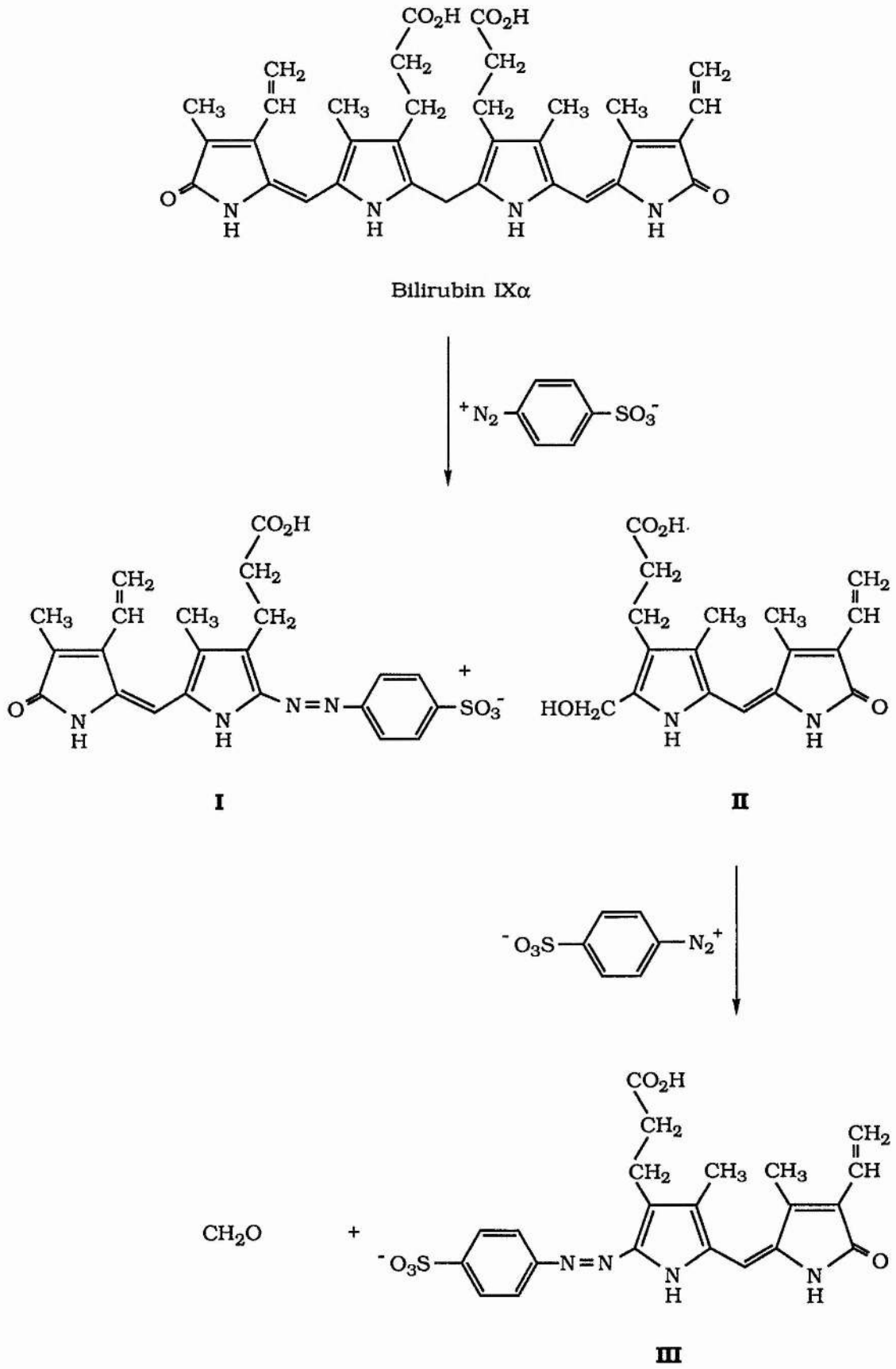

Scheme 7.2 Reaction of bilirubin with diazotised sulphanilic acid.

scission of the methylene bridge. In the first stage, the products are 'vinyl' azobilirubin (I) with its tautomeric arylhydrazone and hydroxypyrromethenecarbinol (II) (Scheme 7.2). In the second stage, II couples slowly with a second molecule of diazonium ion, to form 'isovinyl' azobilirubin (III) and its tautomer with elimination of formaldehyde.[16] In 1980, it was shown by Compernolle *et al*,[17] using ^{1}H and ^{13}C NMR determinations, that the pigments exist predominately as arylhydrazones rather than as azo compounds.

It was thought that binding of bilirubin to albumin prevented reaction with diazotised sulphanilic acid, so before the test was carried out, alcohol was added to the sample to remove all the protein. Under mildly acidic conditions, appropriate for the diazotisation of sulphanilic acid, a red azo pigment was obtained. In later studies two azo reactions were observed suggesting that two types of bilirubin occur naturally in serum.[18] The first reaction occurred almost instantaneously, the second only after the addition of alcohol. It is generally accepted that the first reaction is due to the direct reaction of 'free' or unbound bilirubin. In contrast, bilirubin bound to albumin only reacts quickly once it has been solubilised by the addition of alcohol. The estimation of the total bilirubin content of a sample is therefore established by measuring the amount of direct reacting bilirubin and adding to this the amount of indirect reacting bilirubin detected after the addition of alcohol to the sample. This technique is not entirely satisfactory, however, because co-precipitation of bilirubin to the protein leads to under-estimation of the total bilirubin content. A further refinement of the van den Bergh test for clinical analysis, was the use of a variety of substances which increase the rate at which the diazotisation reaction proceeds. These substances known as

accelerators or promoters include caffeine, sodium benzoate, sodium acetate, urea and mixtures of these. However, in spite of the chemical uncertainty of the processes involved, the van den Bergh test, using accelerators, is routinely used for the clinical estimation of total bilirubin content in plasma. The determination of total bilirubin content by the diazo reaction is crucial in the detection and diagnosis of jaundice and the need to quantify the test has led to many modifications.[19]

In the hope of gaining an insight into the chemistry of the diazo reaction, a kinetic study of the effect of acid and diazo compound on the reaction of bilirubin ditaurate disodium salt with *p*-nitrophenyldiazonium tetrafluoroborate was undertaken. It is reasonable to assume that the above reaction is initiated by electrophilic attack on one of the two central pyrrole rings of the bilirubin conjugate. There are two electrophiles present in the reaction mixture, namely, diazonium ions and protons. Kinetic evidence allows us to determine which is responsible for the cleavage of the central methylene bridge. As the products of diazo-coupling reactions are highly coloured, the kinetics of the above reaction were readily studied by stopped-flow spectrophotometry. The reaction was found to be first-order in the appearance of product (diazonium ions and acid present in large excess).

7.2 Experimental.

7.2.1 Materials.

Bilirubin ditaurate disodium salt was purchased from American Biochemicals Ltd. and used as such. Fluoroboric acid (BDH), sodium nitrite (Aldrich), ethanol, diethyl ether and 1 M HCl (Rhône Poulenc Ltd., analaR) were used as received. *p*-nitrophenyldiazonium tetrafluoroborate was prepared as described in Section 7.2.3.

7.2.2 Instrumentation and General Techniques.

Kinetic studies of the reaction of bilirubin ditaurate disodium salt and *p*-nitrophenyldiazonium tetrafluoroborate were carried out on a Hi-Tech stopped-flow spectrophotometer equipped with a SF-40C photomultiplier, a Data-Lab DC 901 transient recorder and a DT V12-14 Farnell oscilloscope. A very dilute solution of bilirubin ditaurate disodium salt was placed in one arm and a solution of *p*-nitrophenyldiazonium tetrafluoroborate in HCl in the other. Reactions were monitored at λ = 560 nm and 25 °C. Data acquisition and processing were carried out by an Apple II Plus microcomputer, using a Hi-Tech system software kinetics package. Observed rate constants were calculated by a computer programme using the method of Kezdy[20] and Swinbourne.[21] Spectra of the coloured products were recorded on a Philips PU 8732 UV/Visible scanning spectrophotometer fitted with a PU 8732 cell programmer.

7.2.3 Preparation of *p*-nitrophenyldiazonium tetrafluoroborate.

p-nitrophenyldiazonium tetrafluoroborate was prepared according to the method of Starkey.[22]

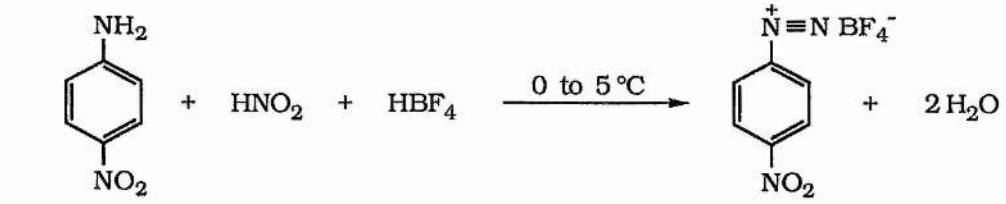

p-nitroaniline

p-nitrophenyldiazonium tetrafluoroborate

p-nitroaniline (17.0 g, 0.125 mol) was dissolved in fluoroboric acid (55 ml) in a 200 ml beaker. The beaker was placed in an ice bath and the solution stirred. A cold solution of sodium nitrite (8.5 g, 0.125 mol) in water (17 ml) was added dropwise. When the addition was complete, the mixture was stirred for a few minutes and filtered by suction on a sintered glass filter. The solid diazonium tetrafluoroborate was washed once with cold fluoroboric acid (15 ml), twice with cold 95% ethanol and several times with diethyl ether. The product weighed 29.3 g (99% yield).

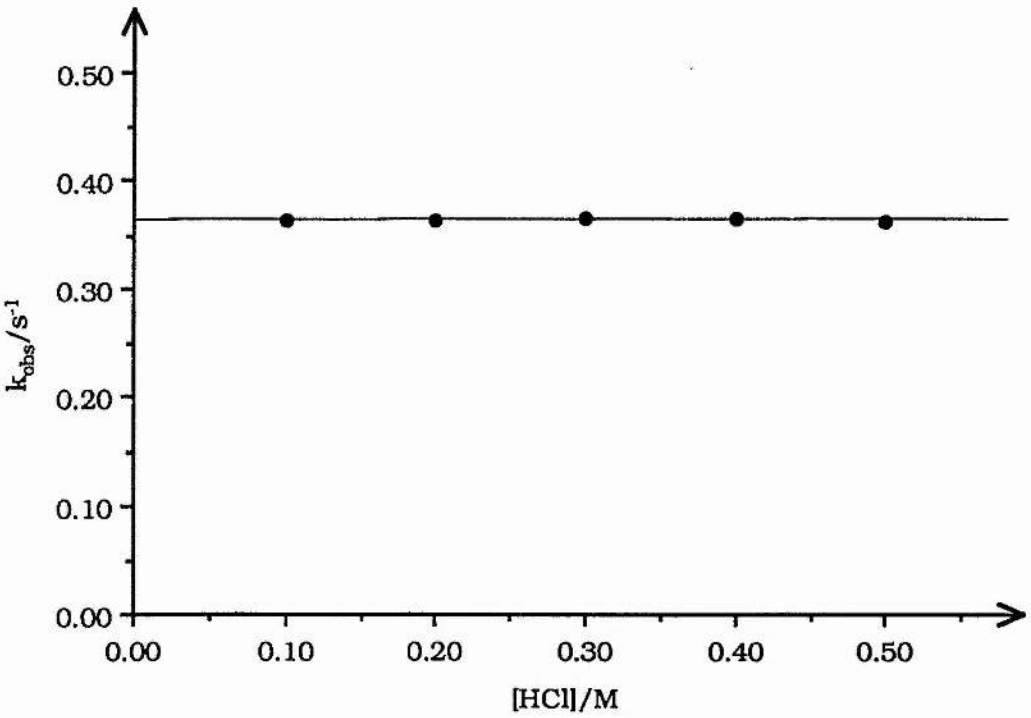

Figure 7.1 Effect of hydrogen ion concentration on the rate of reaction between bilirubin ditaurate disodium salt and *p*-nitrophenyldiazonium tetrafluoroborate.

7.3 Results and Discussion.

7.3.1 Effect of hydrogen ion concentration on the rate of reaction between bilirubin ditaurate disodium salt and *p*-nitrophenyldiazonium tetrafluoroborate.

In order to investigate the effect of hydrogen ion concentration on the rate of reaction between bilirubin ditaurate disodium salt and *p*-nitrophenyldiazonium tetrafluoroborate, the rate of reaction of the above system was determined as a function of hydrogen ion concentration, at constant bilirubin conjugate and diazonium ion concentrations. First order curves were obtained from stopped-flow kinetic experiments on the above system. The observed rate constants, k_{obs}, for a series of reactions (an average of five readings in each case) involving an increasing amount of HCl are listed in Table 7.1. Figure 7.1 illustrates graphically the effect of hydrogen ion concentration on the rate of the reaction.

Table 7.1 Effect of hydrogen ion concentration on the rate of reaction between bilirubin ditaurate disodium salt (A) and *p*-nitrophenyldiazonium tetrafluoroborate (B).

[A]/M	[B]/M	[HCl]/M	k_{obs}/s^{-1}
2×10^{-5}	2.5×10^{-3}	0.1	0.363
2×10^{-5}	2.5×10^{-3}	0.2	0.363
2×10^{-5}	2.5×10^{-3}	0.3	0.367
2×10^{-5}	2.5×10^{-3}	0.4	0.367
2×10^{-5}	2.5×10^{-3}	0.5	0.363

The experimental pseudo first-order rate constant, k_{obs},

remained unchanged with increasing HCl concentration, suggesting that protons are not responsible for the cleavage of the central methylene bridge of the bilirubin conjugate molecule. The above evidence is clear indication of the fact, that the diazo reaction does not proceed as illustrated in Scheme 7.3.

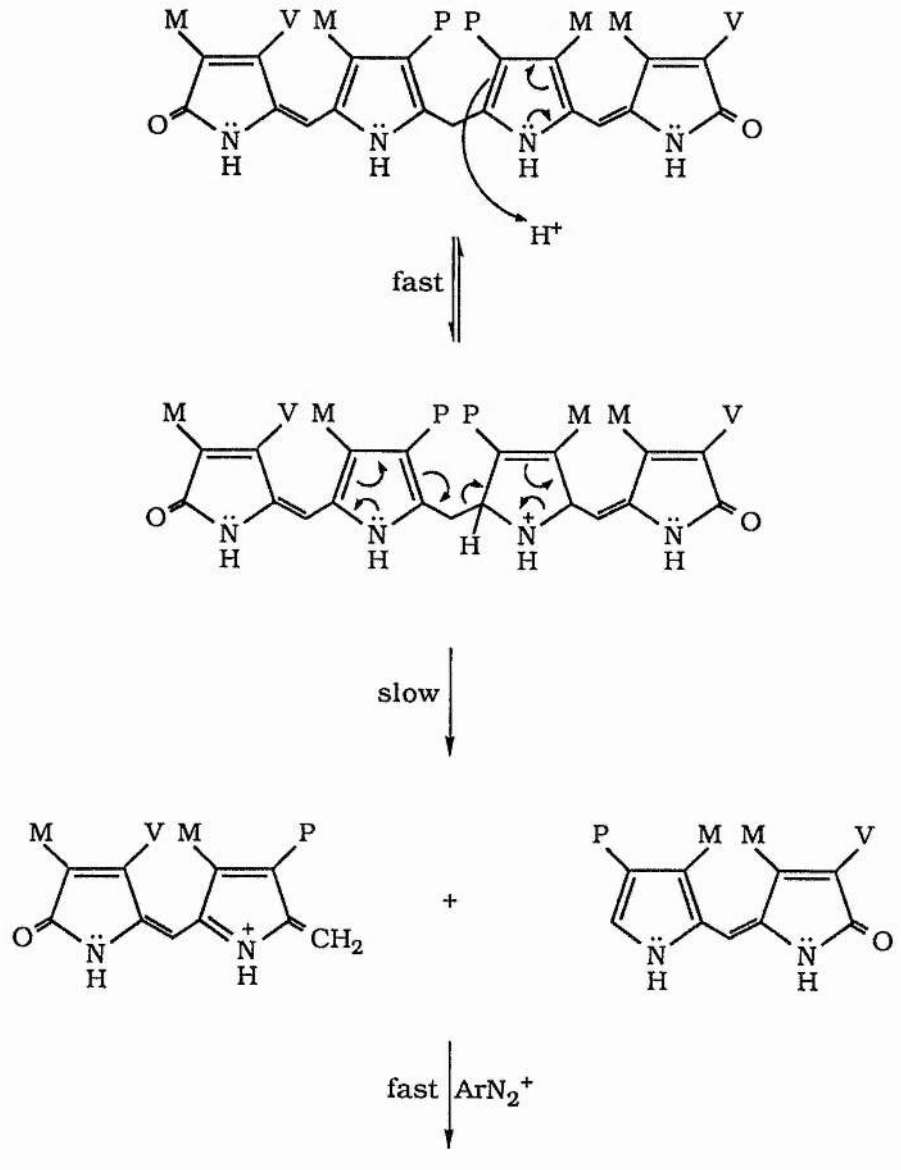

Scheme 7.3

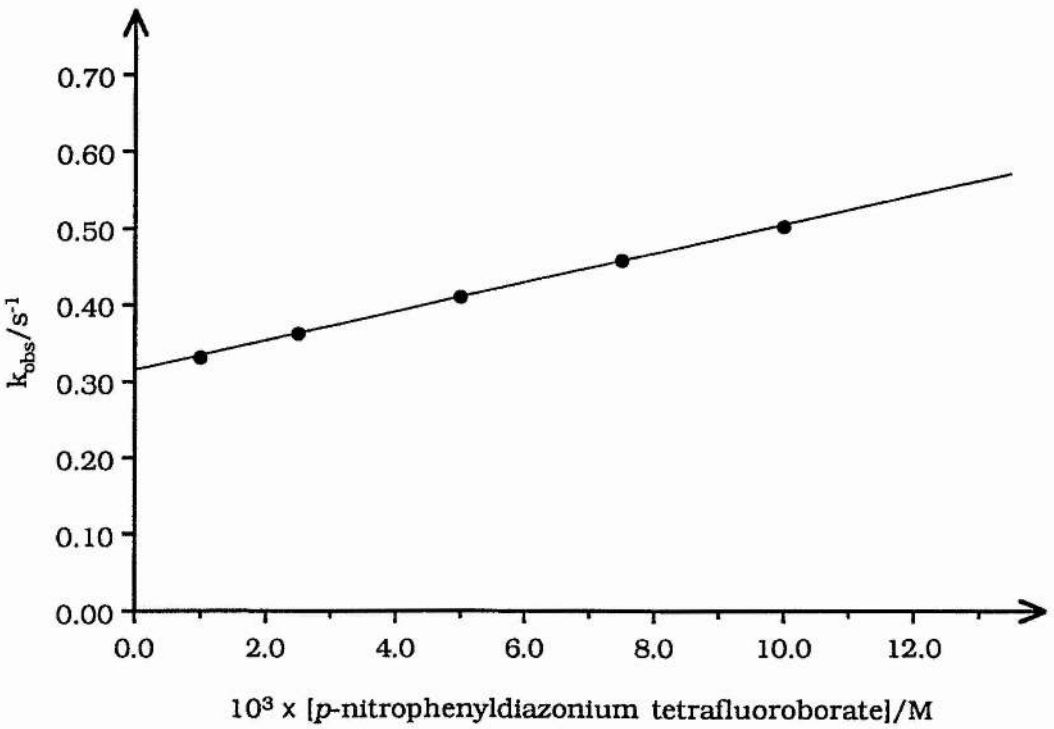

Figure 7.2 Effect of diazonium ion concentration on the rate of reaction between bilirubin ditaurate disodium salt and *p*-nitrophenyldiazonium tetrafluoroborate.

7.3.2 Effect of diazonium ion concentration on the rate of reaction between bilirubin ditaurate disodium salt and *p*-nitrophenyldiazonium tetrafluoroborate.

In order to investigate the effect of diazonium ion concentration on the rate of reaction between bilirubin ditaurate disodium salt and *p*-nitrophenyldiazonium tetrafluoroborate, the rate of reaction of the above system was determined as a function of diazonium ion concentration at constant bilirubin conjugate and hydrogen ion concentrations. The observed rate constants, k_{obs}, for a series of reactions (an average of five readings in each case) involving increasing amounts of *p*-nitrophenyldiazonium tetrafluoroborate are shown in Table 7.2. Figure 7.2 illustrates graphically the effect of the diazonium ion concentration on the rate of reaction of the above system.

Table 7.2 Effect of diazonium ion concentration on the rate of reaction between bilirubin ditaurate disodium salt (A) and *p*-nitrophenyldiazonium tetrafluoroborate (B).

[A]/M	[B]/M	[HCl]/M	k_{obs}/s^{-1}
2×10^{-5}	1.0×10^{-3}	0.1	0.333
2×10^{-5}	2.5×10^{-3}	0.1	0.363
2×10^{-5}	5.0×10^{-3}	0.1	0.412
2×10^{-5}	7.5×10^{-3}	0.1	0.460
2×10^{-5}	10.0×10^{-3}	0.1	0.506

The variation of the experimental pseudo first-order rate

constant, k_{obs}, with diazonium ion concentration was found to be linear with a large positive intercept (Fig. 7.2). This shows that diazo coupling is an equilibrium reaction.

7.3.3 Proposed mechanism of the diazo coupling reaction.

The oscilloscope trace for the diazo coupling reaction (Fig. 7.3), provided strong evidence that the reaction occurs in two steps, which is reasonable if cleavage of the central methylene bridge of the bilirubin conjugate molecule occurs by attack of diazonium ions on each of the central pyrrole rings in two steps.

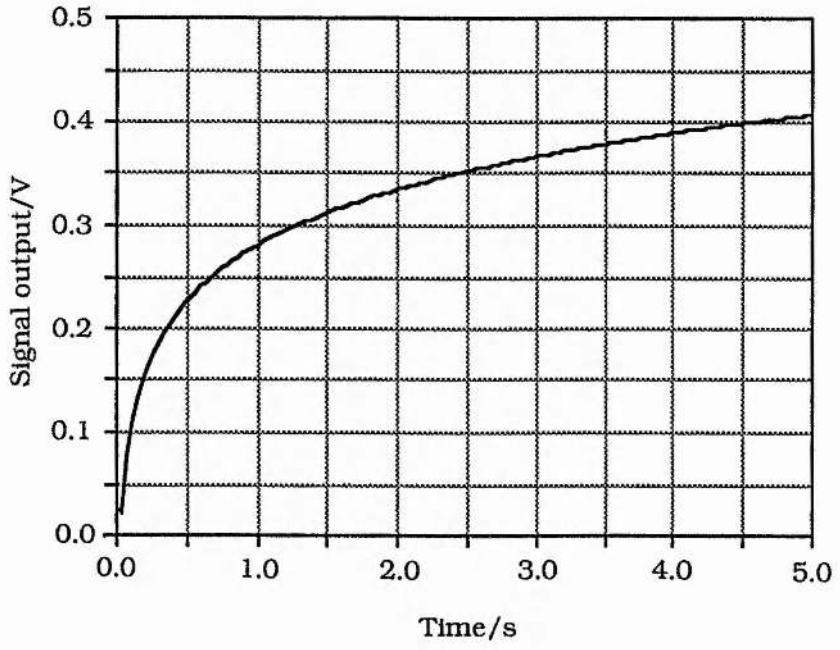

Figure 7.3 Oscilloscope trace obtained for the reaction between bilirubin ditaurate disodium salt and *p*-nitrophenyldiazonium tetrafluoroborate.

Based on the kinetic evidence obtained for the above diazo reaction, a reaction mechanism has been proposed to involve electrophilic attack by diazonium ion on a central pyrrole ring of the bilirubin conjugate molecule, B, at either position 9 or 11 (Scheme 7.4). This leads to the formation of the 'isovinyl' azo

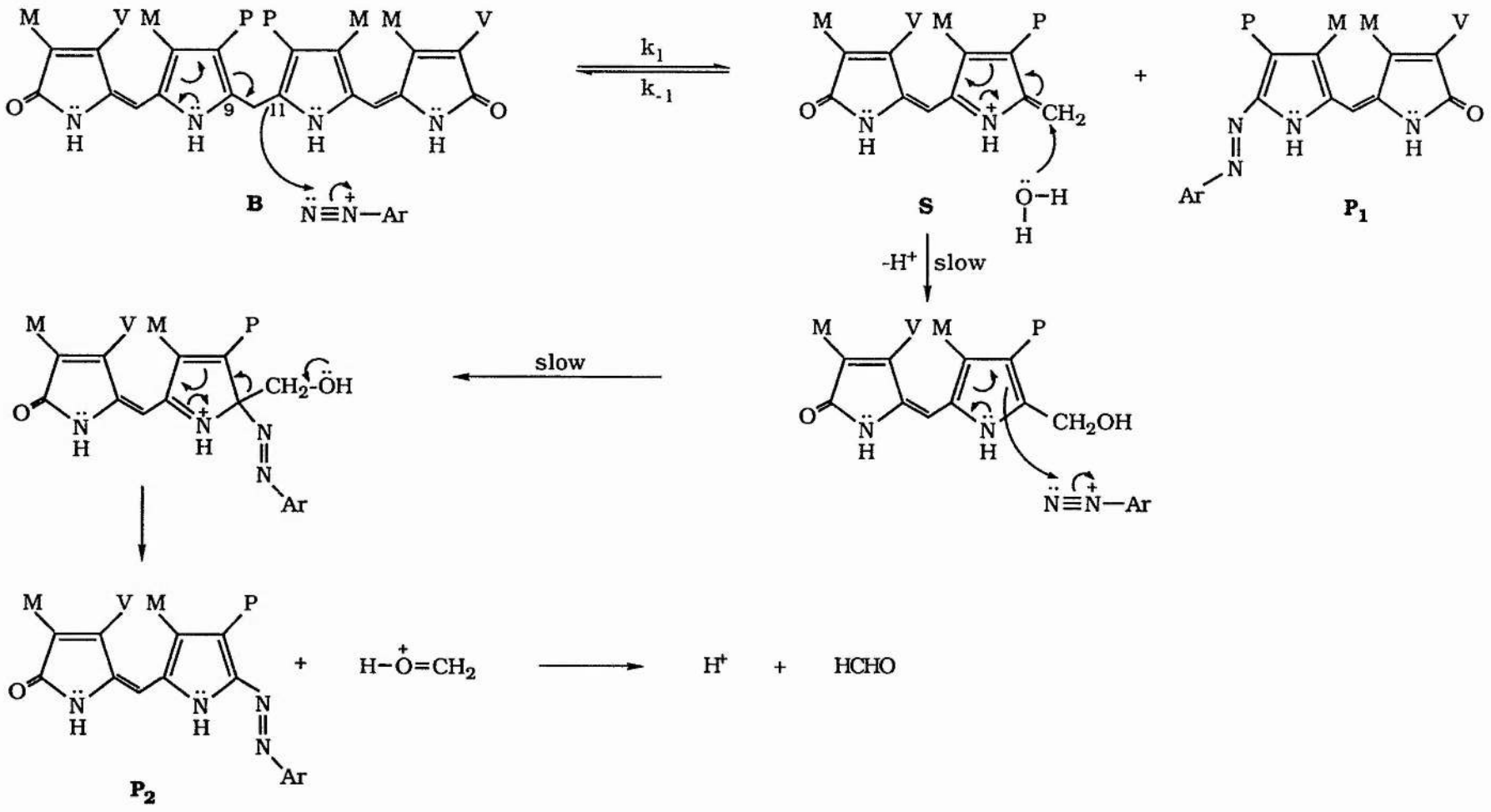

Scheme 7.4 Proposed mechanism for the reaction between bilirubin ditaurate disodium salt and *p*-nitrophenyldiazonium tetrafluoroborate. Ar = $PhNO_2$; M = CH_3; P = $CH_2CH_2CO_2CH(CHOH)_3CHCONHCH_2CH_2SO_3^-Na^+$; V = $CH{=}CH_2$.

pigment, P_1, from initial attack at position 11 (or the 'vinyl' azo pigment, P_2, when the initial point of electrophilic attack is position 9). The remaining oxopyrromethene half of bilirubin, S, is potentially reactive with an additional mole equivalent of diazonium ion, leading to the formation of (in Scheme 7.4) the 'vinyl' azo pigment, P_2, and one equivalent of formaldehyde, in a step which is significantly slower than that leading to the formation of P_1 and S.

The observed rate constant, k_{obs}, measured by the stopped flow apparatus is that of the initial reversible reaction leading to the formation of P_1 and S (Scheme 7.4).

All reactions on approaching equilibrium become first-order,[23] so that the measured value of k_{obs} is given approximately by the expression,

$$k_{obs} = k_1[B][ArN_2^+] - k_{-1}[S][P_1]$$

This explains the dependence of k_{obs} on $[ArN_2^+]$ (Fig. 7.2) and the significance of the intercept which is equal to $k_{-1}[S][P_1]$. All the experimental data are consistent with Scheme 7.4.

Thus, of the two electrophiles present in the reaction mixture, namely, diazonium ions and protons, kinetic evidence suggests that the diazonium ions are solely responsible for the cleavage of the central methylene bridge of the bilirubin ditaurate disodium salt molecule.

References.

1) P. O'Carra and E. Colleran, *FEBS Lett.*, 1969, **5**, 295.

2) R. Schmid and A. F. McDonagh, *Ann. N. Y. Acad. Sci.*, 1975, **244**, 533.

3) R. Schmid and A. F. McDonagh, *in* 'The Porphyrins', (D. Dolphin, ed.), Vol. 6, p. 257, Academic Press, New York, 1979.

4) S. B. Brown and R. F. Troxler, *in* 'Bilirubin', (K. P. M. Heirwegh and S. B. Brown, eds.), Vol. 2, p. 1, CRC Press, Boca Raton, Florida, 1982.

5) J. W. Harris and R. W. Kellermeyer, 'The Red Cell', (rev. ed.), Harvard University Press, Cambridge, Massachusetts, 1970.

6) N. H. Martin, *J. Am. Chem. Soc.*, 1949, **71**, 1230.

7) D. A. Lightner and A. F. McDonagh, *Acc. Chem. Res.*, 1984, **17**, 417.

8) P. Berthelot, Ph. Duvaldestin and J. Fevery, *in* 'Bililrubin', Vol. 2, p. 175, (K. P. M. Heirwegh and S. B. Brown, eds.), CRC Press, Boca Raton, Florida, 1982.

9) A. F. McDonagh, L. A. Palma, F. R. Trull and D. A. Lightner, *J. Am. Chem. Soc.*, 1982, **104**, 6965.

10) A. F. McDonagh, D. A. Lightner and T. A. Wooldridge, *J. Chem. Soc., Chem. Commun.*, 1979, 110.

11) P. Ehrlich, *J. Liebigs Ann. Chem.*, 1883, **8**, 140.

12) A. A. H. van den Bergh and I. Snapper, *Deut. Arch. Klin. Med.*, 1913, **110**, 540.

13) F. H. Jansen and M. S. Stoll, *Biochem. J.*, 1971, **125**, 585.

14) F. Compernolle, F. H. Jansen and K. P. M. Heirwegh, *Biochem. J.*, 1970, **120**, 891.

15) J. Th. G. Overbeek, C. L. J. Vink and H. Deenstra, *Rec. Trav. Chim.*, 1955, **74**, 85.

16) D. W. Hutchison, B. Johnson and A. J. Knell, *Biochem. J.*, 1972, **127**, 907.

17) F. Compernolle, S. Toppet and D. W. Hutchison, *Tetrahedron*, 1980, **36**, 2237.

18) A. A. H. van den Bergh and P. Muller, *Biochem. Z.*, 1916, **77**, 90.

19) H. T. Malloy and K. A. Evelyn, *J. Biol. Chem.*, 1937, **119**, 481.

20) F. J. Kezdy, J. Jaz and A. Bruylants, *Bull. Soc. Chim. Belg.*, 1958, **67**, 687.

21) E. S. Swinbourne, *J. Chem. Soc.*, 1960, 2371.

22) E. B. Starkey, *Org. Syn.*, Coll. Vol. II, 1948, 225.

23) J. W. Moore and R. G. Pearson, *in* 'Kinetics and Mechanism', 3rd ed., p. 309, John Wiley, New York, 1981.